Arg-Trp peptidomimetics as inhibitors of the translocase MraY-E protein interaction site

Rachel Victoria Kerr

Thesis submitted in partial fulfilment of the requirements for the degree of Doctor of Philosophy in Chemistry

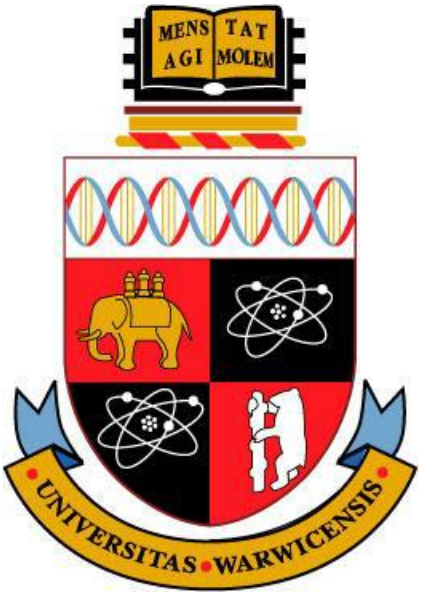

University of Warwick
Department of Chemistry

March 2020

TABLE OF CONTENTS

Abbreviations, Symbols and Formulae

°C	degrees Celcius
A. aeolicus	*Aquifex aeolicus*
aa	Amino acid
Ac	Acetyl
Ala	Alanine
Amp	Ampicillin
AMPs	Antimicrobial peptides
Arg	Arginine
B. subtilis	*Bacillus subtilis*
Boc	*tert*-butyloxycarbonyl
C55-P	Undecaprenyl phosphate
C55-PP	Undecaprenyl pyrophosphate
C. bolteae	*Clostridium bolteae*
CBz	Benzyl chloroformate
CFU	Colony forming units
COOH	Carboxyl
DCC	*N*,*N´*-dicyclohexylcarbodiimide
DCM	Dichloromethane
DIPEA	*N*,*N´*-Diisopropylethylamine
DMF	Dimethylformamide
DMAP	4-dimethylamino pyridine
DMSO	Dimethyl Sulphoxide
E. coli	*Escherichia coli*
EtOAc	Ethyl acetate
EDC	1-ethyl-3-(3-dimethylamino-propyl)carbodiimide
ESI-MS	ElectroSpray Ionisation Mass Spectroscopy
Et_2O	Diethyl ether
Fmoc	Fluorenylmethyloxycarbonyl
FPLC	Fast protein liquid chromatography
FU	Fluorescence units
GlcNAc	*N*-acetylglucosamine

Gln	Glutamine
Glu	Glutamic acid
Gly	Glycine
HATU	2-(7-Aza-1*H*-benzotriazole-1-yl)-1,1,3,3-tetramethyluronium Hexafluorophosphate
HBTU	2-(1*H*-benzotriazol-1-yl)-1,1,3,3-tetramethyluronium hexafluorophosphate
His	Histidine
HOBt	1-hydroxybenzotriazole
HPLC	High-Performance Liquid Chromatography
HRMS	High Resolution Mass Spectrometry
HWoct	H_2N-His-Trp-*O*-octyl ester
Ile	Isoleucine
IPTG	Isopropyl β-D-1-thiogalactopyranoside
Kan	Kanamycin
KG-*N*oct	H_2N-Lys-Gly-*N*-octyl amide
KW-*N*oct	H_2N-Lys-Trp-*N*-octyl amide
KWoct	H_2N-Lys-Trp-*O*-octyl ester
LB	Luria Broth
Lys	Lysine
IC_{50}	Half maximal inhibitory concentration
Leu	Leucine
Lipid I	C55-PP-MurNAc-pentapeptide
LPPS	Liquid/solution phase peptide synthesis
LRMS	Low resolution mass spectrometry
m-DAP	*meso*-diaminopimelic acid
m-Tyr	*meta*-Tyrosine
MBC	Minimum bactericidal concentration
MD2	Muraymycin D2
MDm2	Mouse double minute 2 homolog
MeCN	Acetonitrile
MeOH	Methanol

Met	Methionine
MH	Mueller Hinton broth
MH2	Mueller Hinton cation adjusted broth
MIC	Minimal Inhibitory Concentration
MIC_{50}	Minimum Inhibitory Concentration required to inhibit the growth of 50% of organisms.
MIC_{90}	Minimum Inhibitory Concentration required to inhibit the growth of 90% of organisms
MraY	Phoshpo-MurNAc-pentapeptide translocase, translocase I
$MraY_{AA}$	MraY from *Aquifex aeolicus*
$MraY_{CB}$	MraY from *Clostridium bolteae*
MRSA	Methicillin resistant *S. aureus*
MurNAc	N-acetylmuramic acid
MurA	UDP-*N*-acetylglucosamine enolpyruvyl transferase
MurB	UDP-N-acetylenolpyruvoylglucosamine reductase
MurC	UDP-N-acetylmuramate-L-alanine ligase
MurD	UDP-N-acetylmuramoylalanine-D-glutamate ligase
MurE	UDP-N-acetylmuramoyl-L-alanyl-D-glutamate--2,6-diaminopimelate ligase
MurF	UDP-N-acetylmuramoyl-tripeptide-D-alanyl-D-alanine ligase
MurG	Undecaprenyldiphospho-muramoylpentapeptide beta-NAcetylglucosaminyltransferase
NMR	Nuclear Magnetic Resonance
OD	Optical density
Orn	Ornithine
P. aeruginosa	*Pseudomonas aeruginosa*
P. putida	*Pseudomonas putida*
P. fluorescens	*Pseudomonas fluorescens*
PBP	Penicillin binding proteins
Pbf	2,2,4,6,7-Pentamethyldihydrobenzofuran-5-sulfonyl chloride
Phe	Phenylalanine
PM	Peptidomimetic

Poly	Polymyxin B
Pro	Proline
PPI	Protein-protein interaction
PyBOP	Benzotriazol-1-yl-oxytripyrrolidinophosphonium hexafluorophosphate
R. jostii	*Rhodococcus. jostii*
RFoct	H_2N-Arg-Phe-*O*-octyl ester
RP	Reverse phase
RW-*N*oct	H_2N-Arg-Trp-*N*-octyl amide
RWdec	H_2N-Arg-Trp-*O*-decyl ester
RWhex	H_2N-Arg-Trp-*O*-hexyl ester
RWoct	H_2N-Arg-Trp-*O*-octyl ester
RYoct	H_2N-Arg-Tyr-*O*-octyl ester
S. aureus	*Staphylococcus aureus*
Ser	Serine
SlyD	Sensitive to lysis D
S_NAr	Aromatic nucleophilic substitution
SPPS	Solid phase peptide synthesis
TBAB	Tetra-n-butylammonium bromide
^{t}Bu	*tert*-Butyl
TCA	Trichloroacetic acid
TEA	Triethylamine
Tet	Tetracycline
TFA	Trifluoroacetic acid
THF	Tetrahydrofuran
TIPS	Triisopropylsilyl
TLC	Thin Layer Chromatography
Trp	Tryptophan
Trt	Trityl
Tun	Tunicamycin
Tyr	Tyrosine
UDP	Uridine diphosphate

UMP	Uridine monophosphate
UPA	Uridyl peptide antibiotics
UppP	Undecaprenyl pyrophosphatase
UppS	Undecaprenyl pyrophosphate synthase
UV	Ultraviolet
Val	Valine
VRE	Vancomycin Resistant Enterococci
WT	Wild-type

Declaration

The experimental work reported in this thesis is original research carried out by the author, unless otherwise stated, in the Department of Chemistry, University of Warwick, between October 2016 and March 2020. No material contained herein has been submitted for any other degree, or at any other institution.

Results from other authors are referenced in the usual manner throughout the text.

_____ Date:_____

Rachel Victoria Kerr

Acknowledgments

Firstly I must thank my supervisor Professor Tim Bugg, for the opportunity to carry out my PhD research in his group. I would also like to thank the Bugg group for their help and support over the past three and a half years. Particularly Rahman for his words of wisdom. Goran for his expertise. James and Robb for their help in the biology lab and their friendship. Jess, my MChem student, and now a treasured friend.

I would like to thank the mass spectrometry and NMR technicians, Lijiang Song and Ian Prokes, for their knowledge and expertise.

I would like to thank my industrial supervisor Andy Merritt for the support, opportunity and ideas he has given me. I would also like to thank LifeArc and all the great people there for welcoming me and helping me during my visits. A special thanks must be given to Timur, for his support, optimism and knowledge.

I cannot put into words how much I would like to thank Dan Leng, without whom I probably wouldn't be finishing this PhD. He has helped me every step of the way with chemistry and life in general.

Finally I would like to thank the people closest to me. Firstly my parents and my brother (Bubbles) for the opportunities that they have given me. Who from day one have encouraged me to reach for the stars and not let anyone stand in my way. Secondly Nyle, who has had to listen to my constant complaining every single day, and for that you deserve a second PhD. My time at Warwick has been made worthwhile because of you.

Abstract

The cell wall biosynthesis pathway is made up of a number of steps which can be targeted by a number of antimicrobial natural product inhibitors. These can be utilised in medicine for the treatment of bacterial infection. One of these steps is catalysed by the membrane protein, Phoshpo-MurNAc-pentapeptide translocase, also known as MraY. Although MraY is the target of a number of known natural products there has been little success in developing inhibitors to be used clinically.

MraY is the site of action of bacteriophage ΦX174 which produces lysis protein E. The RWxxW sequence of E protein is thought to be responsible an interaction between it and the ninth transmembrane helix (TM9) of MraY. Previous work showed that MraY could be inhibited by pentapeptides containing this motif. A dipeptide, NH_2-Arg-Trp-octyl ester which was also based on this motif showed antimicrobial activity, but no inhibition of MraY.

This project aimed to synthesise molecules which were able to exhibit antimicrobial activity and inhibit MraY. A series of dipeptides were synthesised based on RWoct. The side chains of the amino acids were changed for other cationic and aromatic residues. The length of the octyl chain was altered. The series of dipeptides was then tested using a MIC_{50} determination assay and the inhibition by the dipeptides was assessed. All of the peptides showed antimicrobial activity, but none showed inhibition of MraY. Four of the most promising dipeptides were selected to be tested against the ESKAPE pathogens, and this showed some promising activity against these clinically relevant strains.

In order to see inhibition and improve the MIC_{50} a series of peptidomimetics were synthesised. The first series were based on a benzamide backbone. These would allow the installation of a second tryptophan residue, incorporating the entire RWxxW motif. The antimicrobial activity was maintained but still no inhibition of MraY was seen. The second series of peptidomimetics utilised a cyclic triazinedione backbone. This provided a more rigid framework and again antimicrobial activity was seen. The ESKAPE pathogen data from this second series of peptidomimetics was an improvement on that seen for the previous groups of compounds.The data obtained indicated that the compounds synthesised are working via several undetermined mechanisms which differ between compounds in the same series.

CHAPTER 1: INTRODUCTION

1.1 PEPTIDOGLYCAN BIOSYNTHESIS

The bacterial cell wall provides structural integrity which allows the bacteria to maintain their shape at different osmotic pressures. [1] If the cell wall is compromised the bacteria cannot maintain normal function and the cell wall lyses due to osmotic stress. As the cell wall is so pivotal to the function of the bacteria, it is a major target for antibiotic design. The biosynthesis of peptidoglycan has many steps which can be targeted to affect the cell wall stability.

Both Gram positive and Gram negative bacteria have a cell wall which is composed of peptidoglycan. The structural cell wall differences between Gram negative and Gram positive are shown in Figure 1. Despite having a thinner cell wall, Gram negative bacteria have a membrane on the outside of the cell wall which makes them more difficult to penetrate that Gram positive bacteria.

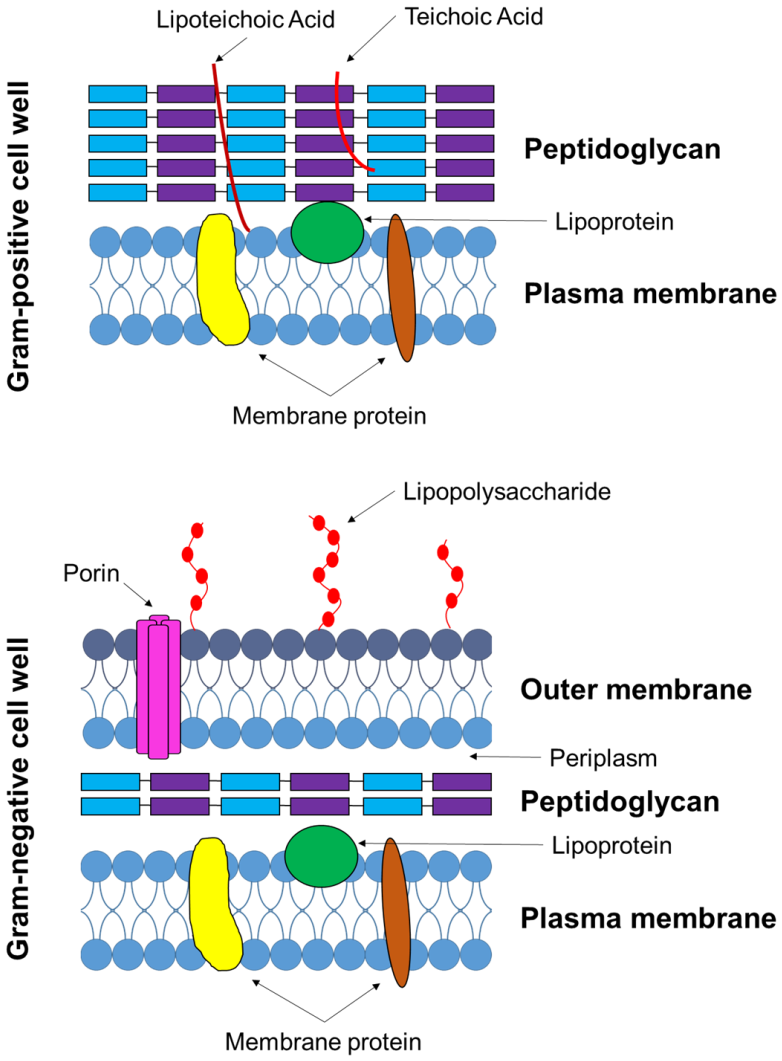

Figure 1: The differences in structure of Gram positive and Gram negative bacteria.

Peptidoglycan is a cross linked polymer of carbohydrates and amino acids. It is a β-1,4-linked polysaccharide consisting of alternating N-acetylglucosamine (GlcNAc) and N-acetylmuramic acid (MurNAc) units.[2] The MurNAc unit's lactyl sidechain is attached to a pentapeptide chain which has the general structure L-Ala-γ-D-Glu-X-D-Ala-D-Ala. The residue X is either L-Lys (found in most Gram positive) or *meso*-diaminopimelic acid (DAP, found mainly in Gram-negative bacteria). The biosynthesis of peptidoglycan is shown in Figure 2, and can be broken down into three steps.

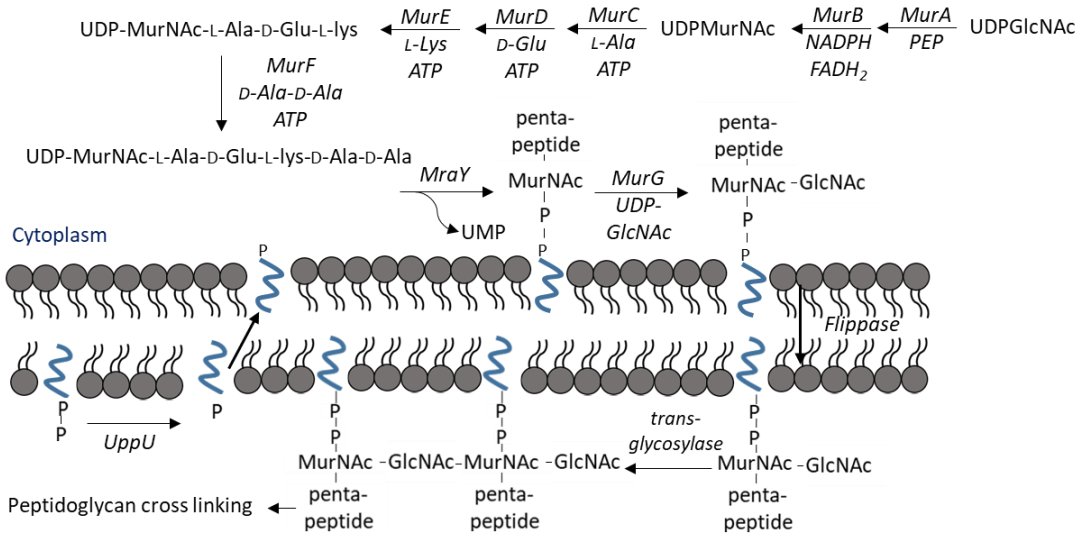

Figure 2: Schematic of peptidoglycan biosynthesis pathway

1.1.1 Synthesis of the peptidoglycan precursors

The synthesis of the components which make up the bacterial cell wall starts in the cytosol. A series of enzymes catalyse the production of the lipid carrier (undecaprenyl phosphate) and the cell wall precursor UDP-MurNAc-pentapeptide.

Undecaprenyl phosphate (C_{55}-P) once synthesised is able to translocate hydrophilic cell wall intermediates across the hydrophobic cellular bilayer.[3] Initially undecaprenyl pyrophosphate (C_{55}-PP), a 55 carbon isoprenoid that is synthesised by undecaprenyl pyrophosphate synthase (UppS), is dephosphorylated at the membrane by undecaprenyl pyrophophatase (UppU), producing C_{55}-P.[4] The synthesis of undecaprenyl phosphate is shown in Figure 3.

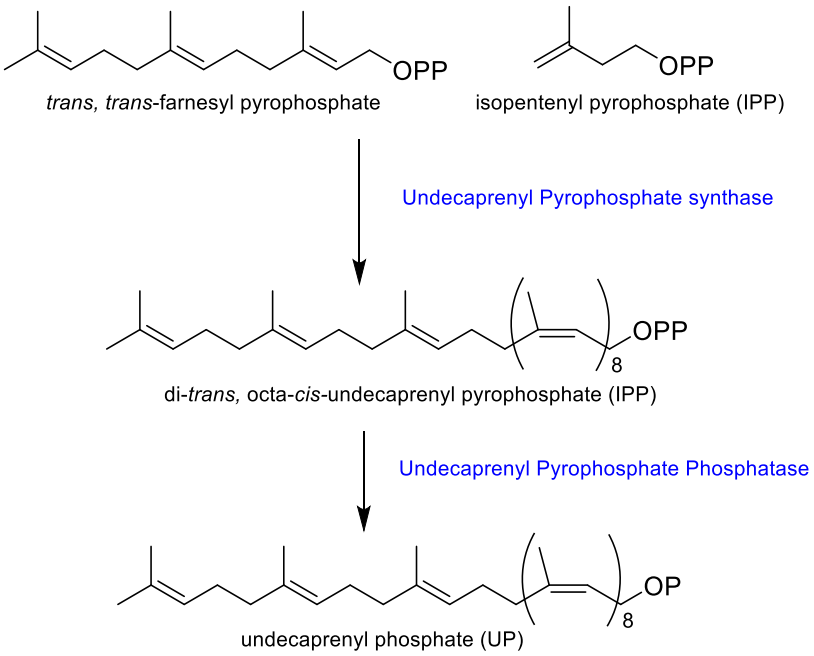

Figure 3: The synthesis of undecaprenyl phosphate (UP). Enzymes are shown in blue.

The second substrate synthesised in the cytoplasm is UDP-Mur-NAc-pentapeptide. Its synthesis is catalysed by the enzymes MurA-MurF from the starting material UDPGlcNAc. This cascade of enzymes is highly conserved across all bacteria. The biosynthetic pathway for UDP-Mur-NAc-pentapeptide is shown in Figure 2, and summarised in Figure 4.

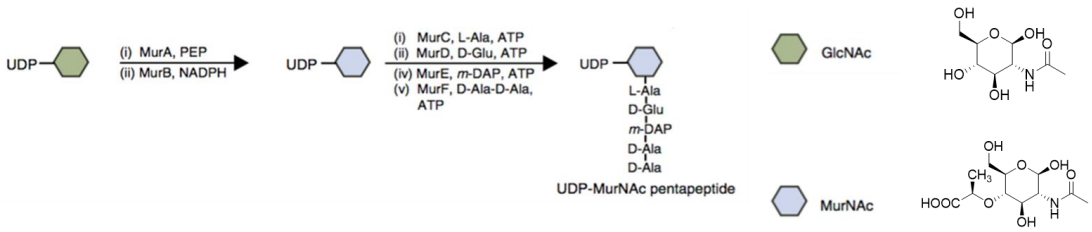

Figure 4: UDPMurNAc-pentapeptide biosynthesis [5]

1.1.2 Biosynthesis of the peptidoglycan monomers

The second stage of cell wall biosynthesis is catalysed by phosphor-MurNAc-pentapeptide translocase, commonly referred to as MraY or translocase 1. MraY is an integral membrane protein which catalyses the reversible transfer of phospho-MurNAc-pentapeptide to the lipid carrier undecaprenyl phosphate (C_{55}-P) to give

Lipid I (undecaprenyl-pyrophosphoryl-MurNAc-pentapeptide).[1,6] The by-product of this reaction is uridine 5'-monophosphate (UMP). This enzymatic reaction is shown in Figure 5.

In the following step, N-acetylglucosamine (GlcNAc) is incorporated into the lipid I intermediate. This is catalysed by the final Mur enzyme, glycotransferase MurG. This transfer gives GlcNAc-β-(1,4)-undecaprenyl-pyrophosphoryl-MurNAc-pentapeptide, also known as lipid II. The by-product is uridine diphosphate (UDP).

Lipid II is transferred across the membrane, by what is thought to be a flippase enzyme. Lipid II is the monomeric building block of peptidoglycan.[2]

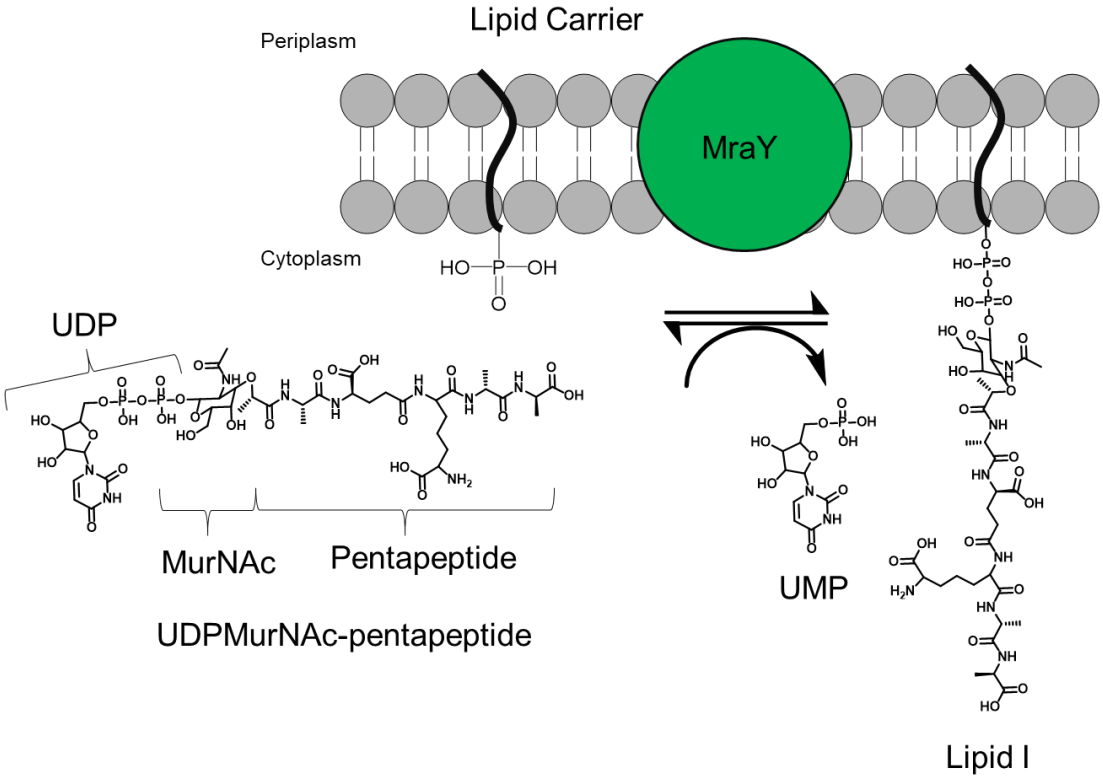

Figure 5: The formation of lipid 1 a reaction catalysed by MraY.

1.1.3 Polymerisation to form peptidoglycan

Lipid II is polymerised to form peptidoglycan by penicillin binding proteins (PBPs).[7] The polymerisation process is catalysed by glycosyltransferases which form glycan

chains and transpeptidases which form peptide cross links. (Shown in Figure 6). The polymerisation continues as further monomers are flipped across the membrane.

The transpeptidation step is the last to occur.[8] These reactions catalysed by transpeptidases cross-link the neighbouring monomers by the pentapeptide chains. The ε-amino group of the residue at the third position of the pentapeptides chain (Lys/DAP), and the D-Ala residues at the fourth position of a neighboring pentapeptides are subjected to transpeptidation catalysed by penicillin binding proteins (PBP).

This stage of the peptidoglycan biosynthesis is the step which varies the most between species, particularly between Gram negative and Gram positive bacteria. The differences in this step are responsible for differences in the rigidity and strength of the cell wall between species.

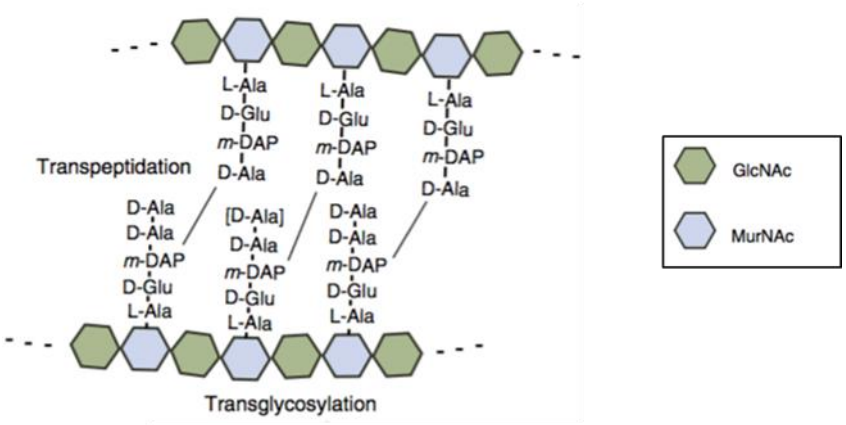

Figure 6: Transpeptidation and transglycosylation in the formation of peptidoglycan.[2]

1.1.4 Antimicrobials targeting cell wall biosynthesis

Several steps of the cell wall biosynthesis pathway are known to be inhibited by natural products, and some examples of these are discussed in this section. This inhibition ultimately leads to cell death. Studying these natural product inhibitors provides a great platform for drug discovery.

Fosfomycin, discovered in 1969, inhibits the synthesis of the cell wall precursor UDPMurNAc.[9] The target of fosfomycin is MurA and its structure is shown in Figure 7. MurA ligates phosphopenol pyruvate (PEP) to the 3'hydroxyl group of

UDPGlcNAc. Fosfomycin is a PEP analog which is able to inhibit MurA by the alkylation of a cysteine residue found within the active site. Sold under the brand name monurol, fosfomycin is commonly used in the treatment of bladder infections.

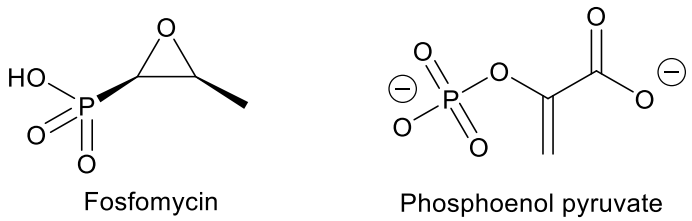

Figure 7: The structure of fosfomycin and phosphoenol pyruvate.

Bacitracin, which was first isolated from *Bacillus licheniformis* in 1945, disrupts the cell wall of Gram positive bacteria by inhibiting UppU, preventing the dephosphorylation of C_{55}-isoprenyl pyrophosphate.[10] Bacitracin is made up of several related cyclic peptides with bacitracin A being the most prevalent. Bacitracin A is shown in Figure 8. It is commonly used in topical medication to prevent skin and eye infections. Resistance to bacitracin is seen in MRSA, likely caused by the drugs overuse in the farming industry.[11]

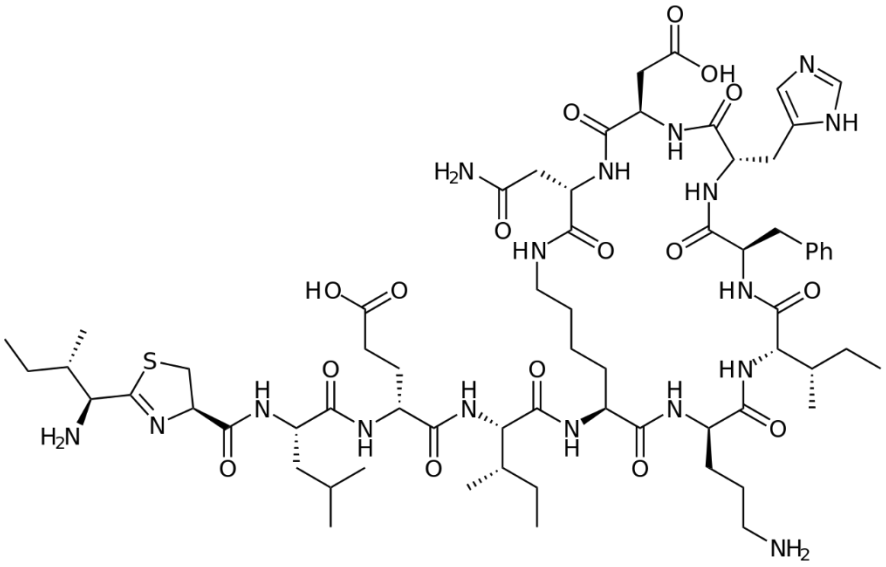

Figure 8: The structure of cyclic peptide bacitracin A.

The class of uridyl natural products inhibitors of MraY, such as tunicamycin, will be discussed in section 1.2.3. These inhibitors prevent the formation of lipid I.

Ramoplanin is a glycolipodepsipeptide antibiotic which inhibits MurG by complexation of lipid I, and so prevents the formation of lipid II.[12] It is used for the treatment of antibiotic-resistant *Clostridium difficile* infection of the gastrointestinal tract after its development was fast-tracked by the US FDA. The structure of ramoplanin A2 is shown in Figure 9.

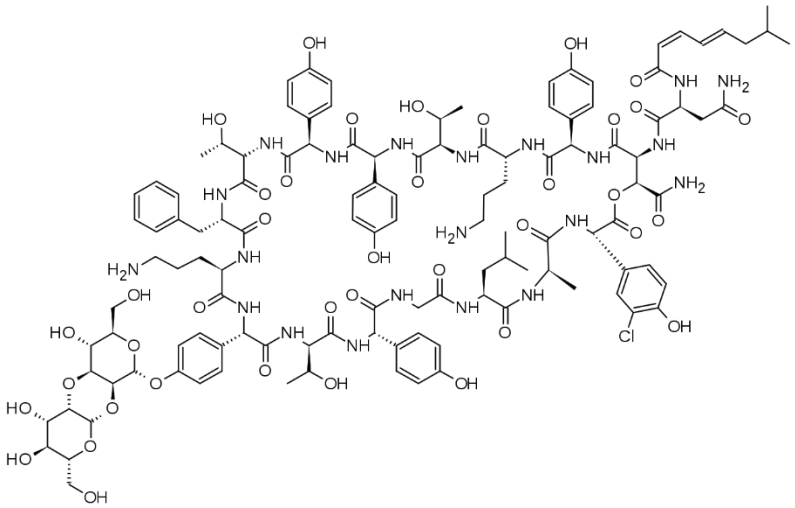

Figure 9: The structure of a glycolipodepsipeptide antibiotic ramoplanin A2.

Penicillins are a well-known class of β-lactam containing antibiotics which inhibit the formation of cross links within the peptidoglycan (Figure 10). Penicillin does this through the inhibition of the penicillin binding protein DD-transpeptidase.[13] Many bacteria have and continue to develop resistance to these compounds due to extensive usage.

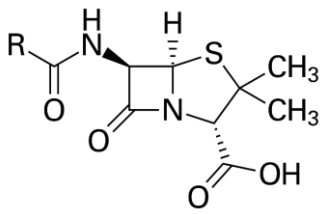

Figure 10: The central structure of penicillin, where the R group varies between compounds.

Moenomycins are a group of phosphoglycolipid antibiotics which are able to bind to bacterial transglycosylases, preventing the extension of the cell wall glycan chain and therefore destabilizing the peptidoglycan.[14] These are the only known compounds which are able to inhibit transglycosylases and no known resistance to them has emerged, making them promising antibiotics. Moenomycins are not currently used in human medicine but are commonly added to cattle feed.[15,16] The general structure of this family of antibiotics is shown in Figure 11.

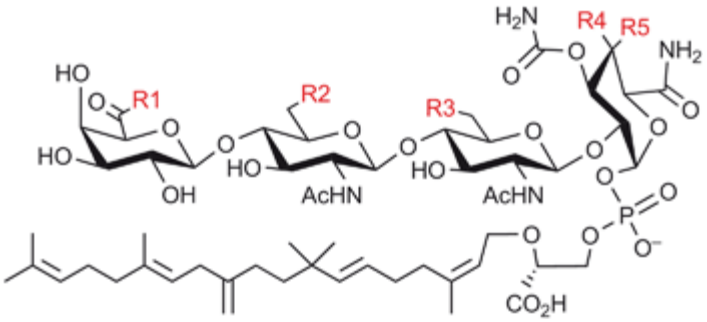

Figure 11: The core structure of the moemycin antibiotic group.

Vancomycin is an antibiotic used to treat many complicated infections caused by MRSA.[17] Vancomycin forms hydrogen bonds with the D-Ala-D-Ala portion of the cell wall pentapeptide. This results in the inhibition of transpeptidases and cell wall cross links cannot be formed.[18,19] Bacteria which have developed resistance against vancomycin have a D-lactate in place of the last D-Ala and this prevents the binding of vancomycin. The structure of vancomycin is shown in Figure 12.

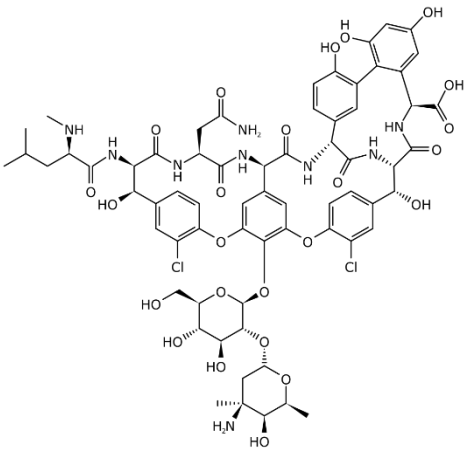

Figure 12: The structure of vancomycin

1.2 TRANSLOCASE MraY

1.2.1 Catalytic mechanism of MraY

Translocase MraY is an integral membrane protein of very low natural abundance, which catalyses the reaction between UDP-MurNAc-pentapeptide and the undecaprenyl phosphate lipid carrier in the presence of Mg^{2+}.[1]

The catalytic mechanism could either be a one step or two step reaction.

One proposal is a single-step phosphotransfer at the β-phosphate of the UDPMurNAc-pentapeptide, via a complex of MraY, UDPMurNAc-pentapeptide and undecaprenyl phosphate.[20]

Alternatively, a two-step mechanism has also been proposed, including an attack by an active site nucleophile. The two-step mechanism suggests UMP is lost to yield a covalently bound phosphate-UDPMurNAc-pentapeptide intermediate, which is then attacked by undecaprenyl phosphate to yield lipid intermediate I.[21]

There are three aspartic acid residues found in the active site which are highly conserved (Asp115, Asp116, Asp267 in *E. coli* MraY).[1] These three residues are the only completely conserved nucleophilic residues in the MraY sequence. Mutation studies showed the importance of these nucleophilic residues which when replaced render the enzyme inactive.[1] One of the proposed roles for the aspartic acids suggested that two of them may form a binding site for the Mg^{2+} cofactor of MraY. The third could then act as a catalytic nucleophile at the active site. Other residues at the active site have also been found to be important for activity, but there is more variation between species.

1.2.2 Crystal structure of MraY

In 2013 it was reported that *A. aeolicus* MraY ($MraY_{AA}$) had been expressed, purified and crystallised by Chung *et al.* and the final model refined.[1] (Figure 13). It was shown that MraY crystallises as a dimer which has an oval shaped tunnel at the interface. The protomers contain ten transmembrane helices (TM1-TM10) linked by four periplasmic loops and five cytoplasmic loops. Both the C- and the N- terminus of MraY are found on the periplasmic face of the membrane. TM9 has a substantial kink in it breaking the helix in to two (TM9a and TM9b). TM9b is circled in yellow in Figure 13.

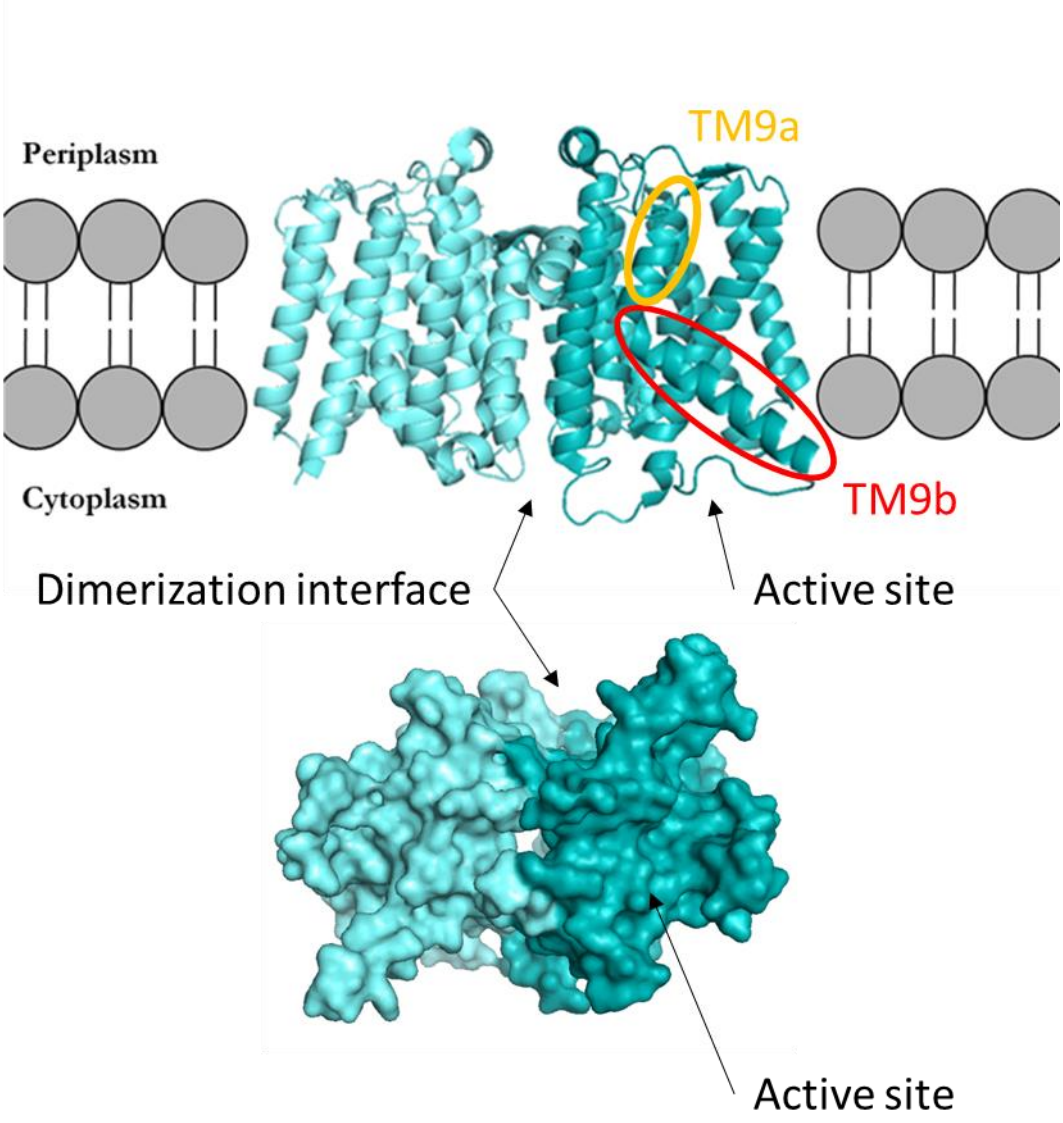

Figure 13: TOP: The MraY dimer showing TM9b circled in yellow. BOTTOM: The surface representation of the MraY dimer, showing the channel formed at the centre. (PDB: 4J72)

Lloyd *et al.* reported the presence of the three conserved nucleophilic aspartate residues (Asp115, Asp116, and Asp267), found on the cytoplasmic face of the membrane that are essential for the catalytic activity of MraY.[22] It was then found by Chung *et* al. that there is also a catalytically active histidine residue (His324) in the active site.[1] There is a triad of histidine residues (His324, His325, and His326; HHH motif) conserved in the bacterial sequences of the polyprenylphosphate N-acetylhexosamine 1-phosphate transferase (PNPT) superfamily, which are positioned on loop E. They also challenged the previously proposed roles of the aspartate residues,

and it is now suggested Asp265 interacts with Mg^{2+} rather than acting as nucleophile. Bouhss proposed that Asp^{117} could in fact deprotonate the phosphate moiety of the lipid carrier.[6] The relevant active site residues are shown in Figure 14.

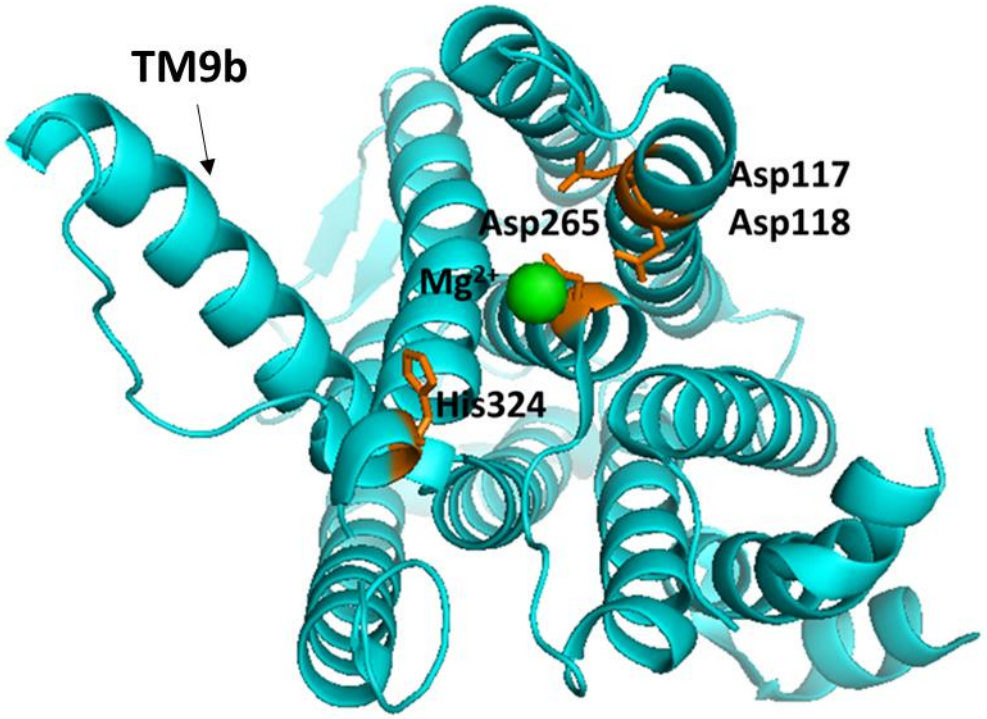

Figure 14: The active site of MraY with the residues consider to be important shown in orange and the Mg^{2+} ion shown in green.[23](PDB: 4J72)

The surface representation of MraY shows a groove that extends from TM9b to the active site where Asp^{117} is located, which could accommodate the lipid chain which is longer than the depth of the membrane. This is shown in Figure 15.

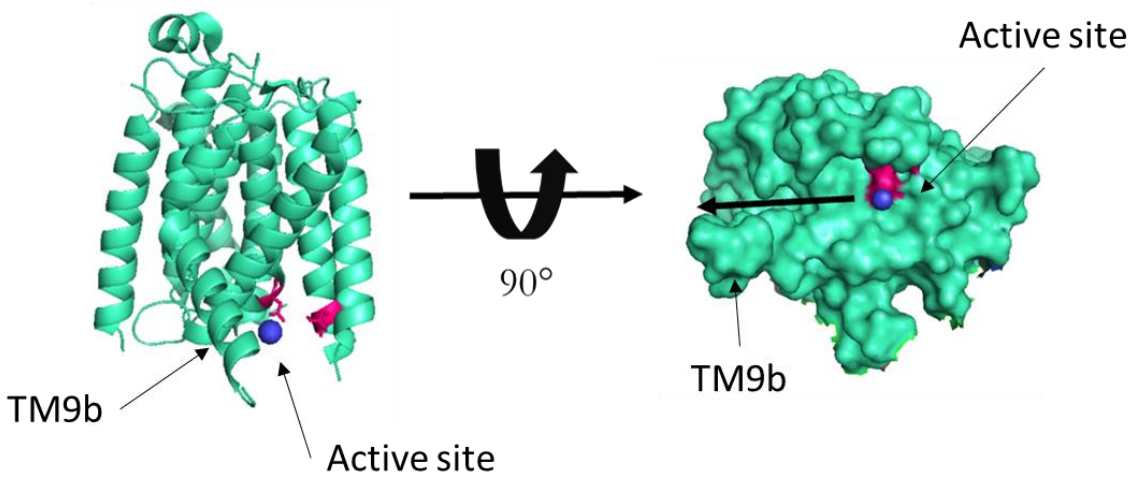

Figure 15: The groove formed by TM9b shown on with a black arrow on the surface representation of the MraY monomer. The catalytic aspartate residues are shown in pink and the Mg^{2+} ion is shown in dark blue. (PDB: 4J72)

1.2.3 Natural product inhibitors

It is well known that natural product inhibitors provide a great resource for the development of new antibiotics. A sub group of natural product inhibitors of MraY are called the uridylpeptide natural product family (or uridyl peptide antibiotics-UPAs). UPAs have shown *in vivo* efficacy against a number of pathogenic bacteria, which include vancomycin-resistant *Enterococcus* (VRE) and methicillin resistant *Staphylococcus aureus* (MRSA).[24–26]

There are several known groups of UPAs, which have the potential to form new groups of antimicrobial agents.[27] The groups of UPAs can be split into pacidamycins (also containing the mureidomycins, napsamycins and sansanmycins), muraymycins, caprazamycins (also containing lipidomycins), capuramycins, and tunicamycins. Their exact mechanism of action is unknown and because of their large size it is unclear how they reach the active site of MraY. This said mureidomycin A and lipidomycin B were shown to be slow binding inhibitors and tunicamycin a reversible inhibitor of MraY.[28,29] Figure 16 shows some examples of UPAs. It is possible that the pore which is seen at the center of the MraY dimer could provide an entry route to the cytoplasmic active site (shown in Figure 13).

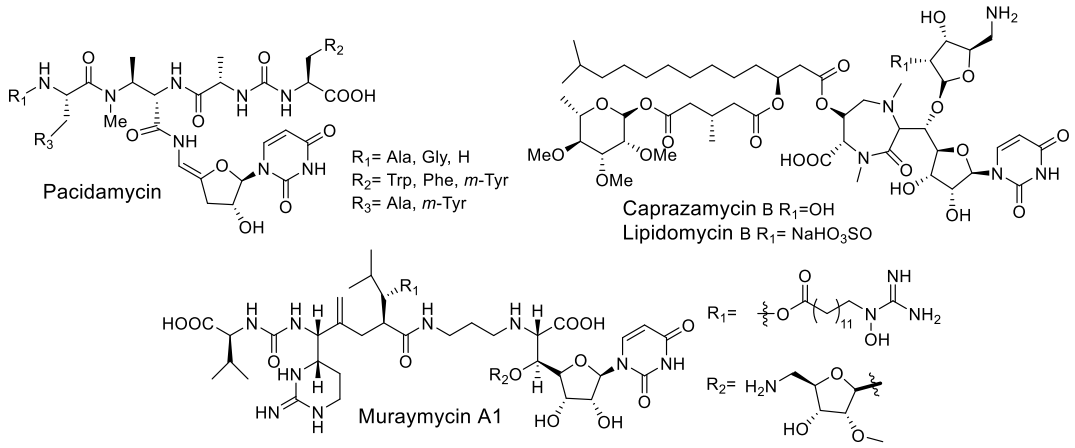

Figure 16: Examples of UPAs

The rapid action of UPAs and their broad spectrum of activity, coupled with microorganisms' low development of resistance against them is promising. Despite this, there are still issues with synthesis, bioavailability, metabolic stability, the route of administration and the cost of production. Recently synthetic analogues of sansanmycin UPAs have been synthesised and show promise for the treatment of TB.[30]

In 2016 and 2017 new co-crystal structures of MraY complexed with tunicamycin and muraymycin D2 were published.[31,32] MraY from the pathogenic Gram-positive bacterium *Clostridium bolteae* ($MraY_{CB}$) was crystallised in complex with tunicamycin and MraY from *Aquifex aeolicus* ($MraY_{AA}$) in complex with muraymycin D2 (MD2). The structures of these uridyl inhibitors are shown in Figure 17. The two crystal structures are shown in Figure 18.

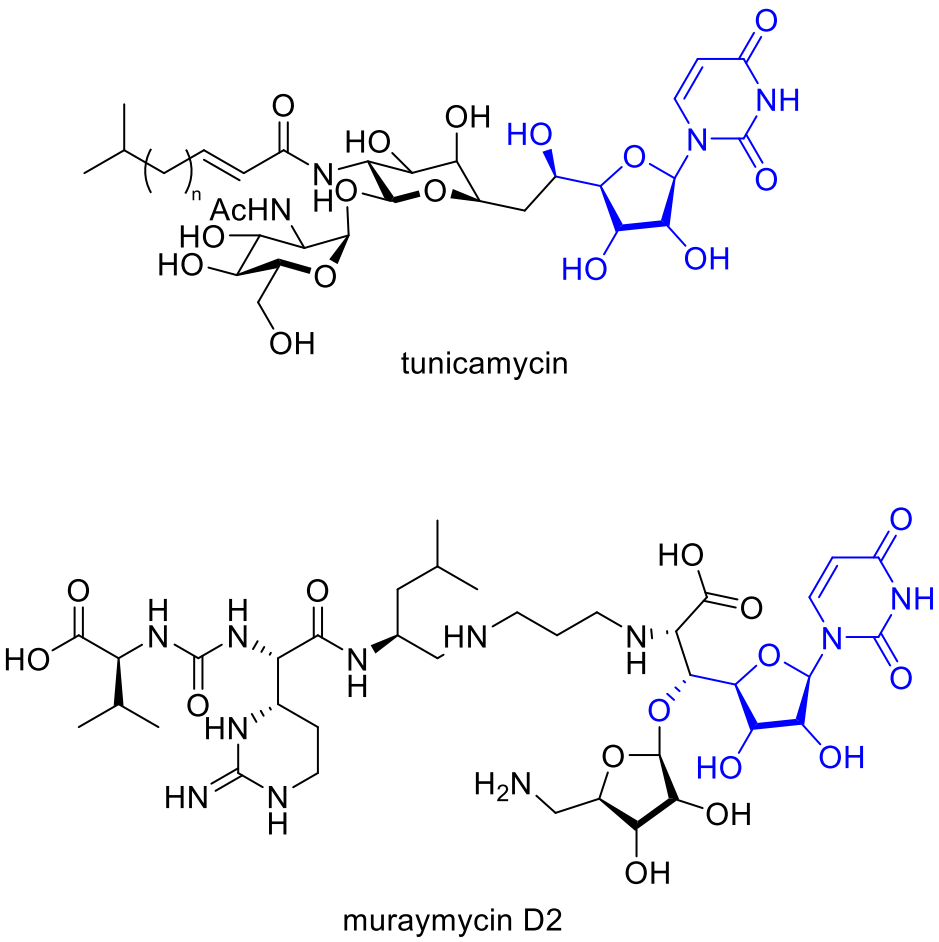

Figure 17: The structures of tunicamycin and muraymycin D2 (MD2). The uridine moiety is highlighted in blue.

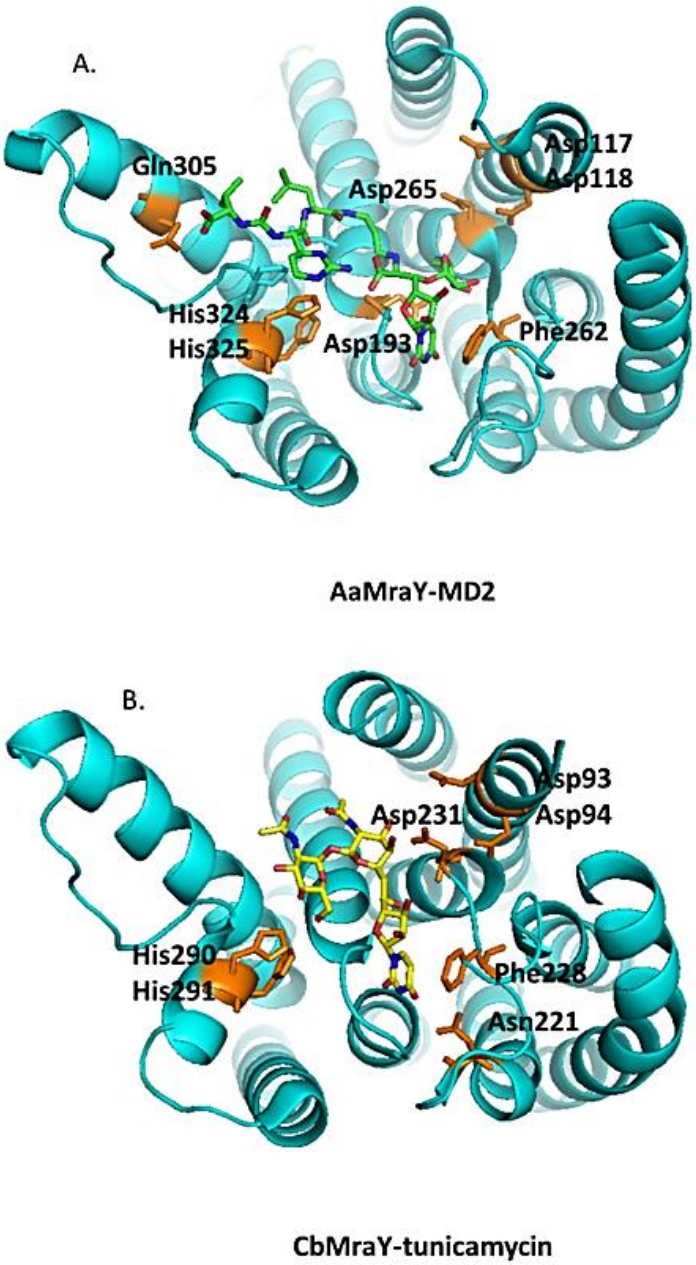

Figure 18: The structures of MraY-Ligand complexes, which show the location of the active site binding interactions. A. MD2 complex B.[31] Tunicamycin complex.[23] (PDB: 5JNQ and 5CKR)

Both crystal structures show that a significant change in active site geometry occurs compared to the previous crystallised apo $MraY_{AA}$, caused by a notable conformational change which occurs on binding. TM9b rotates away from the active site and this can be seen in Figure 19. This leads to a widening of the active site and the HHH motif. The conformational plasticity which the enzyme is able to exhibit may explain how the active site is able to accommodate such a diverse range of inhibitors. The two inhibitors occupy a similar space with the uracil moiety found wedged in a small pocket participating in π-π stacking interactions. In a uridine adjacent pocket the aminoribose moiety participates in hydrogen bonding via its amino group. In the bonding of tunicamycin the conserved HHH motif interacts with the 4'- and 6'-hydroxyl groups of the GlcNAc. The tunicamine hydroxyl group was found to interact with one of the catalytic Asp residues (Asp231). MD2 differs in its binding motif as it does not bind with several of the catalytic residues which were considered to be important, including the three aspartic acid residues. The acyl chain of tunicamycin cannot be seen in the crystal structure due to its flexibility, however the structure supports that it would fill the groove shown in Figure 15.

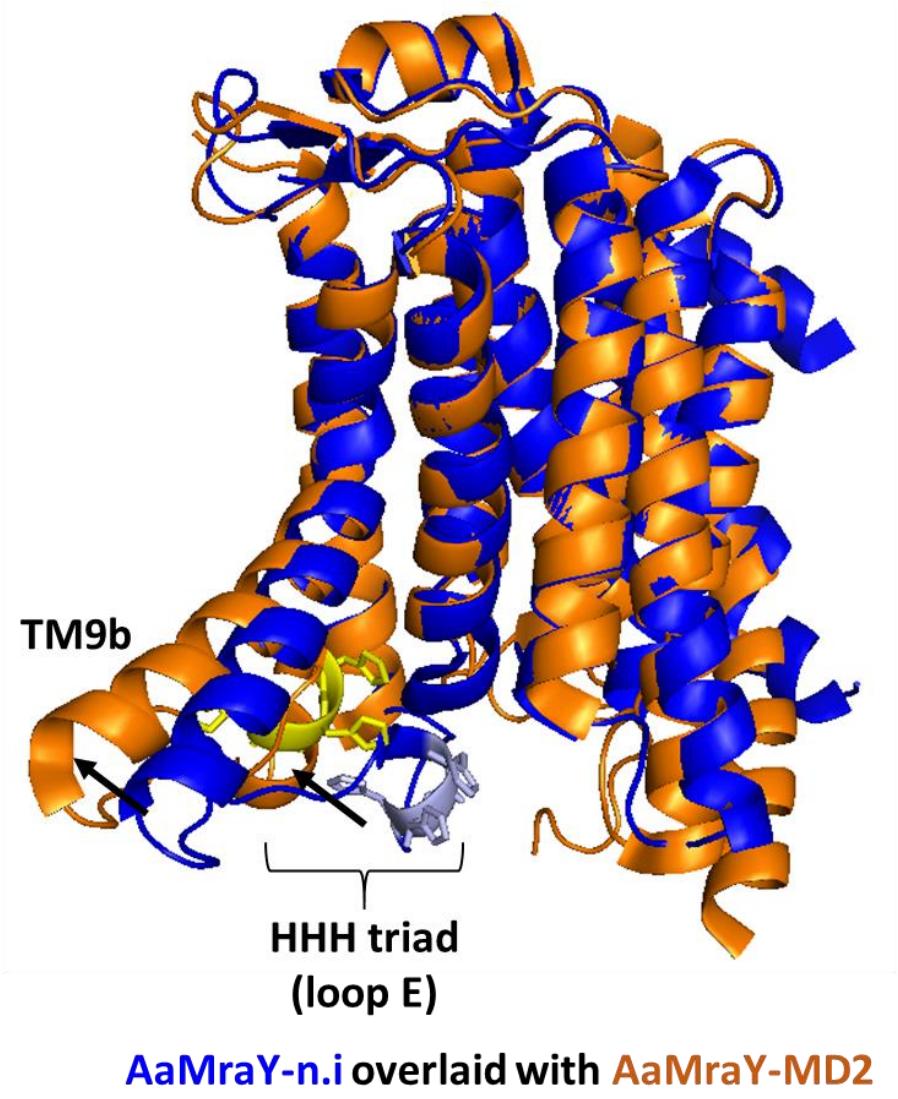

Figure 19: Blue is the Apo MraY and orange shows the complex between MraY and MD2. The two structures are overlaid to show the movement of TM9b when an inhibitor is bound to the active site. The movement of the HHH triad is shown. [23] **(PDB: 5CKR)**

In 2019 Mashalidis *et al.* published three further crystal structures of MraY-inhibitor complexes.[33] This time the inhibitors were the uridyl containing carbacaprazamycin, capuramycin and 3'hydroxymureidomycin. These are potent inhibitors of MraY and the structures are shown in Figure 20. As with MD2, *Aquifex aeolicus* ($MraY_{AA}$) was used.

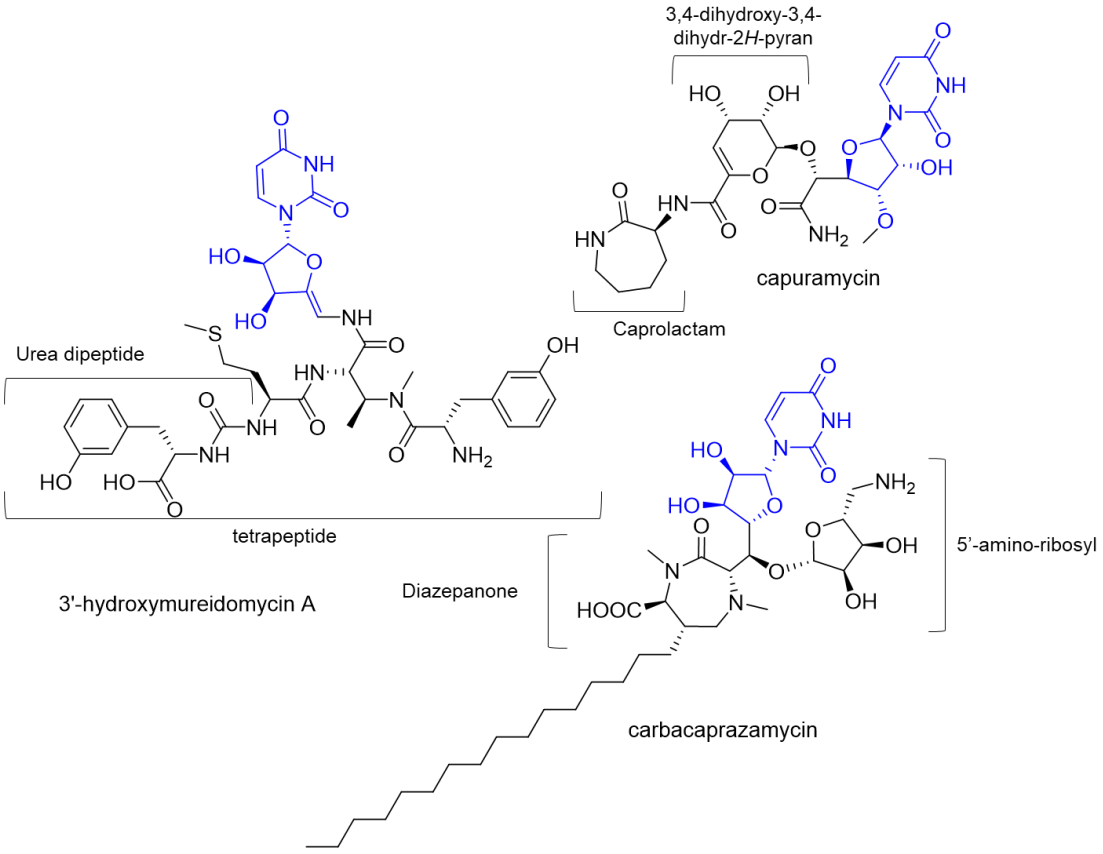

Figure 20: The structures of the three natural product inhibitors co-crystalised with MraY. Uridine shown in blue.

The binding of carbacaprazamycin uridyl moiety and the aminoribose is similar to those of tunicamycin and MD2. The carboxylate group is shown to form a hydrogen bond with H325 of the HHH motif. As with tunicamycin the alkyl chain is presumed to compete with the lipid carrier (C55-P) lying in the groove shown in Figure 15, and is therefore critical for activity.[34] The tunicamycin-MraY complex did not demonstrate this but it can be seen in the carbacaprazamycin-MraY complex and is shown in Figure 21.

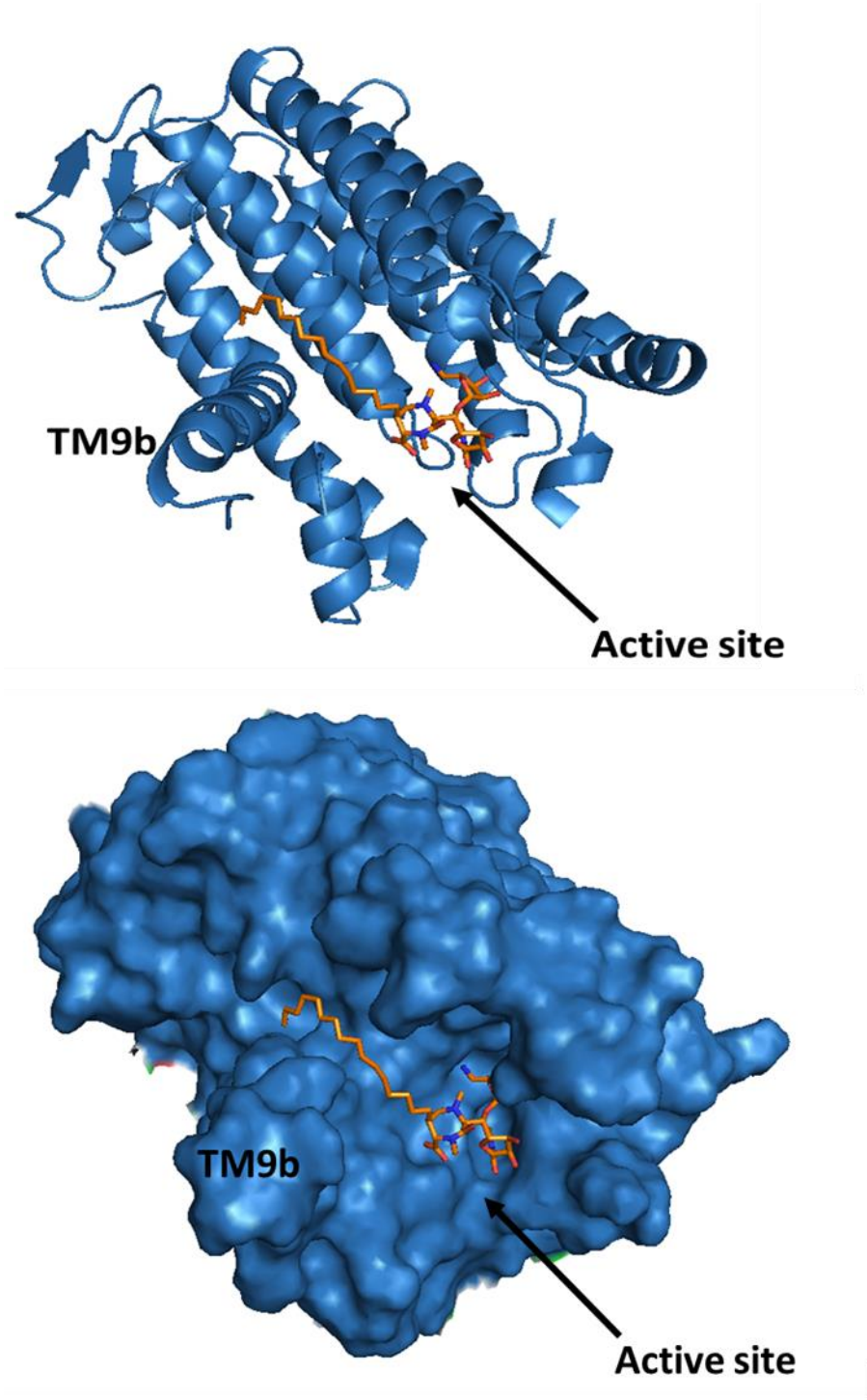

Figure 21: The alkyl chain of caprazamycin shown in TM9 groove. Both images shown the same structure and orientation with the bottom picture on the showing a surface representation. (PDB: 6OYH)

Capuramycin binds in the uridine and uridine adjacent pockets. The caprolactam group binds at a site which is not seen with the other inhibitors. It is on the cytoplasmic face of the enzyme where the caprolactam sits in a shallow hydrophobic pocket. Replacing the caprolactam group with a smaller group such as a hydroxyl leads to a dramatic reduction in inhibitory activity.[35] This binding pocket is shown in Figure 22.

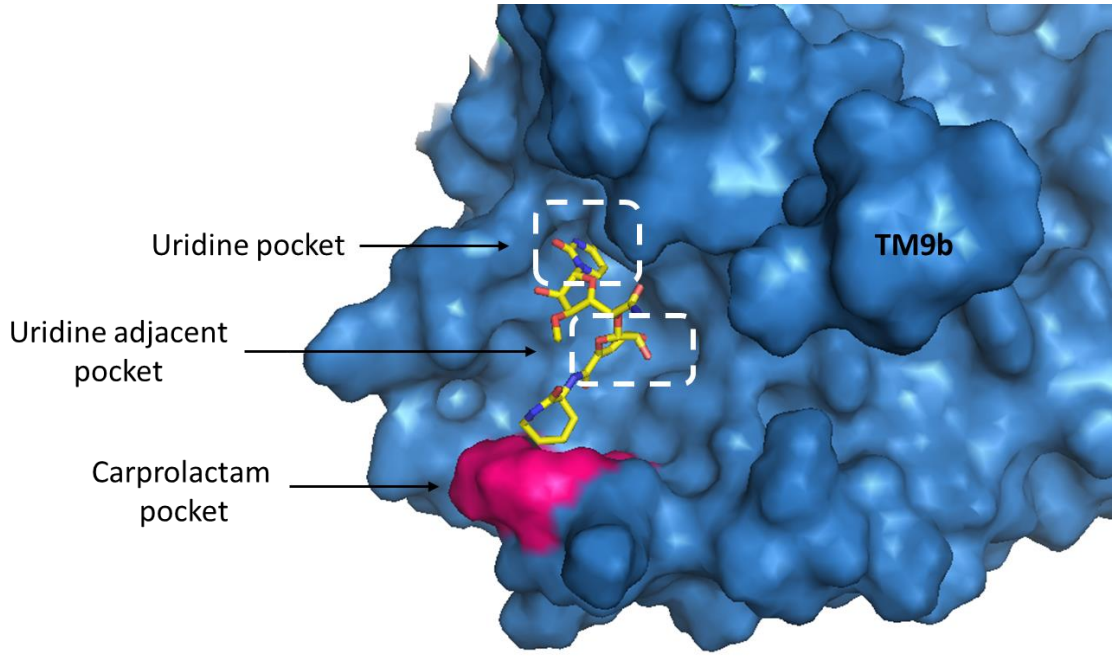

Figure 22: The active site capuramycin complex showing the caprolactam binding site in pink. K121, L122 and K125 are the residues (highlighted in pink) which participate in the binding pocket interactions. (PDB: 6OYZ)

The mureidomycin features a tetrapeptide containing a *meta*-tyrosine which is shown to bind in the uridine adjacent pocket via a hydrogen bond with the hydroxyl group. The urea group in the tetrapeptide binds in the TM9b/loopE pocket, similarly to the urea group seen in MD2. This is shown in Figure 23.

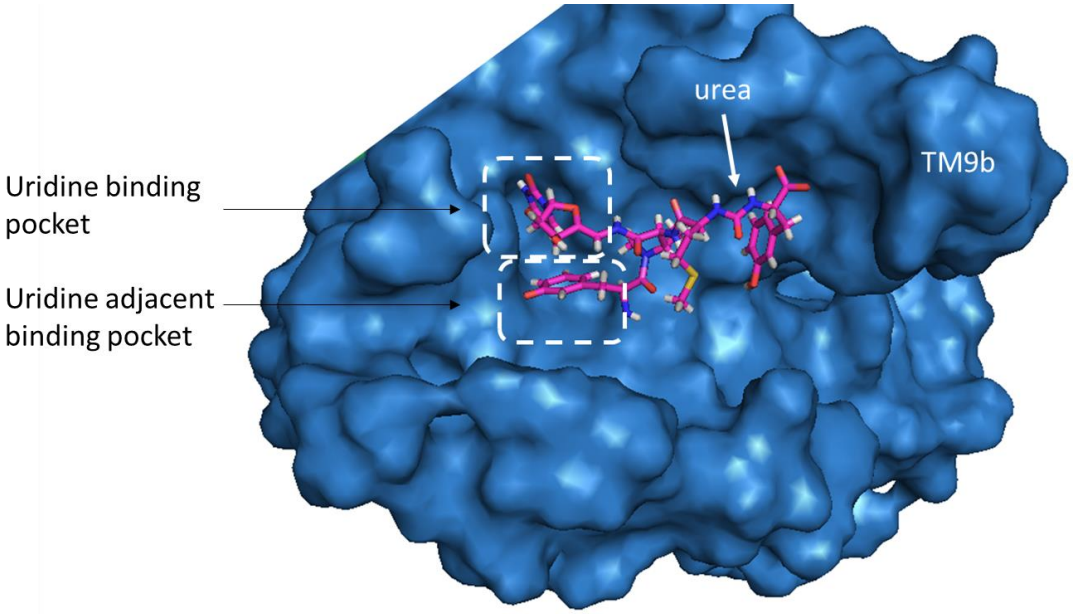

Figure 23: The mureidomycin-MraY complex. (PDB: 6OZ6)

1.3 BACTERIOPHAGE ΦX174 - E PROTEIN

Bacteriophage means "bacteria eater" as they destroy the host cell. They are viruses which infect bacteria. Double stranded DNA bacteriophages are generally composed of two genes which enable them to cause host cell lysis. These two genes code for endolysin and holin. Holin allows endolysin to cross the cytoplasmic membrane and gain access to the cell wall.[36] Endolysin is an enzyme which is able to degrade the cell wall. Once the cell wall has been degraded the cell cannot maintain osmotic pressure and lyses. Small single stranded DNA phage such as ΦX174 in contrast have one single lysis gene *E*.[37] Expression of *E* causes the lysis of *E. coli*.[38,39] Protein E is made up of a hydrophobic transmembrane domain in the N- terminal region and a positively charged soluble domain found near to the C- terminal.[40] The N-terminal 35 residues making up the transmembrane domain are thought to be responsible for causing lysis.[41] The C terminal can be replaced with LacZ without effecting cell lysis, demonstrating that the transmembrane region is of key importance for cell lysis.[42]

There is no evidence to suggest that the E protein is able to degrade the cell wall, and so its mechanism of facilitating cell lysis must be distinct from direct degradation of the cell wall. Due to its simple structure it is unlikely to have enzymatic activity and E-mediated lysis requires cell growth. The exact mechanism by which lysis occurs is unknown and many models have been proposed. Lubitz and co-workers proposed the E protein is able to form "transmembrane tunnels" which then release cytoplasmic contents, which include the progeny virions, but there is little genetic evidence to support this model. [43]

1.3.1 Target of E protein

In order to identify the host genes required in E-mediated lysis, Young and coworkers isolated recessive mutations in the host gene *slyD* which are able to block the effects of E.[44] The gene *slyD* encodes an FK506 binding protein-type peptidyl-prolyl *cis-trans* isomerase (PPIase).[45] It is thought that the *slyD* mutant is able to block accumulation of protein E in the membrane, and based on this it is proposed that SlyD is involved in membrane folding and/or membrane insertion. This proposal fits with the role of PPIase which are associated with protein folding.[46,47] Despite playing a role in the lysis mechanism of protein E, *slyD* is not a target of the bacteriophage.

Bernhardt *et al.* established in 2000 that *E. coli* MraY is the site of action of lysis E protein from bacteriophage ΦX174.[46] Lysis resistant mutations (F288L and ΔL172) were found in MraY genetic mutants. This resistance strongly suggests that E protein is able to induce lysis by inhibiting cell wall biosynthesis. There are two proposals for the role of *slyD*. Firstly it is thought it could allow the accumulation of E, possibility by assisting with folding and stability during membrane insertion. Secondly it is possible that slyD is able to promote the interaction between E and MraY. This is summarised in Figure 24.

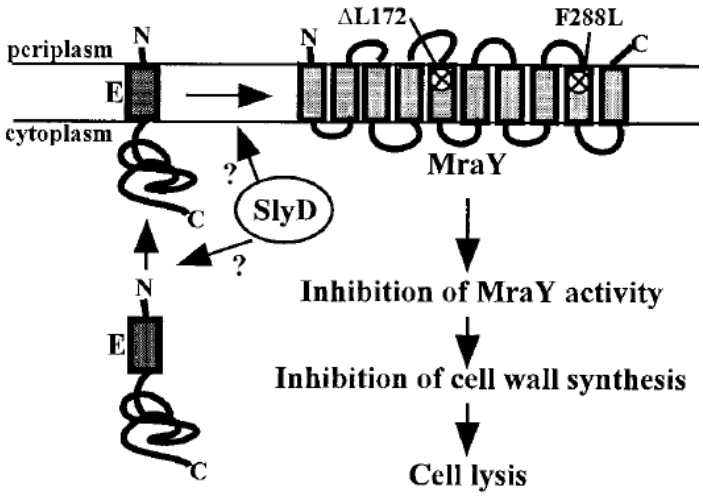

Figure 24: Proposed model for the mechanism of E-mediated cell lysis.

From this it was concluded that the inhibition of MraY by protein E is through a protein-protein interaction distant from the active site. Cell lysis requires a peptidyl-prolyl isomerase SlyD, however the exact role of SlyD is unknown. SlyD was shown by Mendel *et al.* to have a strong interaction with E protein.[42] Later Bernhardt *et al.* proposed that SlyD was able to protect E protein from proteolysis which was consistent with the data collected by Mendel *et al*. From this it was proposed that this protection allowed E protein to disrupt protein-protein interactions with MraY which are essential for the function of MraY.[47] This is shown in Figure 25.

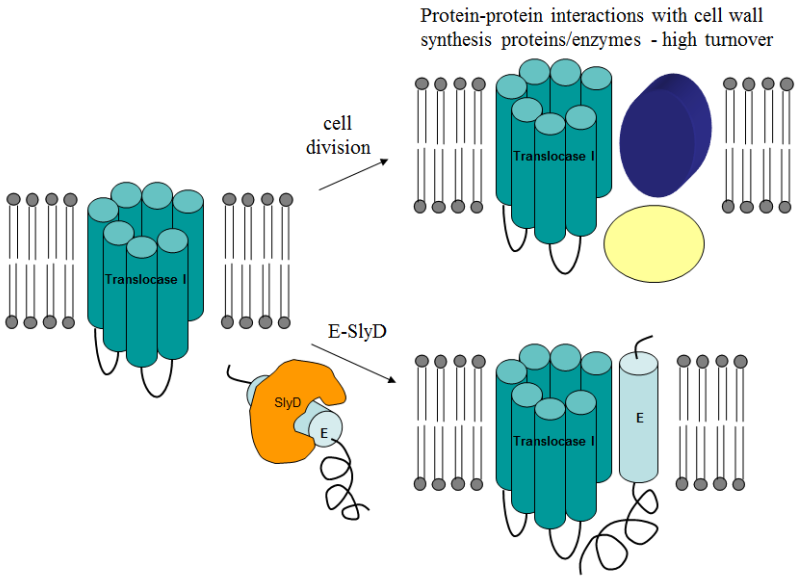

Figure 25: The proposed function of slyD in the E-MraY interaction site.[42]

1.3.2 Protein interaction site with MraY

The 37-residue transmembrane domain was synthesised (E_{pep}) by Mendel *et al.* It was concluded that E_{pep} could inhibit particulate MraY but not detergent solubilized MraY. The mutation F288L in MraY causes resistance to protein E. Phe288 is found in TM9a, close to the exterior face of the membrane, this gives some indication of the interaction site. The fluorescence assay alone is insufficient to conclude that Epep interacts with MraY. Assays such as a pull down assay could be used to definitively conclude this claim.

Based on the fluorescence assay data, Rodolis *et al.* proposed an interaction site between E protein and TM9 of MraY (Figure 26).[48] An alpha-helical wheel based model of TM9 was aligned with the known alpha-helix transmembrane domain of protein E. The proposed model revealed that it was possible for π-stacking interactions to occur between Phe288 and two tryptophan residues (Trp4 and Trp7) found in protein E. It is possible that the guanidinium side chain of Arg3 of E protein could also form favourable hydrogen bonding interactions with Glu287 found in the TM8-TM9 turn of MraY. Glu287 is conserved in all MraY sequences. It is also conceivable that π-cation interactions are occurring between Arg3 and Phe288. From this model the motif Arg-Trp-x-x-Trp (where x is any amino acid) is proposed as an interaction site for Glu287 and Phe288.

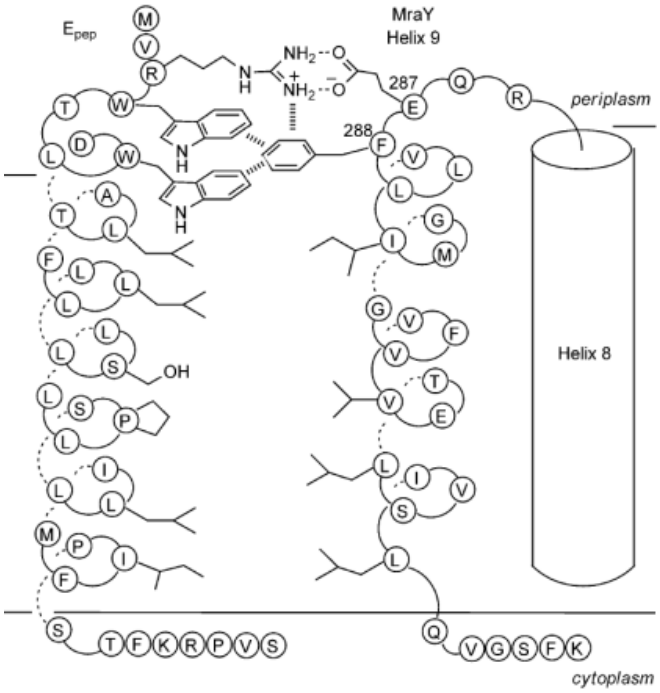

Figure 26: The proposed interaction site between MraY TM9 and E protein.[48]

1.3.3 RWxxW containing antimicrobials

The Arg-Trp-x-x-Trp motif can been seen in other microvirdae bacteriophages related to ΦX174 as well as in several cationic antimicrobial peptides.[48] The RWxxW motif is seen close to the N- or C- terminus of several naturally occurring cationic antimicrobial peptides which are shown in Table 1. Arginine and tryptophan rich peptides are known to have antimicrobial effects and this will be discussed in the next section.[27] Hancock and co-workers have also observed high activity in peptides where Arg and Trp predominate.[49]

Peptide	Sequence
ΦX174 E protein	MVRWTLWDTLAFLLL
Indolicidin	RRWPWWPWKWPLI
MX226	KRRWPWWPWRLI
HHC36	RRWWKWWRK
Lactoferricin	FKCRRWQWRMKKLGAP

Table 1: The sequence similarities between E protein and known antimicrobial peptides.

1.4 ANTIMICROBIAL PEPTIDES

Due to the increasing issue caused by the emergence of antimicrobial resistance there has been an increase in research effort dedicated towards the development of antimicrobial peptides (AMPs).[50] AMPs are produced in the mammalian immune system and in a wide range of plants and insects. This is partly due to their low toxicity and broad spectrum of activity attributed to their bacteriolytic abilities.[51,52] In addition to this, a significant advantage of AMPs over conventional antibiotics is their imperviousness to resistance. Despite this there has been limited success in the development of AMPs that are suitable for clinical use. This is due to a number of reasons including: the high manufacturing costs associated with AMPs, as well as low activities and cytotoxicity toward mammalian cells.[53]

AMPs have multiple target, in contrast to conventional antibiotics which have a single target, and hence for resistance to occur it would be necessary for modifications to arise at all the sites of action.[54] Features of naturally occurring AMPs are often incorporated into the design of new synthetic AMPs and antimicrobial agents. AMPs are known to have intracellular targets such as enzymes, causing the inhibition of cell wall synthesis and protein synthesis, and some are able to interact with RNA and DNA.[55]

1.4.1 Arg-Trp containing antimicrobial peptides

Antimicrobial peptides can be split into several categories. One of these categories are cationic peptides which are rich in arginine and tryptophan residues.[27,56–59] Several subsections of the AMP family are made up of groups of peptides which are rich in particular amino acids.[60] The success of the Arg and Trp containing peptides stems from the physical properties of these two amino acid residues. Examples of peptides found in this group include tritrpticin and indolicidin.[61,62] The arginine residues, which in physiological conditions are always cationic, are able to interact in π-cation interactions and electrostatic interactions with the anionic constituents of the lipid bilayer. This creates specificity, as the peptides can act preferentially with bacteria over the neutral mammalian cell membrane. The sidechain of arginine is also able to participate in hydrogen bonding interactions. Tryptophan is a hydrophobic residue which has a preference to exist in the interfacial region of the lipid bilayer, and is able

to participate in π-cation and π- π- stacking interactions.[63] In combination with one another these two residues are able to participate in stacking interactions which facilitate peptide-membrane interactions and aid with peptide secondary structure formation and stability. Even at short lengths, Arg-Trp AMPs can be highly potent.[61]

Various biophysical studies suggest that AMPs mode of action may be through pore formation which causes the permeabilisation of the lipid membrane of bacteria.[59,64,65] This often leads to cell death. There are a number of mechanisms by which bacteria can make holes in the membrane, and these are described below.

1. The carpet model

The carpet model mechanism involves the AMPs forming a "carpet" of peptide by laying parallel to the membrane. The peptides are able to exhibit detergent like effects which lead to the formation of pores in the membrane. Shown in Figure 27.

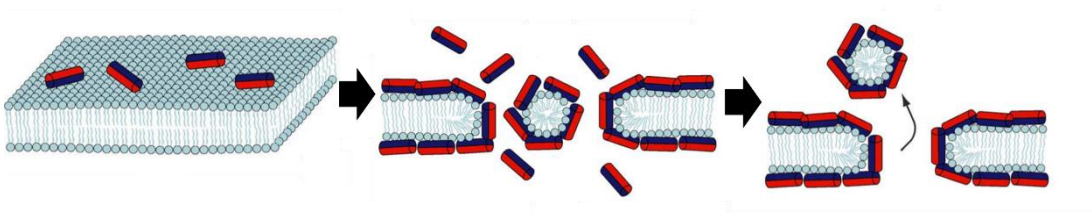

Figure 27: Carpet model mechanism [56] [Red= hydrophilic, Blue= hydrophobic]

2. The toroidal pore

These pores are formed from both AMPs and lipids and curve inwards towards the pore. The longevity of these pores is thought to vary, but is thought to be a mechanism of shuttling AMPs from one side of the membrane to the other. Shown in Figure 28.

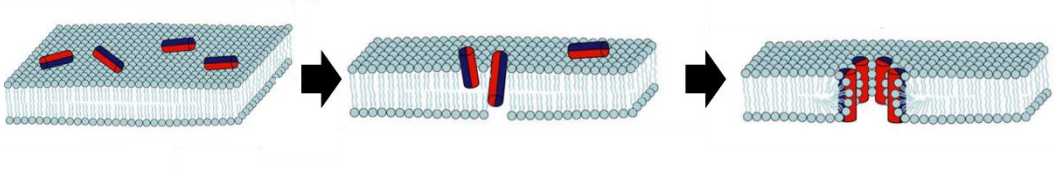

Figure 28:toroidal pore model mechanism [56] [Red= hydrophilic, Blue= hydrophobic]

3. The barrel-stave mechanism

AMPs span the membrane forming barrel-stave pores. These pores are lined with peptides. Shown in Figure 29.

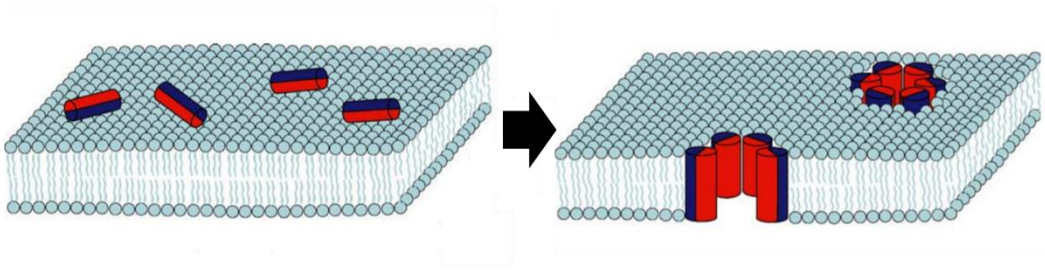

Figure 29: barrel-stave mechanism [56] **[Red= hydrophilic, Blue= hydrophobic]**

AMPs are also known to have intracellular targets such as enzymes, causing the inhibition of cell wall synthesis and protein synthesis, and some are able to interact with RNA and DNA.

A recent example of Arg- and Trp- rich antimicrobial peptides was shown by Castelletto *et al.* (2020) who synthesised three tripeptides with the sequence RXR, where X is an aromatic residue (e.g tryptophan).[66] Their aim was to target *Pseudomonas aeruginosa* through membrane lysis. This was tested using biofilms and theactivity was related to the binding of the second messenger molecule (nucleotide c-di-GMP). There was strong selective activity against *P. aeruginosa* biofilms observed for RFR and RWR. It was observed that all three peptides were able to self assemble into cluster nanostructures. The antimicrobial activity however was attributed to membrane disruption caused by the cationic arginine residues. This membrane disruption likely occurs by one of the mechanisms discussed in this section.

1.5 RWXXW PEPTIDE ANALOGUES

Rodolis *et al.* synthesised a series of Arg-Trp containing dipeptides and pentapeptides to investigate the hypothesis of the RWxxW motif experimentally.[48] Once synthesised, the *in vitro* inhibition of the peptides and the antimicrobial activity were tested. The results of these tests are shown in Table 2.

Peptide Sequence	*E. coli* MraY IC50 [μM]	MIC against *E. coli* K12 [μgmL^{-1}]
RWGLW	590±100	-
RGGLW	210±40	-
RWGLG	274±30	-
RWGGW	233±25	-
GWGLW	209±20	-
EHWGGG	460±30	-
ERWGGW	n.i.	-
H_2N-RW-octyl ester	>1000	31
H_2N-GW-octyl ester	790±160	-
H_2N-RW-methyl ester	n.i.	-
H_2N-GW-methyl ester	n.i.	-

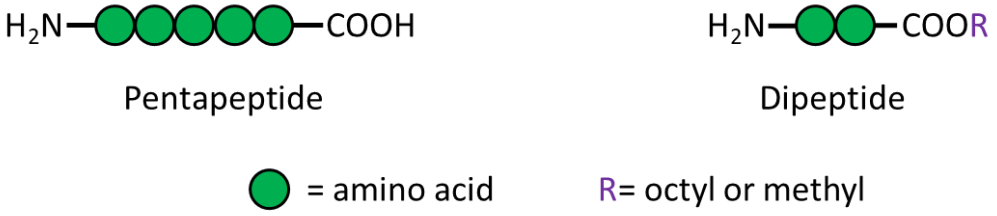

Table 2. The inhibition and antimicrobial data that were obtained for a series of pentapeptides and dipeptides by Rodolis *et al.*[48]

The series of pentapeptides served to identify if any of the residues of the RWxxW motif were solely responsible for the inhibition. The arginine and two tryptophan residues were separately varied for glycine and then the inhibition was tested. This showed that no one residue was responsible for the inhibition of MraY. Inhibition was however seen for all of the pentapeptides suggesting the motif derived for the hypothesised binding region to be correct. The pentapeptides however did not show any antimicrobial activity. It is possible that these pentapeptides did not adequately

mimic the secondary structure of the α-helical E protein. The zwitterionic nature of the pentapeptides may have affected the activity they were able to exhibit.

Looking at the series of dipeptides, the dipeptide Gly-Trp-octyl ester (GWoct) inhibited *E. coli* MraY but not the F288L and E287A varients confirming the importance of the residues Phe288 and Glu287 at the interaction site. Despite this MraY inhibition, no antimicrobial activity was seen. The dipeptide Arg-Trp-octyl ester (RWoct) showed antimicrobial activity against *E. coli* but no measurable inhibition of MraY. It is possible that the arginine and tryptophan residues of the RWxxW motif are responsible for the Epep antimicrobial activity and the final tryptophan of the motif responsible for the inhibition. It is also possible that full inhibition of the enzyme and antimicrobial activity is not possible for the pentapeptides as they may not be able to localise in the membrane. The dipeptides have lipophilic tails which may aid this. Further testing of RWoct was carried out to determine its target. MraY was over expressed in *E. coli* which was then treated with RWoct.[48] Rodolis states that the MIC for RWoct is increased when MraY is being overexpressed and concluded that this indicates an interaction between RWoct and MraY is occurring. This data is shown in Table 3.

	MIC (μg/mL)				
	WT E. coli	**(-) control Empty pET52b**	**MraY**	**F288L**	**E287A**
RWoct	31	31	250	500	300

Table 3: MIC of RWoct against *E. coli* cells overexpressed with MraY

This project aims to build on this observation by synthesising related dipeptides to explore the structure function relationship between MraY and RWoct. Ideally these RWoct peptide analogues will show antimicrobial activity and MraY inhibition. The aims of this project are explained further in section 1.7.

1.6 PEPTIDOMIMETICS

Since the discovery of the first bioactive peptide, insulin, in 1922 there has been an interest in the discovery and use of bioactive peptides in medicine. In 1955 Sanger resolved the amino acid sequence of insulin, which opened the door for the exploration of peptides as therapeutic agents. Both insulin and vasopressin (Figure 30) are peptide drugs which are used in there intact state and are administered into the bloodstream.[67]

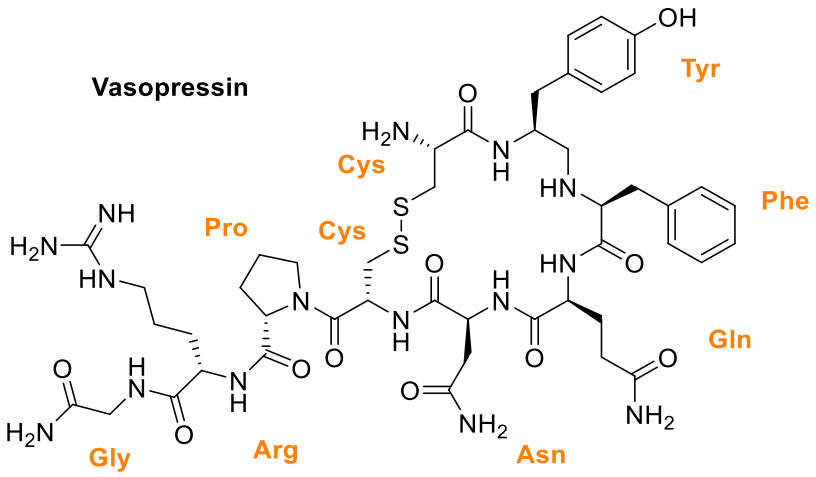

Figure 30: The structure and amino acid sequence of vasopressin

To date the majority of discovered bioactive peptides are not suitable drug candidates as they are not pharmacokinetically favourable, as discussed in section 1.4. Peptide drugs are susceptible to rapid excretion. They have low metabolic stability and lack oral activity. These drawbacks coupled with their low membrane permeability make them unsuitable drug candidates. Despite the drawbacks associated with bioactive peptides, the beneficial properties which they can display cannot be ignored. For this reason functional mimicry of bioactive peptides has become a methodology to overcome many of the issues mentioned. This has given rise to a class of molecules which can be described by the broad term: peptidomimetics.[68] With the emergence of 3-dimensional structural information of the discovered peptides, and the proteins which they target, the discovery of peptidomimetic drugs has been accelerated.

Peptidomimetics can be classified into three groups. The first of these are structures which mimic the local topography of and surrounding the amide bond (type I

peptidomimetics).[69] Amide bond isosteres are examples of this. Examples of the use of isosteres are shown in Figure 31.[70] This class can also include the use of unnatural amino acids (β and γ) and peptoids (poly-N-substituted glycines). The second type are functional mimetics which are small non-peptide molecules that bind to a peptide receptor (type II peptidomimetics). The molecules are often able to produce similar effects to the parent peptide but bind at a different subunit of the receptor, as they do not necessarily mimic its structure. The third type are often referred to as "ideal peptidomimetics" (type III peptidomimetics) and are topographical mimics. These compounds are novel templates which contain the most important groups from the parent compound relating to structure and function, positioned on a non-peptidic scaffold.

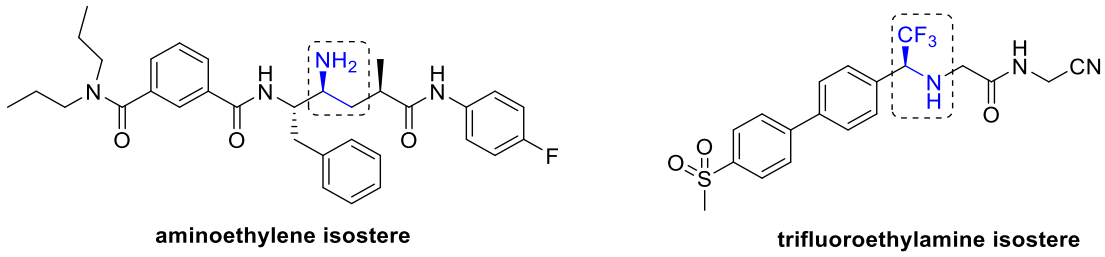

Figure 31: **The aminoethylene isotere in an inhibitor of β-amyloid precursor protein, designed by Sunesis-Merck and a trifluoroethylamine isostere developed by Zanda et al. which is selective a cathepsin K inhibitor.**[70]

The changes made in the classes described improve the bioavailability and stability of the compounds by minimising the breakdown of the compounds in biological conditions (i.e proteolysis), and so increasing the rate of excretion. Coupled with these benefits, peptidomimetics allow us to introduce conformational restriction to a molecule. Conformational restriction can improve the binding ability and the target selectivity, and so increasing the overall activity of a compound. It is possible the lowest energy conformer of the parent compound is not the most active, meaning the active conformer could be unstable, and consequently restricting the conformation to the active one can be beneficial. Additionally conformational restriction can enhance membrane permeability, one of the main disadvantages of peptide drugs. This has been demonstrated thought the incorporation of a cyclopropane scaffold which replaces the amide bond.[68] An example of a cyclopropane scaffold is shown in Figure 32.

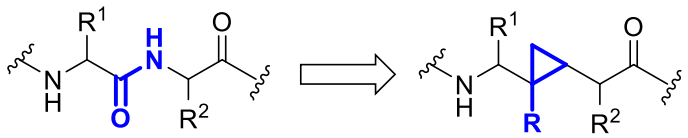

Figure 32: peptidomimetic scaffold designed by Wipf et al. which incorporated a cyclopropane in place of the amide bond.[70]

1.6.1 Secondary structure mimetics

The secondary structure of bioactive peptides are an important consideration when designing peptidomimetics, as many biological targets recognise secondary structure. Examples of this are seen in GPCRs which recognise turn motifs and proteolytic enzymes often recognise beta-sheet structures.[69] The inhibition of protein-protein interaction (PPI) sites relies on both the primary and secondary structure of the proteins involved. The secondary structure influences the binding affinity and so when designing peptidomimetics for these interactions it is important to find ways of replicating the orientation of the important side chain groups.[71]

The α-helical secondary structure is the most abundant of the secondary structures and is commonly seen in PPI interactions.[72] Apoptosis regulators are a predominant target for α-helical mimetics, p53/MDm2 and Bcl-2 family interactions which are targets in the treatment of cancer.[73]

An α-helix is a right handed coil which has a turn every 3.6 residues which creates a binding surface. The residues which occupy the binding surface are denoted *i*, *i*+4, *i*+7, and so on. The development of structural backbone mimics which present the amino acid side chains correctly has been of interest. This usually involves reproducing the characteristics of the *i*, *i* + 3 or *i* + 4, and *i* + 7 residues, located along one face of the helix (Figure 33).

There a several backbone mimics which have been designed which include terphenyls[74] and terpyridines, benzoylureas[75,76] and oligobenzamides[77,78]. The structures of these backbones are shown in Figure 33. A number of these backbones have shown PPI inhibition *in vitro*.

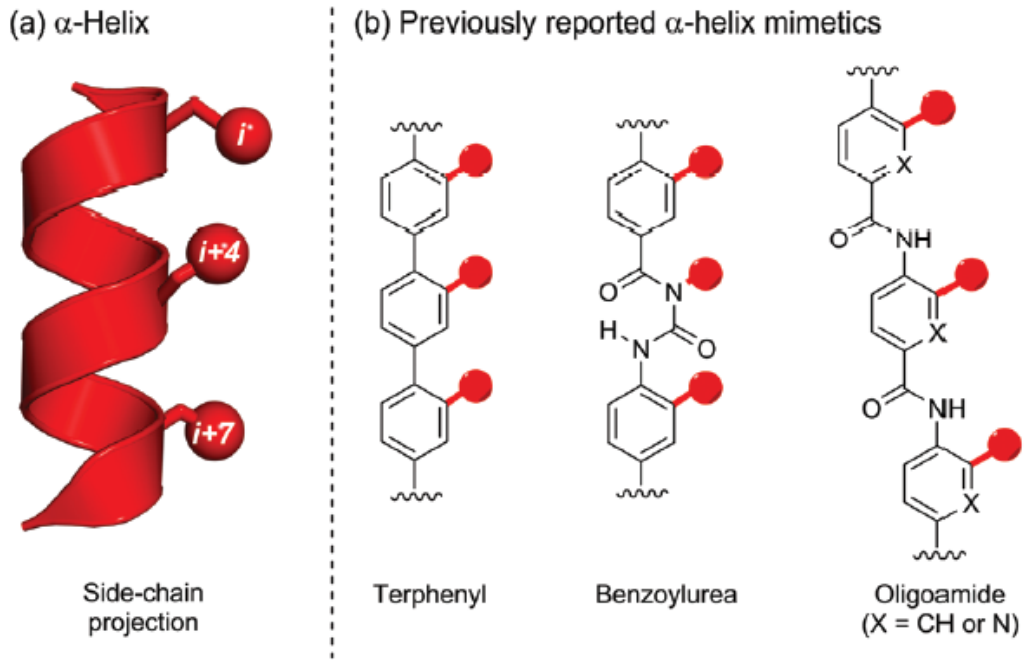

Figure 33: A. shows the alpha helix and the residues which are presented down the same face. B. previously reported a-helix backbone mimetics which present the side chain residues in a similar manner (as shown by the red dots)[79].

The terphenyl[74] (Figure 33) and terpyridine[80] (Figure 34) backbones were designed and synthesised by the Hamilton group who were the first researchers to investigate their use as α-helical PPI inhibitors. Terphenyl backbones have the important residues situated at the *ortho*-positions of the aromatic rings, which take on a staggered conformation. This conformation is a result of the conjugation between the rings and the steric interactions of the side chain groups. Figure 35 shows the comparison of the parent α-helix compared to the terphenyl mimetic. Their use as drug molecules is limited by their poor water solubility. This terphenyl-based backbone was used to mimic Bak BH3 which was able to act as a low-molecular-weight antagonists of Bcl-xL.[81]

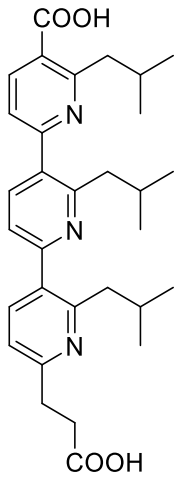

Figure 34: terpyridine α-helix mimetic.

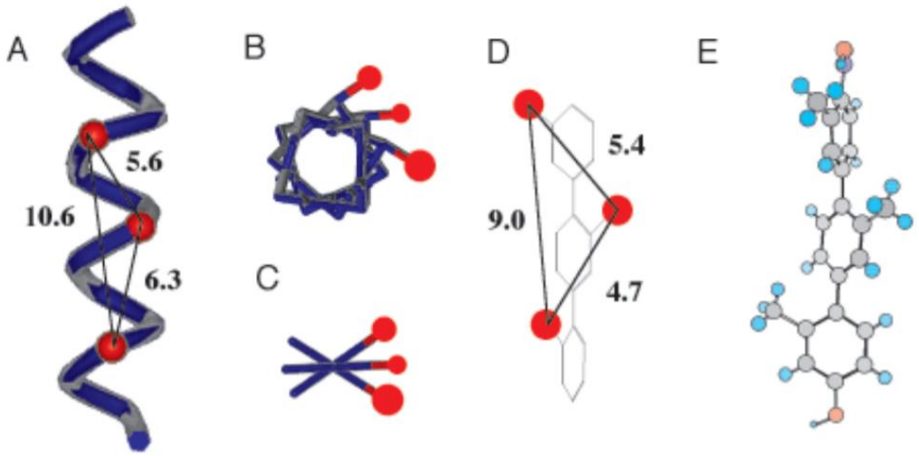

Figure 35: A. The schematic representation of the parent alpha-helix. The i, i+3 and i+7 residues are shown in red. (side view) B. The top view of the parent peptide, residues shown in red. C. The top view of the terphenyl mimetic. D. Side view of the mimetic. E. The crystal structure of the mimetic[74].

The terphenyl backbones are able to rotate freely which is not consistent with an α-helix. In order to prevent this from occuring, both the benzoylureas and oligobenzamides were designed with the ability to form internal hydrogen bonds which would constrain the molecules somewhat, preventing rotation (Figure 36).[74] Hydrogen bonds between amide –NHs and alkoxy groups promote extended conformation in O-alkylated benzamides and restrict the rotation about the aryl amide axes.[82]. Boger *et al.* saw high-affinity against HIV-1 gp41 from a benzamide α-helix mimetic which they had designed and synthesised.[83]

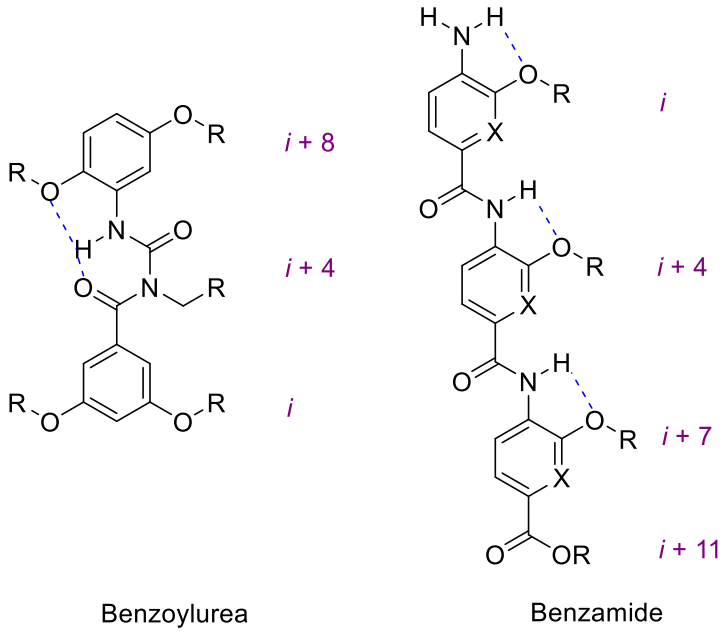

Figure 36: benzoylurea and benzamide backbones constrained by hydrogen bonding. The hydrogen bonds are shown in blue.

A structural mimetic has been shown to inhibit the trans-activator of transcription (TAT) protein interaction with viral TAR-RNA (transactivation response element RNA) which is crucial to HIV proliferation. The formation of the TAR-RNA and TAT complex accelerates the transcription of HIV. An oligopyridylamide-based α-helix mimetic was designed, with the aim of improving upon previous peptide based inhibitors acting at this site.[84] The compound shown in Figure 37 was the most of the effective of the compounds tested against the TAR-RNA-TAT complex (IC_{50} = 1.5 ±0.3 µM) and inhibited HIV-1 pseudovirus proliferation in TZM-bl cells (IC_{50} = 25 µM).

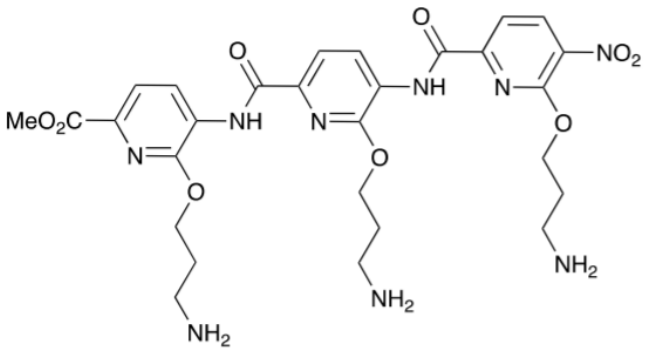

Figure 37: Oligopyridylamide α-helix mimetic designed to inhibit TAR-RNA/TAT PRI.[84]

Our aim is to synthesise peptidomimetics following the synthesis and testing of the dipeptide series. The RWxxW motif is taken from an alpha-helix (E protein) and so aspects of the Hamilton and Boger backbone structures will be utilised in the design of the RWoct mimetics.[76,83] This will be discussed further in section 1.7 and chapter 4.

1.6.2 Cyclic mimetics

These backbone mimetics are designed to mimic peptides which are greater than 10 residues in length. This is mostly because in order for an alpha helix to form there must be enough hydrogen bonds to hold the structure, and therefore there must be enough residues to form at least two turns.[85] So along with these backbone structures we turned our attention to backbone structures designed to mimic shorter peptide sequences. The peptide bond isoteres have already been discussed but will not feature in the design of our mimetics. A cyclic backbone was identified that had been designed and synthesised by Houghten *et al.* which was one of a number of backbones which focused on mimicking di- and tripeptides.[83] These were originally designed to allow the conversion of pre-existing active peptides into cyclic structures which would, as a result of the cyclisation, be more resistance to proteolysis. A diazepine derivative which could be synthesised on a resin bead was chosen as a starting point for the cyclic peptidomimetic design. This is shown in Figure 38. This compound and an alternate cyclic structure will be discussed in more detail in chapter 5.

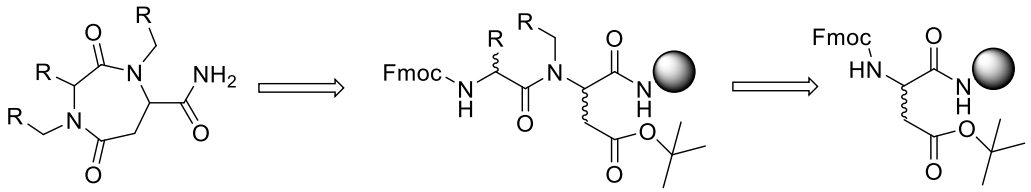

Figure 38: The synthesis of the diazepine mimetic, synthesised on a resin bead.

1.7 AIMS AND OBJECTIVES

1.7.1 Structure activity studies on Arg-Trp-octyl ester

During this project we aimed to synthesise a series of dipeptides which are based on Arg-Trp-octyl ester, the dipeptide synthesized by Rodolis which showed antimicrobial activity.[87] It is hoped that one of these dipeptides may have both antimicrobial activity and is also able to show *in vitro* inhibition of MraY.

The structure of dipeptide RWoct was split into four areas where changes could be applied and these are shown in Figure 39. These areas are the N-terminal, the aromatic tryptophan side chain, the cationic arginine side chain and the *O*-linked alkyl ester chain.

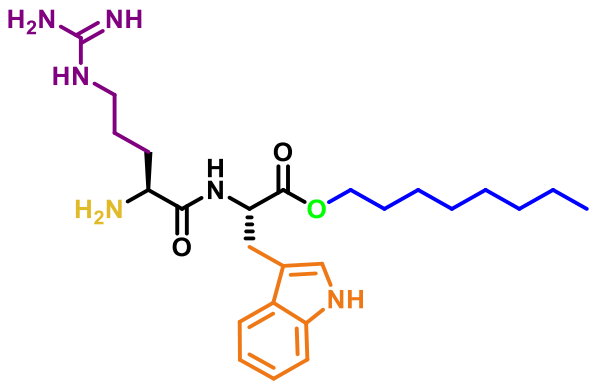

Figure 39: RWoct split into the four regions of interest for the synthesis of new RWxxW based peptides. Purple: cationic side chain, yellow: N-terminal, orange: aromatic tryptophan side chain, green: ester linker and blue: octyl chain

Firstly the length of the ester alkyl chain (blue) was altered to a 6 and a 10 carbon chain. It is thought that this chain aids the insertion of the dipeptide into the membrane. The ester linker (green) was be changed for an amide to prevent break-down by esterases. The N-terminus (yellow) of the dipeptide was protected with a Boc and acetyl group. It has been shown that Boc protection can improve antimicrobial activity of short cationic peptides.[27] The arginine residue was exchanged for a lysine and a histidine residue as well as a non-natural heterocyclic arginine residue. The tryptophan reside was swapped for the other aromatic residues phenylalanine and tyrosine, to determine the importance of the indole. To determine if the aromatic residue is necessary at all, a glycine residue was also be used to replace the tryptophan.

Once the series of dipeptides had been synthesised a series of biological tests were carried out on them. Antimicrobial tests was carried out using a microtitre broth dilution technique. The ability of the dipeptides to inhibit MraY will be determined using a continuous fluorescence assay and a radiochemical assay. This utilizes a fluorescent or radio labelled MraY substrate which when converted to lipid 1 gives an increase in fluorescence. The overexpression of MraY in *E.coli* was also used to demonstrate an interaction. Finally an assay using the dye resazurin was used to help assess how the dipeptides exhibit antimicrobial activity.

1.7.2 Peptidomimetics based on RWxxW motif

Using the data obtained from the biological testing of the dipeptide series, two groups of peptidomimetics will be designed and synthesised. These will be tested using the same biological methods. The aim is to reproduce and/or improve upon the dipeptide's activities.

One group of mimetics will focus on introducing functional groups onto a benzamide backbone and the other group will be peptidomimetics which replace the peptide backbone with a cyclic structure which limits the flexibility of the compound. Examples of these structures are discussed in section 1.7

The basic frameworks which we have chosen are shown below in Figure 40.

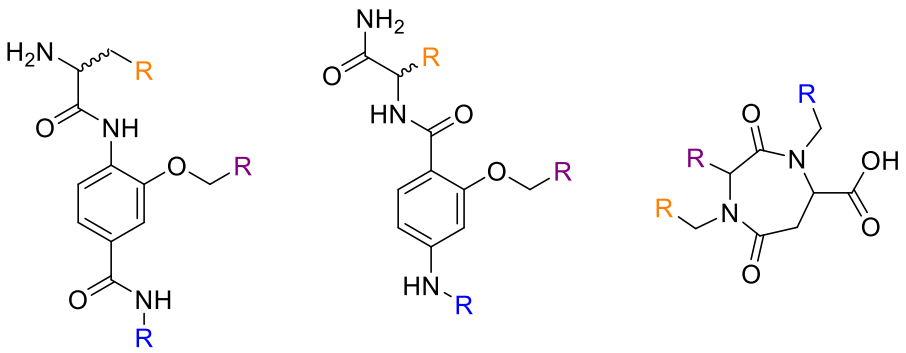

Figure 40: potential peptidomimetic backbone structures based on Hamilton, Boger and Houghten models.[83,85,86]

We will also consider the possibility of using a cyclic structure which was not originally designed as a peptide mimetic but does allow the incorporation of three functional groups in chapter 5.

CHAPTER 2: DIPEPTIDE DESIGN AND SYNTHESIS

The first part of the project was to carry out structure-activity studies on the dipeptide RWoct which was synthesised and tested by Rodolis.[48,87] The alterations described will probe the proposed interaction site of RWoct and the enzyme MraY. Liquid phase peptide synthesis was used to couple appropriately protected amino acids. Purification and deprotections were the carried out to give the final dipeptides.

All of the peptides synthesised contain a residue with an alkyl chain attached by an amide or an ester. The residues used were mostly tryptophan but this was swapped for phenylalanine and a tyrosine. This chain is installed first by an esterification or amide coupling reaction. The length of the chain was also varied with a hexyl and decyl chain linked by an ester to tryptophan. Once this chain had been installed the coupling reaction to the cationic residue could be carried out. The general scheme for this reaction is shown in Figure 41.

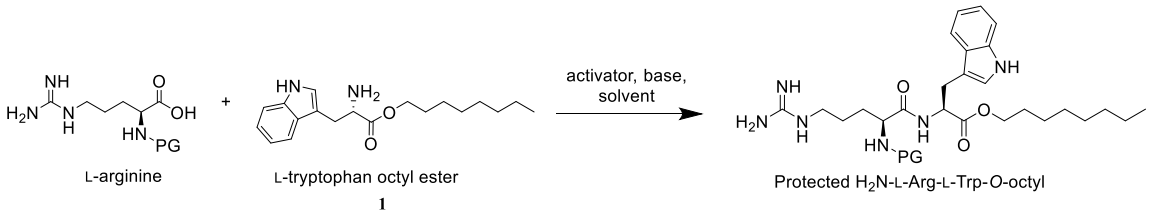

Figure 41: Solution phase peptide synthesis scheme for the general synthesis of the dipeptide series. Show in this scheme is protected RWoct which is not isolated before deprotection. [PG=protecting group)

The coupling reactions mainly used an uronium based coupling reagent as the activator. The cationic residues coupled to the tryptophan ester were arginine, lysine, histidine and a heterocyclic arginine analogue. These residues were protected and following the coupling reaction the protecting groups could be removed.

In some cases the α-amine protecting group was not removed or an alternate protecting group was installed (Boc and Ac).

Making this series of changes gave the series of dipeptides shown in Table 4.

Dipeptide	Abreviated name	Number
NH_2-Arg-Trp-*O*-hexyl ester	RWhex	**7**
NH_2-Arg-Trp-*O*-octyl ester	RWoct	**6**
NH_2-Arg-Trp-*O*-decyl ester	RWdec	**8**
Boc-NH-Arg-Trp-*O*-octyl ester	Boc-RWoct	**11**
Ac-NH-Arg-Trp-*O*-octyl ester	Ac-RWoct	**12**
NH_2-His-Trp-*O*-octyl ester	HWoct	**13**
NH_2-ArgHet-Trp-*O*-octyl ester*	R^1Woct**	**18**
NH_2-Lys-Trp-*O*-octyl ester	KWoct	**16**
NH_2-Arg-Tyr-*O*-octyl ester	RYoct	**10**
NH_2-Arg-Phe-*O*-octyl ester	RFoct	**9**
NH_2-Arg-Trp-*N*-octyl amide	RW-Noct***	**22**
NH_2-Lys-Trp-*N*-octyl amide	KW-Noct***	**24**
NH_2-Lys-Gly-*N*-octyl amide	KG-Noct***	**28**

Table 4: Table of dipeptides synthesised to probe the interaction site between RWoct and MraY. *ArgHet= heterocyclic arginine. **R1=heterocyclic arginine. ***Noct= amide linked octyl chain.

2.1 Synthesis of tryptophan alkyl esters

The majority of the dipeptides that we wanted to synthesise contain a C-terminal ester which is thought to aid insertion into the cytoplasmic membrane. In contrast to the E protein which the dipeptides are modelled, on the dipeptides will approach MraY extracellularly and so the alkyl chain is important. Rodolis showed that a methyl ester at the C terminus showed no inhibition of MraY or antimicrobial activity.[87] In order to optimise the membrane localisation and insertion of the dipeptides, the octyl chain was replaced with a hexyl and decyl chain. The ester chain will also serve as a carboxylic acid protecting group during liquid phase peptide synthesis (LPPS). A Fischer esterification was carried out on L-tryptophan using an excess of the corresponding alcohol (hexanol, octanol or decanol) and a catalytic amount of H_2SO_4.[48,88] (Scheme 1). The long chain alcohols were used as the solvent and were removed by silica chromatography due to their high boiling points. The silica was first deactivated using 5% TEA in petrol to prevent the tryptophan amine sticking.

The nitrogen of the tryptophan side chain, was not protected as it was unlikely to be reactive enough to effect the esterification or coupling reaction which would follow.

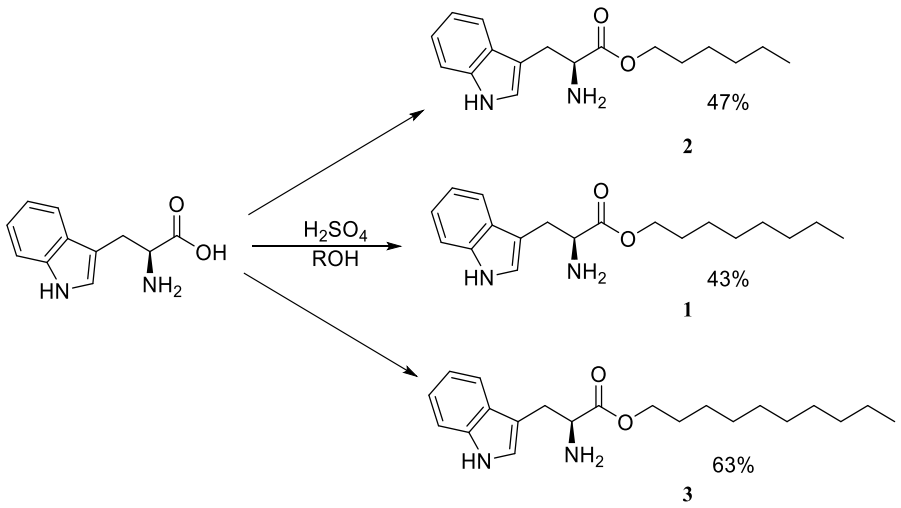

Scheme 1: Fischer esterification of L-tryptophan using 1-hexanol, 1-octanol and 1-decanol as the solvent and reactant with H2SO4 as the catalyst.

2.1.1 Tyrosine and Phenylalanine alkyl esters

The tryptophan was then replaced by phenylalanine and tyrosine (Scheme 2). We wondered whether there was potential for the tyrosine hydroxyl group to be involved in hydrogen bonding at the E-MraY interaction site.

The octyl esters of L-tyrosine and L-phenylalanine were synthesised by the same method as the tryptophan octyl ester. The hydroxyl group of the tyrosine was also not protected as it would not be reactive enough to effect the esterification or coupling reaction.

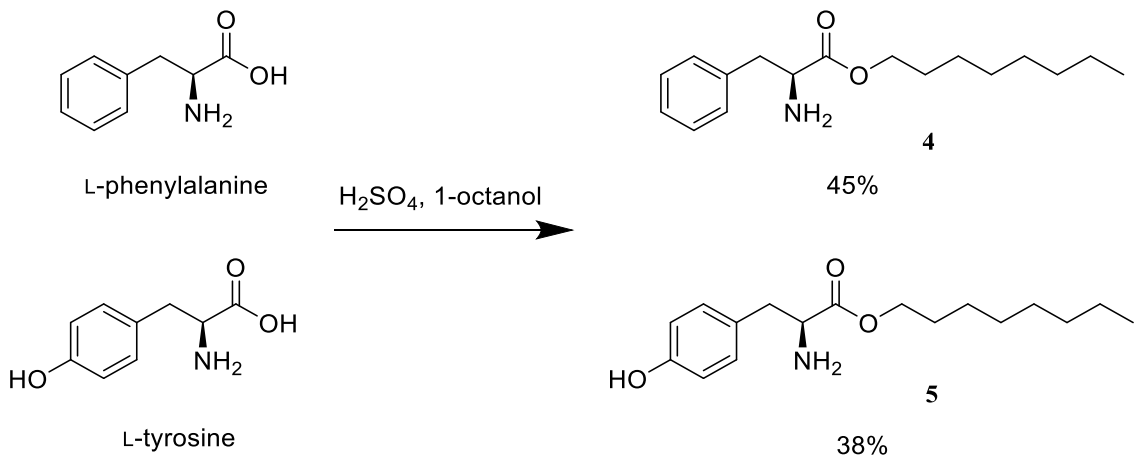

Scheme 2: The esterification of L-phenylalanine and L-tyrosine.

2.2 Peptide coupling methods

Liquid phase peptide synthesis was used for the synthesis of the series of dipeptides designed in this project. The general method is shown in Figure 42. An alternative method would have been to use solid phase peptide synthesis (SPPS) which is usually the more popular choice in the synthesis of peptides.[89] We decided against this method mainly because we only need to carry out one coupling reaction per peptide and carrying out SPPS would require a coupling first to the resin which would increase the number of steps. The coupling to the resin would occur at the C terminus which is where our alkyl esters have already been installed.

LPPS like solid phase peptide synthesis (SPPS) requires an activator and an activator base to be present. In the presence of these reactants an active ester is formed *in situ* which can then be attacked by an amine of a second amino acid, forming an amide bond. (Figure 42). If there is no activation of the carboxylic acid the formation of an amide bond is not energetically favourable.[90] The activated ester has a good leaving group which is electron withdrawing, thus enhancing the electrophilicity of the carbonyl, making it susceptible to nucleophilic attack by the amine.[90]

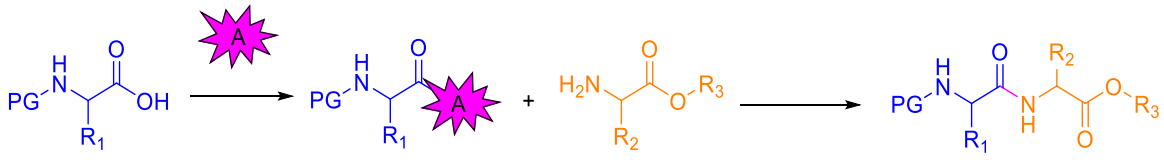

Figure 42: **The general peptide coupling reaction between amino acid 1 (blue) and amino acid 2 (orange). A= activator, R1 and R2= side chain, R3= ester chain, PG= protecting group.**

The activator initially used for the couplings was HATU (a commonly use coupling agent). The activator base used is Hünigs base (DIPEA). The structures of these compounds are shown in Figure 43.

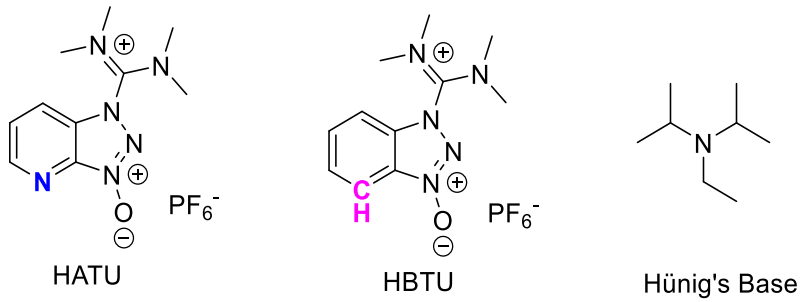

Figure 43*:* The structures of the uronium coupling agents HATU (left) and HBTU (middle). The difference between the two coupling agents are highlighted in blue and pink respectively. DIPEA (right) is the accompanying base.

HATU is in a class of uronium based coupling agents which prevent racemization occurring, something which is sometimes seen when alternate groups of coupling agents are used such as carbodiimides (DCC or DIC). HBTU is a cheaper alternative to HATU. HATU is used as an amine acylation agent where it reacts with a carboxylic acid to form an active ester which can then react with the amine nucleophile to produce the acylated product (amide bond formation). It was first reported by Carpino in 1993.[91] The initial activation step proceeds by the carboxylic anion attacking HATU to form the O-acyl(tetramethyl)isouronium salt (which is highly unstable). The anion attacks the isouronium salt forming the active ester. The step leads to the formation of the tetramethylurea by-product. The active ester is then subject to a nucleophilic attack from the amine. It is possible that the pyridine nitrogen atom is able to stabilise the amine through a hydrogen bond, and it thought that this neighbouring group effect is responsible for the quick reaction times and high coupling efficiency of HATU. The reaction mechanism of the HATU coupling reaction is shown in Figure 44.

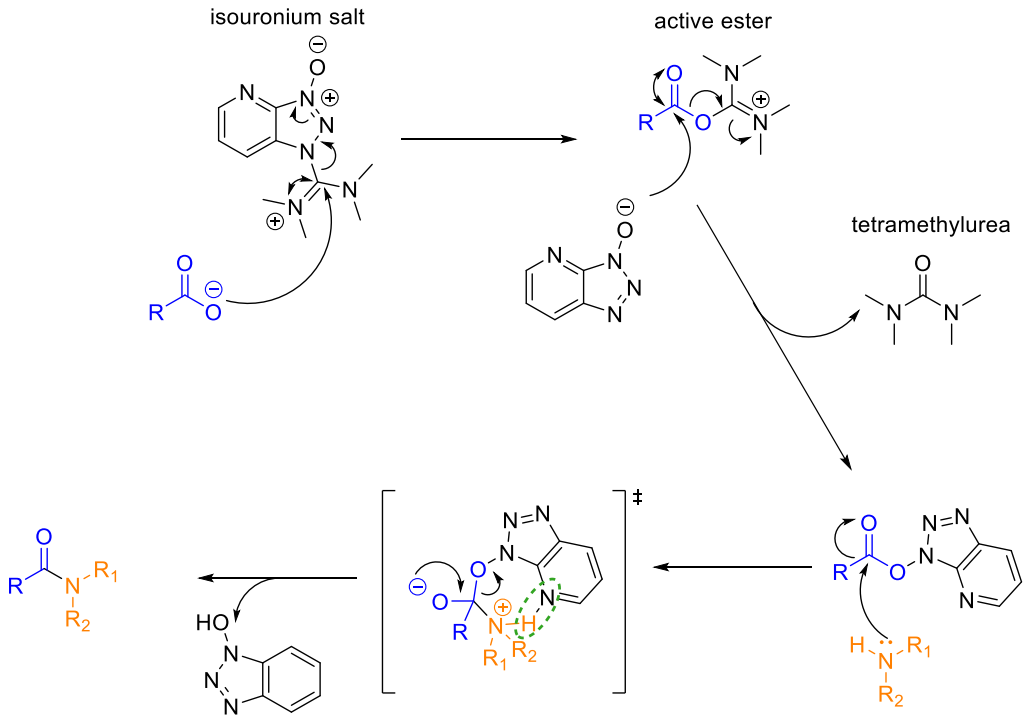

Figure 44: The reaction mechanism of a peptide coupling activated by HATU. The predicted hydrogen bond formed between the pyridine nitrogen and amine hydrogen is circled in green. Amino acid 1 is shown in blue and amino acid 2 is shown in orange.

HBTU is considered to be less effective when synthesising longer peptides.[92] HBTU lacks the pyridine nitrogen that HATU possesses and this may be the reason for a decrease in efficiency. This difference and the structure of HBTU is shown in Figure 43. As our peptide is only two residues in length and ultimately we need milligram quantities of final product, this did not matter. Levels of racemisation are higher when using HBTU, likely due to the lack of the stabilising pyridine nitrogen and this is prevented with the use of DIPEA.[93] DIPEA is a tertiary amine and its approach to the chiral centre of the reacting amino acid intermediate is hindered, and this impedes racemisation. The coupling reactions were monitored using LRMS.

The side product of both coupling agents is tetramethylurea (TMU) which is toxic to cells.[94] It is easily removed by RP-HPLC, but where peptides were purified by other methods its removal was more difficult. It was most effectively removed under vacuum using freeze drying and could take a number of days because of the high boiling point (177 °C). Its complete removal could be verified using ^{1}H-NMR. The 12 protons of TMU are seen as a large singlet at ≈ 2.8 ppm.

2.2.1 Arginine protecting groups.

In order to prevent the side chains of amino acids interfering with the coupling reaction, a variety of protecting groups can be used. These protecting groups are usually labile either in acid or base which allows selective deprotection. This is useful, as the amine of the residue is also protected, and this protecting group is usually removed in different conditions to the side chain to allow further amino acid residues to be coupled.

Fmoc-Arg(Pbf/Pmc)-OH is one of the most commonly used protecting strategies for arginine residues in peptide synthesis.[95,96] The Fmoc protecting group is removed with piperidine and the Pbf/Pmc groups are removed with TFA.

Using this protecting strategy the deprotection of the arginine side chain was unsuccessful. A variety of conditions were used, but LRMS showed that the Pbf or Pmc group had not been removed to form the deprotected dipeptide. The LRMS trace showed a peak at *m/z* 826.4 (Pbf protected compound) but no peak was seen at *m/z* 473.2 (deprotected). The concentration of TFA was increased (from 20%-100%), a scavenger (TIPS) was included and the solution was heated up to 80ºC, but no deprotection was seen. (Alternative methods of deprotection include HF where the risks outweigh the gains.)

Initially it was thought that the Pbf group had not been removed from the arginine. This had previously been seen by Stierandova *et al.* who were able to conclude that an unprotected tryptophan side chain could accept Pmc or Pbf protecting groups from an arginine if the distance between the two did not exceed two residues.[97] (Figure 45).

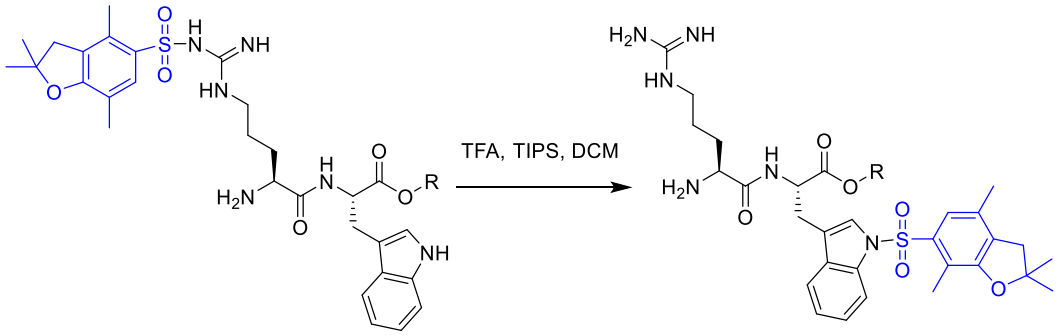

Figure 45: The migration of the Pbf arginine side chain protecting group from the arginine residue to the neighbouring tryptophan residue side chain, and the removal of the N-terminal Boc protecting group.

With the most common protecting strategy being unsuccessful we next used an arginine residue with an unprotected side chain. The guanidinium group was considered to be sufficiently unreactive to not interfere with the coupling reaction. Initially the Boc-Arg-OH was purchased and coupled to the tryptophan octyl ester (**1**) (Scheme 3). This coupling reaction was a success as was the deprotection on the crude coupling product to give Arg-Trp-octyl ester (**6**), which was then purified (section 2.5). The coupling procedure was carried out with the hexyl and decyl tryptophan esters (**2** and **3** respectively) to give RWhex (**7**) and RWdec (**8**).

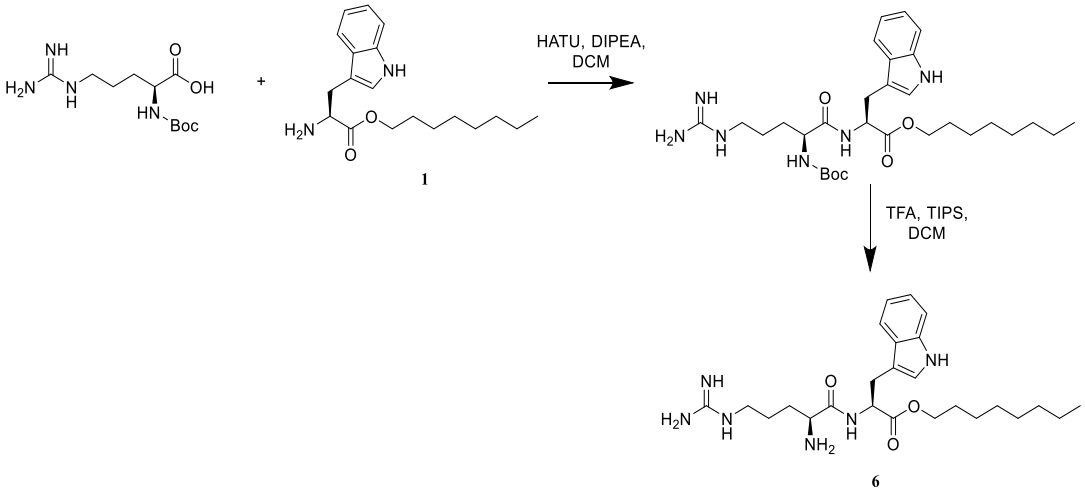

Scheme 3*:* The coupling reaction between Boc-Arg-OH and Trp-octyl ester following by the acid deprotection of the Boc protecting group. There is no protecting group used on the arginine side chain.

2.2.2 Boc deprotection

The mechanism for the removal of Boc protecting groups under acidic (TFA) conditions is shown in Figure 46. The most common deprotection agent for acid labile groups in peptide synthesis is TFA. The *tert*-butyl carbamate is initially protonated by the acid. A carbamic acid is formed due to the loss of the *tert*-butyl cation. The carbamic acid is decarboxylated and this gives a free amine. A TFA salt forms due to the protonation of the amine in the acidic conditions. Dipeptides which were TFA salts were problematic for the biological testing. Erratic cell death has been frequently seen where cells have been treated with compounds which contain the TFA counter ion.[98] The TFA salt can therefore produce variable biological results and false positives.

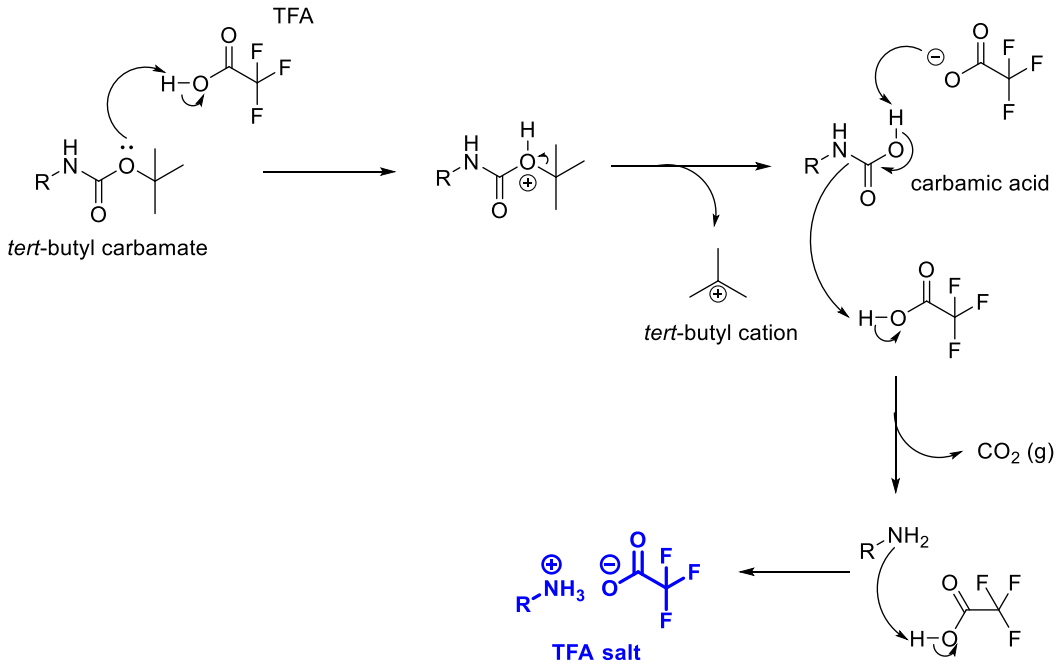

Figure 46: The mechanism of Boc deprotection using TFA and the formation of the toxic TFA salt.

It is possible to remove the TFA salt using Amberlyst A21 (a free base) resin. The dipeptide was stirred with the resin in DCM overnight. All peptides which were treated with TFA were then treated with Amberlyst A21 resin to remove the TFA salt. All dipeptides were analysed by ^{19}F-NMR to confirm the complete removal of the TFA

salt. For a TFA related group the range of ^{19}F chemical shifts is between −85 ppm and −67 ppm (relative to $CFCl_3$).[99,100]

It is possible to avoid using TFA by using 4M HCl in dioxane, as this gives the hydrochloride salt instead. The chloride anion has been shown to have no effect on cells in cell based assays.[98] Towards the end of synthesising the dipeptide series this was used as an alternative to TFA deprotection.

2.2.3 2,5-diketopiperazine formation

Rodolis had previously seen spontaneous cyclisation of dipeptides which contained a less bulky side chain (i.e glycine) in basic conditions.[87] Specifically during a work-up using Na_2CO_3 which we decided not to carry out. The 2,5-diketopiperazine formation is shown in Figure 47. Some of the dipeptides were synthesised using Fmoc-Arg-OH which was deprotected using piperidine and so it was possible that the diketopiperizine formation would occur. There was no evidence for this formation by LRMS analysis and this is likely due to the bulky side chains, and so the cheaper Fmoc protected arginine residues were used in most cases.

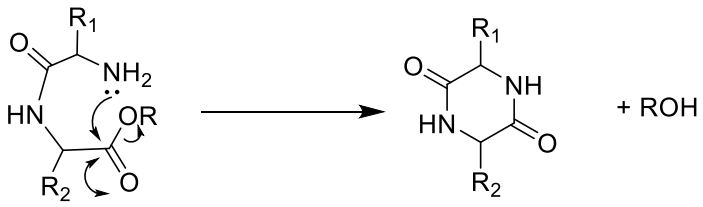

Figure 47*:* Base catalysed cyclisation of a dipeptide ester to for 2,5-diketopiperazine. X=ester chain, R=amino acid side chain.

2.2.4 Fmoc deprotection

As the Fmoc protected amino acids were cheaper and no diketopiperazine formation was seen during the deprotection, most of the couplings were carried out with Fmoc-Arg-OH. The deprotection mechanism is shown in Figure 48, and this shows the Fmoc adduct which is formed as a by-product. The Fmoc adduct is insoluble in water but is soluble in diethyl ether, in which the dipeptides had limited solubility. The majority of the Fmoc adduct needed to be removed as the purification method (RP-HPLC,

discussed in section 2.5) used water, and any precipitation would be damaging to the HPLC machine. The dipeptides where precipitated into diethyl ether and then removed by filtration leaving the by-product in the filtrate. The Fmoc adduct can be seen by mass spectrometry and this allowed the determination of its removal (m/z (ESI) 264.1 $[M+H]^+$).

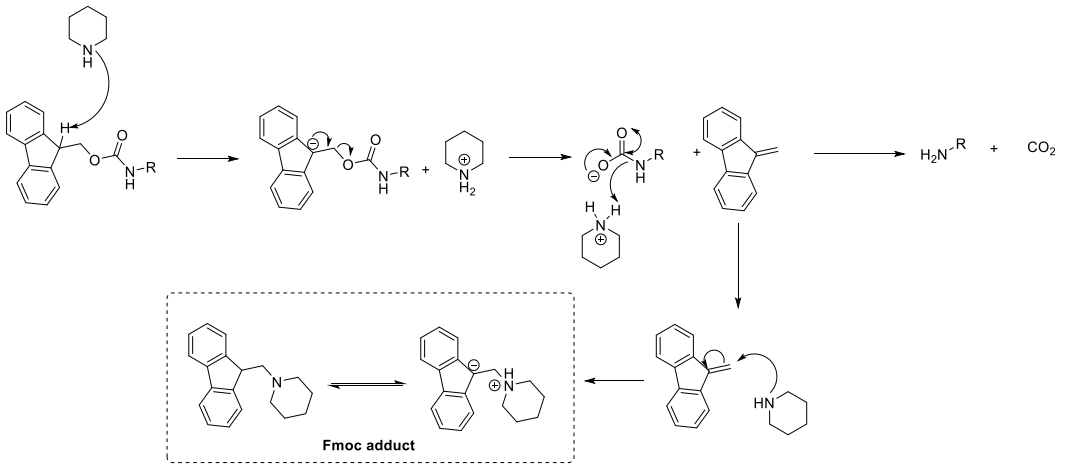

Figure 48*:* The mechanism of Fmoc removal using piperidine and the formation of the Fmoc adduct byproduct.

The coupling procedure was carried out with the hexyl and decyl tryptophan esters (**2** and **3** respectively) which were coupled to either Boc-Arg-OH or Fmoc-Arg-OH to give RWhex (**7**) and RWdec (**8**). Phe-oct (**4**) and Tyr-oct (**5**) were also coupled to either Boc-Arg-OH or Fmoc-Arg-OH to give and RFoct (**9**) and RYoct (**10**) after deprotection.

2.2.5 Protected RWoct analogues

In the literature it has been shown that Arg/Trp containing peptides showed greater antimicrobial activity with an N-terminal protecting group, particularly Boc or one or more amino acids before the cationic residue.[27,101] The exact reason for this is unknown, but it is speculated that the protecting group can help anchor/position the dipeptide correctly. Both the Boc protected and acetylated RWoct analogues were synthesised. For the Boc protected analogue the dipeptide was simply left with the

protecting group attached having been synthesised from Boc-Arg-OH to give Boc-RWoct (**11**). The acetylated analogue was synthesised by combining the crude RWoct (an oil) with acetic anhydride to give Ac-RWoct (**12**) which was then purified. (Shown in Scheme 4).

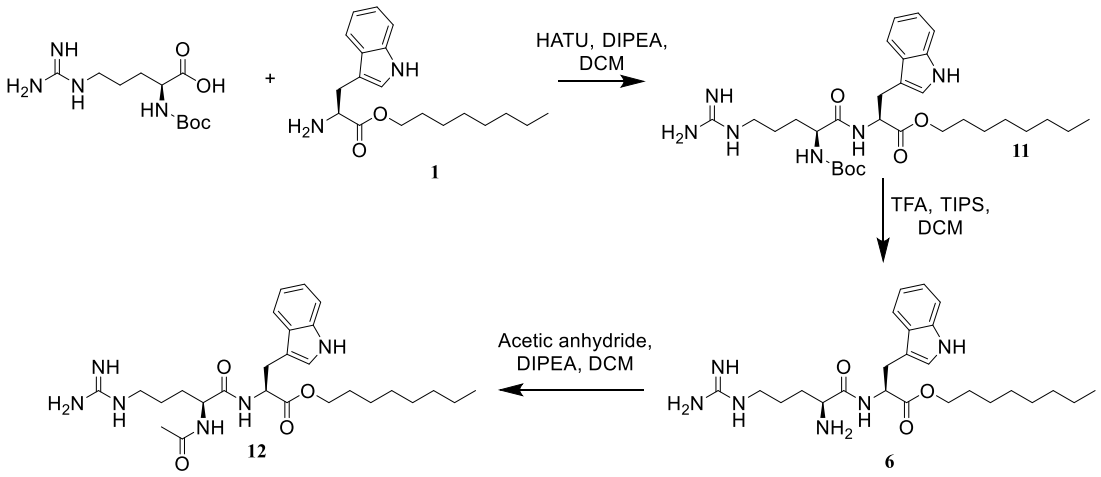

Scheme 4: The synthesis of Boc-RWoct (11) and Ac-RWoct (12)

2.3 Dipeptides containing arginine analogues

The arginine was replaced with other basic residues and a modified arginine residue with the aim to enhance the π-cation and π stacking interactions of the MraY interaction site. The structures of the four residues are shown in Figure 49. The literature shows examples of cationic peptides containing Lys-Arg and some E protein sequences contain His-Arg.[27,101]

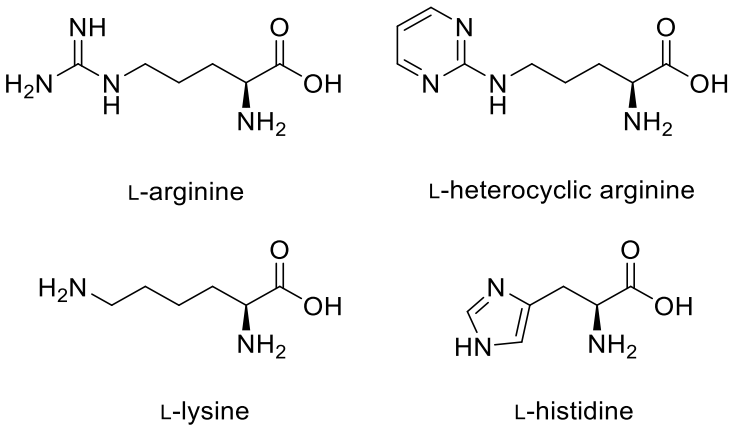

Figure 49*:* Showing arginine and the analogues of it which were incorporated into the dipeptide.

2.3.1 Dipeptide containing histidine in place of arginine

The imidazole side chain of histidine is protonated and partially cationic at pH 7. For this reason it was chosen to enhance π-π stacking, and potentially π-cation interactions, although this is less likely. Histidine residues are also present next to tryptophan residues in some bacteriophage sequences.[48] For the coupling reaction with the tryptophan ester, a doubly protected histidine residue (Boc-His(trt)-OH) was used. By protecting the amines the protecting groups reduced the basicity of the dipeptide, and this meant that the dipeptide could then easily be purified by column chromatography using deactivated silica gel. The acid labile protecting groups were then removed with TFA and the dipeptide His-Trp-octyl ester (**13**) was precipitated from diethyl ether. The dipeptide was then stirred in DCM with Amberlyst A21 (a free base) resin to remove the TFA salt. (Giving a yield of 2 %).

2.3.2 Dipeptide containing lysine in the place of arginine

Lysine is a basic residue which is positively charged at physiological pH. Intially Fmoc-Lys(Boc)-OH was coupled to the tryptophan ester. The dipeptide was deprotected first with piperidine to remove the Fmoc group followed by TFA or HCl to remove the Boc protecting group. To reduce the number of deprotection steps Boc-Lys(Boc)-OH (**14**) was synthesised from L-lysine and Boc_2O in the presence of base (Scheme 5). This meant that following the coupling the protected dipeptide **15**, could be purified by silica chromatography and then deprotected using 4N HCl in dioxane to afford a pure deprotected dipeptide, Lys-Trp-oct. (**16**) (72%)

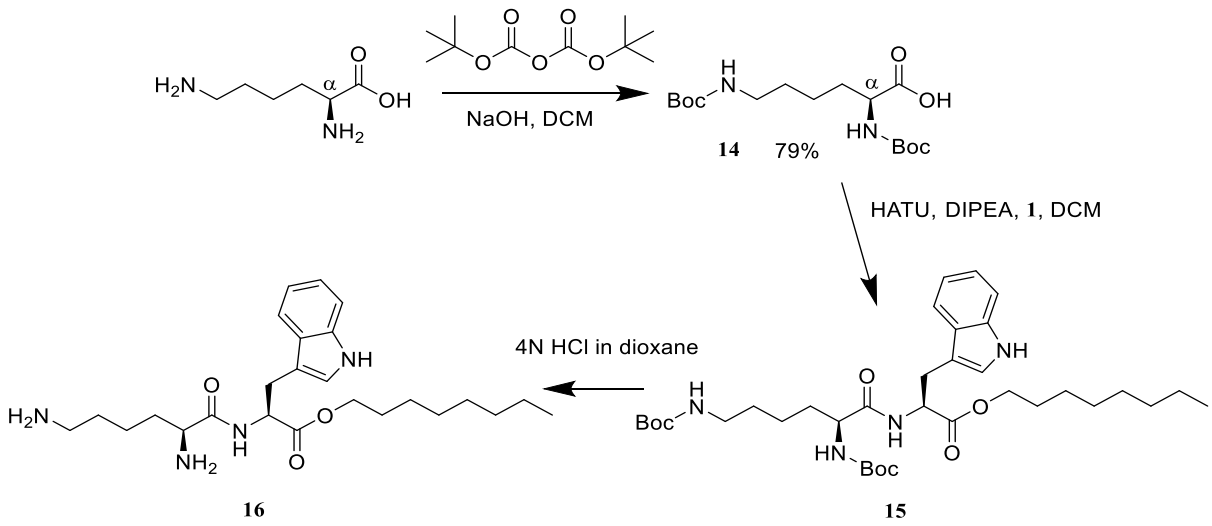

Scheme 5*:* The simultaneous Boc protection of the α-amine and the side change amine of L-lysine, using Boc_2O and NaOH. 14 is then coupled to 1 and the resulting peptide (15) is deprotected using HCl in dioxane

2.3.3 Dipeptide containing heterocyclic arginine analogues

The heterocyclic arginine residue was synthesised from 2-chloropyrimidine and Boc-ornithine under basic conditions to give **17** (Scheme 6). **17** was then coupled to **1** by the procedure previously discussed and deprotected using HCl to give R^1Woct (**18**). This residue had previously been synthesised by Ulhaq *et al*. by a similar method.[102] The α-amino group of the ornithine was protected with a Boc group. This protecting group was used to prevent the S_NAr reaction occurring at the α-amino group as well as the side chain amine. The electron deficient *ortho* carbon is subject to a nucleophilic

attack by the amine side chain, causing the ejection of a chloride ion. This reaction would ideally be carried out at high temperatures (80-100°C), however because the ornithine residue needed to remain protected by the Boc group the temperature used was much lower (40°C) to prevent its removal.[102] This meant the reaction time was approximately 3 days.

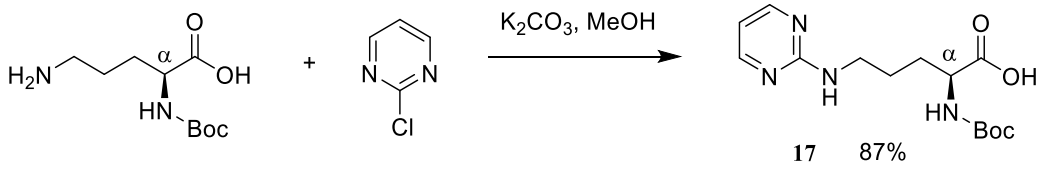

Scheme 6: Synthesis of heterocyclic arginine from 2-chloropyrimidine and Boc-Orn-OH.

Once synthesised it was purified by column chromatography using deactivated silica and coupling to **1** using the same methods described in this chapter and then deprotected using TFA.

2.4 Dipeptides containing n-octyl amide

All of the peptides synthesised up until this point contain an ester bond to the alkyl chain. Ester bonds in drug molecules can be problematic due to the presence of esterases in the body. At the active site of esterases ester bonds can be hydrolysed. During drug design in many cases this is undesirable, as the original compound is no longer intact. Increasingly there are exceptions to this rule. Some drug molecules are designed with an ester bond and until this is hydrolysed the drug is inactive. These are known as prodrugs with esterase triggered release.[103] The purpose of these drugs is to improve stability, solubility and oral bioavailability by masking the polar moieties during administration.[104]

2.4.1 Functional group exchange: ester to amide

To decide whether the ester is susceptible to being broken down by esterases the ester bond must be replaced and the biological data of the two molecules compared. A simple and logical replacement is to change the ester bond to an amide bond. Amide bonds can be broken down by proteases but these are often more specific than esterases, and for this reason the breakdown of this bond should be slower, if not completely stopped.[105] The breakdown of the peptide bond between the two amino acid residues is more likely to breakdown first as proteases breakdown amide bonds between amino acids. Comparing the dipeptides which contain an ester and an amide bond will elucidate whether the ester bond is broken down. This said, it is possible that the removal of the alkyl chain may render the dipeptide more active and this is something that will need to be considered when analysing the biological data obtained.

2.4.2 Synthesis of N-octyl amide dipeptides

The addition of an octyl chain bound by an amide to L-tryptophan can be carried out in 3 steps. To couple 1-octylamine to the acid of L-tryptophan its α-amine must first be protected. (This protection prevents the polymerisation of tryptophan). Boc anhydride was reacted with L-tryptophan under basic conditions. Once Boc-L-tryptophan (**19**) had been synthesised, the acid was activated using DCC and 1-

octylamine was added under basic conditions to give **20**. The reaction scheme is shown in Scheme 7.

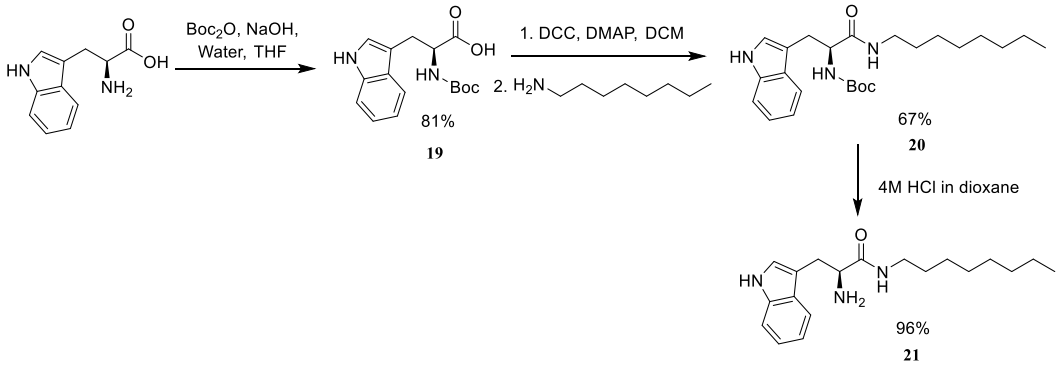

Scheme 7: The synthesis of the tryptophan octyl amide. L-Tryptophan is protected at its α-amine using a Boc group. This is followed by the coupling of 1-octylamine to the free acid. The Boc group can then be removed in acidic conditions.

DCC is one of several carbodiimide condensation reagents. The mechanism for DCC mediated peptide coupling is given in Figure 50. This is the general mechanism for all carbodiimide couplings, but the groups on the nitrogen atoms differ between reagents.[106] (The difference in groups between the carbodiimides alters the urea by-product that is formed). In the case of DCC the by-product *N,N'*-dicyclohexylurea is insoluble and precipitates as the reaction advances.[107] Most of this by-product can be filtered off with any remaining by-product being removed using a silica column. The urea by-product of EDC (another carbodiimide) is water soluble and is easily removed in an aqueous work-up.

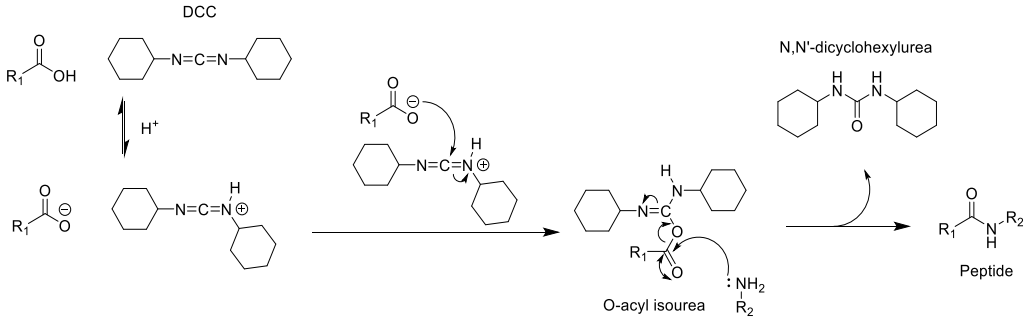

Figure 50: General mechanism of a DCC coupling between and acid and an amine. The insoluble urea by-product is shown.

A problem associated with the use of carbodiimides for peptide coupling is racemisation.[106] The mechanism of racemisation caused by carbodiimides is shown in Figure 51. Racemisation proceeds via an oxazolone intermediate.[90] The α-amine protecting group (Boc) is electron withdrawing, and this promotes the abstraction of a hydrogen atom from the α-carbon by a base. The ion which is formed is resonance stabilised. On opening of the oxazolone intermediate, the conversion between the two enantiomers, at the α-carbon, can occur.

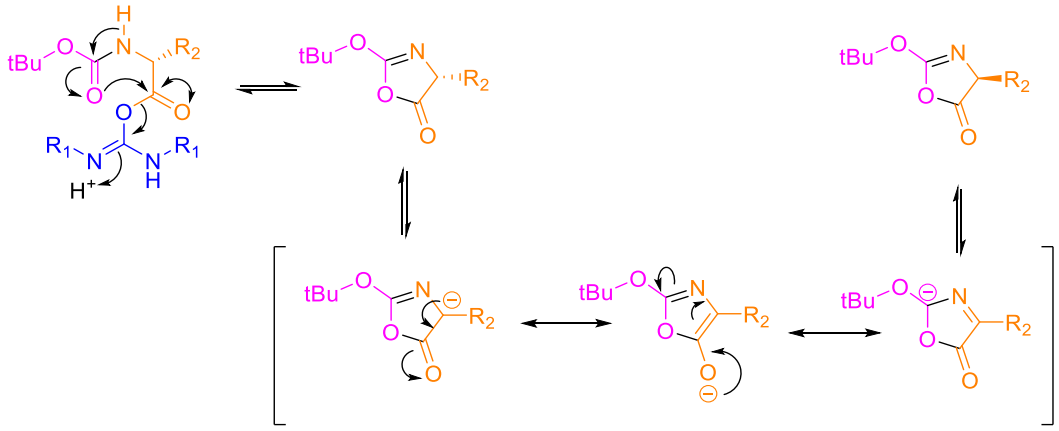

Figure 51: The mechanism by which racemisation occurs when using carbodiimide coupling agents. [Pink=Boc group, Blue=carbodiimide coupling agent, Orange=amino acid]

To reduce the amount of racemisation that occurs, an auxiliary nucleophile can be added. 1-Hydroxybenzotriazole (HOBt) is often used in peptide coupling reactions for this reason. HOBt binds to the carbonyl group which shortens the lifetime of the *O*-acyl-isourea.[108] The amine can now react with the acyl group without racemisation occurring. This is shown in Figure 52.

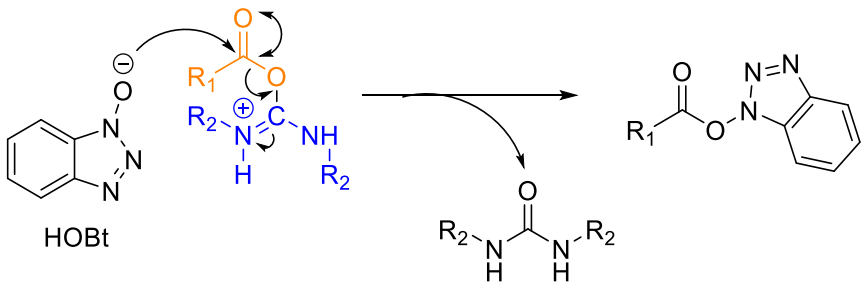

Figure 52: The mechanism by which HOBt prevents racemisation.

The final step of the tryptophan octyl amide synthesis is removing the amine protecting group from **20** which was removed under acidic conditions. The octyl amide tryptophan residue (**21**) was then coupled to protected arginine and purified by RP-HPLC to give RW-Noct (**22**). Fmoc-Lys(Boc)-OH was coupled to **21** to give the protected dipeptide **23** with a yield of 53%. A basic (piperidine) and an acidic (HCl) deprotection afforded KW-Noct (**24**). As not all of the crude was purified and a known concentration was not used at the beginning of the HPLC purification, there are no yields.

From the previous work carried out it is clear that the cationic residue is important for antimicrobial activity.[48] The beginnings of the investigation into the importance of the tryptophan (or an aromatic) residue was described in section 2.1.1.

The replacement of the aromatic residue with a glycine, RGoct, had previously been done and had shown no activity. The ester bond was replaced with an amide in case the ester bond was being broken down by esterases. This was done using the same method which was described earlier in this section. This synthesis route is shown in Scheme 8.

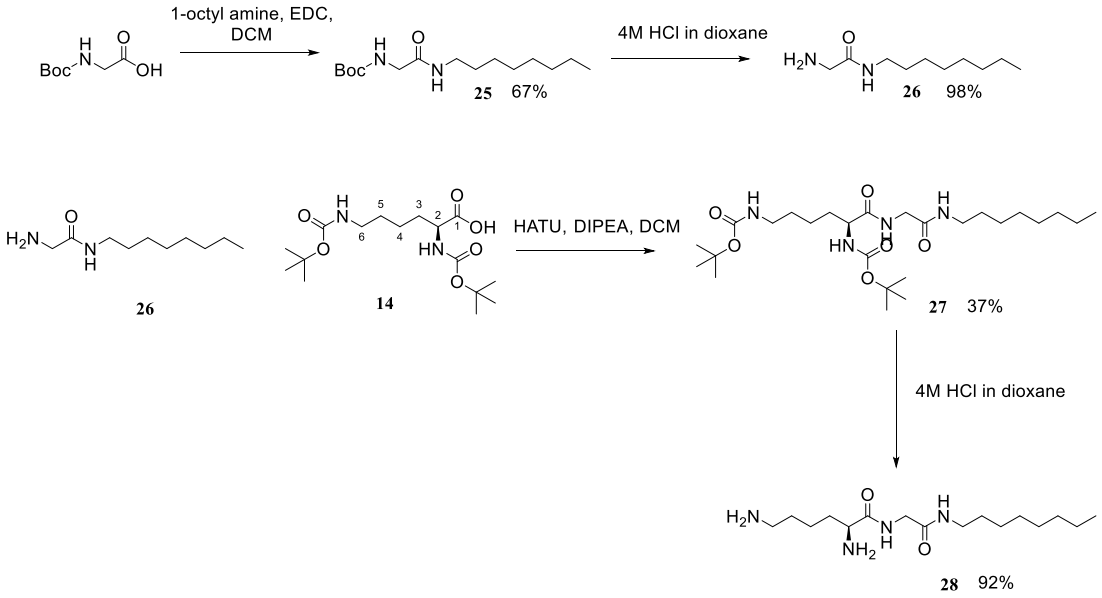

Scheme 8: The synthesis route used for the synthesis of KG-Noct (28)

First Boc-Gly-*N*-oct (**25**) was synthesised by coupling 1-octylamine to Boc-glycine using EDC before being deprotected with HCl to give **26**. For ease of purification we coupled Boc-Lys(Boc)-OH (**14**) to a glycine octyl amide (**26**) using the method previously described. The protected dipeptide **27** was purified by silica chromatography and then deprotected to afford the final dipeptide (KG-Noct **28**).

2.5 Purification of dipeptides

Initial attempts to purify the dipeptides using RP-HPLC were problematic for a number of reasons. The available HPLC machine was intended for analytical separation. Small amounts can be injected into this machine, and the flow rate used and the pressure reached are not suitable for the large scale purification we needed to carry out. The peptide solubility was generally poor, and this could pose issues with precipitation in the machine. Each peak would have to be collected manually and analysed by LRMS in order to determine where the dipeptide eluted. Following the determination of which peak contains the desired product, it would then have to be collected manually which would be time consuming. Finally, each crude material had several side products due to the steps of each reactions carried out without purification prior to the final step. This was the case due to the problems encountered when purifying arginine containing compounds.

In order to avoid this several purification methods were attempted:

1. Recrystallization. Recrystallization from diethyl ether did not leave the dipeptides suitably pure to continue. Attempts to recrystalise from other solvents were also unsuccessful. Liquid-Liquid separations, using Na_2CO_3 (*sat*) and EtOAc were likewise unsuccessful as the arginine side chain remains charged even in the most basic of conditions. An emulsion formed and the layers did not separate.
2. Purification of protected dipeptides. The dipeptides were left protected and then purified using silica chromatography. Boc-Arg(Pbf)-Trp-oct could be purified in this way albeit with a low yield of 2%. As the side chain protecting group could not be removed (Section 2.2.1) the final compound could not be reached. Due to the unprotected arginine side chain being strongly basic and the silica gel being strongly acidic the interaction between the two is strong and irreversible so it was not possible to purify the deprotected dipeptides in this way. Unprotected arginine could not be eluted even when the silica had been deactivated and methanolic ammonia was used as the eluent.
3. Cation exchange chromatography. The arginine side chain was proving to be a hindrance to successful purification so the next purification method was chosen to try and take advantage of the cationic nature of the guanidium group. FPLC using a Mono S cation exchange resin column and a gradient of 0.1M

ammonium acetate to 1M ammonium acetate was used to purify RWhex. A detection wavelength of 280 nm was used for monitoring the elution from the column. All of the peaks were collected but none of the peaks corresponded to the RWhex (determined by LRMS). The dipeptide did not elute. It is likely that on unbinding from the column the poorly soluble dipeptide precipitated in the aqueous conditions and therefore could not elute.

4. Amberlyst 15 cation exchange resin. It is likely that FPLC was unsuccessful because of precipitation. The Amberlyst cation exchange resin uses the same principle but the dipeptide would be more tolerant to the solvent. This is a strongly acidic cation exchange resin which when mixed with the peptide causes the deprotection of the Boc protecting group and binding of the peptide (arginine side chain and amine terminus) to the resin. The resin is washed with a series of solvents and then stirred with ammonia solution (4M in methanol) which exchanges with the peptide. The peptide is now isolated. The concerns with this method were that the ammonia may cause hydrolysis of the ester leading to increased side products and an increased chance of diketopiperazine formation. There is no evidence for this happening from the analysis carried out on the peptides. The method only worked on a small scale (20-50 mg of crude material) and the Boc deprotection was often incomplete. Some peptides were protected with Fmoc and so these could not be successfully purified by this method. Whilst some of the dipeptides were purified in low yield (<8%) using this method the majority of attempts did not yield pure compound therefore this method was not continued.
5. C18-reverse phase silica. This silica resembles that found in RP-HPLC columns. Using this reverse phase silica in a similar manner to a normal silica would mean a larger quantity of material could be loaded onto the column. A gradient of water to acetonitrile was used as eluent. Initially this was carried out in a similar way to normal silica column chromatography however the nature of C18 silica packed very tightly, and this meant the pressure build up from using the bellows was very high and elution was very slow. Changing the apparatus to a Buchner funnel and vacuum pump was more successful. A step wise gradient from of 0% - 100% MeCN + 0.01% TFA was used. This method successfully purified both the Boc protected and acetylated RWoct dipeptides

as small amounts of these dipeptides eluted after the impurities. The unprotected dipeptides eluted at a similar point to the impurities and separation was not possible as the gradient was carried out manually.

6. RP-HPLC. As none of the previously mentioned methods of purification had been suitably successful, RP-HPLC (Synergi™ 4 µm Polar-RP 80 Å) was employed. The peptides were dissolved in MeOH but at the beginning of the gradient (0% MeCN + 0.01% TFA to 100% MeCN + 0.01% TFA (with water + 0.01% TFA) there was precipitation which blocked the machine. The method was optimised so that the run started with a higher concentration of acetonitrile (20%). At this concentration there was not precipitation and the compound had not begun eluting. Some impurities could be washed out at this concentration before the gradient increased to 100% acetonitrile over the next 35 minutes. All the dipeptides from this point were purified by HPLC. TFA is normally used to improve the resolution of the peaks but it was found in our case that there was no need for the addition of TFA and so this was stopped due to toxicity concerns.

Yields are not stated in the experimental section as only the amount of product required for analysis and biological testing was purified (typically 5-10 mg). Some compound is lost during HPLC purification on column and it is possible that there is decomposition under the purification conditions.[109] (As the fractions were collected manually it is hard to account for the delay between the chromatogram on the screen and the collection pipe, and so it is likely that further material is lost here).

2.5.1 Analysis of peptide purity

Following purification using the semi-preparative column (Synergi™ 4 µm Polar-RP 80 Å) the dipeptides were run through the analytic column (Kinetex 5u EVO C18 100A) to ensure they were pure. This is shown in Figure 53. This was used as a method of checking the purity of all of the final compounds synthesised in this project.

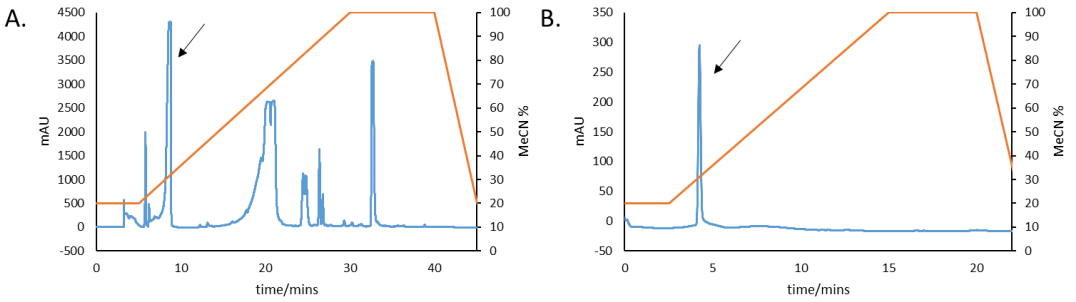

Figure 53. A shows the RP-HPLC trace from the purification of RWoct (blue) with a gradient (orange) of water and MeCN. B. shows the HPLC trace of purified RWoct (blue) and the gradient (orange) of water and MeCN. Both were monitored at 250 nm. The desired compound (RWoct) is indicated with an arrow.

2.6 Conclusion

The series of dipeptides were synthesised using LPPS which was considered to be an advantage in the circumstances over SPPS. A variety of protecting and deprotecting strategies were tested and utilised over the series of dipeptides. Following this the purification by RP-HPLC was carried out. Of the many purification techniques carried out this was the only one which was widely successful. With this series of dipeptides synthesised and purified, the next step was to carry biological tests to determine the antimicrobial activity and the inhibition of MraY. A summary of the synthesis and purification of each dipeptide is shown in Table 5.

Compound	Synthesis issues and solutions
Altering chain length • H_2N-Arg-Trp-*O*-octyl ester (RWoct) **6** • H_2N-Arg-Trp-*O*-hexyl ester (RWhex) **7** • H_2N-Arg-Trp-*O*-decyl ester (RWdec) **8**	▪ Initially the tryptophan esters were synthesised. ▪ Issues arose with the selection of arginine side chain protecting groups. We decided to proceed without a protection of the side chain. ▪ HATU and HBTU used as coupling agents successfully ▪ Several purification methods were tested and success was seen using the Amberlyst 15 resin.
Altering aromatic residue • H_2N-Arg-Tyr-*O*-octyl ester (RYoct) **10** • H_2N-Arg-Phe-*O*-octyl ester (RFoct) **9**	▪ Tyrosine and phenylalanine octyl esters were synthesised and coupled to Fmoc-Arg-OH, this was carried out using HBTU. ▪ It was decided that from this point all arginine containing peptides would be purified using RP-HPLC. Only small amounts were purified due to the limitations of the instrumentation. No meaningful yields were obtained for these and the following arginine containing dipeptides.
Protection of amine • Boc-NH-Arg-Trp-*O*-octyl ester (Boc-RWoct) **11** • Ac-NH-Arg-Trp-*O*-octyl ester (Ac-RWoct) **12**	▪ The Boc protected peptide was synthesised from Boc-Arg-OH and the tryptophan octyl ester with HBTU and purified by RP-HPLC. ▪ RWoct was acetylated with acetic anhydride and purified by RP-HPLC.

Altering cationic residues
• H_2N-Lys-Trp-*O*-octyl ester (KWoct) **16**
• H_2N-His-Trp-*O*-octyl ester (HWoct) **13**
• H_2N-HetArg*-Trp-O-octyl ester (R1Woct) **18**
	▪ Both lysine and histidine can be fully protected with acid labile protecting groups:
	  ▪ Boc-Lys(Boc)-OH
	  ▪ Boc-His(Trt)-OH
	▪ These were coupled to the tryptophan octyl ester using HBTU/HATU and the resulting peptide could be purified used silica column chromatography.
	▪ .The protecting groups were easily removed in HCl and following precipitation in Et_2O no further purification was required.

Functional group change: amide • H_2N-Lys-Trp-*N*-octyl ester (KW-Noct) **24** • H_2N-Lys-Gly-*N*-octyl ester (KG-Noct) **28** • H_2N-Arg-Trp-*N*-octyl ester (RW-Noct) **22**	▪ Firstly the tryptophan/glycine octyl amide was synthesised. ▪ This was then coupled using HATU to the cationic residue and purified using the relevant methods described above for arginine or lysine containing dipeptides.

Table 5: Summary of the synthesis and purification of the dipeptide series.

CHAPTER 3: BIOLOGICAL EVALUATION OF DIPEPTIDE ANALOGUES

In order to determine the antimicrobial activity and inhibition of MraY, a number of biological assays were carried out, which are described in this chapter. Antimicrobial testing was carried out using a microtitre broth serial dilution method. A continuous fluorescence assay and a radiochemical assay were utilised to determine the inhibition of the MraY by the dipeptides, and an assay involving the overexpression of MraY in *E.coli* was also be carried out to determine the same thing. Finally an assay which uses a resazurin based dye to determine the viability of cells was used to determine if pores are being formed in the membranes when treated with the dipeptides.

The results of these assays will determine the functional groups which will be included in the peptidomimetics which was designed and synthesised in chapters 4 and 5. The antimicrobial testing, inhibition assay and cell pore test (described in this chapter) was be carried out on the peptidomimetics.

3.1 Antimicrobial testing

Previous work by Rodolis et al. showed that the dipeptide RWoct (**6**) had antimicrobial activity against *E. coli*, *P. putida* and *B. subtilis.*[48,87] Based on this activity a set of cationic dipeptides with alkyl chains were designed and synthesised (see chapter 2). We will test these compounds to see if the changes we have made will increase the antimicrobial activity.

3.1.1 Microtitre Broth Dilution Method

A microtitre broth dilution method was used to quantify the antibacterial properties of the dipeptides. This method is used commonly for its high throughput screening of potential antimicrobial agents.[110] From the results, it is possible to calculate the minimum inhibitory concentration (MIC) and the concentration at which the growth of the bacteria is reduced by 50% MIC_{50}. Figure 54 shows how these values are calculated.

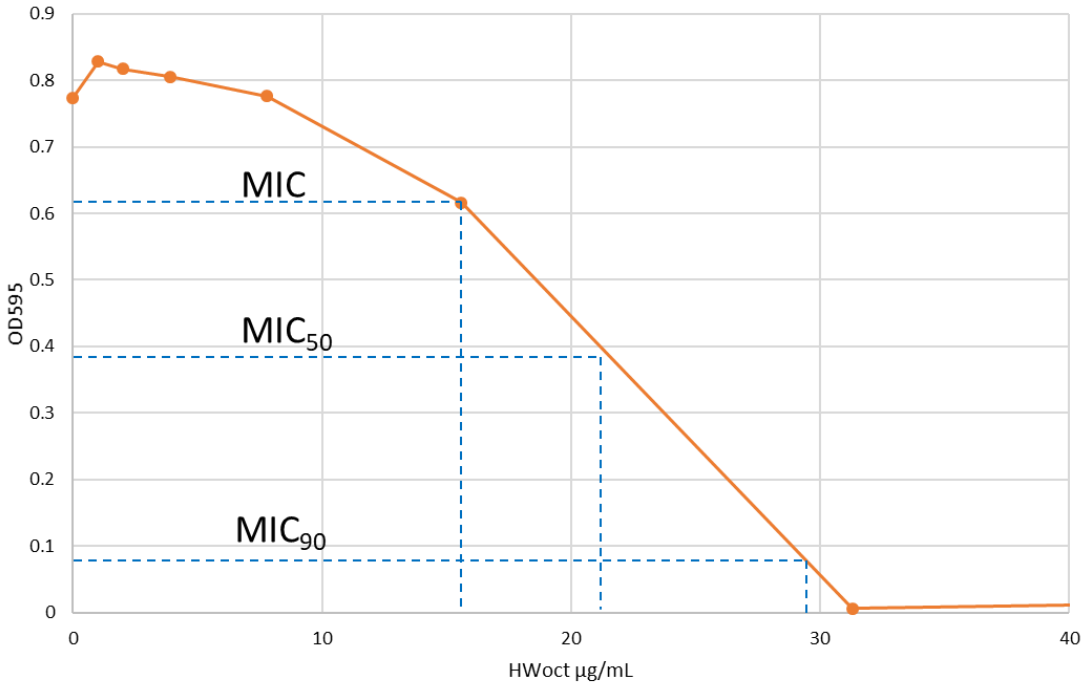

Figure 54: The graph shows how the MIC, MIC_{50} and MIC_{90} are calculated from the results of the antimicrobial testing by microtiter broth dilution. The graph showed the growth inhibition of *Pseudomonas fluorescens* (PF-5) by HWoct.

The number of colony forming units (CFU) of bacteria in the starting culture must be known and maintained for all experiments. To do this the Miles and Misra method was used to calculate the correct dilution factor of the bacterial culture which would give us 1000 colony forming units per mL of culture (CFU/mL) in each well.[111] Each strain of bacteria is inoculated and incubated overnight (at either 30 or 37˚C). The cultures are then diluted. A dilution series carried out (10^{-1}, 10^{-2}, 10^{-3}, 10^{-4}, 10^{-5}, 10^{-6}, 10^{-7} and 10^{-8} fold dilution). From each dilution 20 µL is taken and dropped onto an agar plate and incubated. Some dilutions will not have distinct single colonies but for the dilutions where there are the colonies are counted. The number of colonies is multiplied by 50 to give the CFU/mL. The dilution for which CFU/mL=1000 is chosen.

Once the CFU/mL was found, the overnight bacterial cultures could be diluted to the correct concentration. To a sterile 96-well plate, 190 µL of seeded broth (CFU/mL=10^3) was added to each well. To this, 10 µL of dipeptide solution was added to give a total volume of 200 µL. The inhibitors were prepared by first making a 2.5 mg/mL solution in methanol or DMSO and a twofold dilution series carried out using water. The final inhibitor concentration in the wells was 125, 62.5, 31.25, 15.63, 7.82, 3.90, 1.95 and 0.97 µg/mL. The plates were covered with a sterile lid or film and incubated for 14 hours.

Each compound was tested in triplicate for each bacteria. A number of controls were run which included a media blank, media blank and MeOH/DMSO and media and inhibitor. An example of a typical plate is shown in Figure 55.

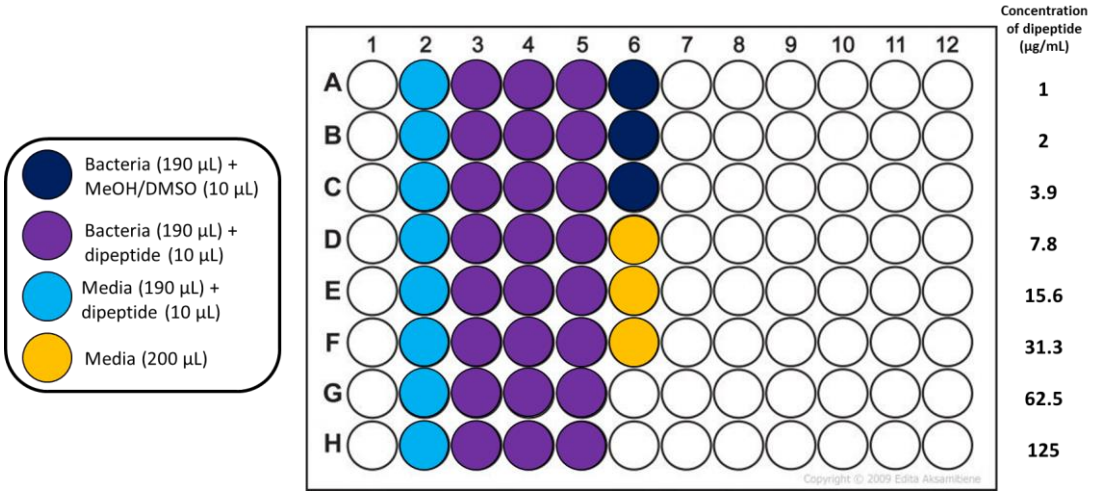

Figure 55: An example of the contents of each well of the 96-well plates used to calculate the MIC_{50} values for each dipeptide.

For each compound three plates were prepared with the compound tested in triplicate on each plate. On each plate the average OD_{595} for each concentration of inhibitor was calculated. The average OD_{595} values were plotted against concentration of inhibitor as shown in Figure 54 and the MIC_{50} was calculated for each plate. An average of these MIC_{50} values was taken for each compound and the standard error calculated. This would allow us to determine whether the differences in MIC_{50} we saw were significant.

3.1.2 Assay optimisation

The original protocol used deep well 96-well plates which can hold up to 1.1 mL of media. These plates needed to be sterilised before each use. From the autoclave process, water often got trapped in the wells. When the assay was run on these plates, the concentration of the bacteria and inhibitor was decreased, and so the results were not reliable. These plates also required a sterile film to be stuck over the top, and this occasionally introduced contamination. To overcome this, normal depth plates with lids which had been pre-sterilised were purchased, and these can hold 300 µL of media.

When checking the growth of the bacteria in the deep well plate, it was found that *Rhodococcus. jostii* did not grow in the time that the plate was incubated. This is likely because the incubation time wasn't long enough, due to the lag phase in the growth of

this organism coupled with the insufficient aeration in the wells. The use of *R. jostii* was withdrawn. The growth of the remaining chosen bacteria was retested in the normal plates. *E. coli* and *P. putida* grew normally in these plates, however *B. subtilis* did not. When testing against *B. subtilis,* the deep well plates were used, and extra care was taken to ensure they were dry after sterilisation.

Initially the bacteria were grown in LB. The results were inconsistent with large variation within each plate. LB media provided a limited amount of carbon sources which can but utilised by bacteria and around a third of the amount of Mg^{2+} (~30 mM) that *E. coli* requires.[112] *E. coli* is thought to need 100 mM Mg^{2+} to bridge the highly negatively charged lipopolysaccharide molecules in its outer membrane.[112,113] It is likely that the integrity of the membrane is compromised and could be causing the variability in the data. Mueller-Hinton broth was designed to be used for MIC determination, containing around 500 µmol per litre of Mg^{2+}. Where the test compounds are cationic Mueller-Hinton 2 (cation adjusted) can be used. The use of this media prevents the inhibitors interacting with the media and affecting the results.[114] All of the tests carried out using LB were repeated using the cation adjusted Mueller-Hinton broth and this method gave consistent MIC values, and so was used for all the testing from this point.

3.1.3 Antimicrobial MIC_{50} testing

After optimising the assay, all of the inhibitors was tested against *P. fluorescens, E.coli* and *B. subtilis.* From this data the MIC_{50} values were calculated and shown in Table 6.

	MIC_{50} µg/mL		
	***E. coli* (TOP10)**	***B. subtilis* (W23)**	***P. Fluorescens* (PF-5)**
Ampicillin	2±0	-	-
RWhex (7)	37±5	13±2	53±3
RWoct (6)	5±1	13±1	18±2
RWdec (8)	3±0	8±1	3±0
Boc-RWoct (11)	12±3	8±3	21±8
Ac-RWoct (12)	42±2	9±2	19±7
HWoct (13)	8±2	12±1	21±3
R^1Woct* (18)	9±0	10±1	45±1
KWoct (16)	2±0	1±1	5±1
RYoct (10)	118±1	25±2	124±5
RFoct (9)	11±3	11±2	64±6
RW-Noct (22)**	3±2	7±1	20±3
KW-Noct (24)**	17±1	11±5	26±6
KG-Noct (28)**	10±1	2±1	18±1

Table 6: The results of the antimicrobial testing carried out on the series of dipeptides. The three organisms tested against were *E. coli, B. Subtilis* and *P. fluorescens*. *R1=heterocyclic arginine. **Noct= amide linked octyl chain.

The MIC_{50} values for each of the compounds against *E. coli* (TOP10) can be compared with the positive control (ampicillin). KWoct is able to match that level of antimicrobial activity and shows the best activity against both *B. subtilis* and *P. fluorescens*. With RW-Noct and RWdec having a comparable activity to amipicillin against *E. coli*.

These values cannot be compared to those obtained by Rodolis (Table 2) due to different strains of bacteria being used.

3.1.4 ESKAPE pathogen MIC data

The six bacterial pathogens which are commonly associated with bacterial disease are combined to give the acronym ESKAPE.[115,116] The ESKAPE pathogens are *Enterococcus faecium*, *Staphylococcus aureus*, *Klebsiella pneumonia*, *Acinetobacter baumannii*, *Pseudomonas aeruginosa* and *Enterobacter*. The acronym is also a reference to their ability to escape the effects of commonly used antibiotics. These pathogens have an increased resistance to antibiotics which are commonly used clinicaly, including penicillin and vancomycin. Mechanisms of resistance displayed by these pathogens include β-lactamases deactivating β-lactams, biofilm production and modification of the target site. Efflux pumps are also able to pump antibiotics out of some of the Gram-negative pathogens.[117]

A selection of dipeptides were submitted to the Warwick University antimicrobial screening facility and the MIC and MBC values against the ESKAPE pathogens were determined by John Moat and Julie Todd. The results are shown in Table 8. The positive controls which were carried out are shown in Table 7. The positive controls are ciprofloxacin, penicillin G and colistin. Ciproflaxin is a fluoroquinolone which works by inhibiting DNA gyrase. Penicillin G inhibits peptidoglycan biosynthesis. Colistin is polymyxin E which is a last resort drug which behaves as a detergent.

The MBC is the minimum bactericidal concentration. This is the lowest concentration of compound which is require to kill a given pathogen. Antimicrobial agents are usually considered to be bactericidal if the MBC is no more than four times the MIC.[118]

	ciprofloxacin	penicillin G	colistin
	MIC	MIC	MIC
Enterobacter cloacae NCTC 13405			
Staphylococcus aureus ATCC 29213	1.6	<0.5	
Klebsiella pueumoniae ATCC 700603			
Acinetobacter baumanni ATCC 19606			
Pseudomonas aeruginosa NCTC 13437			4
Enterococcus faecium JH2			

Table 7: Positive controls of ciprofloxacin, penicillin G and colistin against some of the ESKAPE pathogens

	RWoct (6)		KWoct (16)		RWNoct (22)		KWNoct (24)	
	MIC	MBC	MIC	MBC	MIC	MBC	MIC	MBC
Enterobacter cloacae NCTC 13405	>256	-	32	32	64	64	64	64
Staphylococcus aureus ATCC 29213	>256	-	16	32	8	8	32	32
Klebsiella pueumoniae ATCC 700603	>256	-	64	64	>128	>128	>128	>128
Acinetobacter baumanni ATCC 19606	>256	-	64	64	64	64	64	64
Pseudomonas aeruginosa NCTC 13437	>256	-	8	128	64	128	64	128
Enterococcus faecium JH2	>256	-	8	32	64	64	64	64

Table 8: The MIC and MBC values in µg/mL of the four selected dipeptides against the ESKAPE pathogens

The dipeptide RWoct showed no observable activity against the ESKAPE pathogens. The activity of RWNoct and KWNoct was very similar, with both showing the best activity against *S. aureus*. However when comparing the dipeptide data to the positive controls none reach that level of antimicrobial activity The data for both implies that they are bactericidal agents, based on the relationship between the MIC and the MBC values. KWoct has the best activity overall against the ESKAPE pathogens out of the

four dipeptides tested. This data indicates that KWoct is also acting in a bactericidal manner.

3.1.5 Conclusion

After optimising the protocol, antimicrobial data was obtained for all of the dipeptides. All of the dipeptides synthesised had activity against the 3 strains of bacteria.

Based on this data (Table 6) we can conclude that the tryptophan residue is important for antimicrobial activity, more so than the other aromatic residues tested. The dipeptide containing phenylalanine shows better activity than the tyrosine containing peptide. (Order of activity Trp>Phe>Tyr). This shows that there is not a favourable hydrogen bonding occurring at the hydroxyl group of the tyrosine side chain. Rodolis *et al.* showed the importance of the tryptophan residue by replacing it with a glycine residue. RGoct showed no antimicrobial activity. However the dipeptide KG-Noct showed activity which was comparable to RWoct. This may be because of the amide bond linker (which replaced the ester linker), or that KG-Noct has a different mechanism of action to RGoct.

Of the dipeptides with the varied chain length the decyl ester gave the lowest MIC_{50} value, this could be because its longer alkyl chain allows it to insert into the membrane more readily.

The protected dipeptides showed no improvement of MIC_{50}, although they were still active, and so protecting groups will not be used when designing the peptidomimetics.

Several cationic residues were used and both arginine and lysine showed the good activity over all the bacterial strains, but the KWoct showed the best activity. Both the HWoct and R1Woct were incorporated in the hope they would be involved in π-cation stacking, but showed no improvement on the MIC_{50} of RWoct.

When comparing the amides and the esters to each other it has not been possible to conclude which is a better choice. In the arginine series, RW-Noct has a lower MIC_{50} than RWoct, whereas in the lysine series, KWoct has a lower MIC_{50} than KW-Noct. This suggests that the arginine dipeptides may be working via a different mechanism

to the lysine dipeptides. It is also possible that alkyl chains (mainly the ester linked) could be removed *in vivo* by esterase and peptidase activity.

Through these observations it is likely that there are a number of mechanisms of action occurring within this series of dipeptides. Further tests will be needed to help elucidate these.

Based on the data obtained against the ESKAPE pathogens it is likely that KWoct, RWNoct and KWNoct are acting in a bactericidal manner. The data also supports the conclusion already made that the ester and amide linkers may have different mechanisms of action, as well as there being differences between the arginine and lysine residues.

3.2 Continuous Fluorescence Assay for MraY Activity

One of the main aims of this project was to synthesise a compound which showed antimicrobial activity and inhibited MraY. Previously Maria Rodolis showed that RWoct did not inhibit MraY, whereas GWoct did show inhibition.[87] However GWoct showed no antimicrobial activity, whereas RWoct did. The series of dipeptides which we have synthesised was tested using a continuous fluorescence assay, to determine whether the compounds inhibit MraY as well as having antimicrobial activity.

The continuous fluorescence assay was developed by Brandish (1995) and was then further optimised by Mihalyi (2013). This assay can quantitatively measure the *in vitro* inhibition of MraY.[28,119] The substrate of MraY (UDPMurNAc-pentapeptide) is isolated and then a dansyl fluorescent group is attached, which exhibits polarity dependent fluorescence. (Figure 56) When lipid 1 is formed by MraY using the dansylated substrate, this polarity dependent change in fluorescence gives a two fold increase in fluorescence intensity.

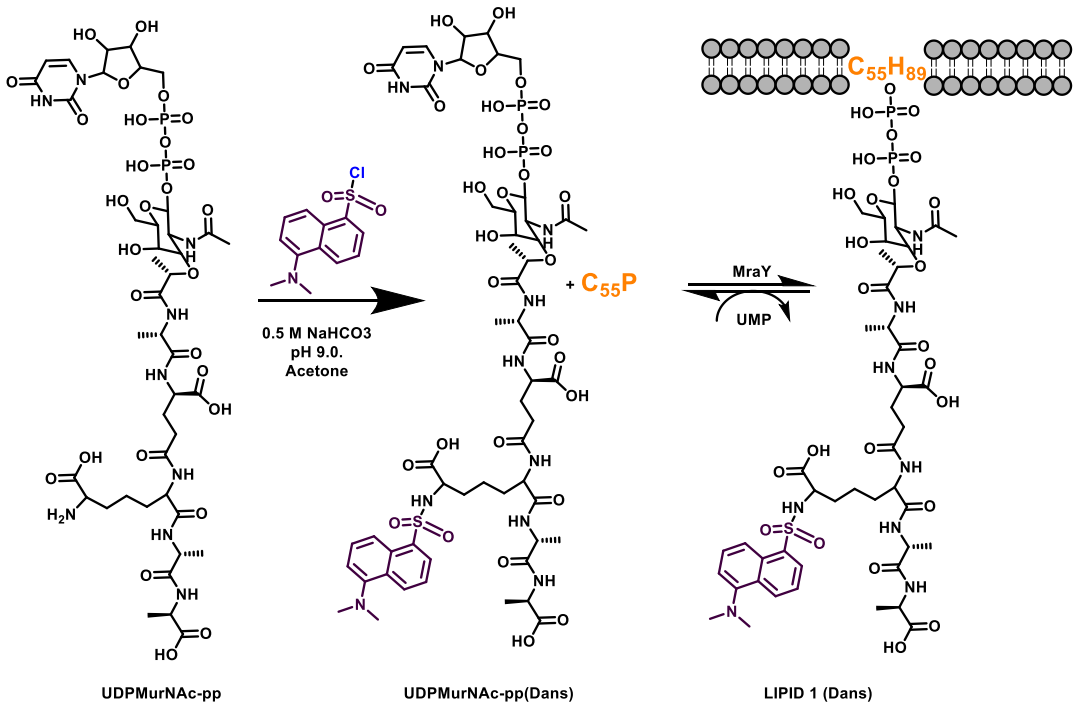

Figure 56: The reaction of UDPMurNAc-pp and dansyl chloride to give the dansylated MraY substrate UDPMurNAc-pp(Dans). This is followed by the dansylated substrates reaction with the lipid carrier to form Lipid 1 (Dans).

3.2.1 Preparation of UDPMurNAc-pentapeptide from Bacillus subtillis

A dansyl group can be attached to DAP residue of the UDPMurNAc-pentapeptide (Figure 56). This was previously prepared by a summer student (Namrita Modgill), using UDPMurNAc-pentapeptide purchased from BaCWAN. The preparation of cell wall intermediates was not continued after 2015 by BaCWAN and no other providers are available.

The substrate for MraY (UDPMurNAc-pentapeptide) was previously isolated from antibiotic treated cells of *B. subtilis* by Brandish *et al.*[28] As *B. subtilis* is a Gram positive bacteria it is more suitable for producing cell wall intermediates, but differs from other Gram positive bacteria as it uses diamiopimelic acid (DAP) at the third position of the pentapeptide instead of lysine. This DAP containing pentapeptide is the natural substrate for *E. coli* MraY. The preparation of UDP-MurNAc-pentapeptide involved growing *B. subtilis* W23 in a rich medium (PYP) to mid-logarithmic phase, when the rate of cell wall synthesis is at its highest. The cell pellets were then collected and resuspended in cell wall synthesis medium (CWSM). This medium contains 12.5 mg/mL vancomycin, 50 mg/mL chloroamphenicol and 50 mg/mL ampicillin. Vancomycin is a glycopeptide which inhibits the second stage of cell wall biosynthesis but inhibiting the polymerization of the phosphodisaccharide-pentapeptide lipid complex.[120] It binds to D-Ala-D-Ala of the pentapeptide unit of lipid 2, leading to the accumulation of UDPMurNAc-pentapeptide. The use of ampicillin (transpeptidase inhibitor) gave Brandish *et al.* greater yields, whereas Chloroamphenicol has a damaging effect on bacterial protein synthesis.[121] This medium also contains uracil, and the amino acids found in the pentapeptide unit, to increase the yield. The cells were grown in CWSM for 45 minutes at 37°C and the cells were then collected by centrifugation. The pellets were initially resuspended in 5% (w/v) TCA (5 mL/g cells). to precipitate the macromolecules as done by Brandish. After several attempts with little success, the cells were lysed using the cell disruptor. This prevented the cell wall intermediates being treated with strong acid which may lead to their breakdown. The sample was initially purified by gel filtration (Sephadex G25, 3 x 80 cm), eluting with water. The fractions were analysed using UV spectroscopy. Any fractions containing an absorbance at 262 nm were collected and analysed. Mass spectrometry was needed to identify which peak contained the desired product. UDPMurNAc-pp was not seen in any of the fractions collected. Attempts to purify UDPMurNAc-pentapeptide were

then carried out using C_{18} reverse phase HPLC, using a gradient of 0:100 to 30:70 Acetonitrile/ 0.05M aqueous NH_4HCO_3 as previously carried out by Siricilla *et al.*[122] The peaks were collected and de-salted before submitting to Lijiang Song for LC-MS analysis. One peak did showed 1194.3464 $[M+H]^+$ corresponding to UDPMurNAcpp, and this peak was collected. After many runs the amount of material collected was less than 2 mg, which was not sufficient for analysis by NMR. A small scale dansylation was carried out on the product. The reaction is shown in Figure 57. LC-MS analysis provided no evidence that the dansylated substrate had been formed.

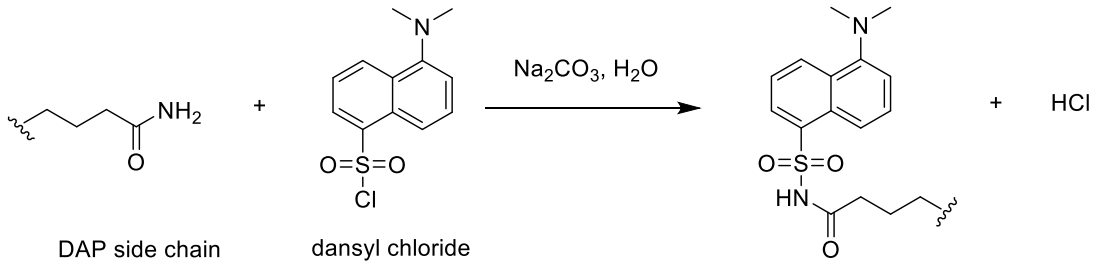

Figure 57: The reactions which occurs between the DAP side chain amide and dansyl chloride under basic conditions (pH ≅ 9.5) in water. This reaction was carried out on the DAP containing UDPMurNAc-pentapeptide.

The substrate preparation was attempted more than ten times with a variety of techniques (including changes to the cell lysis technique, alterations to the antibiotics used and purification techniques and eluents) used to try and improve the success of the substrate synthesis and isolation. None were successful and the stocks made by Namrita Modgill were used on the inhibition assay for the duration of this project.

3.2.2 Continuous fluorescence assay protocol

For this assay the preparation of *E. coli* membranes overexpressing MraY must be done in advance. This was previously carried out by Mihalyi (2013) using the C43 strain of *E. coli* containing plasmid pET52b-MraY, overexpressing *E. coli* MraY. These membranes were aliquoted and stored at -80 °C are still viable and was used in the assay.

The dansyl group is able to exhibit polarity dependent fluorescence. The polarity dependent change in fluorescence is seen when the transfer of phosphor-MurNAc-pentapeptide to the lipid carrier (undecaprenyl phosphate) has occurred, forming lipid 1. When UDPMurNAc-pentapeptide is added to the membranes with MraY overexpressed and undecaprenyl phosphate a blue shift in fluorescence is seen indicating the formation of Lipid 1. When tunicamycin a natural inhibitor of MraY is added no increase in fluorescence is observed as lipid 1 is not formed.

The entire dipeptide series was subjected to the assay in triplicate. The inhibitors were added to the well of the 96-well plate to give a final concentration of 125 µg/mL. The excitation wavelength was 340 nm and the emission was measured at 530 nm. The results of the assay of the dipeptides which were considered to have the best antimicrobial activity based on the previous assay are shown in Figure 58. Also in Figure 58 are shown the two controls, a methanol blank and tunicamycin. None of the dipeptides show inhibition of MraY under these conditions.

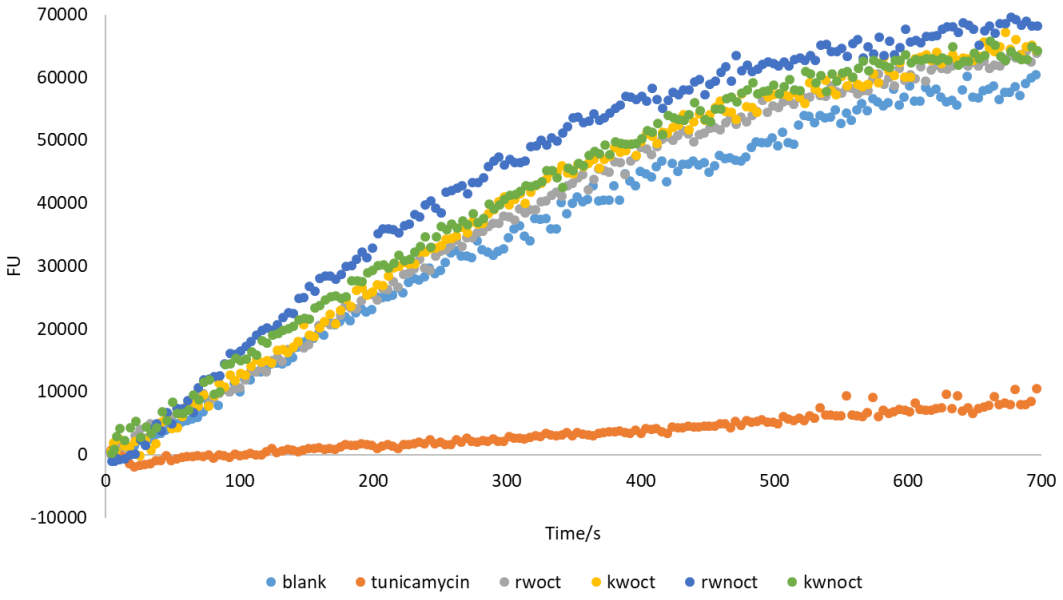

Figure 58: The fluorescence reading of the MraY inhibition assay over 700 seconds of four of the dipeptides which are considered to have the best antimicrobial activity. The final concentrations of the peptides is 125 µg/mL. The MeOH blank and tunicamycin (20 µg/mL) controls are shown.

3.2.2 Conclusion

No inhibition was seen by RWoct or related dipeptides, which is consistent with the observations made by Rodolis. Rodolis then examined the effect of MraY overexpression on the MIC of RWoct. Their data from this assay indicated an interaction between MraY and RWoct. This assay will be discussed in section 3.4.

This assay alone is insufficient in the determination of an interaction between MraY and the dipeptides. There is no observable evidence that the protein complex which is predicted to form is actually forming. In order to confirm an interaction at MraY further biological data would need to be obtained. One method of doing this would have been to carry out a pull down assay. Pull down assays allow the isolation of protein complexes by adsorbing the complex onto beads. Firstly however it would be important to determine if there is truly an interaction between Epep and MraY as this is the interaction which the dipeptides are based on.

3.3 Radiochemical assay for the determination of MraY inhibition

Due to the limited amount of dansylated UDPMurNAc-pentapeptide not all of the compounds synthesised in this project could be tested using the fluorescence based inhibition assay (section 3.2).

An alternate method to determine the inhibition of MraY uses [^{14}C]-UDPMurNAc-pentapeptide (phosphor-MurNAc-L-Ala-γ-D-Glu-m-DAP-[^{14}C]-D-Ala-[^{14}C]-D-Ala). The preparation of the substrate was carried out by Agnes Mihalyi using a procedure based on the method used by P. Brandish at Smith Kline Beecham Pharmaceuticals in 1991.

The radiolabelled substrate is mixed with C_{55}-P, inhibitor and over expressed E. coli membranes (prepared by Maria Rodolis) and then left for 30 minutes to allow the formation of radiolabelled lipid I.[22] The reaction is quenched with pyridinium acetate and butanol is added. Separation occurs between the organic butanol and aqueous reaction mixture. The unconverted radiolabelled substrate remains in the aqueous layer whilst the radiolabelled lipid I is extracted into the organic butanol layer. This butanol layer is carefully removed and added to scintillation fluid. The ionizing radiation of these samples can be detected and measured using a liquid scintillation counter. By comparing the counts of the samples containing inhibitor to those of the controls it is possible to determine the percentage inhibition of the inhibitors.

The controls used are as follows: scintillation fluid on its own, substrate with no enzyme, tunicamycin and no inhibitor. The scintillation fluid control allows the deduction of the background radiation from all of the samples. The substrate with no enzyme serves as an extraction control. Tunicamycin is an inhibitor of MraY and serves as a negative control. The sample with no inhibitor gives a value which represents 100 % activity of MraY.

The assay was carried out with the help of Prof. Tim Bugg, and the samples were analysed by the Warwick Univeristy Life Sciences Radiochemical Department.

3.3.1 Radiochemical inhibition assay results dipeptides

Two of the dipeptides were tested with this assay to allow comparison with the peptidomimetics which will be described in chapters 4 and 5. The results are shown in the bar chart below (Figure 59).

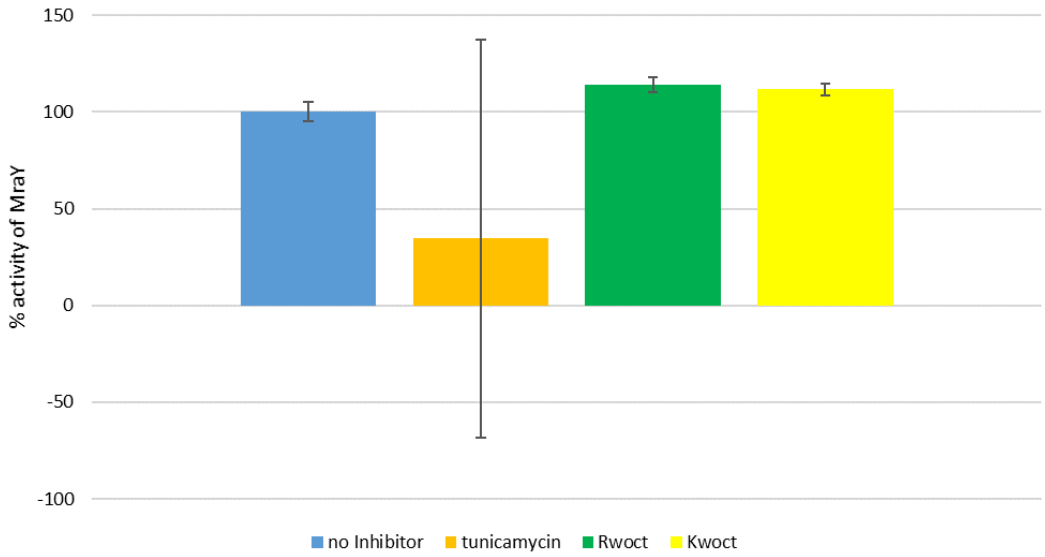

Figure 59: A bar chart showing the % activity of MraY with no inhibitors and when treated with 200 µM RWoct (6) and KWoct (16) with the controls which use no inhibitor (100% activity) and tunicamycin (100 µg/mL)

The large error bars seen on the tunicamycin value are due to a reading which is thought to be higher because of static interference, which is occasionally seen in assays of this type. In an assay previously run by Prof. Tim Bugg the tunicamycin inhibition of MraY was 96%.

The percentage activity calculated for MraY when treated with both RWoct (**6**) and KWoct (**16**) is higher than the no inhibitor sample which gives the 100% MraY activity value. Prior to commencing the assay the error was estimated to be around 5% however based on this assay it is higher this. Whilst the error between duplicates is low (see error bars on bar chart), the RWoct (**6**) and KWoct (**16**) samples compared to the no inhibitor sample show some disagreement. Possible causes of this error could be from pipetting errors. For future assays it may be advisable to remove a smaller portion of butanol to insure no aqueous layer is removed. Due to time restraints no further assays

were carried out and so this data is preliminary. From this data however there is no evidence of RWoct (**6**) and KWoct (**16**) inhibiting MraY.

3.4 Effect of overexpression of MraY on antimicrobial MIC

Zheng *et al.* (2008) showed that when MraY was overexpressed on a pBAD30 plasmid it was able to protect against infection by the ΦX174 E gene, which was expressed on a λ prophage. This can be explained by a 1:1 complex being formed formed between the enzyme and inhibitor, therefore increasing the amount of MraY can protect against inhitibitors. As RWoct had shown antimicrobial activity against *E. coli* this method could be used to investigate the interaction with MraY *in vivo*. An increase in IC_{50} would be seen if a complex than led to inhibition formed between MraY and RWoct. This is shown pictorially in

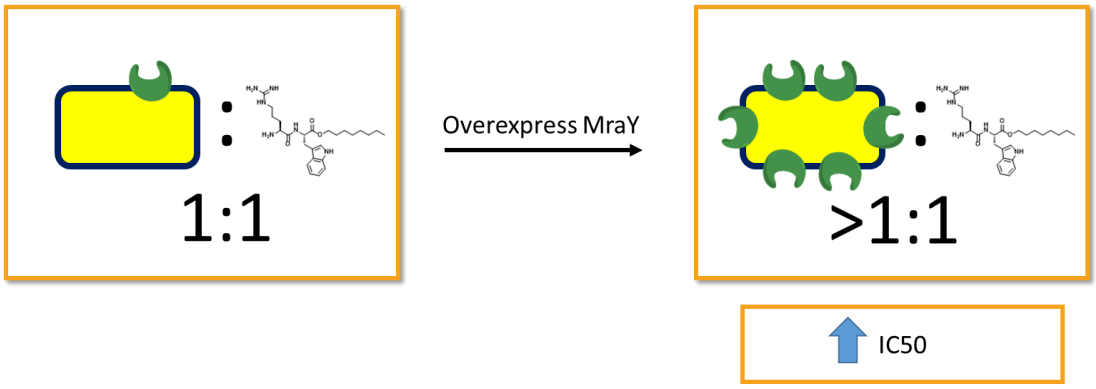

Figure 60: schematic of the overexpression of MraY protecting against RWoct. [Yellow rectangle represents bacteria and green shape represents MraY]

This result was seen by Rodolis and is shown in Table 9.[87] This time a pET52b plasmid was used instead of pBAD30.

	MIC (µg/mL)				
	WT E. coli	**(-) control Empty pET52b**	**MraY**	**F288L**	**E287A**
RWoct	31	31	250	500	300

Table 9: The MIC results seen by Rodolis when MraY (and the two mutants F288L and E287A) were over expressed in the presence of RWoct.

3.4.1 Testing of dipeptides

The four most promising compounds (based on the antimicrobial testing) from the series of dipeptides: RWoct (**6**), RW-Noct (**22**), KWoct (**16**) and KW-Noct (**24**) were chosen to initially test via this method. None of these compounds showed inhibition of MraY based on the data obtained from the *in vitro* fluorescence assay (section 3.2.2) but had all shown antimicrobial activity (section 3.1.3).

The overexpression experiment was carried out using a similar protocol to Rodolis.[87] A pET52b vector which contained WT MraY, E287A MraY or F288L MraY was used. This vector contains a T7 RNA polymerase promoter and terminator which allowed the transcription of the *mraY* genes when induced with IPTG. The target gene which is downstream from the T7 promoter is transcribed from the vector by the bacteriophage T7 polymerase.[123] The overexpression of integral membrane proteins has been shown to be toxic to *E.coli* in some instances and had been observed earlier by Lloyd *et al*. (2004).[22] Rodolis conducted a growth experiment to ensure the concentration of IPTG did not cause toxic levels of overexpression and normal cell growth occurred.[87] It was found that 0.5 mM IPTG did not affect the growth of the bacteria.

Usually BL21 *E. coli* is used as the host strain in T7 promoter systems, however Lloyd *et al.* (2004) previously showed that higher levels of MraY expression can be achieved using *E.coli* C43. C43 is a mutant strain of BL21, which has been shown to tolerate the overexpression of integral membrane proteins without the toxic effects.[22,124]

The overexpression assay was carried out on 96-well plates in a similar way to the antimicrobial testing with the controls previously mentioned. The addition of ampicillin (100 μg/mL) to the media of *E.coli* was included where the plasmids were present to ensure plasmid maintenance.

An explanation of the further controls and the expected results are shown in Table 10.

C43 + plasmid	Title on MIC_{50} table	Expected result
No plasmid	C43	MIC_{50} value of dipeptide against C43
pET52b 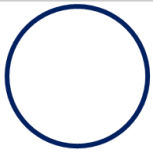	Empty	MIC_{50} value should be the same as C43 as this plasmid does not contain any genes for the overexpression of MraY
pET52b with WT MraY 	WT	MIC_{50} value should be higher than both empty and C43 as WT MraY is overexpressed
pET52b with F288L MraY 	F288L	MIC_{50} value should be higher that wild type. This variant is thought to protect against Epep.
pET52b with E287A MraY 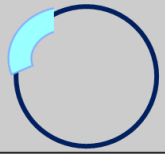	E287A	MIC_{50} value should be higher that wild type. This variant is thought to protect against Epep.

Table 10: an explanation of the controls used to determine the results of the overexpression assay. The expected results are explained and the nomenclature used in table 10.

The plates were incubated for 8 hours at 37˚C and then absorbance measurements taken at 595 nm (OD_{595}). The IC_{50} values calculated are shown below in Table 11 and Figure 61.

	MIC_{50} µg/mL					
	C43	**pET52b**	**WT**	**E287A**	**F288L**	**TOP10**
RWoct (6)	80	>250	239	200	156	5
RW-Noct (22)	14	200	236	>250	200	3
KWoct (16)	24	50	26	100	15	2
KW-Noct (24)	44	>250	>250	>250	>250	17

Table 11: The table shows the calculated IC50 values for the four selected peptides against the 5 C43 *E. coli* which contain no plasmid, an empty plasmid, WT MraY or one of the two mutant MraY (E287A or F288L) which are under control of the T7 promotor. This data is displayed in Figure 61.

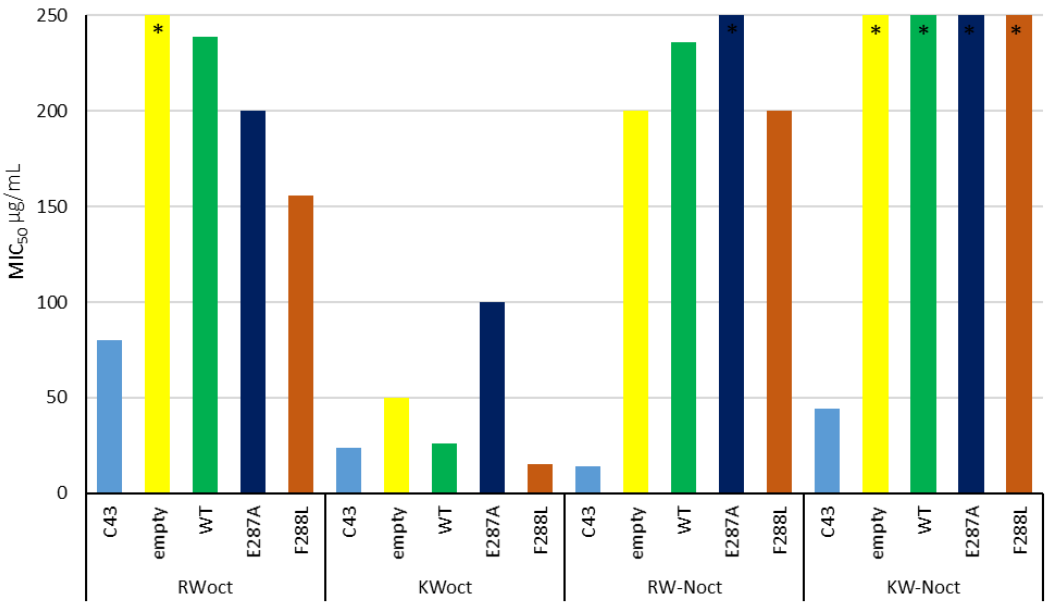

Figure 61: The graph shows the calculated MIC_{50} values for the four selected peptides against the 5 C43 *E. coli* which contain no plasmid, an empty plasmid, WT MraY or one of the two mutant MraY (E287A or F288L) which are under control of the T7 promotor. This data is shown in Table 11. (* shows where the MIC50 exceeds 250 µg/mL)

The MIC_{50} values for all of the inhibitors were higher in C43 *E. coli* than in TOP10 *E. coli*. The C43 strain is more resistant to toxic proteins and this might indicate why the MIC_{50} is higher that the TOP10 strain.

The MIC_{50} values for the empty plasmid are higher than the MIC_{50} values for the C43 strain. Therefore, although the MIC_{50} values are higher than C43 when MraY is overexpressed, this is primarily due to some effect of the pET52b plasmid, so the increase in MIC observed by Rodolis may not be due to MraY overexpression.

Also the data obtained for KWoct (**16**) shows a different pattern, so it is possible that its mechanism of action differs from the other dipeptides. Based on the results the initial conclusion is that there is a gene on the pET52b plasmid which is leading to an increase in MIC_{50}, which is not *mraY*.

3.4.2 Troubleshooting of the overexpression assay

In order to be able to interpret this data it is first necessary to determine why the empty plasmid increases the MIC_{50} against the four inhibitors. The three differences between the conditions was the addition of 0.5 mM IPTG, the addition of 0.29 mM ampicillin and the pET52b plasmid. Ampicillin, an antibiotic, would cause a decrease in growth rather than protecting the bacteria. Ampicillin does cause the plasmid to be retained but this was accounted for in the controls used. As IPTG has been used in this sort of assay many times it was unlikely to be the reason for the increased IC50. However an increase in MraY expression could make the bacteria more vulnerable to lysis. This said where pET52b was present (with and without *mraY* over expression) an increase in MIC_{50} was seen, and the growth of the bacteria was not stunted by the addition of IPTG when compared to C43. TOP10 and C43 were tested against RWoct (**6**) in the presence of 0.5 mM IPTG to establish whether IPTG was effecting the growth. This is shown in Figure 62.

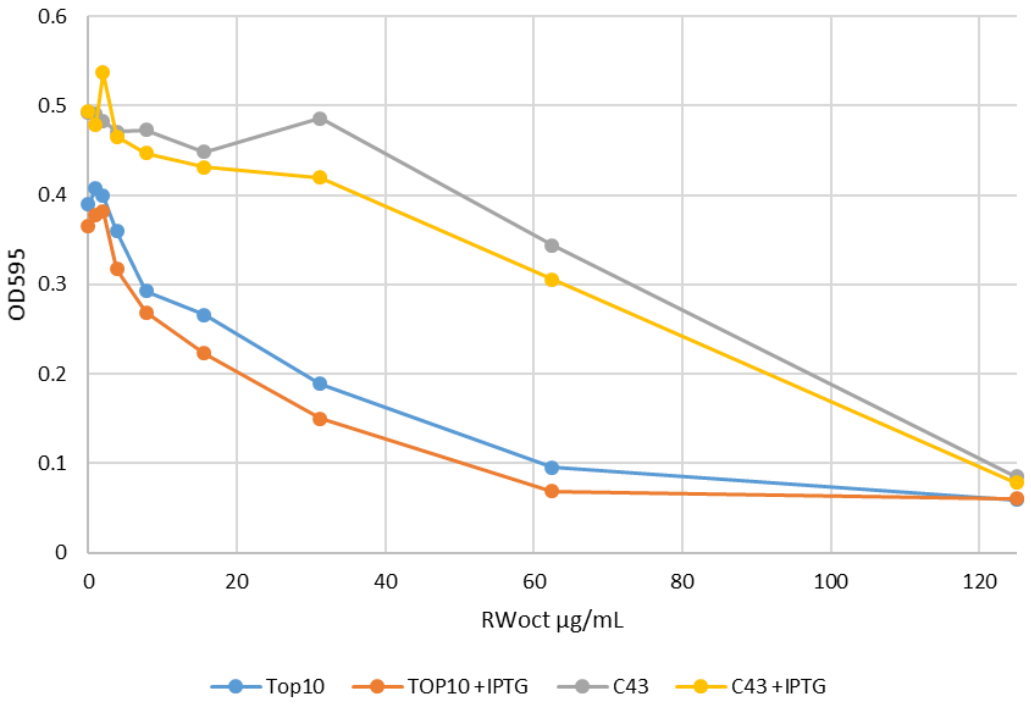

Figure 62: This graph shows the effect that the concentration of RWoct (6) has on the concentration of E. coli TOP10 and C43, with and without the 0.5 mM IPTG

A notable change which had been caused by the introduction of the pET52b plasmid is the resistance to ampicillin which is caused by the β-lactamase gene.

With the aim of determining whether the β-lactamase gene caused the protection against the inhibitors an IC_{50} determination experiment was carried out with RWoct. This time 3 "empty" plasmids containing different resistance genes were transformed into TOP10 *E. coli*. For the ampicillin resistance pET52b was used again and pET28a (kanamycin resistance) and pBR322 (tetracycline resistance) were used. Colonies were picked and grown overnight in LB with the associated antibiotic. The cultures were diluted 100-fold in the morning with MH2 plus the working concentration of antibiotic. The seeded broth was added to 96-well plates with RWoct and KWoct as previously described. The plates were incubated at 37˚C for 8 hours. The data from this experiment is shown below in Table 12 and Figure 63.

	MIC_{50} µg/mL			
	E. coli (TOP10)	**pET52b + 100 µg/mL Amp**	**pET28a + 50 µg/mL Kan**	**pET28a + 50 µg/mL Tet**
RWoct (6)	18	250	38	42
KWoct (16)	5	14	4	4

Table 12: The IC_{50} values calculated when E. coli TOP10 with and without plasmids conferring resistance to ampicillin, kanamycin and tetracycline were treated with the respective antibiotic and RWoct and KWoct.

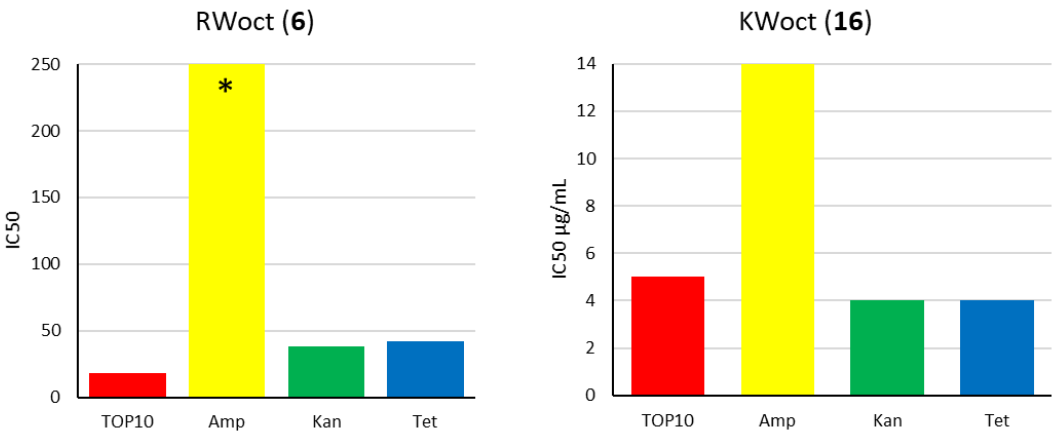

Figure 63: Graphs showing The IC50 values calculated when E. coli TOP10 with and without plasmids conferring resistance to ampicillin, kanamycin and tetracycline were treated with the respective antibiotic and RWoct (Left) and KWoct (Right). Amp=ampicillin resistance gene, Kan=kanamycin resistance gene and Tet=tetracycline resistance gene.

The data obtained from this experiment clearly shows that the plasmid containing the β-lactamase gene (ampicillin resistance) increases MIC_{50} RWoct and KWoct. Both the kanamycin and tetracycline resistant *E. coli* showed a similar IC_{50} to TOP10 (without a resistance gene). The protection which seems to be caused by the ampicillin resistance gene rather than the kanamycin or tetracycline resistance genes could be due to the differing mechanisms of action of these antibiotics.

Ampicillin is a β-lactam containing antibiotic which inhibits cell wall biosynthesis. Ampicillin is able to penetrate the cell wall where it then binds irreversibly to transpeptidases,[125] which catalyse the last step of peptidoglycan biosynthesis. The β-lactamase gene found in the pET52b vectors, leads to the production of the β-lactamase enzyme which opens the β-lactam ring of ampicillin, rendering it inactive (Figure 64).[126]

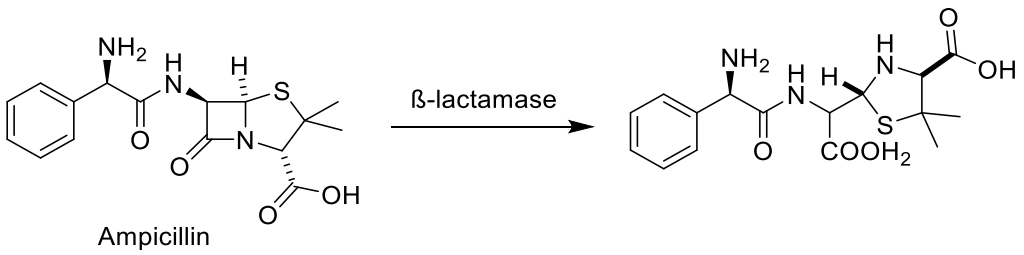

Figure 64: The chemical change that ampicillin undergoes at the active site of a β-lactamase. The β-lactamase gene on the pET52b plasmid allows the bacteria to be resistant to ampicillin.

Kanamycin is an aminoglycoside antibiotic which inhibits protein synthesis. Kanamycin irreversibly binds to the 30S subunit of prokaryote ribosomes.[127] This causes the incorrect alignment of mRNA triggering mistranslation and the incorrect amino acid being inserted. As a result a non-functional peptide is produced. The gene which encodes kanamycin resistance (found is pET28a) is the neomycin phosphotransferase (*npt*) gene.[128] The gene encodes for aminoglycoside 3'-phosphotransferase enzyme. Kanamycin is inactivated by this enzyme by the addition of a phosphate group (from ATP) to the 3'-hydroxyl group (Figure 65).

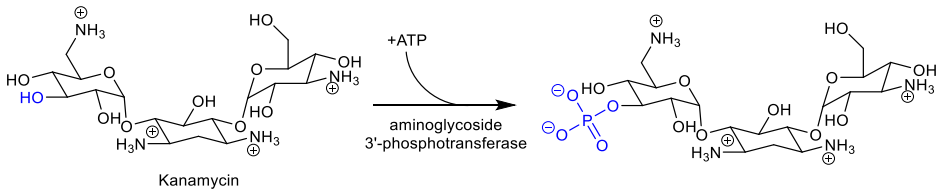

Figure 65: The addition of a phosphate group to kanamycin by aminoglycoside 3'-phosphotransferase enzyme causing its inactivation. This is the reaction which occurs allowing bacteria with which possess the pET28a plasmid to be resistant to kanamycin.

The two antibiotics have very different mechanisms of action and the resistance genes have very different effects on the drug molecules. Ampicillin has a site of action in the cell wall which we expect our dipeptides also do. A possible cause for the β-lactamase gene causing resistance against our compounds could be hydrolysis of the peptides causing them to become inactive. However this is unlikely as two of the peptides tested did not contain ester bonds, and there is no literature evidence to support this. As our

compounds do not have a 3'-hydroxyl group or a phosphate group, phosphorylation will not occur and the compound's activity will not be effected by this gene. So we decided to use a kanamycin resistance cassette for this assay instead of the ampicillin resistance gene.

A further consideration is that ampicillin interacts with the peptides in some way and deactivating them. To determine if this is the case an MIC_{50} was carried out as described in section 3.1 with RWoct. The cells were also treated with a sub MIC_{50} amount of ampicillin (0.8 μg/mL). If ampicillin was inactivating the peptide the MIC_{50} would increase. The results of this assay are shown in Table 13.

	MIC_{50} μg/mL	
	RWoct without ampicillin	**RWoct with ampicillin (0.8 μg/mL)**
***E. coli* TOP10**	5	4

Table 13: The MIC_{50} values calculated for the treatment of *E. coli* C43 treated with RWoct (6) with and without ampicillin (0.8 μg/mL).

The MIC_{50} of RWoct (**6**) is decreased upon the addition of ampicillin. This shows that ampicillin is not deactivating RWoct (**6**). *E. coli* C43 was did not grow when treated with 0.8 μg/mL of ampicillin and so whilst it is unlikely that ampicillin interacts with RWoct in C43 it is not possible to definitively conclude that.

3.4.3 Antibiotic Cassette Replacement - Transferring the MraY gene from pET52b to pET28a

We wanted to create a plasmid which contained the *mraY* gene under control of the T7 promotor and the kanamycin resistance cassette. It was important that the plasmid did not contain an active β-lactamase gene.

Our first attempt would remove the *mraY* gene from the pET52b vector (Figure 66) and place this into the kanamycin resistance gene containing vector: pET28a (Figure 67).

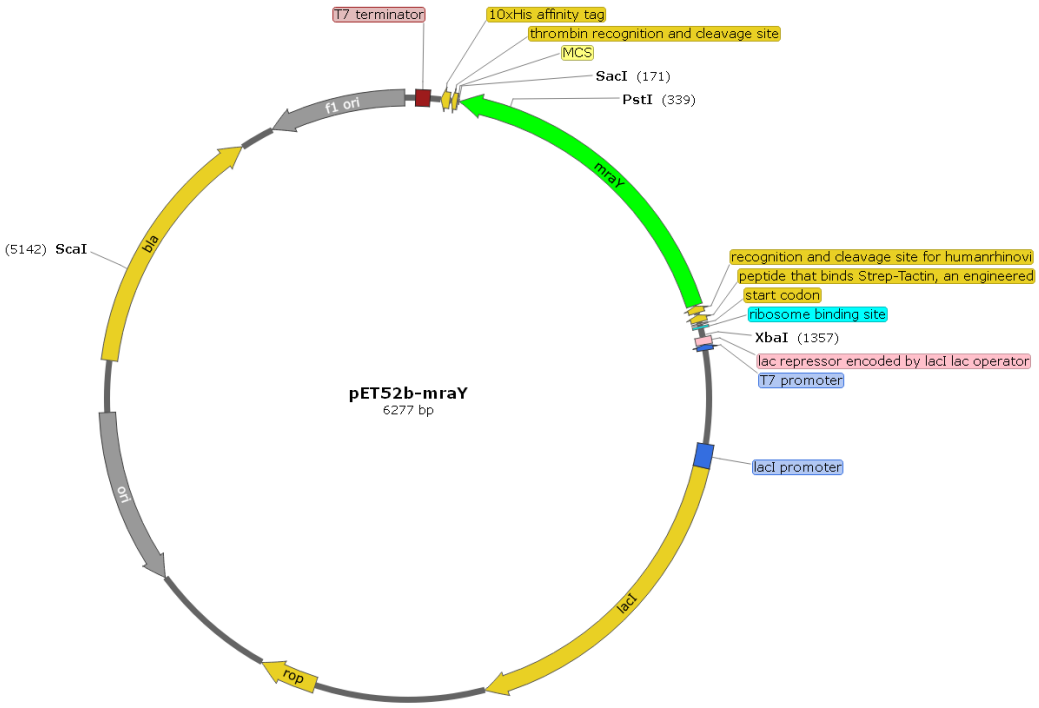

Figure 66: Plasmid map showing the pET52b plasmid containing the *mraY* gene under the control of a T7 promoter. (β-lactamase gene are abbreviated to "bla")

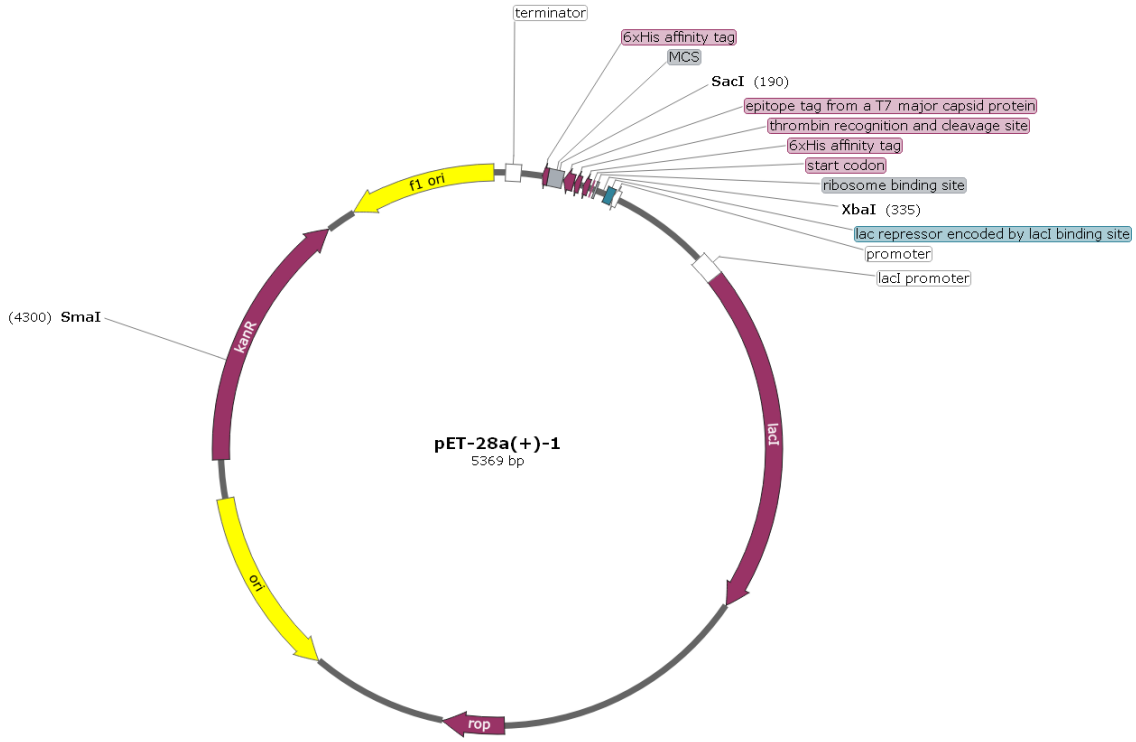

Figure 67: Plasmid map of pET28a

To do this, appropriate restriction sites on both plasmids needed to be found. *Sac*I and *Xba*I were the enzymes used to digest the two plasmids (restriction sites shown on both plasmid maps in Figure 66 and Figure 67). This released the *mraY* insert from pET52b and opened the pET28a vector in the appropriate place. The insert and vector were combined with T4 DNA ligase overnight at 16˚C. The ligation mix was transformed into *E. coli* TOP10, and then spread onto LB+Kan (50 µg/mL) agar plates, which were incubated at 37˚C overnight. A ligation mix which contained no insert was also prepared in the same way, and this would show whether self-ligation was occurring. This plate showed that self-ligation was occurring. The number of self-ligating colonies was similar to the number of colonies on the pET28a-MraY ligation plate. This indicated that it was likely these colonies had self-ligated and did not contain the MraY gene. Both of the enzymes cut the DNA and left sticky ends (Figure 68), which should have prevented self-ligation occurring,

Figure 68: The restriction sites for *Sac*I and *Xba*I which give sticky ends.

To further confirm that self-ligation had occurred 30 colonies were picked and the plasmid DNA extracted. To confirm if the *mraY* gene had been inserted, a restriction site within the gene and in the vector were chosen. *Pst*I and *Sma*I are shown on the plasmid maps in Figure 66 and Figure 67. Then the cut DNA was run on an agarose electrophoresis gel only two bands were seen. (Figure 69). We would expect to see three bands if the desired plasmid had been successfully cut with these two enzymes. This coupled with the evidence of self ligation showed that the insertion of the *mraY* gene under the control of a T7 promoter had been unsuccessful.

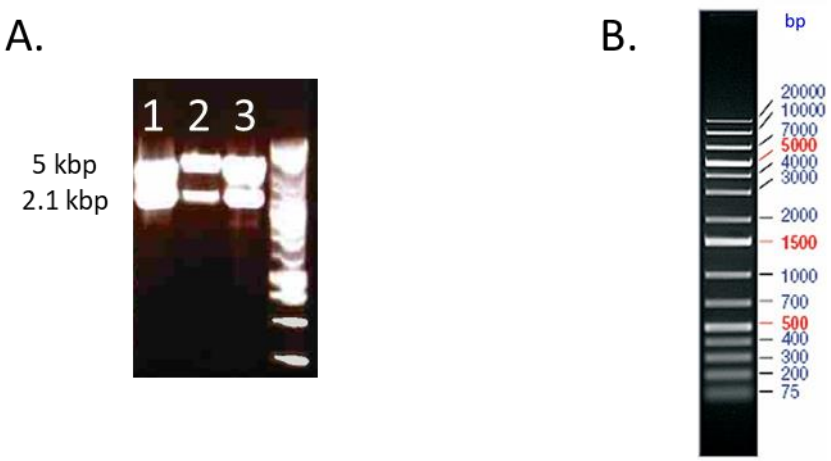

Figure 69: A. The agarose electrophoresis gel of plasmids created from the ligation of the MraY insert and a cut pET28a plasmid using *Pst*I and *Sma*I (1-3 show the same reaction but 3 separate attempts). The presence of only two bands showed that the ligation was not successful. B. the 1kb gene ruler purchased from thermofisher used for all the agarose electrophoresis gels in this chapter.

3.4.4 Antibiotic Cassette Replacement - Transferring the kanamycin cassette to pET52b

As we could not insert the *mraY* gene into pET28a, we then attempted to place the kanamycin resistance gene into the pET52b plasmid which already contains the *mraY* gene. This method would require us to remove or disrupt the ampicillin resistance gene. Within this gene there is a *Sca*I restriction site (Figure 70). This enzyme was used to digest pET52b and the enzyme was then denatured by heating the mixture to 80˚C for 20 minutes.

*Sca*I

Figure 70: The restriction site of *Sca*I which creates blunt ends.

To the now open pET52b plasmid we needed to ligate the kanamycin resistance cassette. The kanamycin cassette from the plasmid pALM-kan was amplified using PCR. (Figure 71). The kanamycin cassette which was 1.4 kbp was isolated on an agarose electrophoresis gel and then extracted.

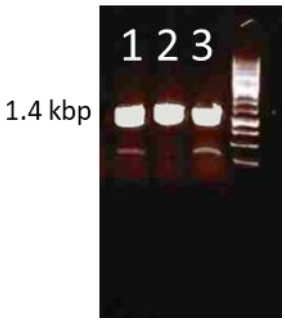

Figure 71: This agarose electrophoresis gel shows the kanamycin resistance cassette (approximately 1.4 kbp) which had been amplified by PCR from the plasmid pALM-kan. The DNA from this band was extracted. (Lanes 1-3 shows three successful attempts of the same reaction).

The cassette was added to the open pET52b vector and ligase was added. The ligation mix was transformed into *E. coli* TOP10, which was spread onto LB+Kan (50 μg/mL)

agar plates, which were incubated at 37˚C overnight. Any colonies which grew on these plates had to contain the kanamycin resistance gene and 10 colonies were obtained. It was therefore very likely these were the desired plasmid, however because the cut plasmid and insert had blunt ends it was possible other products had formed. This plasmid is shown in Figure 72.

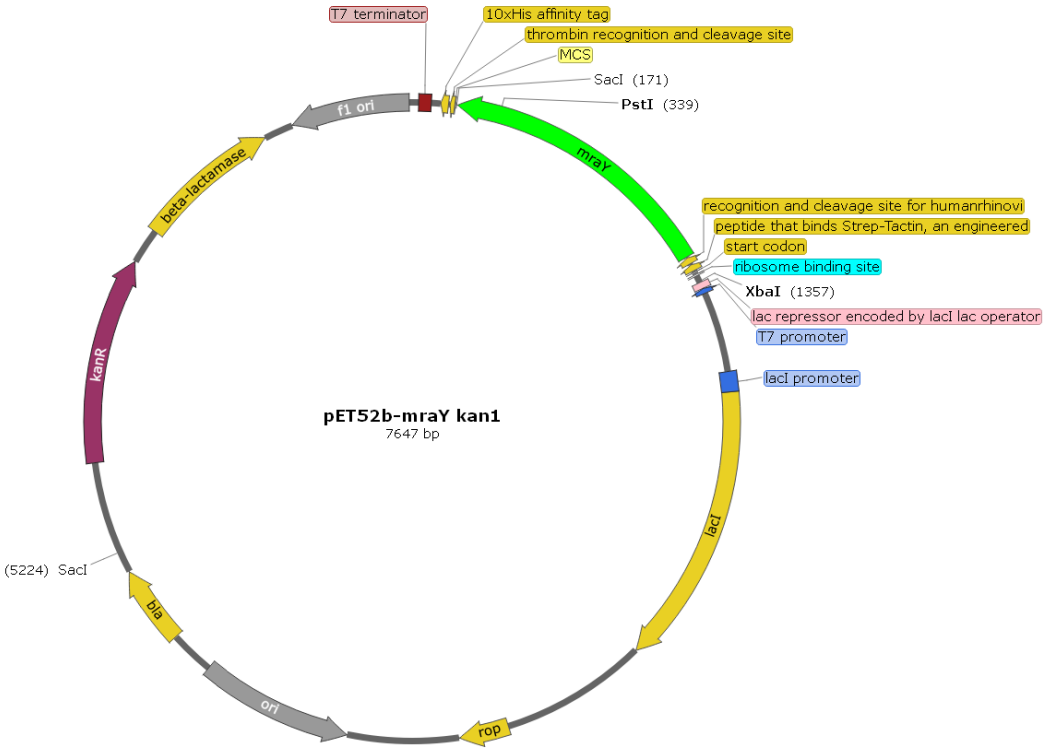

Figure 72: Plasmid map the pET52b-MraY plasmid with the kanamycin resistance gene inserted and the β-lactamase gene disrupted (shown in two parts "bla" and "beta-lactamase".

To confirm that the product was correct, the plasmid DNA was extracted from the 10 colonies which had grown, and then digested with PstI and XbaI. From this digest we would expect to see bands at around 1.0 and 6.6 kbp on an agarose electrophoresis gel. The gel is shown in Figure 73, and it shows that colonies 3-10 had been cut as expected.

Figure 73: The agarose electrophoresis gel which shows the plasmid DNA extracted from the 10 colonies which grew after the ligation between pET52b (cut with *Sac*I) and the kanamycin resistance cassette. This DNA had been digested with *Pst*I and *Xba*I. The expected bands of 1 (orange box) and 6.6 kbp (blue box) can be seen in samples 3-10. (lanes 1-10 show the 10 different colonies which were obtained)

As the cut sites were both blunt ended it meant the kanamycin resistance gene (*kan*) could be inserted into the plasmid running forwards and backwards. Whilst it was thought it wouldn't affect the function of the gene, this still needed to be checked. If both the forward and backward gene behaved the same one direction would be selected and this choice would be maintained for all of the plasmids.

To determine the direction of the cassette *Sac*I was employed to digest the extracted plasmid. The digestion was run on an agarose electrophoresis gel and gave two different patterns depending on the direction of the cassette. This result is seen as the *SacI* cut site is at one end of the kanamycin cassette. The forward direct was considered to be the same direction as the β-lactamase gene. (Forward: 5 and 2.6 kbp. Backward: 6.2 and 1.2 kbp). The results of the gel are shown in Figure 74. Both directions of the *kan* cassette had the same activity when tested against kanamycin.

The creation of the new plasmid and determination of the kanamycin cassette direction were repeated for the two mutant plasmids and the empty plasmid.

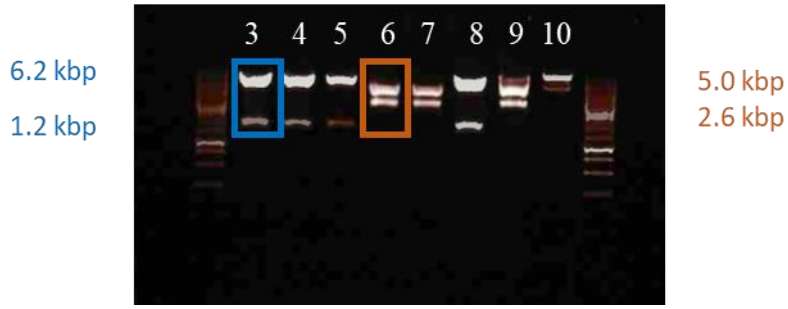

Figure 74: The agarose electrophoresis gel which shows the pET52b-MraY-Kan plasmid when cut with *Sac*I. This digest was used to determine the direction of the kanamycin resistance cassette which had been inserted into the pET52b plasmid which contained the MraY gene under the control of a T7 promoter. This plasmid had been cut in the β-lactamase gene to disrupt the ampicillin resistance. The orange box shows the band pattern from the cassette being inserted forwards and the blue box backwards. (lanes 3-10 show the 7 of the 10 different colonies which were obtained)

After successfully cloning the kanamycin resistance gene into the pET52b vectors by cutting the β-lactamase gene it was important to confirm that that gene was no longer functional. The forwards and backwards pET52b-MraYKan were transformed into *E. coli* TOP10 and a single colony was inoculated in LB+Kan and incubated at 37 ˚C overnight. *E. coli* TOP10 was also inoculated in LB and incubated overnight. The cultures were diluted to 1000 CFU/mL and 190 µL of seeded broth was added to the wells of a sterile 96-well plate. To this 10 µL of ampicillin (final concentrations 125, 62.5, 31.25, 15.63, 7.82, 3.90, 1.95 and 0.98 µg/mL) was added. The plates were incubated for 16 hours at 37˚C and then absorbance measurements taken at 595 nm (OD_{595}).

The results are shown in Figure 75. The data shows that β-lactamase gene is no longer active as the MIC for the two pET52b-MraYKan plasmids is the same as *E. coli* TOP10. The graph also shows pET52b which has the intact β-lactamase gene and so the growth of the bacteria is not affected by ampicillin. Based on this we deemed the forward pET52b-MraYKan plasmids suitable to be transformed in *E. coli* C43 and to be used in the overexpression protection assay. The results obtained should now reflect the effects of over expressing MraY rather than that of the β-lactamase gene.

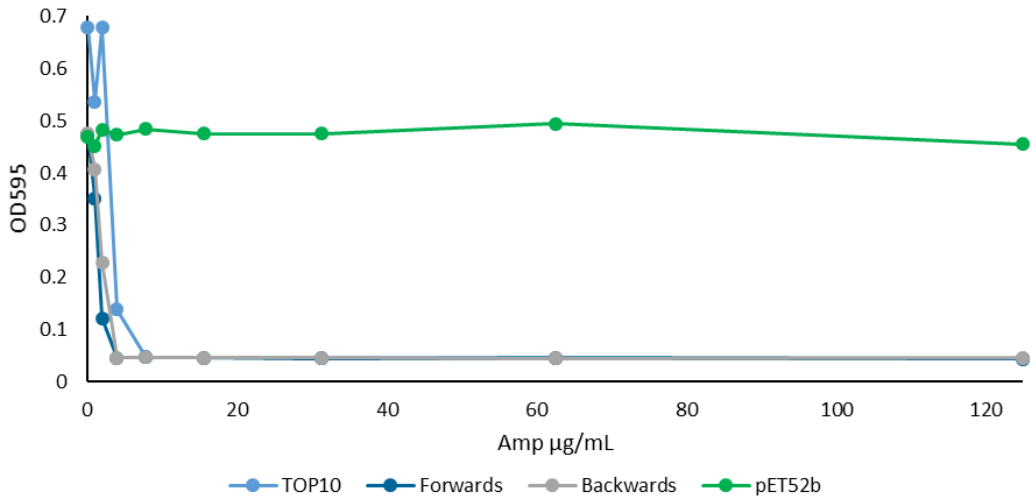

Figure 75: The graph shows the concentration of four bacteria containing different plasmids which had been treated with increasing concentrations of ampicillin and incubated for 16 hours. The four bacteria were *E. coli* TOP10 containing no plasmid, pET52b-MraYKan with the kanamycin cassette forwards and backwards and pET52b (ampicillin resistant).

3.4.5 Testing the overexpression of MraY using a kanamycin resistance cassette

The overexpression assay could now be repeated as before (using kanamycin resistance instead of ampicillin). This time the assay was run using only RWoct.

The MIC_{50} values calculated from this data are shown in Table 14.

	MIC_{50} µg/mL				
	C43	**empty**	**WT**	**E287A**	**F288L**
RWoct	75	135	86	60	75

Table 14: The table showing the MIC_{50} results of the protection assay with the new kanamycin resistant plasmids which were made in section 3.4.4

The MIC_{50} values with the exception of the empty plasmid do not differ greatly. However, Figure 76 clearly shows that when MraY is overexpressed the growth of the bacteria inhibited compared to both the empty and C43 (no plasmid). This indicates that the overexpression of MraY is having toxic effects which were not seen when the

assay was previously carried out. The empty plasmid which was treated with IPTG shows no stunted growth further indicating that the MraY overexpression is responsible for the effect seen. Therefore, it is not possible to determine if there is a relationship between RWoct and MraY from this data.

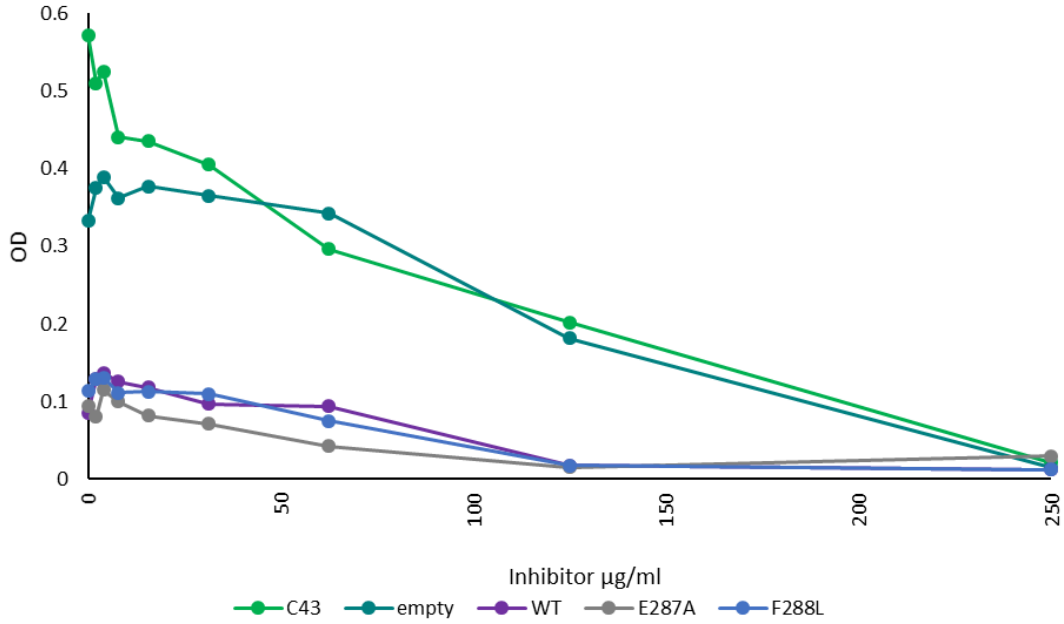

Figure 76: The graph generated from the determination of the IC50 values of the protection assay with RWoct. This shows that the growth of the bacteria in the samples where MraY is overexpressed (WT, E287A and F288L) and no RWoct was added is inhibited when compared to C43 (no plasmid) and empty (no overexpression of MraY).

The growth of the E. coli was not effected when overexpressing MraY using the original pET52b plasmids. This might indicate that MraY was not being overexpressed, and this could be a result of the plasmids not being maintained. During the course of the assay the concentration of ampicillin will decrease as it is inactivated by the β-lactamase. These enzymes will continue to deactivate ampicillin in the media even after the host cell has lysed. As the concentration of the ampicillin drops there is no advantage maintain the plasmids, particularly because of the overexpression of a toxic protein (MraY). Therefore the population of bacteria seen at the end of the assay my not contain the pET52b plasmids.

3.4.6 Conclusion

Evidence to determine whether inhibition of MraY was occurring *in vivo* could not be obtained from the data acquired from the multiple attempts at this assay.

3.5 Membrane permeabilisation assay

It is known that many cationic antimicrobial peptides have multiple mechanisms of action, and so it is possible that this is the case for the series of dipeptide synthesised in this project.[56]

An alternate or additional mechanism of action would be that the peptides could permeabilise the membrane. The dipeptides have a lipophilic alkyl chain and polar charged head group which are the two properties which make up surfactants. An example of a cationic surfactant is shown in Figure 77. Surfactants can act as detergents and disrupt membranes, and this characteristic would make the dipeptides toxic to both bacteria and human cells. Cationic antimicrobial peptides (notably ones containing arginine and tryptophan) are known to create pores in cell membranes because of their detergent-like abilities.[56,59]

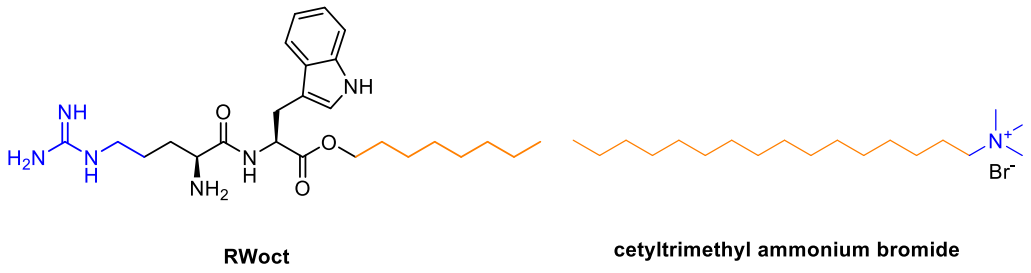

Figure 77: The comparison of RWoct to cationic surfactant cetltrimethyl ammonium bromide. The cationic head groups of the two compounds are shown in blue and the lipophilic tales are shown in orange.

Previously Rodolis carried out an assay using a fluorescent dye, NPN, to determine whether membrane permeabilisation was occurring.[87] NPN is a fluorescent dye which is non-polar and exhibits an increase in fluorescence when in phospholipid environments compared to aqueous environments (Figure 78).[129] There was no evidence of membrane permeabilisation by RWoct. Attempts to repeat this assay were unsuccessful, and this was likely due to the insolubility of the dye. As this assay was time consuming and not suitable for screening many compounds an alternate protocol would be beneficial.

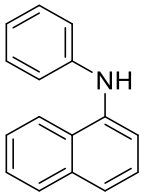

Figure 78: The fluorescent dye N-phenylnaphthalen-1-amine (NPN)

3.5.1 Resazurin Based Assay

In order to test the new series of dipeptides which may differ in their mechanism of action compared to RWoct an alternate dye was sourced.

Resazurin is a blue dye that is weakly fluorescent but can be reduced irreversibly to resorufin which is red and highly fluorescent.[130] (Figure 79). Resazurin was first used to quantify bacterial content in milk by Pesch and Simmert in 1929.[131] It is commonly used in cell viability assays as an indicator of oxidation/reduction.[132,133] Resazurin is able to cross the cell membrane and there the irreversible reaction is proportional to aerobic respiration. Resazurin is the active ingredient in the cell viability reagent alamarBlue™. There are other reagents which can be used in a similar manner (MTT/XTT) but alamarBlue™ has a much lower toxicity and therefore can be used over longer periods of time.[134]

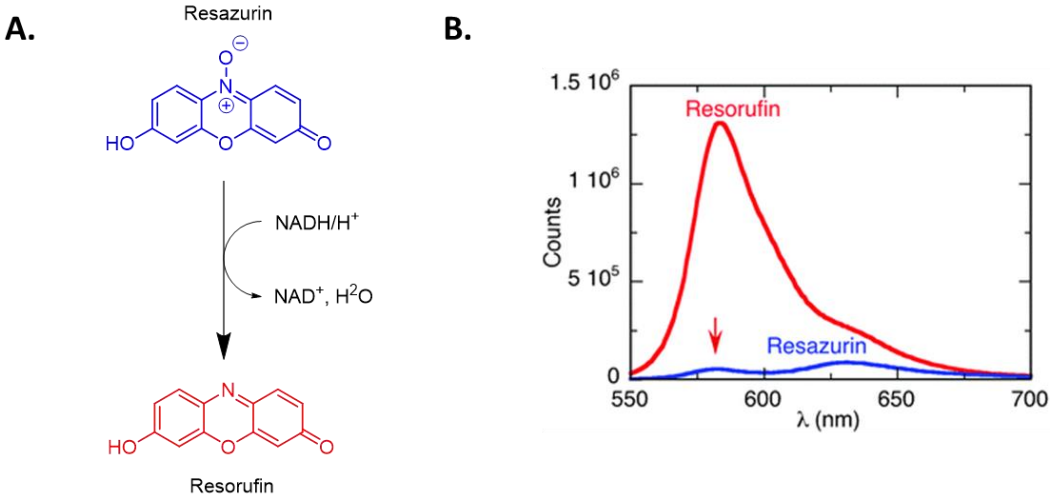

Figure 79: A. The irreversible reduction of blue dye resazurin that takes place inside the cell, forming the red resorufin. B. The fluorescence difference between resazurin (blue) and resorufin (red).[133]

This dye can be used to analyse a number of cell assays but for the purpose of this project it will be used to determine whether the dipeptides are bacteriostatic or bactericidal. If bacteriostatic the growth of the bacteria will be slowed or completely halted but the cell will remain intact and will not necessarily die. If bactericidal the compounds will kill the bacteria, and this will likely be due to them acting as in a detergent like manner. Where the dye is added to cultures which have been treated with a bacteriostatic agent a colour change from blue to red will be seen and there will be a large increase in fluorescence. The colour change can be seen because respiration is still occurring and the dye is being reduced. Where the dye is added to a culture which has been treated with bactericidal agent the dye will remain blue as there is no respiration occurring.

An assay protocol was developed and carried out. An overnight culture of LB was diluted 100 fold with MH2 media and then grown to exponential phase at 37 °C. It was then added to a 96-well plate with 90 µL per well. The antimicrobial compounds were added (10 µL per well giving a final concentration 250 µg/mL) and the plate was incubated at 37 °C for one hour. An hour was considered long enough for the compound to have an effect on the bacteria. The alamarBlue™ reagent was added (10 µL per well) and incubated for a further 3 hours at 37 °C. The plate was then read on the Hidex microplate reader with an excitation of 540 nm and emission of 590 nm.

A number of controls were used, and it is the comparison of the dipeptide readings to these controls which determine the results of this assay.

In order to show that it was not the antimicrobial agents causing the reduction of the dye, media blanks with the antimicrobial agents were used. In these wells the dye remained blue, showing that the compounds do not reduce the dye. Further controls containing media only, boiled *E.coli* or bacterial culture with no inhibitor were also tested. These wells gave the minimum and maximum fluorescence readings.

Ampicillin was used as a control to demonstrate the effects of a bacteriostatic agent. Ampicillin inhibits transpeptidases, preventing the third stage of bacterial cell wall synthesis.[125] As cell wall synthesis cannot proceed the bacteria cannot multiply. In the wells treated with 250 µg/mL ampicillin the dye turned pink.

The final control used was polymyxin B (Figure 80). This antimicrobial agent alters the membrane permeability by binding to the lipopolysaccharide layer via an

electrostatic interaction.[53,135] The positively charged cyclic amino group of the polymyxin B interacts with the negatively charged lipopolysaccharide layer. The lipophilic tail of polymyxin B is then able to disrupt the cytoplasmic membrane. It is non-specific and disrupts all membranes making the drug highly toxic and a last resort in treatment of resistant bacteria. Despite this it is on the World Health Organization's List of Essential Medicines, which details the most effective and safest medicines needed in the healthcare system.[136] In the wells treated with 250 μg/mL polymyxin the dye remained blue, showing no respiration was occurring, due to the polymyxin induced lysis of the cells.

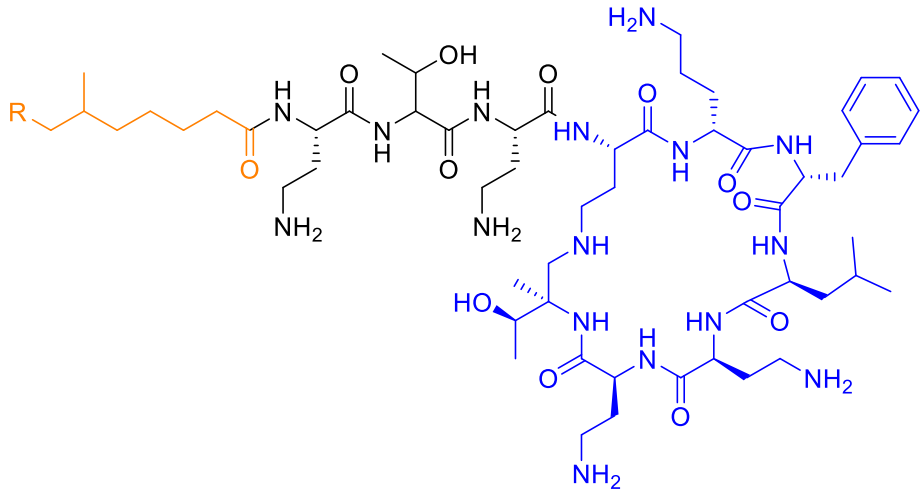

Figure 80: The structure of polymyxin B. The lipophilic portion is coloured in orange and the polar, charged head group is shown in blue.

3.5.2 AlamarBlue™ Assay results

The assay was carried out as described in the previous section with the dipeptides RWoct (**6**), KWoct (**16**), RW-Noct (**22**), KG-Noct (**28**) and KW-Noct (**24**). The results of this are presented in a bar chart in Figure 81.

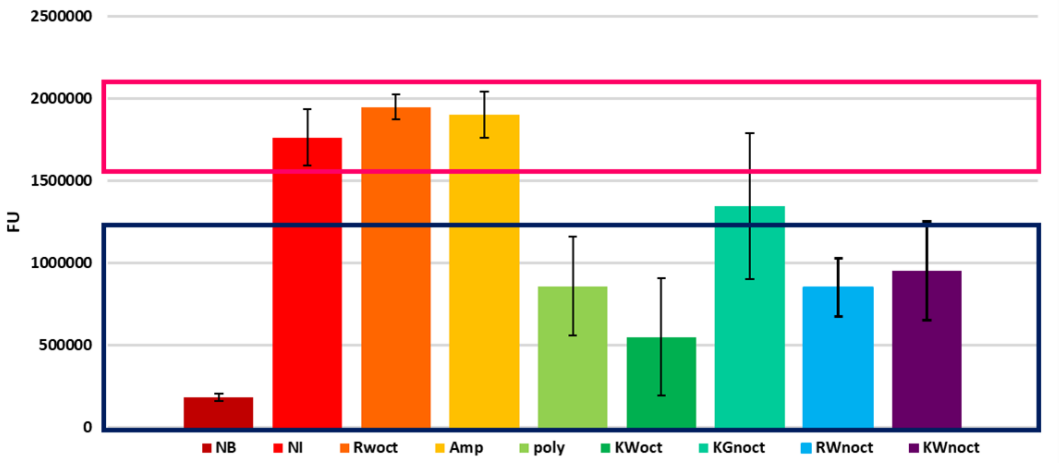

Figure 81: A graph to show the fluorescence readings from the AlamarBlue™ assay. [NB= no bacteria, NI= no inhibitor, Poly= polymyxin, Amp= ampicillin]. The pink box shows the fluorescence readings considered to be bacteriostatic agents and the blue box the bactericidal agents. All compounds were tested at 250 µg/mL.

The results from wells with no inhibitor and ampicillin were considered to be the maximum fluorescence that could be obtained from this assay and represent bacteria which were respiring. These wells were pink in colour showing that the conversion of resazurin to resorufin had occurred. The results from the wells with no bacteria and polymyxin were considered to be the lowest range of fluorescence. These wells were blue in colour indicating there had been no reduction of resazurin. The colours of the wells under all of the conditions described are shown in Table 15. These controls provided two ranges of fluorescence shown on Figure 81 by a pink and a blue box. The pink box represents the range in which the fluorescence reading of a sample containing only resorufin would fall and the blue box a range of resazurin.

Well contents	Well colour
No bacteria	
No inhibitor	
Ampicillin	
Polymyxin	
RWoct (**6**)	
KWoct (**16**)	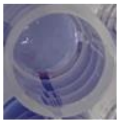
KG-Noct (**28**)	
RW-Noct (**22**)	
KW-Noct (**24**)	

Table 15: A table showing the colours of the alamarBlue™ dye after 2 hours in the different conditions used in the assay.

3.5.3 Conclusion

The dipeptides RWoct and KWoct were tested as the results from the protection assay suggested that there was a difference in mode of action. RWoct shown in Figure 81 and Table 15 is clearly comparable to the resorufin controls and could be considered bacteriostatic and not creating pores in the membrane. KWoct on the other hand falls in the blue box and is comparable to polymyxin. This indicates that it acts differently

to RWoct and is bactericidal, likely because it exhibits detergent like properties leading to the formation of pores in the membrane. The amide containing dipeptides RWnoct and KWnoct were tested and showed similar effects to KWoct. This suggests that the incorporation of an amide linked octyl chain alters the mechanism of action.

Finally KGnoct was tested as is does not have the aromatic group and so it is a cationic group and a lipophilic chain. The results from this peptide are inconclusive. The FU value falls between the two regions with the error bars extending into both the blue and pink region. The colour of this well was purple (as shown in Table 15) and this is consistent with the fluorescent results.

3.6 Conclusion

The conclusions drawn from this chapter will influence functionality which will be installed onto the peptidomimetics in the next part of the project.

As no inhibition was seen, in the fluorescence assay and the overexpression assay could not be carried out due to the toxicity of MraY. The radiochemical inhibition assay carried out also showed no evidence of MraY inhibition. The majority of the conclusions must be drawn from the antimicrobial testing.

The antimicrobial testing results were discussed in section 3.1. Based on this the groups which were carried forward to the peptidomimetic design are the guandinium group, the indole group and an alkyl chain. Initially an octyl chain will be used which can later be optimised. The ester linkages will not be include due to the known break down of the bonds by esterase enzymes.[105]

The results obtained from the resazurin based assay indicate that the dipeptides differ in mechanism of action. It is not however possible to determine what these mechanism might be. The most promising peptide based on this assay is RWoct. It may be that the octyl chain is being removed by esterases to give NH_2-RW-OH.

As no inhibition of MraY was seen development of the peptidomimetics will focus mainly on improving the antimicrobial activity of RWoct.

CHAPTER 4: Peptidomimetics based on α-helical mimetics – design, synthesis and testing

The use of peptides as therapeutic agents is limited by poor membrane permeability, rapid excretion and bad stability.[137] To overcome the downfalls which peptides as drug molecules have, peptidomimetics can be designed and synthesised to produce molecules which mimic the parent peptide but are more "drug-like". This often involves altering the peptide backbone structure to make the compound less susceptible to breakdown by proteases.

4.1 Dipeptide Peptidomimetic Design

The series of dipeptides are proposed to interact at a PPI site rather than at the active site of MraY. The interaction site of E and MraY is shown in Figure 82. (section 1.3.2).

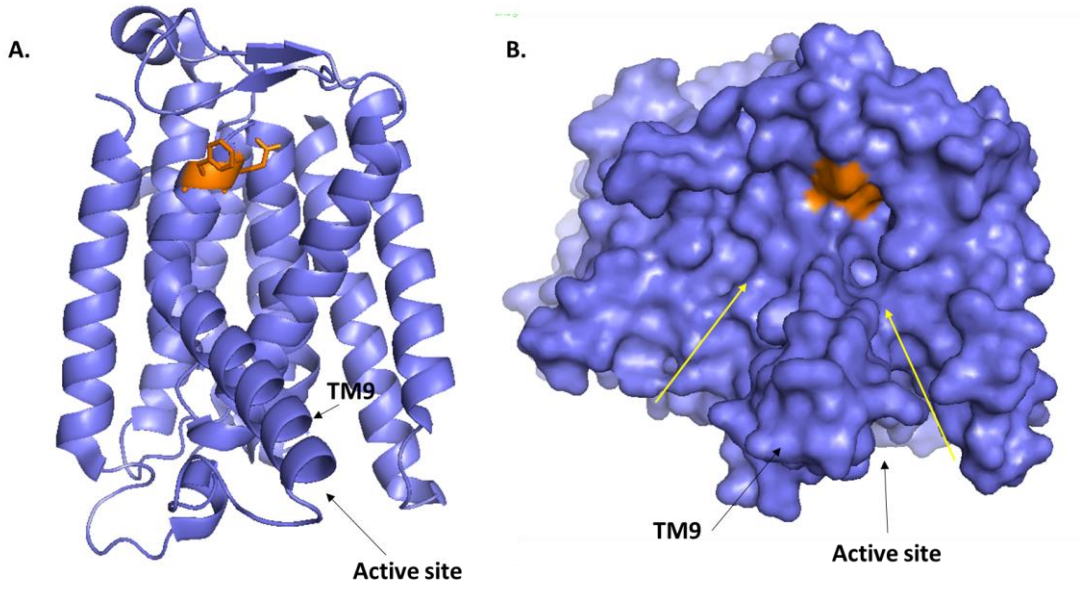

Figure 82: A. The crystal structure of the MraY monomer with the proposed E protein-MraY protein-protein interaction site shown in orange. The orange residues are E287 and F288. B. shows the surface representation and the channels (yellow arrows) lead to the interaction site. (PDB: 4J72)

PPI sites are large, solvent exposed and do not have contiguous binding sites, and this complicates the design process.[138] For this reason small-molecules drugs which directly disrupt PPIs are relatively rare, with many sites unable to support binding interactions with such molecules and are considered "undruggable" targets.[139] Recent developments in the area have seen some success disrupting interactions between globular proteins and single chain peptides, particularly where there are binding pockets on the surface of the globular proteins. A recent review by Scott *et al.* (2016) lists examples of drugs which are currently in clinical trials which target PPI sites.[139]

The design of PPI disrupters is usually aided by X-ray crystallography and protein based NMR spectroscopy. Crystal structures with inhibitors bound at the active site

are available, but none exist for the site which we are trying to target. MraY is a membrane protein and obtaining this sort of structural data is difficult.

It is important to consider the secondary structures involved in the interaction, such as α-helices and β-sheets. The E protein is α-helical but our dipeptides contain too few residues to adopt this structure, and this could have caused the side chain groups to be orientated incorrectly, and is therefore the reason no inhibition of MraY was seen. Each turn of an α-helix is 3.6 residues with 2-3 turns (minimum) needed to actually maintain the structure through hydrogen bonding.[140] It is also important to consider the flexibility of the dipeptides. The peptide backbones are not constrained structures and the arginine side chain and the alkyl chain are both very flexible.

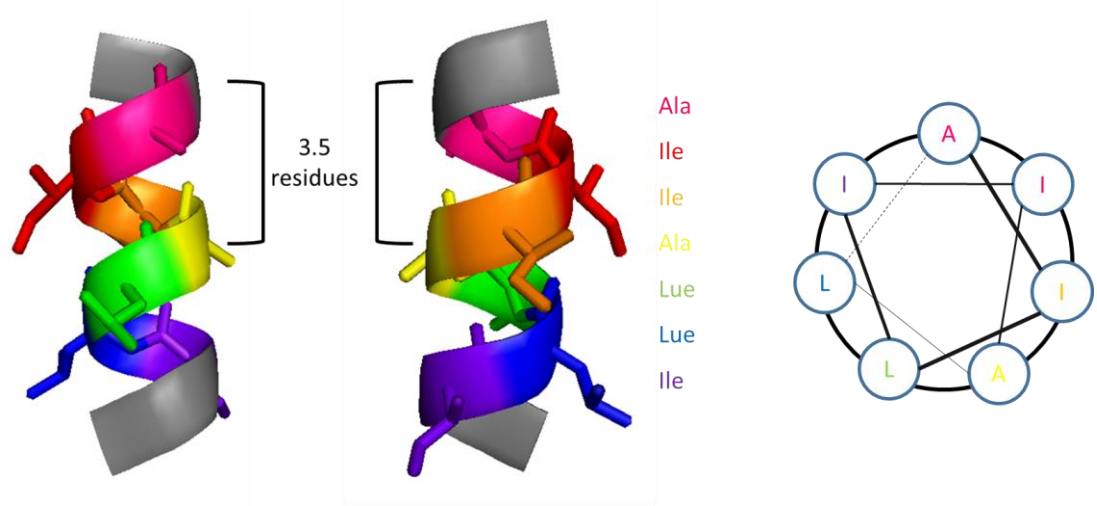

Figure 83: A. Examples showing the 3.5 residues in one turn of a section of α-helix (TM10 of MraY. The side chain groups are presented outwards. B. The corresponding wheel diagram showing a representation of the α-helix from above.

In order to synthesise peptidomimetics which would inhibit MraY, two α-helical backbone structures were chosen to install an arginine or a lysine residue, an indole ring and an octyl chain. The side chain groups would now more closely mimic the orientation and spatial arraignment which is seen in the RWxxW motif. Onto these backbones it would also be possible to install a second indole group and so completing the full motif.

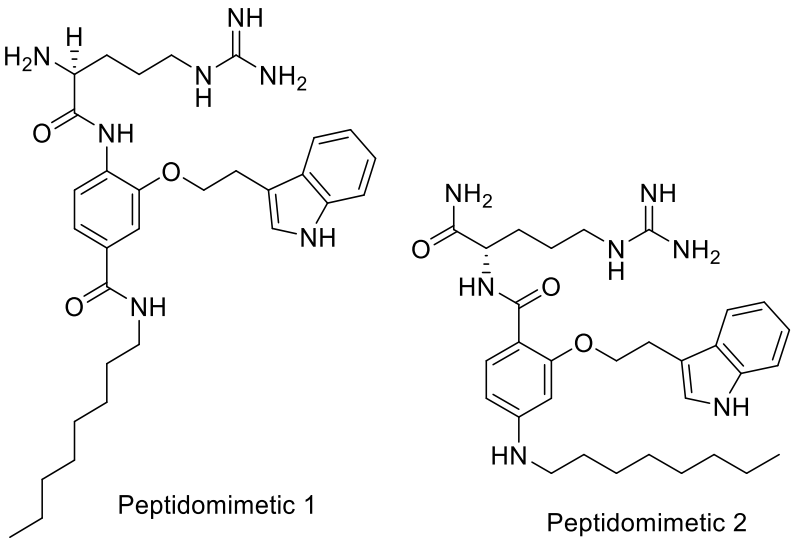

Figure 84: Proposed structures of the peptidomimetics designed based on the antibacterial data obtained for the series of dipeptides (PM 2 is based on a Hamilton model.[140] PM 1 is based on a Boger model.[83])

Peptidomimetic 1 and 2 are based on α-helical backbone mimetic models designed by Hamilton[140] and Boger[83], which were discussed in more detail in section 1.6 and 1.7

4.2 Dipeptide peptidomimetic: Peptidomimetic 1

Figure 85 shows the initial synthetic route that was proposed for the synthesis of peptidomimetic 1.

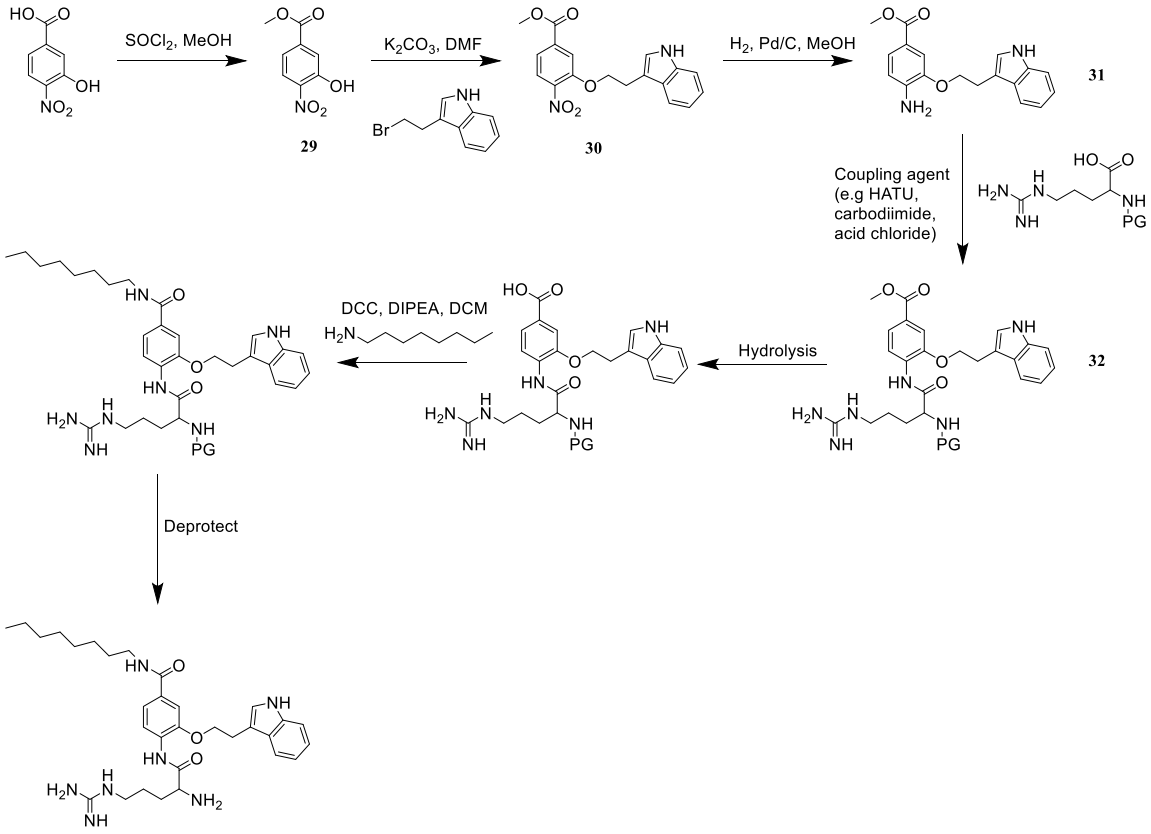

Figure 85: The synthetic route proposed for the synthesis of peptidomimetic 1. [PG= protecting group]

The first step of the synthesis is the alkylation of the hydroxyl group of ***3-hydroxy-4-nitrobenzoic acid*** to give the benzoic acid alkyl ether. Hydroxyl groups can be reacted with organohalides under basic conditions, by a Williamson reaction to form ethers.[141] The alkoxide ion which forms, reacts with a primary halide via an S_N2 reaction. To attach an indole by the ether linker the primary halide, 3-(2-Bromoethyl)indole, was used.

The success of this synthesis required the chemoselective alkylation of the hydroxyl group over the carboxylic acid. The difference in pK_a of the hydroxyl group should allow this to be achieved. Tetrabutylammonium bromide (TBAB) can be used as a

phase transfer catalyst and enhances nucleophilicity.[142] Pandey *et al.* showed that the use of (tetrabutylammonium hydroxide) TBAH instead of TBAB lead to the alkylation of a benzoic acid group as well as a hydroxyl group during a similar syntheis.[143] However the alkylation did not proceed when the benzoic acid was not protected. The carboxylic acid group of ***3-hydroxy-4-nitrobenzoic acid*** was protected using thionyl chloride and methanol to form the methyl ester **29**. Initally H_2SO_4 was used, this gave a yield of 49% compared to a 78% yield using thionyl chloride. After the installation of the methyl ester the alkylation was successful to give **30** (Scheme 9).

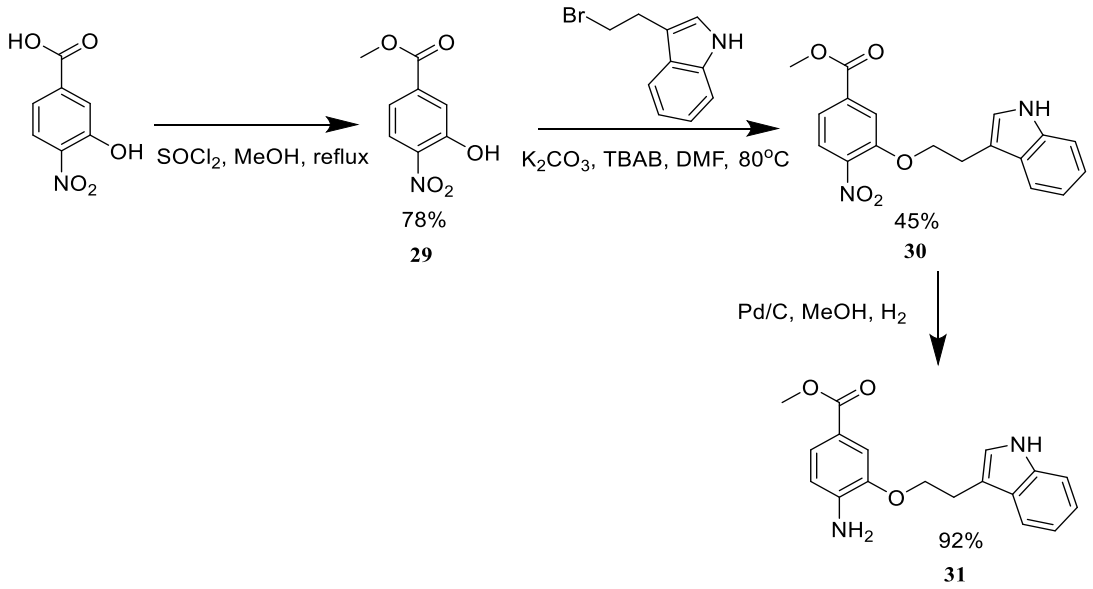

Scheme 9: Protection of the carboxylic acid using thionyl chloride and MeOH to give a methyl ester followed by alkylating the hydroxyl group using K_2CO_3 and TBAB. The nitro group is then reduced in the presence of Pd/C under H_2(g).

Following the alkylation, the nitro group was reduced by hydrogenation using Pd/C under hydrogen to give aniline **31**. Some literature states that indoles can be reduced under these conditions[96]. There was no evidence of this occurring based on the HRMS and NMR data obtained for **31.**

Anilines ($pK_a \approx 4.6$) are less basic than amines which are bonded to an aliphatic group (i.e amino acids, $pK_a \approx 9.5$). The weak basicity is attributed to a resonance effect and the inductive effect of the neighbouring more electronegative sp^2 carbon. The weak

bascicity of the aniline made coupling the arginine residue more difficult as the nitrogen lone pair in its sp^2 orbital is delocalised into the π system of the ring.

Figure 86 shows the reagents used initially to couple the arginine residue to the aniline. Both uronium based and carbodiimide activating agents were used with the appropriate organic bases and solvent. None of these conditions gave the desired product by LRMS analysis.

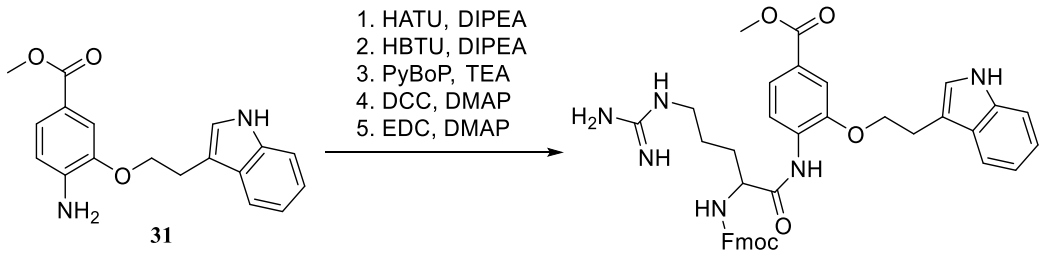

Figure 86: The conditions tested to couple an arginine residue to an aniline 31.

N-hydroxysuccinimide was coupled to Fmoc-Arg-OH to form the active ester and then was added to the aniline again using the conditions described in **Error! Reference source not found.**.[144] This coupling was also unsuccessful, despite the formation of the succinimide active ester, which was identified by LRMS.

Coupled with the lack of reactivity from the aniline it is possible that the arginine residue was undergoing δ-lactam ring formation once activated with the coupling agent (see Figure 87).[145] This was not a side reaction which had been identified when synthesising the dipeptides.

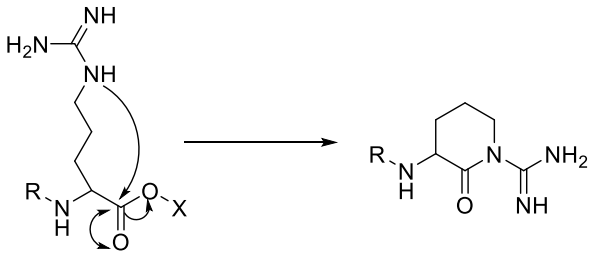

Figure 87: Mechanism of arginine δ-lactam ring formation.

Protecting the side chain of arginine can prevent the δ-lactam ring formation (as well as the loss of the guanidine side chain).[145] Traditionally Pmc and Pbf groups are used to protect the arginine side chain, however earlier in the project, during the dipeptide synthesis problems were encountered removing these groups in chapter 2. An alternate protecting strategy is to use ω-nitro group to protect the side chain. Boc-Arg(NO_2)-OH was used instead of Fmoc-Arg-OH. This meant that δ-lactam ring formation was prevented, however the coupling was still unsuccessful. Tests to remove the NO_2 protecting group using hydrogenation were also unsuccessful after 24 hours, and with the only other deprotection method for this group being HF, the use of ω-nitro group arginine was discontinued.[96]

We hypothesised that a more reactive activated carboxylic acid derivative was needed to successfully couple an arginine residue to the aniline, and so thionyl chloride was used (Scheme 10) to generate the acid chloride of Fmoc-Arg-OH, and then added to the aniline with DIPEA. This coupling was successful, and **32** was identified using HR-MS. **32** was isolated using RP-HPLC (Synergi™ 4 μm Polar-RP 80 Å). The use of thionyl chloride was a concern because of epimerisation, however Carpino *et al.* showed that amino acids protected with Fmoc did not undergo epimerisation due to the neighbouring atoms of the Fmoc group.[146] The reactivity of the acid chloride caused the formation of many side reactions, and this lead to a difficult purification by RP-HPLC and a low yield (<2%).

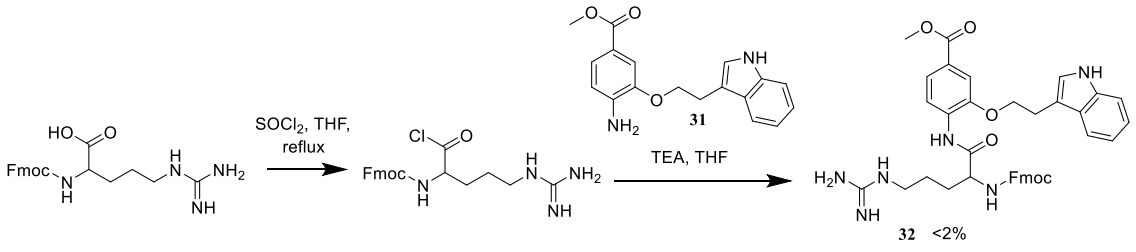

Scheme 10: The synthesis of arginine acid chloride using thionyl chloride following by the coupling to 31 in basic conditions.

It was found that the removal of the methyl ester could not be carried out without removing the Fmoc group. Without the α-amino group protected the synthesis could

not be continued. Non-basic conditions were used in a further attempt remove the methyl group (NaI and $SiCl_4$), however this was unsuccessful.[147]

Protecting the arginine with a Boc group would not be suitable due to the strongly acidic coupling conditions.

Ghosez's reagent is used to form acid chlorides in neutral conditions (Figure 88).[148] This would allow the use of acid labile protecting groups. Boc-Arg-OH was treated with Ghosez's reagent. NMR was used to assess whether the acid chloride had formed, however after 7 hours it had not. The intermediates and by product also could not be seen, indicating that Ghosez's reagent was not sufficiently reactive or compatible to form an acid chloride of Boc-Arg-OH.

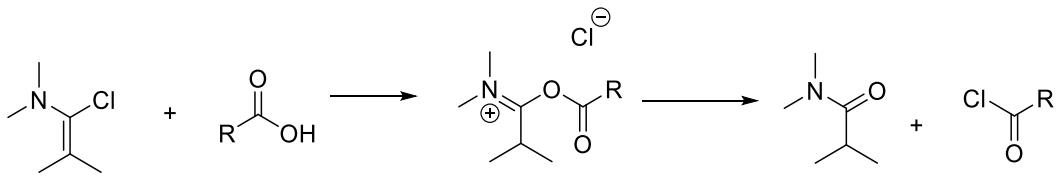

Figure 88: Reaction of Ghosez's reagent with carboxylic acids.[148]

As both Fmoc and Boc amine protection were unsuitable, the next option was to try Cbz protection. When reacted with thionyl chloride, Cbz-Arg-OH formed a tar-like residue which would not dissolve in DMF, and therefore was not suitable for the coupling reaction with the aniline.

It is possible that the arginine side chain was affecting the coupling. Once coupled it made the purification of the compound more difficult (using RP-HPLC) and during this purification, yield was lost. In order to get around this, if a protected ornithine derivative could be coupled to the aniline, then the guanidinium group could be added as the final step. This would allow silica column chromatography to be used for the purification prior to the installation of the guanidinium group. A possible method of installing the guanidinium group is shown in Figure 89, using o-isomethylurea at pH10.[149] It is possible to carry out this reaction using S-methylisothiourea, but this releases methanethiol which is an undesirable side product.[150]

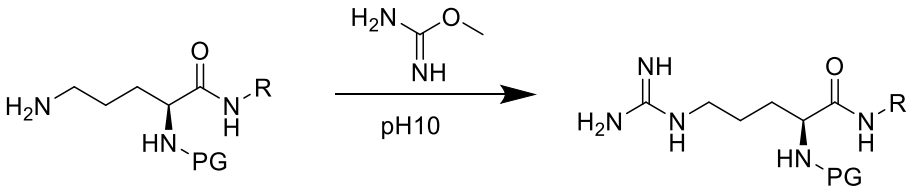

Figure 89: Guanidination of ornithine using o-isomethylurea at pH 10.[149]

In order to carry out this reaction, L-ornithine must be suitably protected (Scheme 11) using a method described by Rzeszotarskat *et al.*[151] The side chain was protected with Boc and the amine was protected with Cbz. In order to selectively protect the ornithine side chain with a Boc group, L-ornithine was chelated to copper, combining with $Cu(OAc)_2$, which left the side chain free. This was followed by the addition of Boc_2O to install the Boc group on the side chain. To remove the copper from the ornithine, the chelating agent, 8-quinolinol was used. The α-amine was now free to react with benzyl chloroformate to give Cbz-Orn(Boc)-OH.

The presence of an acid labile Boc group meant that the thionyl chloride coupling method would not be suitable since it generates SO_2 and HCl. The coupling reagent HATU was used again, but was unsuccessful.

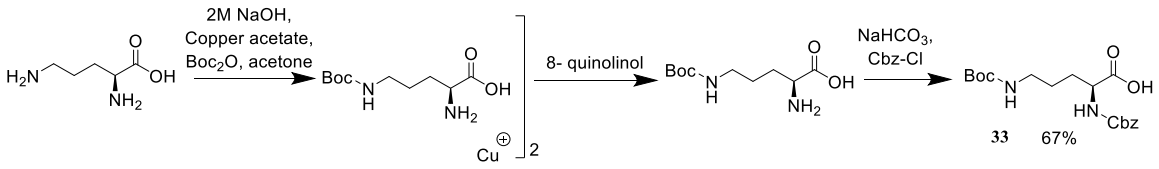

Scheme 11: Synthesis of Cbz-Orn(Boc)-OH from L-ornithine using copper acetate and Boc_2O following be Cbz-Cl.[151]

Having exhausted the possible protecting and deprotecting strategies available, including a variety of conditions to remove the methyl ester (Na_2CO_3, LiOH and NaOH) this synthesis route was discontinued.

In order to synthesise peptidomimetic 1 a new route was designed. As the coupling step would likely be the lowest yielding it was decided to make this the last step. The first step could be changed to the coupling of the octyl chain. This would remove the

need to deprotect the acid later in the synthesis, and so the overall number of steps in the synthesis was decreased. The new synthesis route is shown in Scheme 12.

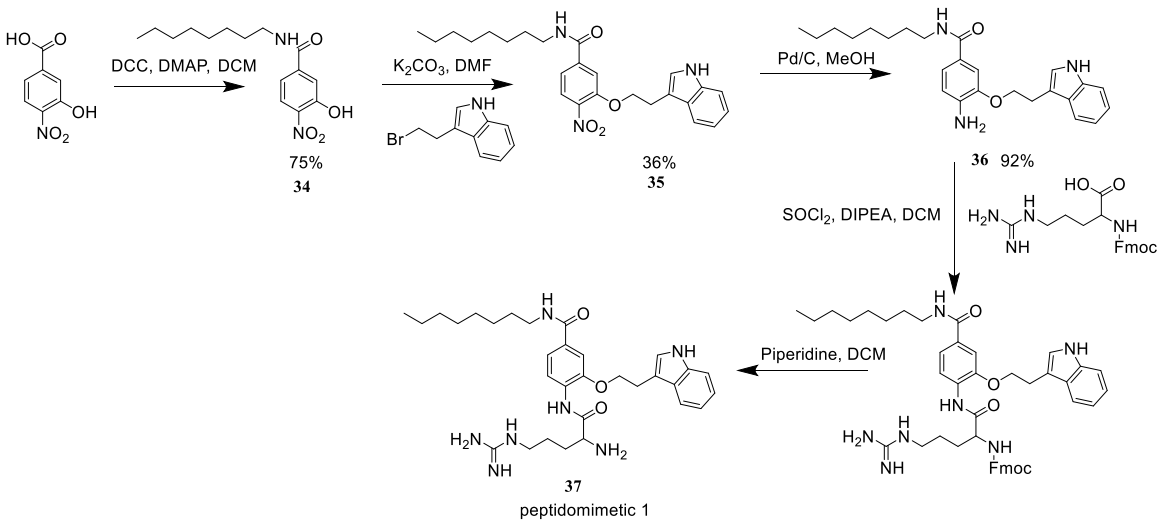

Scheme 12: The revised synthetic route for peptidomimetic peptidomimetic 1. Yields are not given for the last two steps as the first was carried out in situ and only some of the second was purified.

To install the octyl chain, the benzoic acid was activated with DCC in the presence of DMAP and then 1-octylamine was added to afford **34**. This step was followed by the alkylation of the 3'hydroxyl group (**35**) and reduction of the nitro group (**36**), as previously carried out. Fmoc-Arg-OH was coupled to the aniline using thionyl chloride, and then deprotected using 20% piperidine in DCM. RP-HPLC (Synergi™ 4 µm Polar-RP 80 Å) was carried out to isolate peptidomimetic 1 (**37**).

4.3 Dipeptide peptidomimetic: Peptidomimetic 2

Scheme 13shows the initial synthetic route that was proposed for the synthesis of peptidomimetic 2.

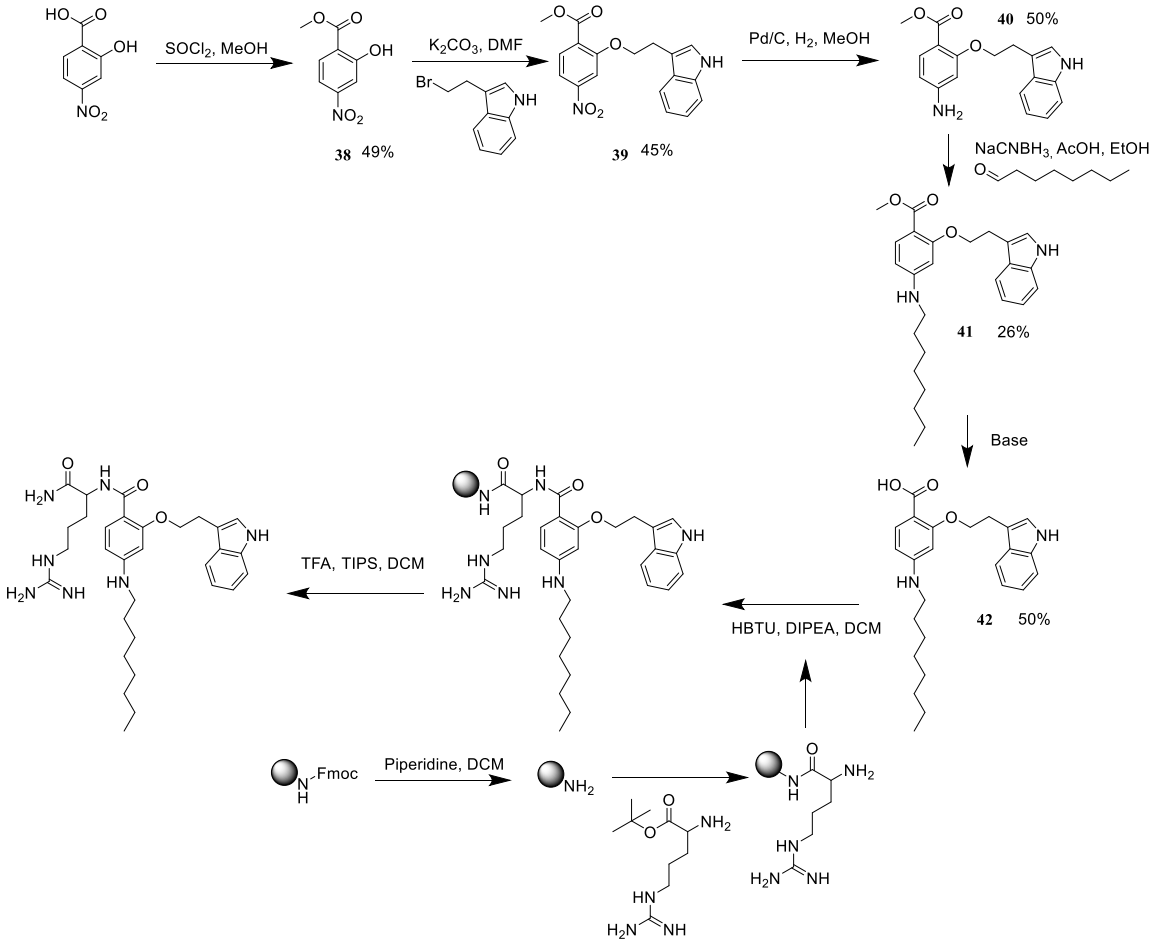

Scheme 13: The synthetic route proposed for the synthesis of peptidomimetic 2

The starting compound, ***2-hydroxy-4-nitrobenzoic acid***, was protected as its methyl ester **38**, before the alkylation (**39**) and reduction of the nitro group (**40**) were carried out as described in section 4.2. To incorporate the octyl chain onto the aniline nitrogen $NaCNBH_3$ and 1-octanal were initially used with acetic acid at pH 4 to give **41**. The yield of this reaction was low (<20%), and was not sufficient to carry out the following steps. Optimisation of the reductive amination was attempted. Using the same reactants as before, the amine and the aldehyde were refluxed (to form the imine) prior to the addition of $NaCNBH_4$.[152] The only product which now formed had two octyl chains attached to the aniline. Acidic and basic conditions were used to try and form and then isolate the imine, but this was not successful. Next, $NaBH_4$ was used, also

yielding mainly the doubly alkylated product.[153] An alkylation using 1-bromooctane and K_2CO_3 was carried out as previously described, but again the doubly alkylated product was formed (summarised in Scheme 14). The initial reaction conditions were therefore used, and the synthesis continued.

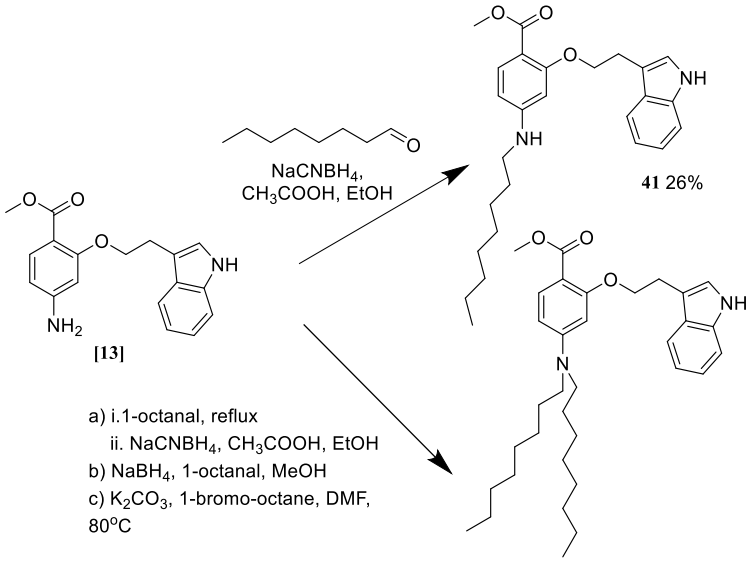

Scheme 14: The reaction conditions used to optimise the reductive amination step and the incorrect double octyl chain product formed.

As with the synthesis of peptidomimetic 1, the methyl ester was difficult to remove under basic conditions, and at higher pH some degradation of the compound was seen. After purification of **42**, the yield was 36%, giving little material for the next reaction.

In order to couple L-arginine to the benzoic acid, the carboxylic acid of the L-arginine must be protected. The initial strategy for this was to couple Fmoc-Arg-OH to MBHA rink amide resin, and then remove the Fmoc group using piperidine. Coupling to this resin would leave the product amidated at the C terminus, which is preferable to a free acid. This is because the product will be cationic rather than zwitterionic, like the parent peptides. The benzoic acid **42** was then coupled to the resin bound arginine using HBTU (Scheme 15). TFA was used to cleave the product from the resin and HRMS and LC-MS were used to confirm presence of the desired product. In order to purify the product RP-HPLC was used, however the coupling was low yielding, and the product could not be isolated. It is possible that the coupling conditions could be

optimised to improve the coupling, but this would require more of the benzoic acid starting material.

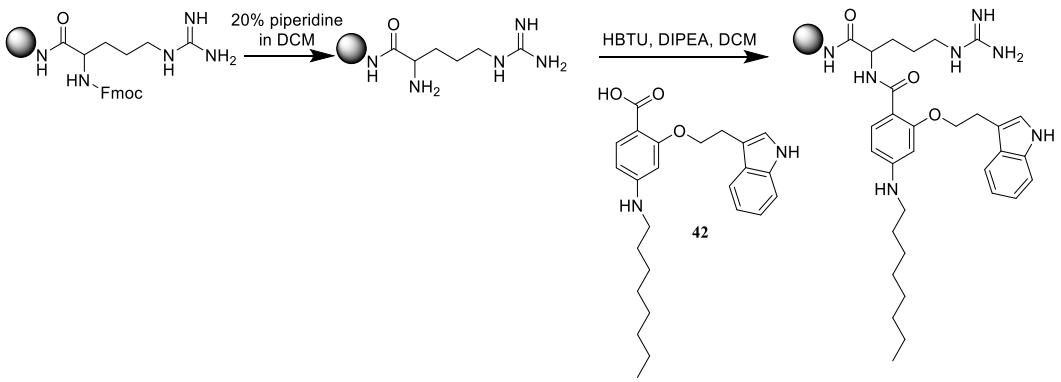

Scheme 15: The coupling of Fmoc-Arg-OH to MBHA rink amide resin followed by the deprotection of the Fmoc group and coupling of using HBTU.

The low yield of several steps in this synthetic route meant obtaining enough of the final compound to allow complete analysis and the subsequent biological testing was not easily achievable.

4.4 Dipeptide peptidomimetic: Peptidomimetic 3

At this point, we decided to change the final compound (Figure 90). Since alkylating the aniline nitrogen had been surprisingly difficult, we decided to attach the octyl chain through a carbon-carbon bond instead of a carbon-nitrogen bond as before, using a palladium-catalysed coupling to form the C-C bond.

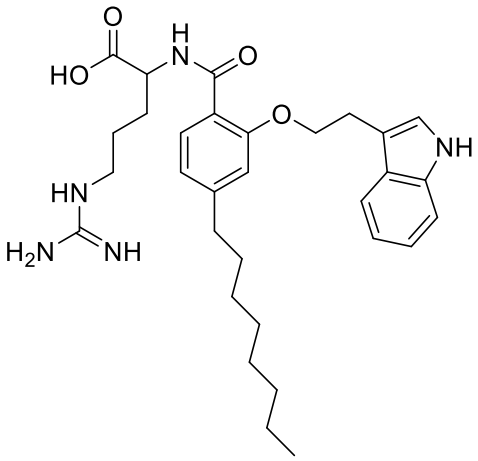

Figure 90: New design, peptidomimetic 3

The starting material used was 4-bromo-2-hydroxybenzoic acid, to which a methyl ester was introduced by the same method as before to give **43**. A Sonogashira cross coupling was carried out with 1-octyne and $Pd(PPh_3)_4$ (0.1 eq) and this afforded **44.**[154] (Scheme 16).

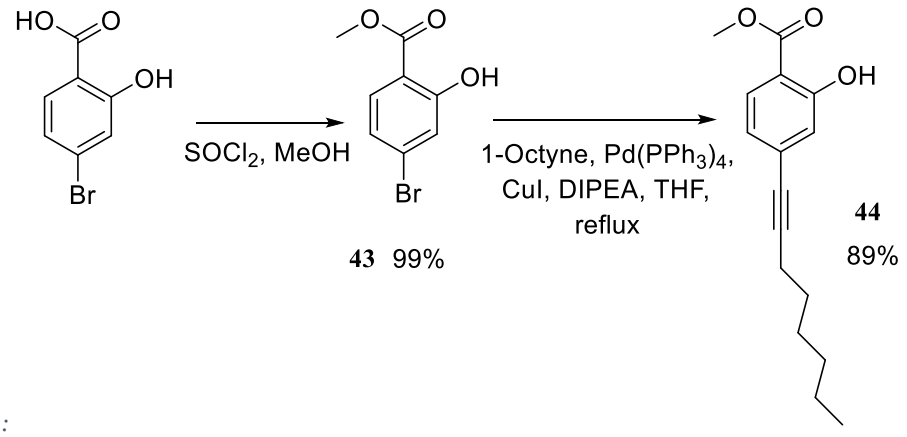

Scheme 16: The esterification of the benzoic acid of 4-bromo-2-hydroxybenzoic acid followed by the Songashira coupling at the aryl bromide.

This method introduces a carbon-carbon bond which is catalysed by palladium and co-catalysed by copper. The new bond is formed between a terminal alkyne and an aryl (or vinyl) halide.[154] The catalytic cycle of this reaction is shown in Figure 91.

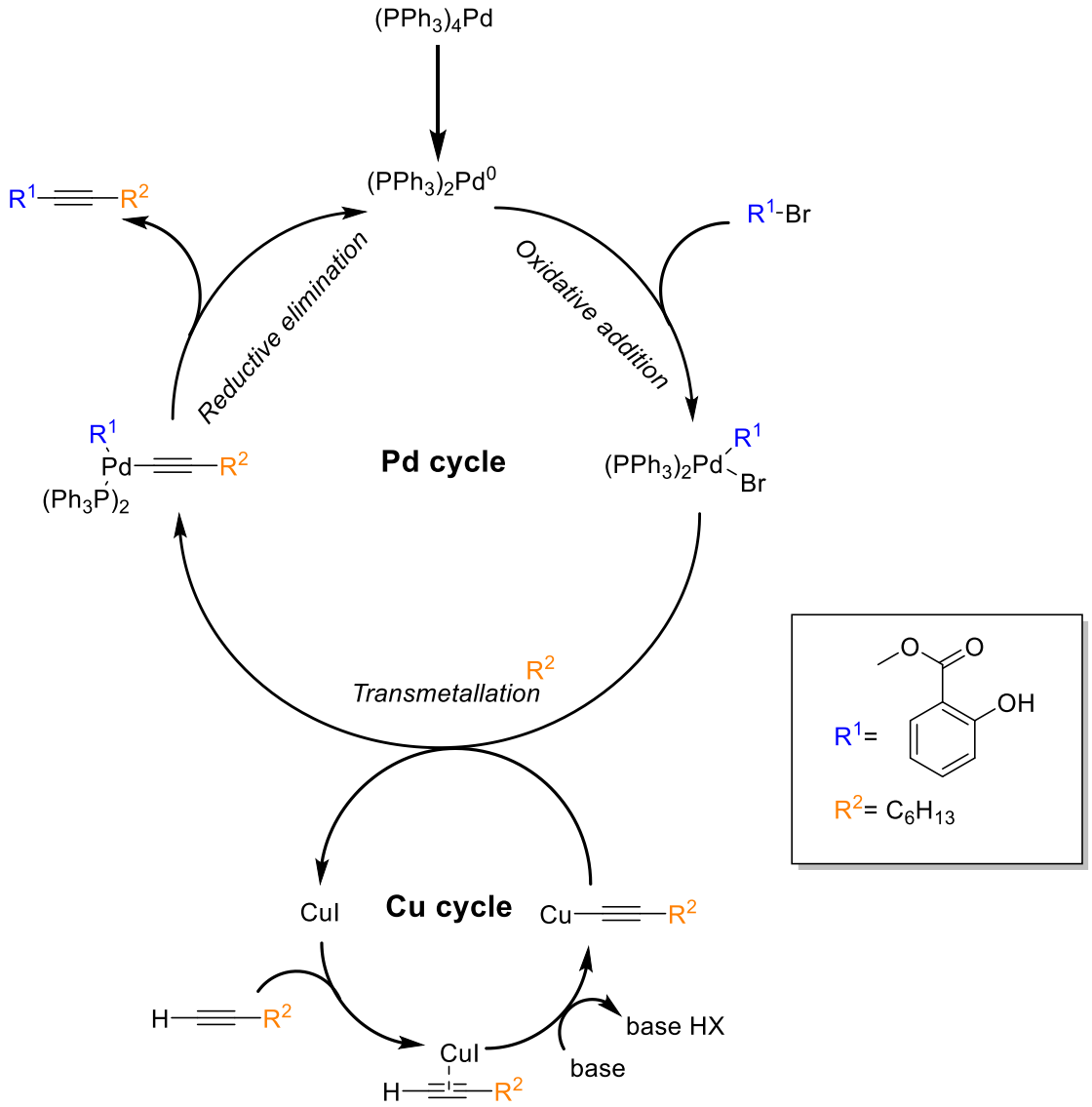

Figure 91: Sonogashira catalytic cycle.

Tetrakis(triphenylphosphine)palladium(0) was the catalyst used in this instance. The reaction proceeded with a high yield (89%).

Following this, the alkylation to incorporate the indole group was attempted as previously described, but was unsuccessful. However, carrying out the alkylation reaction in anhydrous acetone gave the desired product, **45**, in 52% yield. This is a less

hygroscopic solvent that DMF and full precipitation of the salt would occur. (Scheme 17).

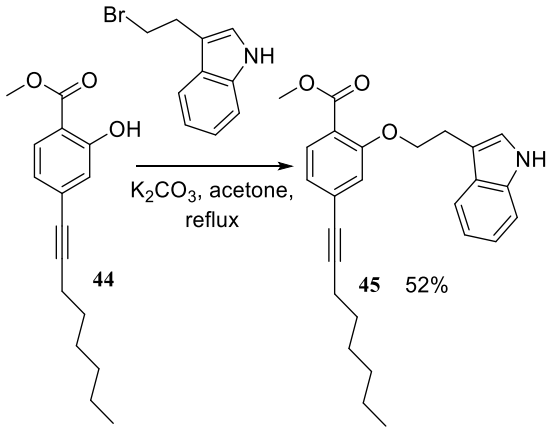

Scheme 17: Alkylation between the hydroxyl group of 44 and 3-(2-bromoethyl)indole, using K_2CO_3 and acetone.

The methyl ester could now be removed in base to give **46** with a yield of 98%, which was an improvement on the previous deprotection of this kind (section 4.3).

An alternative method to couple the arginine residue to the benzoic acid was also carried out to improve the yield seen when using the MBHA resin. An arginine residue which was acid protected (Arg-O^{t}Bu) was purchased, and coupled using HATU to **46**. Then the t-butyl ester was removed with HCl in dioxane, before being purified by RP-HPLC to give **47**. (Scheme 18). The alkyne was reduced with hydrogen and Pd/C. The final compound, peptidomimetic 3 **48**, was purified by RP-HPLC.

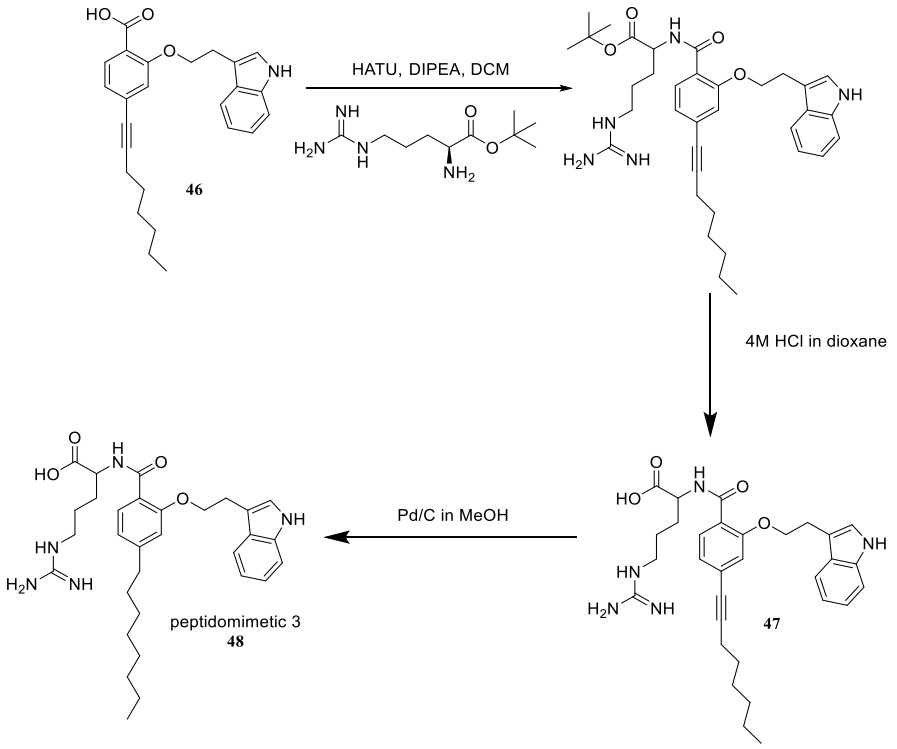

Scheme 18: This scheme shows the coupling of NH_2-Arg-O^{t}Bu to 46 followed by the deprotection of the arginine acid using HCl. Finally the reduction of the alkyne using Pd/C. No yields are given as no purification was carried out between each of thesis steps. The final HPLC purification was incomplete and carried out on unknown concentrations of compound.

4.5 Biological testing of set one peptidomimetics

Following purification the two peptidomimetics were tested using the same methods as the series of dipeptides.

4.5.1 Microtitre broth dilution antimicrobial testing

The antimicrobial testing was carried out using a microtitre broth dilution technique described in section 3.1. The results are shown in Table 16.

	MIC_{50} µg/mL		
	***E. coli* (TOP10)**	***B. subtilis* (W23)**	***P. Fluorescens* *(PF-5)***
PM 1 (37)	>125	10±8	>125
PM 3 (48)	30±6	10±5	>125

Table 16: MIC_{50} calculation results.

4.6 Tripeptide peptidomimetic: Peptidomimetic 4

The dipeptides synthesised in chapter 2 showed no inhibition of MraY, but they only contain the first two residues of the RWxxW motif. Rodolis synthesised a series of pentapeptides containing the entire motif and saw inhibition of MraY.[48] It is possible that that entire motif is necessary for a compound to successfully inhibit MraY. A second aromatic residue could be incorporated into one of the peptidomimetics in order to try to mimic the full motif.

The most obvious way to introduce the remainder of the RWxxW motif is to install and aromatic group at the top of the octyl amide of peptidomimetic 1 (**37**) (Figure 92).

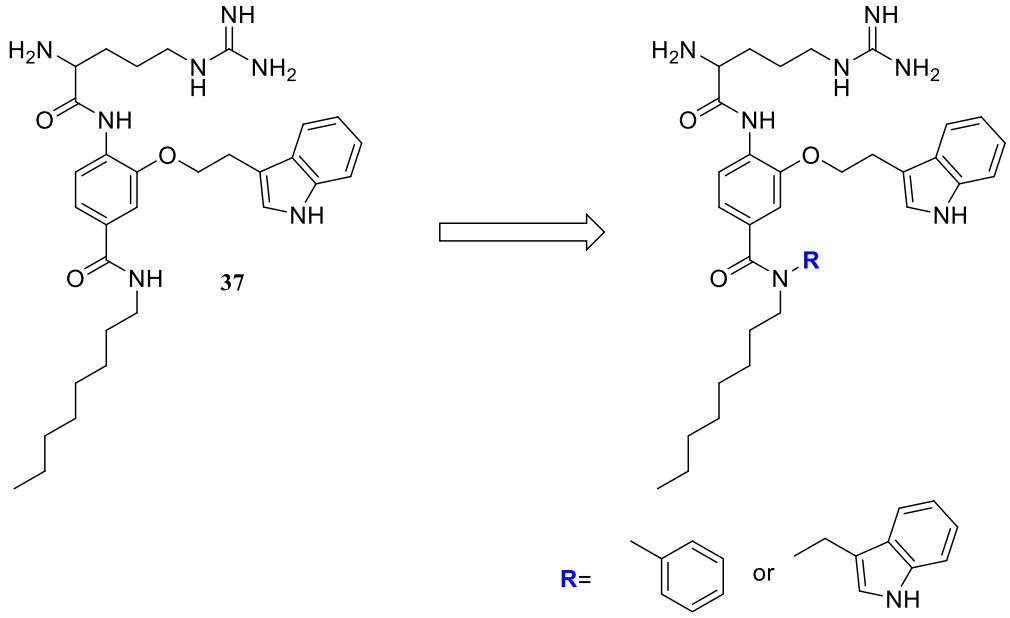

Figure 92: The proposed site for installing a second aromatic group (here shown as "R" in blue) to peptidomimetic 4

The synthesis route was similar to that of peptidomimetic 1 and is shown in Scheme 19.

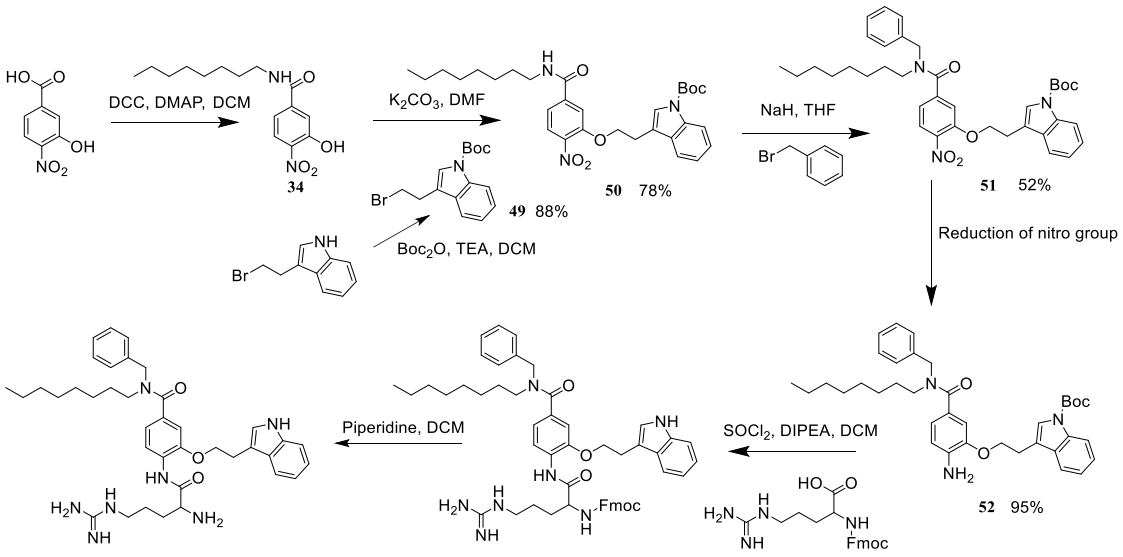

Scheme 19: The proposed synthetic route for the tripeptide peptidomimetic 4

Octylamine was coupled to the ***3-hydroxy-4-nitrobenzoic acid***, using DCC and DMAP, to form an octyl amide **34**. The bromo-indole was protected with a Boc group using Boc anhydride to give **49** (88% yeild). The Boc protected indole was alkylated to the hydroxyl group as previously described to give **50**. Benzyl bromide was alkylated onto the octyl amide nitrogen using sodium hydride giving **51** in 52% yield. The next step, reducing the nitro group, had previously been carried out using a hydrogenation reaction. These conditions could not be used with this compound as it led to the removal of the benzyl group. Iron (with NH_4Cl) was successful at reducing the nitro group, to give **52** with a yield of 95%. As with the previous synthesis, the L-arginine needed to be coupled to the aniline. This had previously been very challenging. The coupling was carried out using $SOCl_2$ and DIPEA as before, but the desired product was not seen by LRMS. RP-HPLC was carried out on the crude material and the peaks collected separately and MS repeated, but still no product was observed.

At this point it was decided that the synthesis of this compound would be discontinued. This backbone and synthesis route were not suitable for making a library of di- and tri-peptidomimetics.

4.7 Optimisation of the benzamide backbone and synthetic route

In order to be able to synthesise a library of peptidomimetics it was necessary to develop a new route which allowed the easy installation of different functional groups on a benzamide backbone. Three changes were introduced:

1. Changing arginine to lysine. Throughout the project the arginine residues and its associated protecting groups have posed problems with couplings, purification, protection and deprotection reactions. This in many cases led to insufficient yields or unsuccessful reactions. Lysine-containing dipeptides were shown to have antimicrobial activity, and the introduction of L-Lys-OMe in the synthetic route seemed more straightforward in terms of protection and purification.
2. Acylation of the aniline nitrogen. Since the reductive amination of the aniline nitrogen had been very problematic, we decided to acylate the nitrogen instead.
3. Replacement of the indole group by a phenyl group. This change was made as it would limit the number of possible side reactions. This would allow the optimisation of the full route before the indole group could be reintroduced.

The revised synthetic route is shown in Scheme 20.

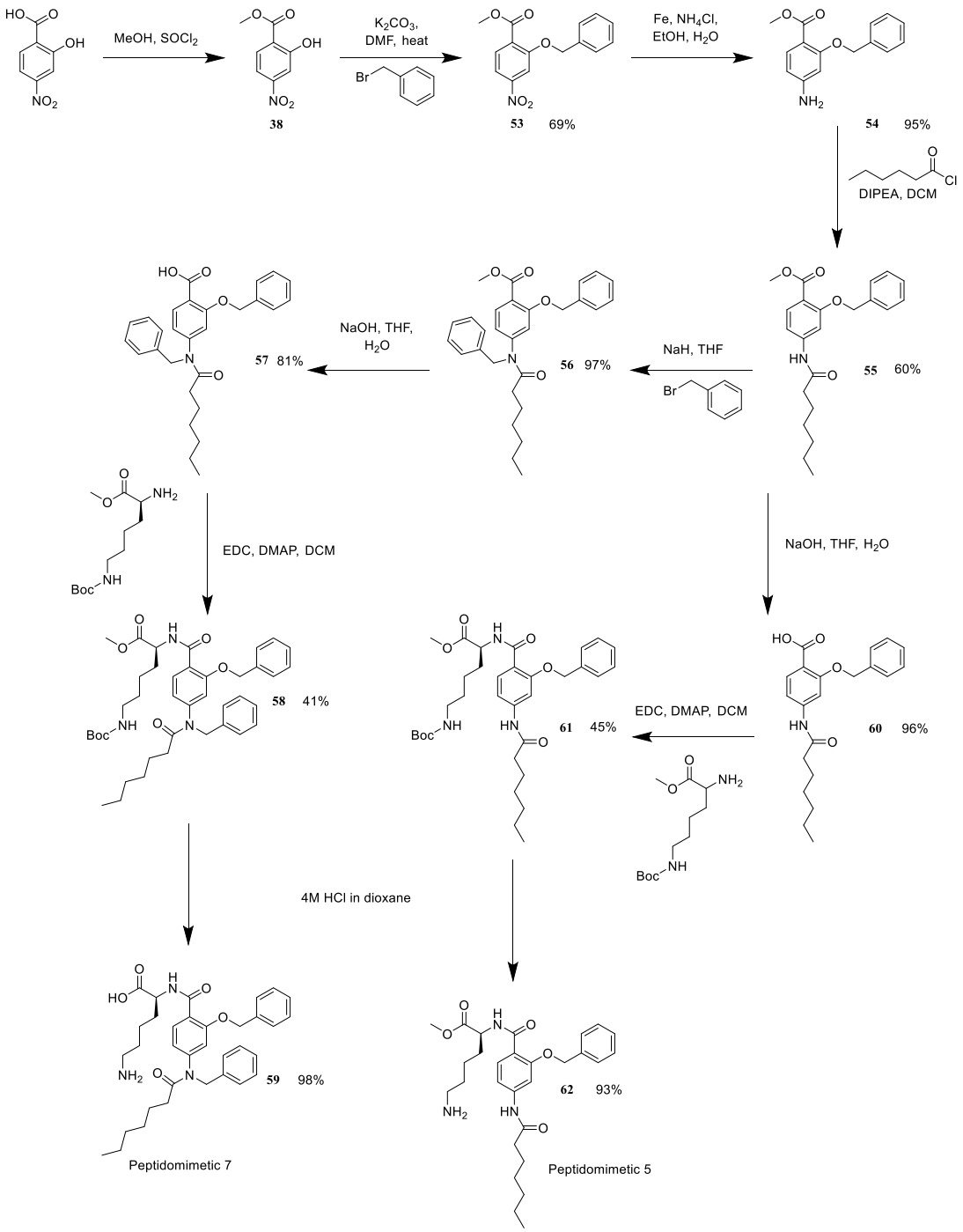

Scheme 20: The synthetic route proposed to achieve peptidomimetics 5 and 7

Scheme 20 shows routes to a di- and tri- peptidomimetic which both contain a lysine residue and benzyl groups. The initial synthesis was carried out with benzyl groups instead of indole groups so that the reactions could initially be tested without hindrance from the indole nitrogen. Once a successful route had been established, the indole groups could be installed.

The initial steps are similar to those of the previous dipeptides (Scheme 21).

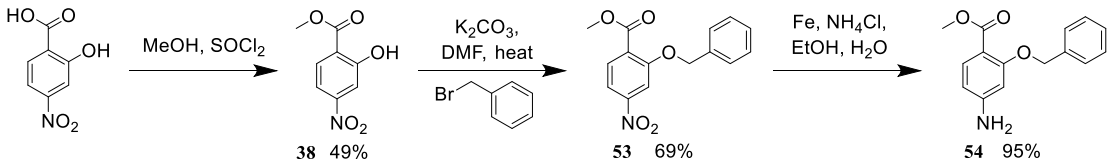

Scheme 21: The synthesis of the methyl ester 38. Alkylation of 38 with benzyl bromide was followed by the reduction of the nitro group with Fe to give 54.

Heptanoyl chloride was added to the aniline and TEA in DCM dropwise at 0 °C, forming the amide **55** in 60 % yield. In the case of the tripeptide a further alkylation of this amide was carried out, using benzyl bromide and sodium hydride in THF, to give **56** in 97% yield. (Scheme 22).

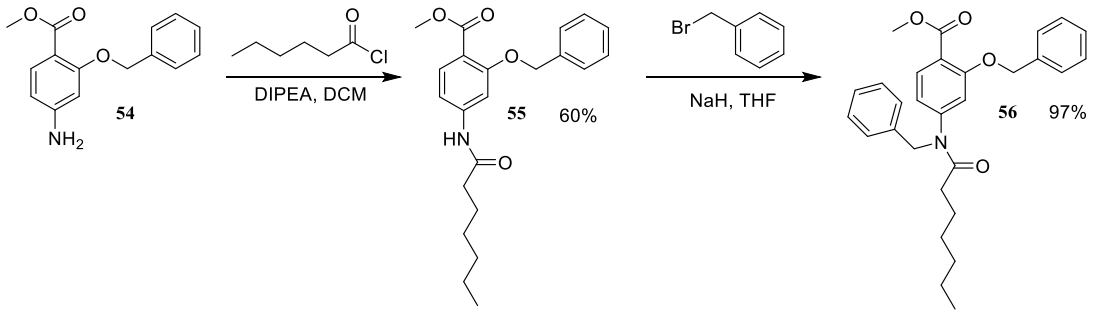

Scheme 22: Acylation and subsequent alkylation of the aniline 54

The methyl ester was deprotected using NaOH and THF/water to give **57**, and the Lys(Boc)-OMe was successfully coupled to the benzoic acid using EDC to give **58**. (Scheme 23). The Boc side chain was then deprotected using HCl (98% yield) which gave the final peptidomimetic 7 (**59**). This was repeated on **55** to give peptidomimetic 5 (**62**).

The carboxylic acid of the lysine residue was protected as a methyl ester and this was not removed. Previously when an amino acid residue was coupled to the benzoic acid (peptidomimetic 3), its acid protecting group (^{t}Bu) was removed giving a zwitterionic final compound. The aim was to mimic the cationic antimicrobial peptides, and so zwitterionic character is probably not desirable. It is possible that this characteristic

caused a reduction in antimicrobial activity, so in this case the methyl ester was left, so that the final compound was cationic, at pH 7.

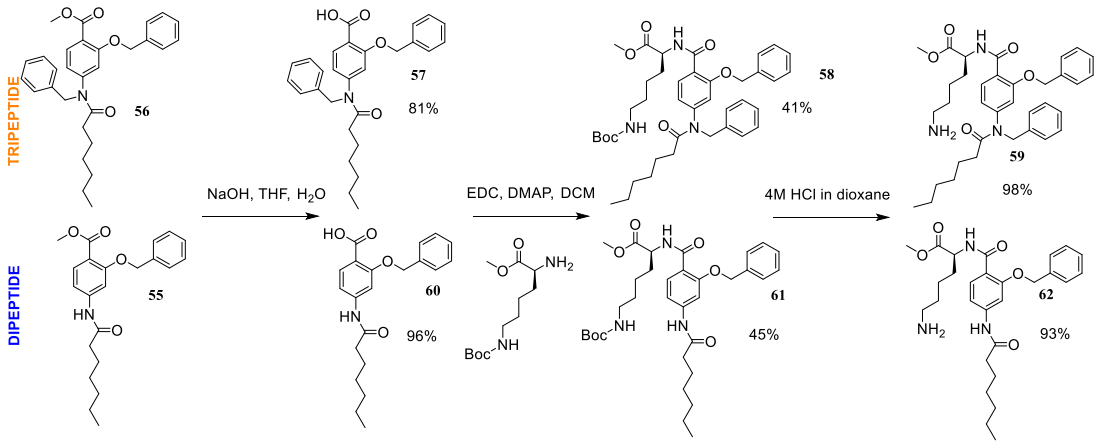

Scheme 23: The final steps of the di and tri peptidomimetic syntheses.

All of the steps were successful, with yields of >60% and the synthetic intermediates could easily be purified using silica column chromatography and did not require HPLC purification at any stage. The success of this route meant that different functionality could be introduced onto this backbone.

The next step was replacing the benzyl groups with indole groups to give a compound that contained the RWxxW motif. The di- peptidomimetic was synthesised by the same route as shown in Scheme 20 but using 3-(2-bromoethyl)indole compound instead of benzyl bromide to give peptidomimetic 6 (**66**) shown in Scheme 24.

The tripeptidomimetic required extra synthetic steps. To prevent possible side reactions the bromoindole was protected with a Boc group. Alkyation using NaH was unsuccessful. The amide starting material was broken down when treated with sodium hydride (shown by TLC and MS). It was unclear why this happened. The base was changed to potassium tert-butoxide, which is weaker than sodium hydride, but still strong enough to deprotonate the amide. The reaction was tested first using benzyl bromide to give **70**. This was successful with a yield of 90%. The remaining steps of the synthesis were carried out on this compound to give peptidomimetic 8 (**73**) shown in Scheme 24. The alkylation using potassium t-butoxide was repeated with the bromo-indole but only gave **74** with a yield of 5%. The reaction was repeated this time

refluxing for 4 hours which increased the yield to 12%. The reaction was run on a large enough scale so that the remaining steps of the synthesis could be carried out to give peptidomimetic 9 (**77**).

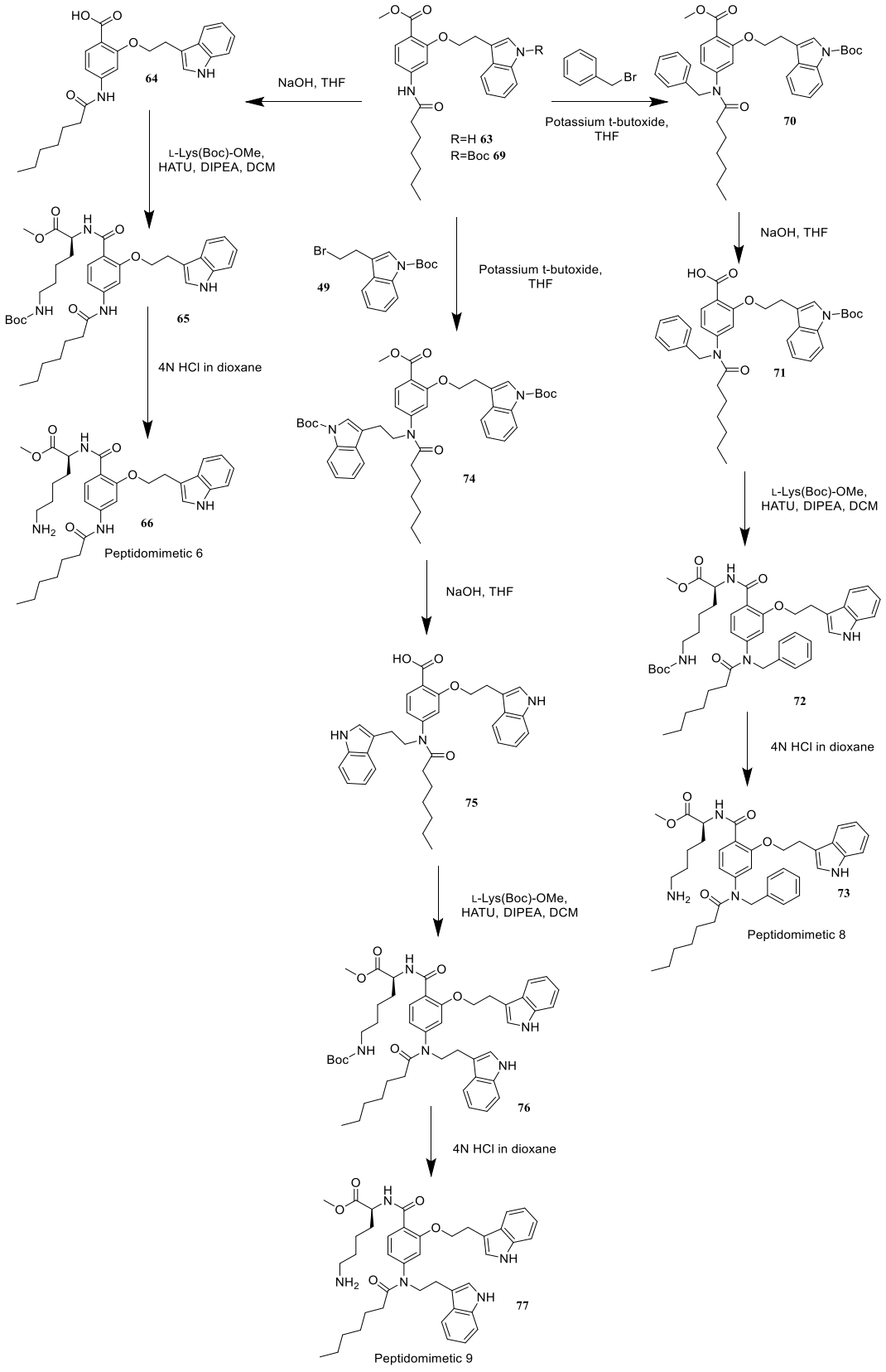

Scheme 24: The synthetic route proposed to achieve peptidomimetics 6, 8 and 9

From the new synthetic route, 5 peptidomimetics were successfully synthesised, and are shown in Figure 93. These compounds will be tested using the assays described. It is hoped that the compounds which contain the full RWxxW motif will inhibit MraY.

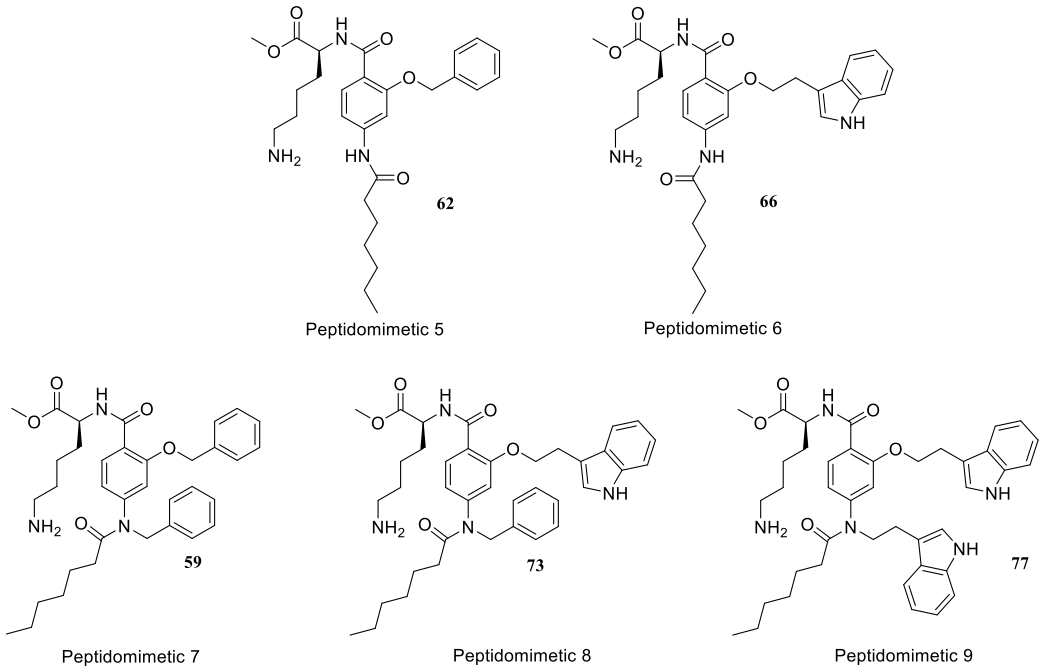

Figure 93: The five peptidomimetics synthesised using the optimised route.

The optimised route was a successful method to introduce the desired functionality onto the benzamide backbone. Whilst L-lysine was used in this instance, an L-arginine residue could be introduced, but would require the final purification to be carried out using RP-HPLC. It is also possible that L-ornithine could be used and then the guanidinium sidechain of L-arginine introduced as the last step. (The method for this will be described in section 5.5).

4.8 Biological testing of set two peptidomimetics

4.8.1 Microtitre broth dilution antimicrobial testing

The antimicrobial testing of these compounds was carried out as previously described. The results of which are shown in Table 17.

	MIC_{50} µg/mL		
	***E. coli* (TOP10)**	***B. subtilis* (W23)**	***P. fluorescens (PF-5)***
PM 5 (62)	8±2	44±1	>125
PM 6 (66)	28±3	28±3	56±4
PM 7 (59)	7±2	12±3	46±4
PM 8 (73)	4±2	28±5	>125
PM 9 (77)	4±1	58±5	>125

Table 17: The antimicrobial results for peptidomimetics 5-9

The results show that there is a notable improvement in the antimicrobial activity of these peptidomimetics against *E. coli* when compared to set one (section 4.5), and some activity against *P. fluorescens* was observed. Peptidomimetic 7 (**59**) has the best activity across the three species tested. Peptidomimetic 8 (**73**) and 9 (**77**) had the best activity against *E. coli*.

The MIC_{50} values are not representative of the effect on the bacteria that was caused by the peptidomimetics. Figure 94 shows the raw data obtained from the antimicrobial testing of peptidomimetic 8 (**73**). When the concentration of peptidomimetic 8 (**73**) increases to ≈ 63 µg/mL The OD_{595} of the bacterial cultures begin to increase. This is seen across all three species that were tested and for all of the peptidomimetics (peptidomimetic 5-9). This is an effect which was not seen when testing the previous peptidomimetics or the dipeptides. One possible explanation for the cause of this is that when the compounds reach a certain concentration the bacteria are able to break down the compound, and utilise the components for growth. At higher concentrations hydrolysis of the ester may occur and this could lead to a reduction in activity. It is also possible that the compounds form micelles at higher concentrations, leading to the increase in MIC_{50} that is seen.

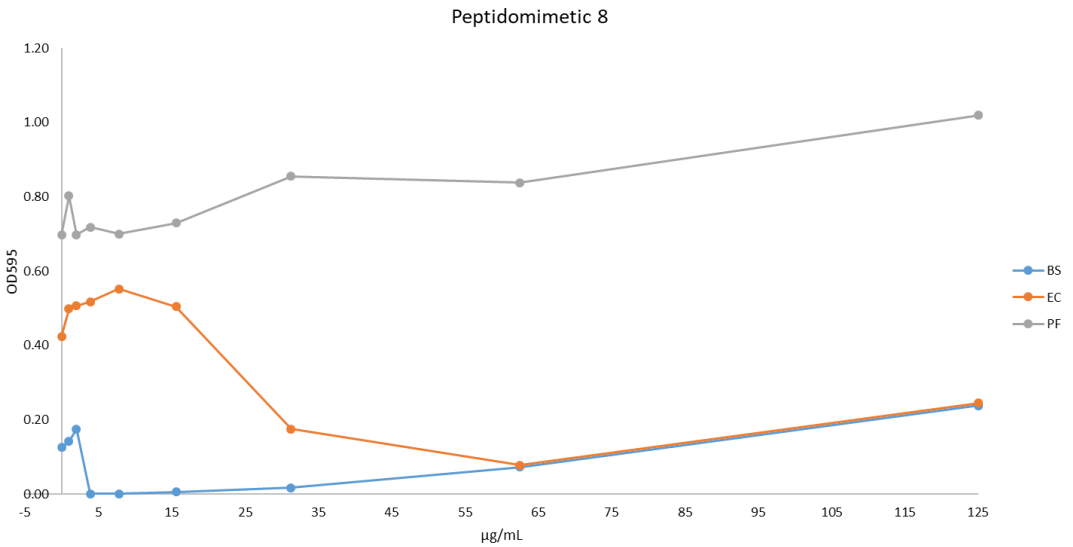

Figure 94: The graph showing the results of the antimicrobial testing of peptidomimetic 8 against *B.subtilis* (BS), *E.coli* (EC) and *P. fluorescens*

4.8.2 MIC and MBC testing against ESKAPE pathogens

Peptidomimetic 5-9 were submitted to the Warwick university antimicrobial screening facility and the MIC and MBC values against the ESKAPE pathogens were determined by John Moat and Julie Todd. This data is shown in Table 18.

	PM 5 (62)		**PM 6 (66)**		**PM 7 (59)**		**PM 8 (73)**		**PM 9 (77)**	
	MIC	MBC	MIC	MBC	MIC	MBC	MIC	MBC	MIC	MBC
Enterobacter cloacae NCTC 13405	>256	-	>256	-	>256	-	>256	-	>256	-
Staphylococcus aureus ATCC 29213	32	32	128	128	16	16	16	16	16	16
Klebsiella pueumoniae ATCC 700603	>256	-	>256	-	>256	-	>256	-	>256	-
Acinetobacter baumanni ATCC 19606	>256	-	>256	-	>256	-	>256	-	>256	-
Pseudomonas aeruginosa NCTC 13437	>256	-	>256	-	>256	-	>256	-	>256	-
Enterococcus faecium JH2	16	64	64	256	16	64	8	16	16	32

Table 18: The MIC and MBC values in µg/mL of Peptidomimetic 5-9 against the ESKAPE pathogens

These peptidomimetics did not show an improvement in activity across the ESKAPE pathogens when compared with the data obtained for the dipeptides in section 3.1.4. The peptidomimetics only showed activity against *S. aureus* and *E. faecium*, with the MIC and MBC implying bactericidal charateristics.

4.8.3 Fluorescence inhibition assay

The fluorescence inhibition assay was carried out as described in section 3.2 on peptidomimetic 9 (**77**). No inhibition of MraY was seen when tested at 100 µg/mL. Peptidomimetic 9 is the compound which is the most similar in structure to the RWxxW motif but still no inhibition of MraY is observed. Shown in Figure 95.

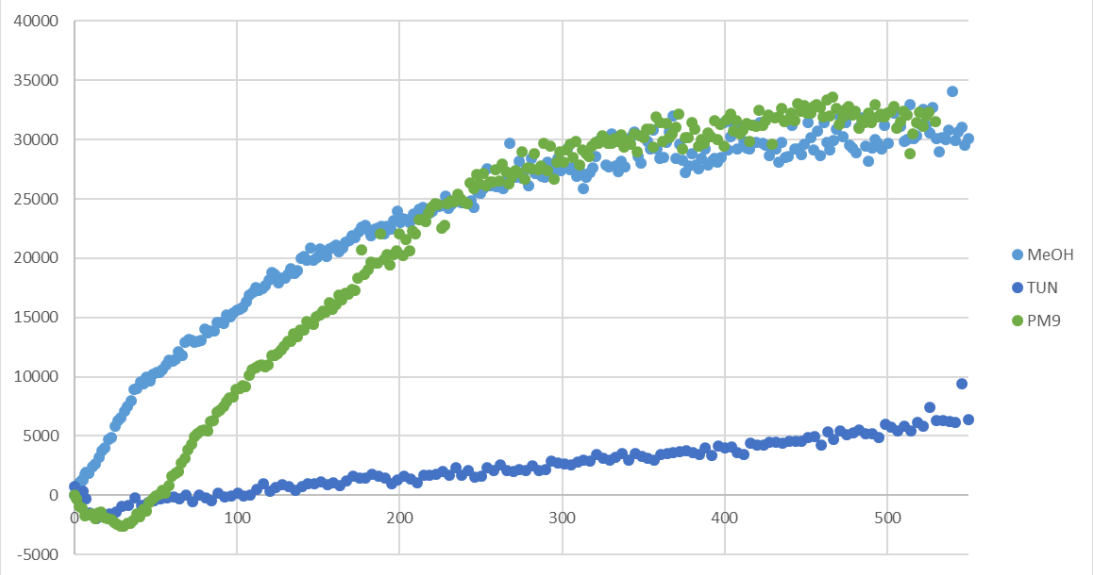

Figure 95: The continuous fluorescence assay run on Peptidomimetic 9 at 100 µg/mL. TUN=tunicamycin 20 µg/mL

4.8.4 Radiochemical inhibition assay results

The 5 benzamide peptidomimetics were tested using the radiochemical inhibition assay, described in section 3.3. The results are shown in the bar chart below (Figure 96).

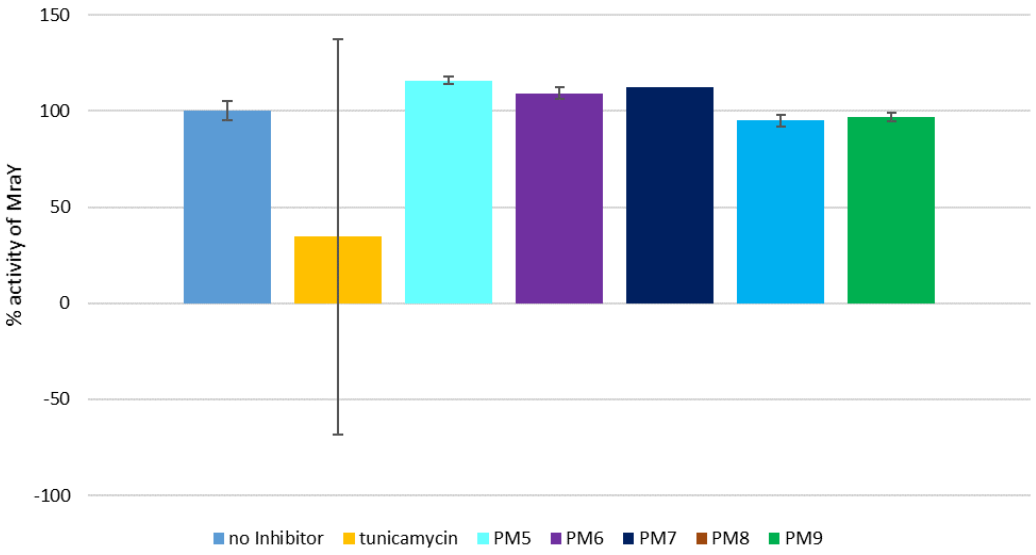

Figure 96: A bar chart showing the % activity of MraY with no inhibitors and when treated with 200 µM peptidomimetic 5 (62), peptidomimetic 6 (66), peptidomimetic 7 (59), peptidomimetic 8 (73) and peptidomimetic 9 (77) with the controls which use no inhibitor (100% activity) and tunicamycin (100 µg/mL)

The cause of the large error bar on the tunicamycin data point is discussed in section 3.3.

As with the tested dipeptides MraY showed >100% activity when treated with some of the peptidomimetics. Based on this data there is no apparent inhibition of MraY by these compounds. Further assays need to be carried out as discussed in section 3.3.

4.8.5 AlamarBlue ™ Assay

The AlamarBlue ™ Assay was carried out on peptidomimetics 5-9 using the same method described in section 3.5. The results of which are shown in Figure 97 and Table 19.

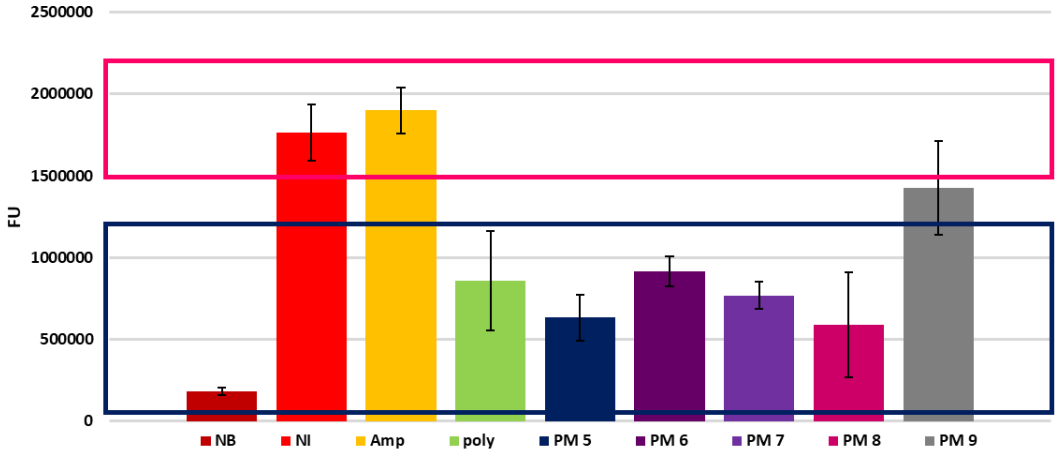

Figure 97: The fluorescence results of the alamarBlue™ assay carried out on peptidomimetics 5-9. The pink box shows the fluorescence readings which fall in a similar area to bacteriostatic agents and the blue box shows the regions which bactericidal compounds are expected to fall in. [NB= no bacteria, NI= no inhibitor, Amp= amipicillin, Poly= Polymyxin B]. All compounds were tested at 250 µg/mL.

Well contents	Well colour
No bacteria	
No inhibitor	
Ampicillin	
Polymyxin	
PM5 (**62**)	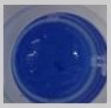
PM6 (**66**)	
PM7 (**59**)	
PM8 (**73**)	
PM9 (**77**)	

Table 19: A table showing the colours of the alamarBlue™ dye after 2 hours in the different conditions used in the assay.

With the exception of peptidomimetic 9, all of the peptidomimetics fell within the bactericidal range which was determined based on the results of the controls run in this assay. It is possible that this is due to the peptidomimetics making pores in the membrane. These results are not comparable to RWoct, and therefore it is unlikely that they are interacting with the same mechanism of action.

4.9 Conclusion

The second set of peptidomimetics had more promising antimicrobial activity against all three strains tested against, with peptidomimetic 7 having the best activity of this set. The increase of OD_{595} at higher concentrations of compounds is not a favourable property for drug molecules.

The inhibition fluorescence assay was run with peptidomimetic 9 (**77**) which was most closely related to the RWxxW motif. No inhibition was seen. No inhibition of MraY was seen by the 5 benzamide peptidomimetics when tested using the radiochemical inhibition assay.

The resazurin dye assay indicated that the peptidomimetics may be toxic. The potential adverse effects exhibited on the membrane by these compounds may affect any results seen in assays containing membranes and therefore the results would not be reliable. It is not possible to have control samples which would allow the determination between membrane disruption and MraY inhibition.

Further alterations to the structures could be made. Swapping the lysine residue for an arginine may help the peptidomimetics interact similarly to RWoct (**6**). RWoct (**6**) had shown the most favourable antimicrobial activity overall (section 3.1). This would require more time and a more difficult purification which would extend beyond the timeframe of this project. RW-Noct (**22**) which contained the amide linker did not show as favourable results in section 3.1 as RWoct (**6**). This is due to the amide bond which replaced the ester linker. The benzamide backbone uses amide linkers, which could potentially be changed to ester linkers, however ester linkers are not favourable in the design of drug molecules. Alterations to the chain length may also lead to an improvement of activity, but it is likely that this would only enhance the surfactant effect which may be occurring.

CHAPTER 5: Additional Arg-Trp peptidomimetics and molecular modelling

Additional peptidomimetic structures on which Arg and Trp sidechains could be positioned were also explored. This chapter focuses on a cyclic structure which will replace the peptide backbone with the aim of maintaining or improving the MIC_{50} of the dipeptides.

5.1 cyclic backbone designs

Two cyclic structures which have been designed based on the results obtained from the dipeptide series and the peptidomimetics synthesised in the previous chapter are shown in Figure 98.

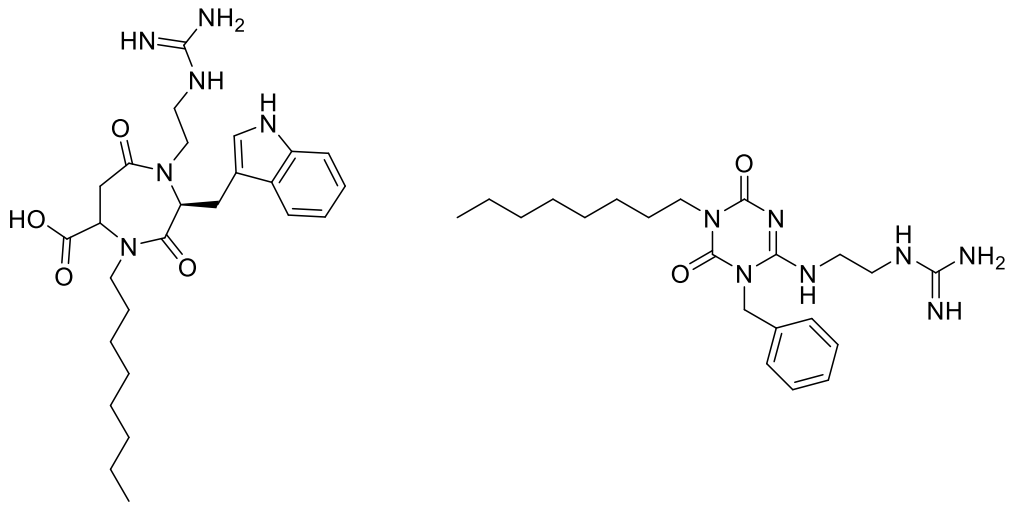

Figure 98: The structures of two peptidomimetics which incorporate a cyclic backbone replacement

Peptidomimetic 13 is based on a Houghten model and peptidomimetic 14 is based on a triazinedione model proposed by Congiu.[86,155]

The triazinedione structure had previously been used by Ralbovsky *et al.* (2009) and Congiu *et al.* (2014) in the design and synthesis of prokineticin receptor antagonists.[155,156] Congiu refined the synthetic route which Ralbovsky had previously proposed. Whilst the prokineticin interaction was not of interest for the design of antimicrobial peptidomimetics, the triazinedione backbone provided a structure onto which functionality could be installed. The central ring is more constrained than the parent peptide backbone reducing the overall flexibility of the molecule. By testing peptidomimetics with more constrained backbones a better picture of the interaction can be built up.

The Houghten model is one of a series of backbones designed by the group for the conversion of dipeptides into peptidomimetics.[86] This series of peptidomimetic backbones are synthesised using solid phase peptide chemistry.

5.2 Design and synthesis of triazinedione peptidomimetic backbone- Peptidomimetic 11

Using the general synthetic route described by Congiu different reagents could be employed to allow the installation of an octyl chain, an aromatic group and cationic lysine and/or arginine mimic onto the triazinedione backbone.[155] The route is shown in Scheme 25.

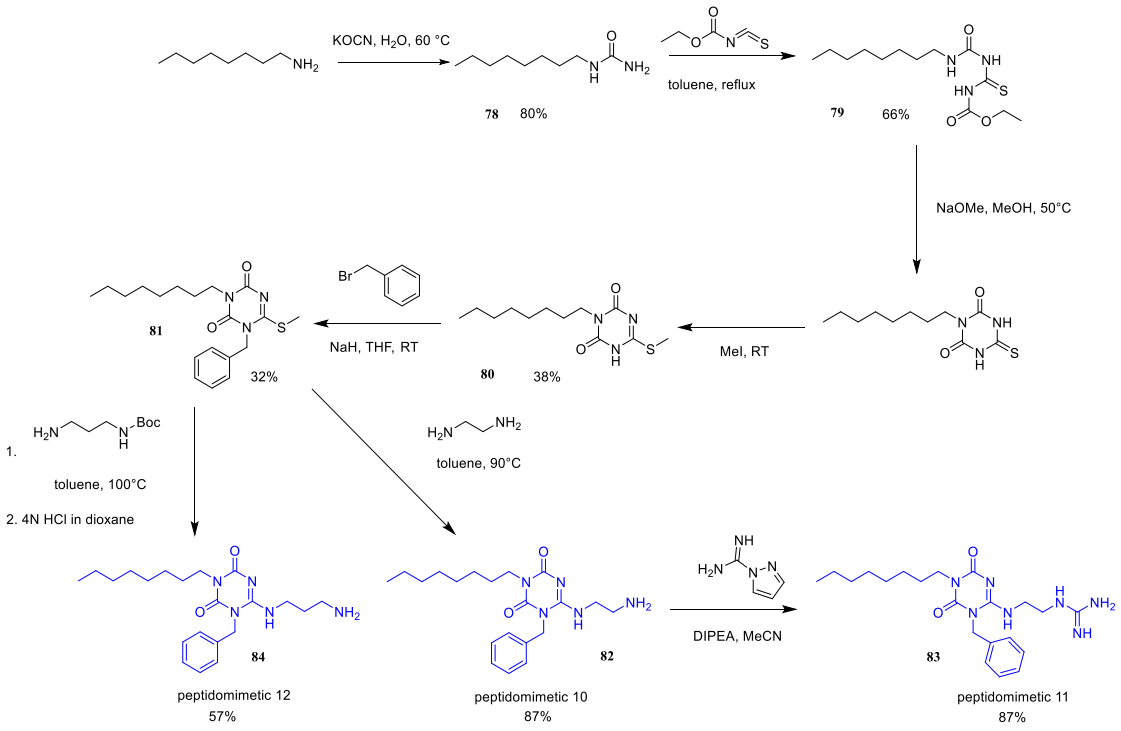

Scheme 25: The synthetic route to PM 10, 11 and 12. The final compounds are shown in blue.

Three peptidomimetics could be synthesised using the same route. Peptidomimetic 10 has a free amine which is linked to the ring by two carbons whereas peptidomimetic 12 has a three carbon linker (more closely mimicking lysine). This will aid the determination of how flexible the cationic moiety needs to be. Peptidomimetic 11 contains a guanidinium group to mimic the arginine moiety.

The first step involves the formation of octyl urea **78** from 1-octylamine and potassium cyanate under acidic conditions (80% yield). **78** is precipitated from the solution and was isolated using suction filtration. Octyl urea was then coupled with ethyl isothiocyante to give the N-ethoxycarbonylthiourea **79** which was precipitated from

diethyl ether (66% yield). The thiourea was cyclised and alkylated *in situ* using MeI to give **80** (38% yield).The resulting intermediate was purified using silica gel chromatography. A second alkylation was then carried out using benzyl bromide in the presence of NaH to give **81** (33% yield). Ethylenediamine was then used to displace the thiomethyl group to give peptidomimetic 10 (**82**) (87% yield). The solvents from this reaction were removed *in vacuo* in a fumehood due to the liberation of methanethiol.

To give the peptidomimetic 12 (**84**), *N*-Boc-1,3-propanediamine was used in place of ethylenediamine. The Boc protection was necessary as 1,3-diaminopropane is very toxic. The Boc group was removed in the 100 °C reaction conditions used, so no deprotection step was necessary. Both peptidomimetic 10 (**82**) and peptidomimetic 12 (**84**) were purified using silica gel chromatography, where the silica had been deactivated using TEA.

Peptidomimetic 11 (**83**) was formed when **82** was reacted with 1H-Pyrazole-1-carboxamidine hydrochloride in the presence of DIPEA. The desired product precipitated from the reaction mixture, and after filtration, required no further purification.

5.3 Biological testing of triazinedione peptidomimetics

5.3.1 Microtitre broth dilution antimicrobial testing

The antimicrobial testing of these compounds was carried out as previously described. The results of which are shown in Table 20.

	MIC_{50} µg/mL		
	***E. coli* (TOP10)**	***B. subtilis* (W23)**	***P. Fluorescens (PF-5)***
PM 10 (82)	12±3	25±2	21±3
PM 11 (83)	2±1	4±1	11±1
PM 12 (84)	12±1	4±1	24±2

Table 20: The results of the antimicrobial testing carried out on the series of dipeptides. The three organisms tested against were *E. coli*, *B. subtilis* and *P. fluorescens*.

All three compounds showed promising antimicrobial activity but, PM 11 (**83**) shows the best activity across the three bacteria, which might be attributed to the guanidinium group.

5.3.2 MIC and MBC testing against ESKAPE pathogens

PM10-PM12 were submitted to the Warwick university antimicrobial screening facility and the MIC and MBC values against the ESKAPE pathogens were determined by John Moat and Julie Todd. This data is shown in Table 21.

	PM 10 (82)		PM 11 (83)		PM 12 (84)	
	MIC	MBC	MIC	MBC	MIC	MBC
Enterobacter cloacae NCTC 13405	32	32	64	64	32	32
Staphylococcus aureus ATCC 29213	8	16	8	32	4	16
Klebsiella pueumoniae ATCC 700603	32	32	64	64	64	64
Acinetobacter baumanni ATCC 19606	32	32	32	32	64	64
Pseudomonas aeruginosa NCTC 13437	64	64	64	64	64	128
Enterococcus faecium JH2	8	32	8	32	16	32

Table 21: The MIC and MBC values in µg/mL of PM10-PM12 against the ESKAPE pathogens

Of all the groups of compounds synthesised in this project PM10-PM12 have the best overall data when tested against the ESKAPE pathogens with MIC values of less than 64 µg/mL against all of the pathogens. There are no clear trends with the differing cationic functionality. As with the other groups of compounds, these peptidomimetics appear to also be bactericidal.

5.3.3 Radiochemical inhibition assay results peptidomimetics 2

The 3 heterocyclic peptidomimetics were tested using the radiochemical inhibition assay, described in section 3.3. The results are shown in the bar chart below (Figure 99).

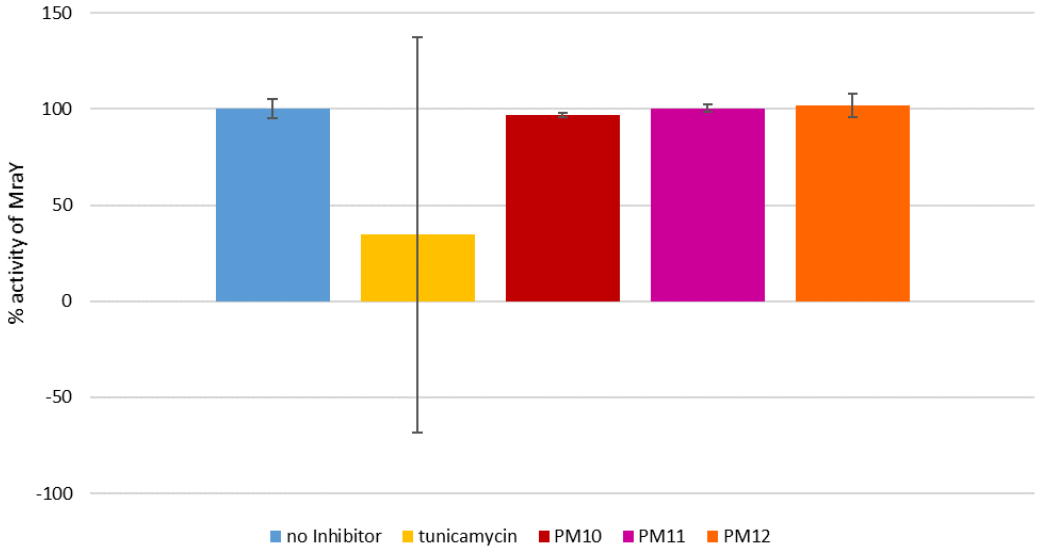

Figure 99: A bar chart showing the % activity of MraY with no inhibitors and when treated with 200 µM PM10 (62), PM11 (83), and PM 12 (84) with the controls which use no inhibitor (100% activity) and tunicamycin (100 µg/mL)

The cause of the large error bar on the tunicamycin data point is discussed in section 3.3.

Based on this data there is no apparent inhibition of MraY by these compounds. Further assays need to be carried out as discussed in section 3.3.

5.3.4 AlamarBlue ™ Assay

The alamarBlue ™ Assay was carried out on peptidomimetics 10-12 using the same method described in section 3.3. The results of which are shown in Figure 100 and Table 22.

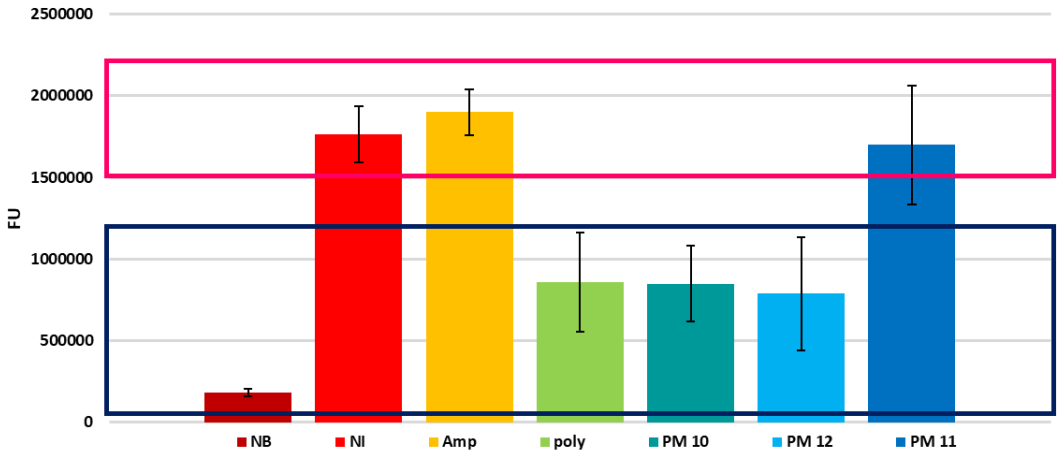

Figure 100: A graph to show the fluorescence readings from the AlamarBlue™ assay. [NB= no bacteria, NI= no inhibitor, Poly= polymyxin, Amp= ampicillin]. The pink box shows the fluorescence readings considered to be bacteriostatic agents and the blue box the bactericidal agents. All compounds were tested at 250 µg/mL. All compounds were tested at 250 µg/mL.

Well contents	Well colour
No bacteria	
No inhibitor	
Ampicillin	
Polymyxin	
PM10 (**82**)	
PM11 (**83**)	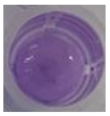
PM12 (**84**)	

Table 22: A table showing the colours of the alamarBlue™ dye after 2 hours in the different conditions used in the assay. All compounds were tested at 250 µg/mL.

Both peptidomimetics with the free amine (10 and 12) show results which are more similar to polymyxin. Peptidomimetic 11 which had the best antimicrobial activity appears to be bacteriostatic in the alamarBlue assay. From the biological assay results peptidomimetic 11 is the most promising candidate.

5.5 Peptidomimetic 13

The synthesis route design had a number of steps which would need a lot of optimisation to allow the full route to be carried out. For these reasons the synthesis of this molecule was not pursued due to time constraints.

5.6 Conclusion

From the molecular modelling peptidomimetic 11 was chosen to be synthesised and tested. The simple synthesis route designed by Congiu *et al.* was easily executed and three new peptidomimetics were synthesised.[155]

The antimicrobial testing showed that the guanidinium had the best activity and this compound also gave the most favourable results based on the alamarblue assay.

Based on this data and the data gained in the previous chapters the guanidinium group is preferable over the free amine of lysine (or lysine mimics). This is most apparent in this chapter and that could be due to the simplified and constrained nature of the new peptidomimetics.

It would be interesting to introduce an indole in place of the benzyl group. This would allow further determination of the important functionality.

The MraY inhibition of the heterocyclic peptidomimetics was tested using this radiochemical inhibition assay. There was no inhibition seen.

CHAPTER 6: CONCLUSIONS AND FUTURE WORK

The synthesis route for the Arg-Trp dipeptide series was optimised during this project along with the purification methods. The series of dipeptides was tested using several biological tests to determine the antimicrobial activity and the inhibition of MraY.

From the MIC_{50} calculations there was only one clear trend which showed that increasing the alkyl chain length improved the activity. Both the arginine and lysine residues showed promising activity when coupled with tryptophan and so these were the residues that would be carried forward to the peptidomimetic design. The dipeptide series were also tested in a continuous fluorescence assay to determine if the compounds were able to inhibit MraY. None of the peptides showed inhibition of MraY in this assay. Both RWoct (**6**) and KWoct (**16**) were tested using the radiochemical inhibition assay also. This confirmed the results of the fluorescence based assay. Previous work proclaimed that when MraY was overexpressed the MIC_{50} for RWoct (**6**) increased, implying that MraY was infact the target. These results could not be replicated and following the optimisation of this assay no conclusive data could be obtained. This indicates that the dipeptides exhibit their antimicrobial effects via different mechanisms, and this theory is corroborated by the alamarBlue assay which was carried out. This indicated that most of the dipeptides were acting in a bactericidal manner, which is not consistent with the proposed MraY inhibition. When considering that the increase in alkyl chain length increased the antimicrobial activity, it may indicate that the dipeptides are acting similarly to detergents.

The next step was to use this data to design a series of peptidomimetics. The first series were based on a benzamide backbone described in chapter 1. Following the synthesis of dipeptide mimetics and synthesis route optimisation a second tryptophan side chain was installed so the peptidomimetics included the entire RWxxW motif. It was hoped that the addition of this third residue would confer the inhibition of MraY. The tripeptide mimetic did not show inhibition of MraY. The mimetics did however have antimicrobial activity, which was improved upon in the second round of mimetics. The mechanism of action could be similar to the dipeptide but it is impossible to say based on the biological data that was obtained. The MraY inhibition of the final five benzamide peptidomimetics were tested using the radiochemical inhibition assay, however none showed inhibition.

The cyclic backbone of the second round of mimetics was chosen based on computation modelling analysis. The diazepine backbone was furnished with the same groups as the benzamide backbone. These compounds showed antimicrobial activity which was comparable to the parent dipeptides but no inhibition of MraY.

A summary of the antimicrobial data and the radiochemical inhibition data is shown in Table 23 and Figure 101 respectively.

	MIC_{50} µg/mL		
Compound	*E. coli* (TOP10)	*B. subtilis* (W23)	*P. Fluorescens* (PF-5)
RWhex (7)	37	13	53
RWoct (6)	5	13	18
RWdec (8)	3	8	3
Boc-RWoct (11)	12	8	21
Ac-RWoct (12)	42	9	19
HWoct (13)	8	12	21
R^1Woct* (18)	9	10	45
KWoct (16)	2	1	5
RYoct (10)	118	25	124
RFoct (9)	11	11	64
RW-Noct (22)**	3	7	20
KW-Noct (24)**	17	11	26
KG-Noct (28)**	10	2	18
PM 1 (37)	>125	10	>125
PM 3 (48)	30	10	>125
PM 5 (62)	8	44	>125
PM 6 (66)	28	28	56
PM 7 (59)	7	12	46
PM 8 (73)	4	28	>125
PM 9 (77)	4	58	>125
PM 10 (82)	12	25	21
PM 11 (83)	2	4	11
PM 12 (84)	12	4	24

Table 23: The summary of the antimicrobial data obtained for the compounds synthesised in this project.

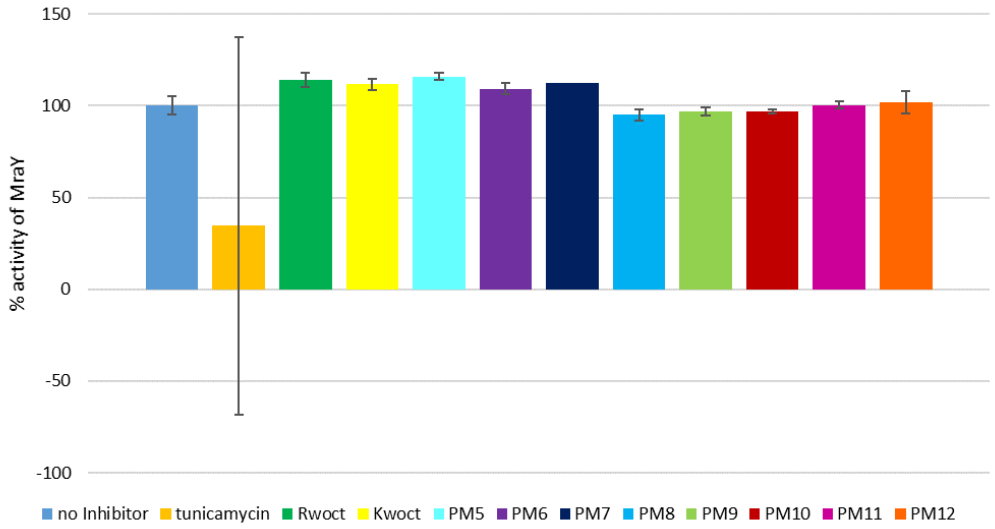

Figure 101: The summary of the antimicrobial data obtained for the compounds synthesised in this project.

Despite having series of dipeptides and peptidomimetics which have antimicrobial activity, we were unable to obtain data which allows us to draw conclusions of how they exhibit these effects. Based on the data obtained in this project there is no evidence to suggest that there is an interaction between MraY and any of the compounds tested. The data shows the MBC and MIC are the same and this coupled with the alamarBlue data indicated that many of the compounds are acting in a bactericidal manner and could indicate that the peptides and mimetics are toxic. Based on the structures of the compounds it would not be unrealistic to think that they could lead to pore formation in the membrane.

The future work could take two routes. The first would be to go back to the pentapeptides which show inhibition of the enzyme and make changes and peptidomimetics based on these.[48] It would also be advisable to confirm there is actually an interaction occurring at this site, by carrying out more conclusive biological tests on Epep and MraY (such as a pull down assay). The second would be to pursue the antimicrobial activity and develop the peptidomimetics. However it may be wise to first test for toxicity against mammalian cell lines. More testing could be carried out in order to determine the true mechanism of action.

CHAPTER 7: EXPERIMENTAL

All chemicals used during this research project were purchased from Merck, Sigma Aldrich, Fluorochem and Fisher scientific.

The biological reagent C_{55}-P was purchased from Larodan Fine Chemicals. The substrate UDP-MurNAc pentapeptide was purchased from UK Bacterial Cell Wall Assembly Network (BaCWAN) and fluorescently tagged by summer student Namrita Modgill. Water used during these experimental procedures was deionized and autoclaved when necessary.

Deuterated methanol, acetone and DMSO used for recording NMR spectra were purchased from Sigma Aldrich. HPLC grade solvents were purchased from Fischer Scientific. Anhydrous solvents which were used were obtained from Sigma Aldrich. Solvents were evaporated using a Buchi Rotavapor R-114 equipped with a Buchi Vacuum pump V-700 and a Buchi Heating bath B-480.

Flash column chromatography was conducted on silica gel (40-63μm, 60Å) purchased from Sigma Aldrich.

Thin Layer Chromatograpy (TLC) was performed on aluminum backed plates precoated with Merck TLC Silica Gel 60 F_{254} and were visualized under UV radiation, permanganate, ninhydrin or vanillin.

Semi-preparative HPLC purification was conducted on an Agilent Technologies series 1200 Preparative HPLC instrument equipped with a Synergi™ (4 μm Polar-RP 80 Å) column and analytical HPLC was carried out using the same machine but equipped with a Kinetex (5u EVO C18 100A) column.

Low resolution ESI mass spectra were recorded using a Bruker Esquire 2000 electrospray ionization spectrometer. High resolution mass spectra were recorded on a Bruker Micro TOF spectrometer equipped with an electrospray ionization source (by Lijiang Song).

^{1}H-NMR spectra were recorded at 300, 400 or 600 MHz using Bruker DPX300, DPX400 or AV III-600 spectrometers, respectively. Chemical shifts (δ_H) are quoted in ppm with reference to the residual solvent peak. The data in parenthesis follow the order (i) multiplicity: s, singlet; d, doublet, t, triplet; q, quartet; m, multiplet (ii) number

of equivalent protons (iii) coupling constant (*J*) in Hz (iv) assignment. HMBC, HMQC, COSY and NOESY were used in selected cases to aid in assignments.

Fluorescence data and bacterial growth data were recorded using a HIDEX Sense Microplate Reader 425-301.

The optical purity of the compounds could not be tested due to lack of instrumentation

7.1 Synthesis of the amino acid precursors and dipeptides

Octyl L-tryptophanate; L-Trp-oct[48] ***(1)***

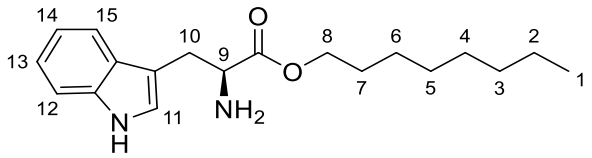

L-Tryptophan (2.04 g, 0.01 mol, 1 eq) was added to 1-octanol (10 mL, 8.24 g, 0.06 mol, 6.3 eq) and was refluxed at 80°C. H_2SO_4 conc. (1 mL) was added to the reaction mixture and stirred for 1 hour. The reaction mixture was taken up in EtOAc (25 mL) and then washed with sat. Na_2CO_3 (3x25 mL). The organic layer was separated and dried under $MgSO_4$ and then concentrated. To remove the excess 1-octanol from the tryptophan octyl ester, purification by silica column chromatography was carried out using deactivated silica and eluted with 1:9/MeOH:EtOAc. The resulting product was an off white solid. The procedure was modified from literature reference[87]; (1.35 g, 4.2 mmol, 43%). $\mathbf{R_f}$ = 0.54 (1:9/MeOH:EtOAc) **^{1}H-NMR:** (400 MHz, MeOD) δ_H: 0.90 (t, 3H, J=6.5 Hz, H-1), 1.18-1.32 (m, 10H, H-2, H-3, H-4, H5, H-6), 1.51 (m, 2H, H-7), 3.14 (qd, J= 6.0 Hz, 3.5 Hz, 2H, H-10), 3.76 (t, 1H, J=6.5 Hz, H-9), 3.99 (t, 2H, J=6.5 Hz, H-8), 7.00 (t, 1H, J=7.5, H-13), 7.08 (s, 1H, H-11), 7.09 (t, 1H, J=7.5 Hz, H-14) , 7.31 (d, 1H, J=8.0, H-12), 7.52 (d, 1H, J=8.0, H-15). **^{13}C-NMR** (125 MHz, MeOD): 13.39 (*C*H_3), 22.30 (*C*H_2), 25.63 (*C*H_2), 27.44 (CH*C*H_2), 28.48 (*C*H_2), 29.08 (*C*H_2), 31.60 (*C*H_2), 32.23 (*C*H_2), 54.32 (CO*C*H), 64.20 (*C*H_2), 110.06 (NHC*C*H), 111.35 (CH_2*C*), 118.48 (CCH*C*H), 120.94 (NHCCH*C*H), 121.37 (C*C*H), 123.86 (C*C*HNH), 127.24 (C*C*), 136.74 (NHC), 172.84 (O*C*HO). **LRMS** *m/z* (ESI): 317.3 $[M+H]^+$. **HRMS** *m/z* (ESI): calculated for $C_{19}H_{29}N_2O_2^+$ $[M+H]^+$: Exact Mass: 317.2224 found 317.2225.

Hexyl L-tryptophanate; L-Trp-hex[157] ***(2)***

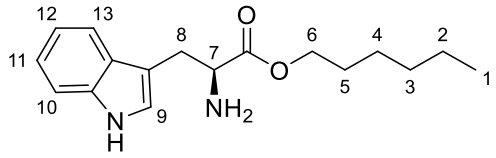

L-Tryptophan (4.12 g, 0.02 mol, 1eq) was added to 1-hexanol (20 mL, 16.3 g, 0.16 mol, 8 eq) and was refluxed at 80°C. H_2SO_4 *conc.* (1 mL) was added to the reaction mixture and stirred for 45 minutes. The reaction mixture was taken up in EtOAc (25 mL) and then washed with *sat.* Na_2CO_3 (3x25 mL). The organic layer was separated and dried under $MgSO_4$ and then concentrated. To remove the excess 1-hexanol from the tryptophan hexyl ester, purification by silica column chromatography was carried out using deactivated silica and eluted with 1:9/MeOH:EtOAc. The resulting product was an off white solid; (2.69g, $9.3x10^{-3}$mol, 47%). **R_f =** 0.54 (1:9/MeOH:EtOAc) **^{1}H-NMR:** (400 MHz, MeOD) δ_H: 0.88 (t, 3H, J=7.0 Hz, H-1), 1.12-1.33 (m, 8H, H-2, H-3, H-4), 1.47 (m, 2H, J=6.5 Hz, H-5), 3.14 ((qd, J= 6.0 Hz, 3.5 Hz, 2H, H-8), 3.76 (t, 1H, J=6.0 Hz, H-7), 3.99 (t, 2H, J=6.5 Hz, H-6), 7.00 (t, 1H, J=7.13, H-11), 7.08 (s, 1H, J=6.0 Hz, H-9), 7.09 (t, 1H, J=7.0 Hz, H-12) , 7.33 (d, 1H, J=8.0 Hz, H-10), 7.52 (d, 1H, J=8.0 Hz, H-13). **^{13}C-NMR** (125 MHz, MeOD): 13.01 (CH_3), 22.30 (CH_2), 25.63 (CH_2), 27.09 (CHCH_2), 28.48 (CH_2), 29.08 (CH_2), 53.72 (CO*C*H), 64.88 (OCH_2), 109.32 (CH_2*C*), 112.02 (NHC*C*H), 118.02 (CCH*C*H), 120.18 (NHCCH*C*H), 121.68 (C*C*H), 123.18 (C*C*HNH), 127.14 (C*C*), 136.74 (NH*C*CH), 175.07 (O*C*HO). **LRMS** *m/z* (ESI): 289.2 $[M+H]^+$. **HRMS** *m/z* (ESI): calculated for $C_{17}H_{25}N_2O_2^+$ $[M+H]^+$: Exact Mass: 289.1911 found 289.1914.

*Decyl L-tryptophanate; L-Trp-dec (**3**)*

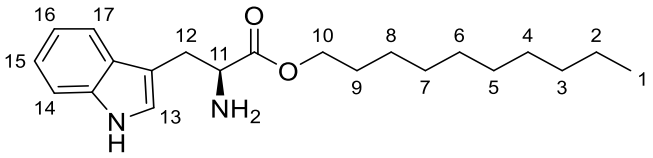

L-Tryptophan (4.12 g, 0.02 mol, 1eq) was added to 1-decanol (20 mL, 16.59 g, 0.10 mol, 5eq) and was refluxed at 80°C. H_2SO_4 *conc.* (1 mL) was added to the reaction mixture and stirred for 1 hour. The reaction mixture was taken up in EtOAc (25 mL) and then washed with *sat.* Na_2CO_3 (3x25 mL). The organic layer was separated and dried under $MgSO_4$ and then concentrated. To remove the excess 1-decanol from the tryptophan decyl ester, purification by silica column chromatography was carried out using deactivated silica and eluted with 1:9/MeOH:EtOAc. The resulting product was an off white solid; (4.36g, 0.13 mol, 63%). $\mathbf{R_f}$ = 0.57 (1:9/MeOH:EtOAc). **^{1}H-NMR:** (400 MHz, MeOD) δ_H: 0.9 (t, 3H, J=7.0 Hz, H-1), 1.12-1.39 (m, 8H, H-2, H-3, H-4, H-5, H-6, H-7, H-8), 1.48 (m, 2H, J=7.0 Hz, H-9), 3.14 ((qd, J= 6.0 Hz, 3.5 Hz, 2H, H-12), 3.76 (t, 1H, J=6.5, H-11), 4.00 (t, 2H, J=6.5 Hz, H-10), 7.00 (t, 1H, J=7.0 Hz, H-15), 7.08 (s, 1H, H-13), 7.09 (t, 1H, J=7.0 Hz, H-16) , 7.33 (d, 1H, J=8.0 Hz, H-14), 7.52 (d, 1H, J=8.0 Hz, H-17). **^{13}C-NMR** (125 MHz, MeOD): 13.27 (*C*H_3), 22.45 (*C*H_2), 25.62 (*C*H_2), 30.38 (*C*H_2), 25.43 (*C*H_2), 27.35 (*C*H_2), 29.44 (*C*H_2), 28.21 (*C*H_2), 31.77 (*C*H_2), 65.50 (O*C*H_2), 174.93 (O*C*HO), 53.29 (CO*C*H), 28.09 (CH*C*H_2), 109.29 (CH_2*C*), 123.39 (C*C*HNH), 136.70 (NH*C*CH), 111.07 (NHC*C*H), 120.15 (NHCCH*C*H), 121.85 (C*C*H), 118.45 (CCH*C*H). 127.43 (C*C*). **LRMS** *m/z* (ESI): 367.3 $[M+Na]^+$. **HRMS** *m/z* (ESI): calculated for $C_{21}H_{32}N_2NaO_2^+$ $[M+Na]^+$: Exact Mass: 367.2356 found 367.2357.

*Octyl L-phenylalaninate; L-Phe-oct (**4**)*

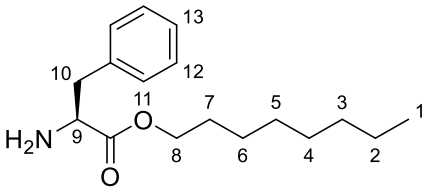

L-phenylalanine (1.00 g, 6.1 mmol) was added to 1-octanol (10mL, 8.24 g, 0.06 mol) and was refluxed at 80°C. H_2SO_4 *conc*. (0.5 mL) was added to the reaction mixture and stirred for 45 minutes. The reaction mixture was taken up in EtOAc (25 mL) and then washed with Na_2CO_3 *sat.* (3x25 mL). The organic layer was separated and dried under MgSO4 and then concentrated. To remove the excess 1-octanol from the tryptophan octyl ester purification by silica column chromatography was carried out using deactivated silica, eluting with EtOAc. The resulting product was an off white solid. The procedure was modified from literature reference[48]; (0.44 g, 2.7 mmol, 45%). **R_f** = 0.41 (EtOAc) **^{1}H-NMR:** (400 MHz, MeOD) δ_H: 0.90 (t, 3H, J=6.5 Hz, H-1), 1.21-1.40 (m, 10H, H-2, H-3, H-4, H5, H-6), 1.45-1.59 (m, 2H, H-7), 2.89-3.04 (m, 2H, H-10), 3.70 (t, 1H, J=6.5 Hz, H-9), 4.05 (t, 2H, J=6.5 Hz, H-8), 7.16-7.32 (m, 5H, H-11, H-12, H-13). **^{13}C-NMR** (125 MHz, MeOD): 14.49 (*C*H_3), 23.76 (*C*H_2), 27.00 (*C*H_2), 29.66 (*C*H_2), 30.34 (*C*H_2), 30.63 (*C*H_2), 33.06 (*C*H_2), 41.97 (CH*C*H_2), 56.78 (*C*H_2), 66.11 (CO*C*H), 127.90 (CHCH*C*H), 129.58 (C*C*H), 130.38 (CCH*C*H), 138.35 (CH_2*C*), 175.91 (O*C*HO). **LRMS** *m/z* (ESI): 278.3 $[M+H]^+$. **HRMS** *m/z* (ESI): calculated for $C_{17}H_{28}NO_2^+$ $[M+H]^+$: Exact Mass: 278.2115 found 278.2116.

*Octyl L-tyrosinate; L-Tyr-oct (**5**)*

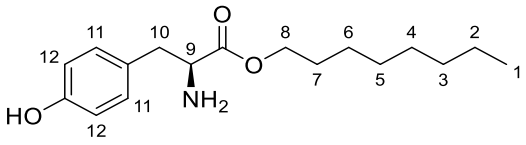

L-Tyrosine (1.00 g, 5.5 mmol) was added to 1-octanol (10mL, 8.24 g, 0.06 mol) and was refluxed at 80°C. H_2SO_4 *conc*. (0.5 mL) was added to the reaction mixture and stirred for 45 minutes. The reaction mixture was taken up in EtOAc (25 mL) and then washed with Na_2CO_3 *sat.* (3x25 mL). The organic layer was separated and dried under $MgSO_4$ and then concentrated. To remove the excess 1-octanol from the tryptophan octyl ester purification by silica column chromatography was carried out using deactivated silica, eluting with 1:9/MeOH:EtOAc. The resulting product was an off white solid. The procedure was modified from literature reference[48]; (0.64 g, 2.1 mmol, 38%). **R_f =** 0.67 (1:9/MeOH:EtOAc) **^{1}H-NMR:** (400 MHz, MeOD) δ_H: 0.90 (t, 3H, J=6.8 Hz, H-1), 1.25-1.38 (m, 10H, H-2, H-3, H-4, H5, H-6), 1.53 (m, 2H, J=6.5 Hz, H-7), 2.87 (m, 2H, H-10), 3.63 (t, 1H, J=6.5 Hz, H-9), 4.05 (t, 2H, J=6.5 Hz, H-8), 6.72 (d, 2H, J=7.0 Hz, H-11) , 6.99 (d, 2H, J=7.0 Hz, H-12). **^{13}C-NMR** (125 MHz, MeOD): 13.13 (*C*H_3), 22.29 (*C*H_2), 25.50 (*C*H_2), 28.38 (*C*H_2), 29.13 (*C*H_2), 32.01 (*C*H_2), 32.50 (*C*H_2), 39.58 (CH*C*H_2), 48.27 (*C*H_2), 55.15 (CO*C*H), 127.78 (CH_2*C*), 130.17 (C*C*H), 144.44 (CCH*C*H), 156.19 (*C*OH), 174.48 (O*C*HO). **LRMS** *m/z* (ESI): 294.3 $[M+H]^+$. **HRMS** *m/z* (ESI): calculated for $C_{17}H_{28}NO_3^+$ $[M+H]^+$: Exact Mass: 294.2064 found 294.2064.

*L-Arginyl-L-tryptophan octyl ester; H_2N-RW-oct (**6**)*[87]

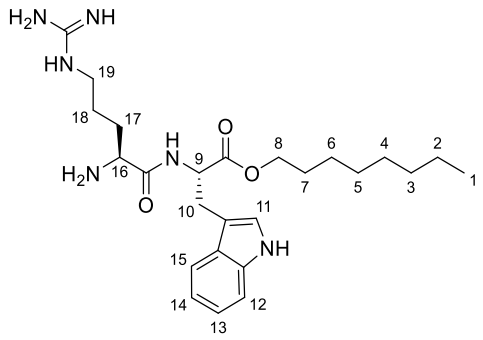

Boc-Arg-OH (0.69 g, 2.5 mmol, 1 eq), HATU (0.95 g, 2.5 mmol, 1 eq), **1** (0.79 g, 2.5 mmol, 1 eq) and DIPEA (0.32 g, 0.45 mL, 2.5 mmol, 1 eq) were stirred in anhydrous DCM (15 mL) and stirred for 18 hours. The solvent was removed *in vacuo*. The resulting oil (50 mg) was added to Amberlyst 15 resin (1.5 g) in DCM (10 mL) and stirred overnight. The DCM was removed by suction filtration. The resin was then successively washed with hexane, THF and methanol. The resin was then stirred with 3M ammonia in methanol for 30 minutes. The solvent was then evaporated *in vacuo* and the product was dried under high vacuum to produce a brown oil. The procedure was modified from a literature reference[48,158] **^{1}H-NMR:** (400 MHz, MeOD) δ_H: 0.90 (t, 3H, J=7.0 Hz, H-1), 1.15-1.40 (m, 10H, H-2, H-3, H-4, H5, H-6), 1-44-1.50 (m, 2H, H-7), 1. 67-1.73 (m, 2H, H-18), 1.77-1.83 (m, 2H, H-17), 3.14 (dd, J=8.5, 2.5 Hz, 2H, H-19), 3.20-3.27 (m, 2H, H-10), 3.70-3.77 (m, 1H, H-16), 3.92-3.98 (m, 1H, H-9), 4.02 (t, 2H, J=6.5 Hz, H-8), 7.01 (t, 1H, J= 6.0 Hz, H-13), 7.09 (t, 1H, J=7.5 Hz, H-14), 7.17 (s, 1H, H-11), 7.35 (d, 1H, J=8.0 Hz, H-15), 8.34 (d, 1H, J=8.0 Hz, H-12). **^{13}C-NMR** (125 MHz, MeOD): 13.04 (CH_3), 22.30 (CH_2), 22.35 (CH_2), 22.65 (CH_2), 23.66 (CH_2CH_2), 25.48 ($CHCH_2$), 28.09 (CH_2), 28.88 (CH_2), 28.89 ($CHCH_2$), 31.56 (CH_2), 44.32 (CH_2NH), 52.33 ($COCH$), 53.85 ($NHCOCH$), 65.72 (CH_2), 172.13 ($OCHO$), 108.98 (CH_2C), 111.06 ($NHCCH$), 117.60 ($CHCHC$), 118.49 ($CHCHC$), 123.16 ($NHCCHCH$), 123.23 ($CCHNH$), 127.13 (CHC), 136.73 (NHC), 157.27 ($NHCNH$), 168.59 ($NHCO$). **LRMS** *m/z* (ESI): 473.2 $[M+H]^+$. **HRMS** *m/z* (ESI): calculated for $C_{21}H_{32}N_2O_3^+$ $[M+H]^+$: Exact Mass: 473.3235 found 473.3239.

*L-Arginyl-L-tryptophan hexyl ester; H_2N-RW-hex (**7**)*

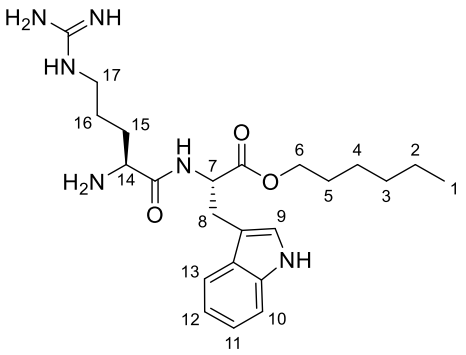

Boc-Arg-OH (0.69 g, 2.5 mmol, 1 eq), HATU (0.95 g, 2.5 mmol, 1 eq), **2** (0.72 g, 2.5 mmol, 1 eq) and DIPEA (0.32 g, 0.45 mL, 2.5 mmol, 1 eq) were stirred in anhydrous DCM (15 mL) and stirred for 18 hours. The solvent was removed *in vacuo*. The resulting oil (50 mg) was added to Amberlyst 15 resin (1.5 g) in DCM (10 mL) and stirred overnight. The DCM was removed by suction filtration. The resin was then successively washed with hexane, THF and methanol. The resin was then stirred with 3M ammonia in methanol for 30 minutes. The solvent was then evaporated and the product was dried under high vacuum to produce a brown oil; **^{1}H-NMR:** (400 MHz, MeOD) δ_H: 0.89 (t, 3H, J=7.0 Hz, H-1), 1.16-1.32 (m, 8H, H-2, H-3, H-4), 1.37-1.42 (m, 2H, H-5), 1.68-1.70 (m, 2H, H-16), 1.79-1.91 (m, 2H, H-15), 2.92-3.08 (m, 2H, H-17), 3.17 (dd, J=8.5, 2.5 Hz, 2H, H-8), 3.91 (t, 1H, J=6.5 Hz, H-7), 4.02 (t, 2H, J=6.5 Hz, H-6), 4.10 (t, 1H, J=7.0 Hz, H-14), 7.01 (t, 1H, J=7.5 Hz, H-11), 7.08 (s, 1H, H-9), 7.09 (t, 1H, J=7.5 Hz, H-12), 8.15 (d, 1H, J=8.0 Hz, H-10), 8.49 (d, 1H, J=8.0 Hz, H-13). **^{13}C-NMR** (125 MHz, MeOD): 13.04 (CH$_3$), 22.30 (CH$_2$), 22.65 (CH$_2$), 23.66 (CH$_2C$H$_2$), 25.48 (CHCH$_2$), 28.88 (CH$_2$), 28.89 (CHCH$_2$), 31.56 (CH$_2$), 44.32 (CH$_2$NH), 52.33 (COCH), 53.85 (NHCOCH), 65.72 (OCH$_2$), 108.98 (CH$_2C$), 111.06 (NHCCH), 118.49 (CHCHC), 123.16 (NHCCHCH), 123.23 (CCHNH), 136.73 (NHC), 172.13 (OCHO), 117.60 (CHCHC), 127.13 (CHC), 157.27 (NHCNH), 168.59 (NHCO). **LRMS** *m/z* (ESI): 445.2 $[M+H]^+$. **HRMS** *m/z* (ESI): calculated for $C_{23}H_{37}N_6O_3^+$ $[M+H]^+$: Exact Mass: 445.2922 found 445.2947.

*L-Arginyl-L-tryptophan decyl ester; H_2N-RW-dec (**8**)*

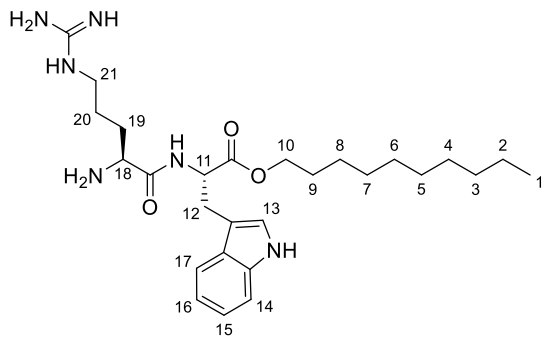

Boc-Arg-OH (0.69 g, 2.5 mmol, 1 eq), HATU (0.95 g, 2.5 mmol, 1 eq), **3** (0.86 g, 2.5 mmol, 1 eq) and DIPEA (0.32 g, 0.45 mL, 2.5 mmol, 1 eq) were stirred in anhydrous DCM (15 mL) and stirred for 18 hours. The solvent was removed *in vacuo*. The resulting oil (50 mg) was added to Amberlyst 15 resin (1.5 g) in DCM (10 mL) and stirred overnight. The DCM was removed by suction filtration. The resin was then successively washed with hexane, THF and methanol. The resin was then stirred with 3M ammonia in methanol for 30 minutes. The solvent was then evaporated *in vacuo* and the product was dried under high vacuum to produce a brown oil. The procedure was modified from literature reference[48,158]; **^{1}H-NMR:** (400 MHz, MeOD) δ_H: 0.89 (t, 3H, J=7.0 Hz, H-1), 1.15-1.35 (m, 12H, H-2, H-3, H-4, H-5, H-6, H-7, H-8), 1.43-1.52 (m, 2H, H-9), 1.60-1. 72 (m, 2H, H-20), 1.78-1.91 (m, 2H, H-19), 3.20 (dd, J=8.5, 2.5 Hz, 2H, H-12), 3.54 (t, 2H, J=6.5 Hz, H-21), 4.00 (t, 1H, J=7.0 Hz, H-11), 4.09 (t, 2H, J=6.5 Hz, H-10), 4.27 (t, 1H, J=7.5 Hz, H-18), 7.11 (t, 1H, J=7.5 Hz, H-15), 7.31 (t, 1H, J=7.5 Hz, H-16), 7.33 (s, 1H, H-13), 8.17 (d, 1H, J=8.5 Hz, H-17), 8.49 (d, 1H, J=8.0 Hz, H-14). **^{13}C-NMR** (125 MHz, MeOD): 14.41 (*C*H_3), 22.35 (*C*H_2), 23.61 (CH_2*C*H_2), 26.21 (*C*H_2), 27.42 (CH*C*H_2), 27.49 (*C*H_2), 27.55 (CH*C*H_2), 28.24 (*C*H_2), 28.35 (*C*H_2), 28.88 (*C*H_2), 28.91 (*C*H_2), 30.80 (*C*H_2), 42.11 (*C*H_2NH), 53.68 (CO*C*H), 54.51 (NHCO*C*H), 63.22 (*C*H_2), 109.18 (CH_2*C*), 110.62 (NHC*C*H), 117.22 (CH*C*HC), 118.50 (*C*HCHC), 122.22 (C*C*HNH), 123.43 (NHCCH*C*H), 127.67 (CH*C*), 136.60 (NH*C*), 156.55 (NH*C*NH), 170.10 (NH*C*O), 172.90 (O*C*HO). **LRMS** *m/z* (ESI): 501.2 $[M+H]^+$. **HRMS** *m/z* (ESI): calculated for $C_{27}H_{45}N_6O_3^+$ $[M+H]^+$: Exact Mass: 501.3548 found 501.3550.

*Octyl L-arginyl-L-phenylalanate- H_2N-RF-oct (**9**)*

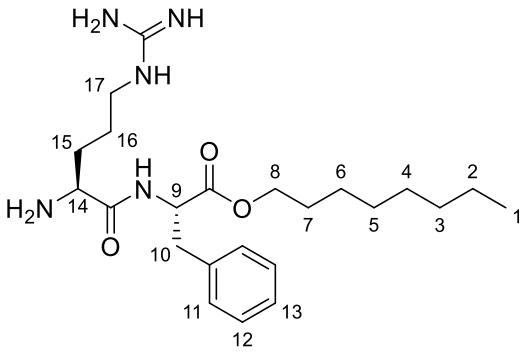

Fmoc-Arg-OH (0.99 g, 2.5 mmol, 1 eq), HBTU (0.10 g, 2.75 mmol, 1.1 eq), **4** (0.76 g, 2.75 mmol, 1.1 eq) and DIPEA (0.1.92 g, 2.60 mL, 2.5 mmol, 6 eq) were stirred in anhydrous DCM under N_2 gas for 18 hours. The solvent was removed *in vacuo*. The dipeptide was deprotected with 20% piperidine in THF (10 mL). Once the deprotection was complete the solution was concentrated under high vacuum to remove the piperidine and then precipitated from Et_2O. The sample was then purified by RP-HPLC using Synergi™ 4 µm Polar-RP 80 Å and an elution gradient of H_2O + 0.1% TFA /MeCN + 0.1% TFA (80:20 to 0:100) over 30 minutes with a flow rate of 2 mL/min. The fractions were pooled and lyophilized. **^{1}H-NMR:** (400 MHz, MeOD) δ_H: 0.91 (t, 3H, J=6.5 Hz, H-1), 1.23-1.35 (m, 10H, H-2, H-3, H-4, H5, H-6) 1.42-1.49 (m, 2H, H-7), 1.66- 1.78 (m, 2H, H-16), 1.84- 1.96 (m, 2H, H-15), 3.00-3.09 (m, 2h, H-16), 3.22 (t, 2H, J=7.0 Hz, H-8), 3.89 (t, 1H, J=6.0 Hz H-9), 4.07 (t, 2H, J=6.5 Hz, H-10), 4.72 (t, 1H, J=7.5 Hz H-14), 7.21-7.36 (m, 5H, H-11, H-12, H-13). **^{13}C-NMR** (125 MHz, MeOD): 12.97 (*C*H_3), 21.97 (*C*H_2), 23.66 (*C*H_2), 25.54 (CH_2*C*H_2), 28.16 (CH*C*H_2), 28.49 (*C*H_2), 28.89 (*C*H_2), 31.36 (*C*H_2), 32.82 (*C*H_2), 36.81 (CH*C*H_2), 40.46 (CH_2CH_2*C*H_2), 52.48 (CO*C*H), 54.26 (CO*C*H), 65.35 (O*C*H_2), 126.73 (CCHCH*C*H), 128.27 (CH_2*C*), 128.72 (CCH*C*H), 136.54 (CH_2*C*) 156.21 (NH*C*NH), 171.59 (O*C*O), 174.20 (NH*C*O). **LRMS** *m/z* (ESI): 434.4 $[M+H]^+$. **HRMS** *m/z* (ESI): calculated for $C_{23}H_{40}N_5O_3^+$ $[M+H]^+$: Exact Mass: 434.3126 found 434.3129.

*Octyl L-arginyl-L-tyrosinate - H_2N-RY-oct **(10)***

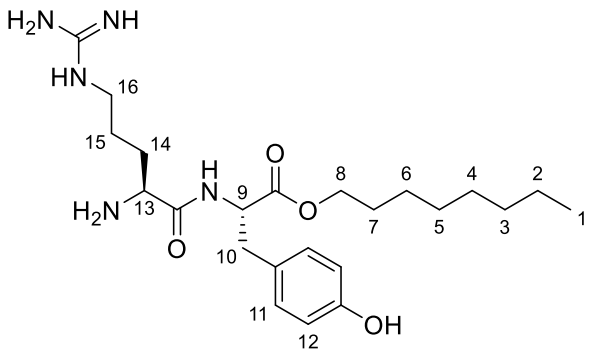

Fmoc-Arg-OH (0.99 g, 2.5 mmol, 1 eq), HBTU (0.96 g, 2.5 mmol, 1 eq), **5** (0.74 g, 2.5 mmol, 1 eq) and DIPEA (0.32 g, 0.45 mL, 2.5 mmol, 1 eq) were stirred in anhydrous DCM under N_2 gas for 18 hours. The dipeptide was deprotected with 20% piperidine in DCM (10 mL). Once the deprotection was complete the solution was concentrated under high vacuum to remove the piperidine and precipitated from Et_2O. The sample was then purified by RP-HPLC using Synergi™ 4 µm Polar-RP 80 Å and an elution gradient of H_2O + 0.1% TFA /MeCN + 0.1% TFA (100:0 to 0:100) over 30 minutes with a flow rate of 2 mL/min. The fractions were pooled and lyophilized. **^{1}H-NMR:** (400 MHz, MeOD) δ_H: 0.91 (t, 3H, J=7.0 Hz, H-1), 1.20-1.35 (m, 10H, H-2, H-3, H-4, H5, H-6) 1.53-1.62 (m, 2H, H-7), 1.65- 1.75 (m, 2H, H-15), 1.76- 1.82 (m, 2H, H-14), 1.89- 1.95 (m, 2h, H-16), 2.87 (m, 2H, H-10), 3.22 (t, 2H, J=7.0 Hz, H-8), 3.90-3.94 (m, 1H, H-9), 4.60-4.64 (m, 1H, H-13), 6.71 (d, 2H, J=8.0 Hz, H-11), 7.04 (d, 2H, J=8.0 Hz, H-12). **^{13}C-NMR** (125 MHz, MeOD): 13.31 (CH_3), 21.80 (CH_2), 23.53 (CH_2), 25.37 (CH_2), 28.37 (CH_2), 28.44 (CH_2), 28.81 (CH_2), 31.54 ($CHCH_2$), 35.92 (CH_2CH_2), 40.20 ($CHCH_2$), 44.38 ($CH_2CH_2CH_2$), 52.43 (COCH), 54.52 (COCH), 65.17 (OCH_2), 115.00 (CCHCH), 126.96 (CH_2C), 129.82 (CCH), 156.26 (COH), 160.81 (NHCNH), 168.38 (OCO), 171.78 (NHCO). **LRMS** *m/z* (ESI): 450.4 $[M+H]^+$. **HRMS** *m/z* (ESI): calculated for $C_{23}H_{40}N_5O_4^+$ $[M+H]^+$: Exact Mass: 450.3075 found 450.3075.

*Boc-L-Arginyl-L-tryptophan octyl ester; Boc-RW-Oct (**11**)*

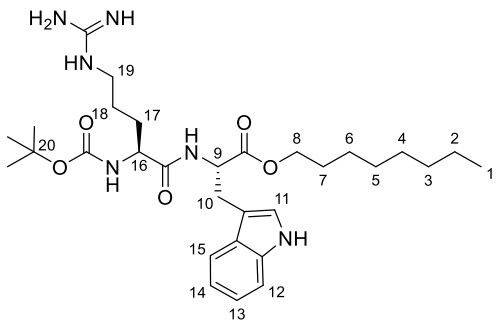

Boc-Arg-OH (1 g, 2.5 mmol, 1 eq), HATU (0.95 g, 2.5 mmol, 1 eq), **1** (0.69 g, 2.5 mmol, 1 eq) were stirred in minimum DCM. DIPEA (0.32 g, 0.45 mL, 2.5 mmol, 1 eq) was added to the reaction mixture which was then stirred over 3 days. The reaction was monitored with LC-MS. The reaction mixture was concentrated to dryness. The dipeptide was precipitated from Et_2O. The sample was then purified by RP-HPLC using Synergi™ 4 µm Polar-RP 80 Å and an elution gradient of H_2O + 0.1% TFA /MeCN + 0.1% TFA (100:0 to 0:100) over 30 minutes with a flow rate of 2 mL/min. The fractions were pooled and lyophilized; **^{1}H-NMR:** (400 MHz, MeOD) δ_H: 0.90 (t, 3H, J=7.0 Hz, H-1), 1.21-1.34 (m, 12H, H-2, H-3, H-4, H5, H-6), 1.39 (s, 9H, H-20), 1.44-1.51 (m, 2H, H-7), 1.64-1.70 (m, 2H, H-18), 1.71-1.80 (m, 2H, H-17), 3.13-3.19 (m, 2H, H-19), 3.20 (dd, J=8.5, 2.5 Hz, 2H, H-10), 3.93-4.00 (t, 2H, H-16), 4.10 (t, 1H, J=6.5 Hz, H-8), 4.32 (t, 1H, J=6.5 Hz, H-9), 7.04 (t, 1H, J=7.5 Hz, H-13), 7.29 (s, 1H, H-11), 7.30 (t, 1H, J=7.5 Hz, H-14), 7.68 (dd, 2H, J=8.0 Hz, H-12, H-15). **^{13}C-NMR** (125 MHz, MeOD): 12.24 (*C*H_3), 21.52 (*C*H_2), 22.62 (CH_2*C*H_2), 23.45 (*C*H_2), 24.60 (*C*H_2), 27.89 (CH*C*H_2), 28.19 (3*C*H_3), 28.24 (*C*H_2), 29.80 (CH*C*H_2), 29.82 (*C*H_2), 30.24 (*C*H_2), 44.32 (*C*H_2NH), 52.50 (NHCO*C*H), 54.30 (CO*C*H), 64.21 (*C*H_2), 80.21 (CH_3*C*), 109.29 (CH_2*C*), 110.61 (NHC*C*H), 118.02 (CH*C*HC), 119.92 (*C*HCHC), 122.16 (NHCCH*C*H), 122.49 (C*C*HNH), 128.13 (CH*C*), 136.73 (NH*C*), 157.27 (NH*C*NH), 156.33 (NH*C*OOC), 169.10 (NH*C*O), 170.23 (O*C*HO). **LRMS LRMS** *m/z* (ESI): 573.3 $[M+H]^+$. **HRMS** *m/z* (ESI): calculated for $C_{30}H_{49}N_6O_5^+$ $[M+H]^+$: Exact Mass: 573.3759 found 573.3759.

Ac-L-Arginyl-L-tryptophan octyl ester; Ac-RW-Oct ***(12)***

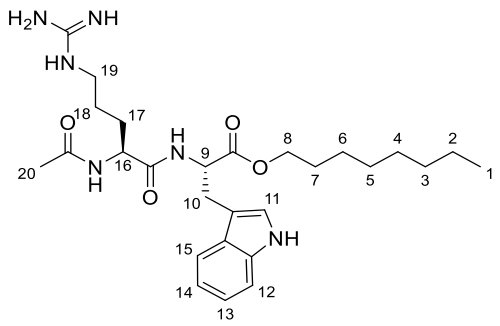

Boc-Arg-OH (1 g, 2.5 mmol, 1 eq), HATU (0.95 g, 2.5 mmol, 1 eq), **1** (0.79 g, 2.5 mmol, 1 eq) and DIPEA (0.32 g, 0.45 mL, 2.5 mmol, 1 eq) were stirred in anhydrous DCM under N_2 gas for 18 hours. The solvent was removed and the resulting oil was stirred in 4N HCl in dioxane (4 mL) for 4 hours. The solvent was removed and the resulting oil containing H_2N-RW-Oct was added to acetic anhydride (4 mL, 4.32 g, 0.042 mol) and DIPEA (4 mL, 2.98 g, 0.023 mol) in DCM (12 mL) and stirred for 30 minutes. The solvent was then evaporated. The sample was then purified by RP-HPLC using Synergi™ 4 μm Polar-RP 80 Å and an elution gradient of H_2O + 0.1% TFA /MeCN + 0.1% TFA (100:0 to 0:100) over 30 minutes with a flow rate of 2 mL/min. The fractions were pooled and lyophilized; **^{1}H-NMR:** (400 MHz, MeOD) δ_H: 0.90 (t, 3H, J=7.0 Hz, H-1), 1.18-1.38 (m, 10H, H-2, H-3, H-4, H5, H-6), 1-41-1.48 (m, 2H, H-7), 1. 60-1.69 (m, 2H, H-18), 1.72-1.80 (m, 2H, H-17), 1.94 (s, 3H, H-20), 3.14 (dd, J=8.5, 2.5 Hz, 2H, H-19), 3.21-3.27 (m, 2H, H-10), 3.69-3.75 (m, 1H, H-16), 3.93-3.98 (m, 1H, H-9), 4.00 (t, 2H, J=6.5 Hz, H-8), 7.03 (t, 1H, J= 6.0 Hz, H-13), 7.09 (t, 1H, J=7.5 Hz, H-14), 7.15 (s, 1H, H-11), 7.38 (d, 1H, J=8.0 Hz, H-15), 8.34 (d, 1H, J=8.0 Hz, H-12). **^{13}C-NMR** (125 MHz, MeOD): 13.09 (*C*H_3), 22.47 (*C*H_2), 23.09 (CO*C*H_3),23.42 (*C*H_2), 23.63 (CH_2*C*H_2), 24.85 (*C*H_2), 28.92 (CH*C*H_2), 29.10 (*C*H_2), 29.71 (*C*H_2), 29.80 (CH*C*H_2), 30.90 (*C*H_2), 46.28 (*C*H_2NH), 52.50 (NHCO*C*H), 54.28 (CO*C*H), 64.22 (O*C*H_2), 110.27 (CH_2*C*), 111.42 (NHC*C*H), 119.12 (CH*C*HC), 119.59 (*C*HCHC), 121.29 (C*C*HNH), 121.97 (NHCCH*C*H), 128.13 (CH*C*), 136.32 (NH*C*), 157.27 (NH*C*NH), 169.89 (NH*C*OCH_3), 170.10 (NH*C*O), 172.99 (O*C*HO). **LRMS** *m/z* (ESI): 515.2 $[M+H]^+$. **HRMS** *m/z* (ESI): calculated for $C_{27}H_{43}N_6O_4^+$ $[M+H]^+$: Exact Mass: 515.3340 found 515.3344.

*L-Histidyl-L-tryptophan octyl ester; H_2N-HW-Oct (**13**)*

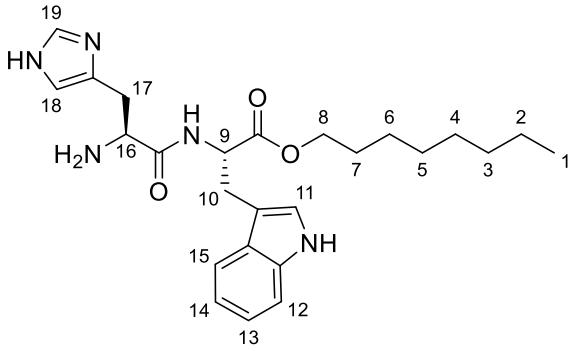

Boc-His(Trt)-OH (0.62 g, 1.25 mmol, 1 eq), HBTU (0.48 g, 1.25 mmol, 1 eq), **1** (0.40 g, 1.25 mmol, 1 eq)and DIPEA (0.16 g, 0.23 mL, 1.25 mmol, 1 eq) were stirred in anhydrous DCM (15 mL) under N_2 gas for 18 hours. The solvent was removed *in vacuo*. The resulting oil was purified using silica column chromatography, using deactivated silica, and the product was eluted with 2:8/EtOAc:petroleum ether. The solvent was removed and the resulting oil was stirred in 4N HCl in dioxane (4 mL) for 4 hours. The solvent was removed *in vacuo*. to give an orange oil; (8 mg, 0.02 mmol, 2%). **^{1}H-NMR:** (400 MHz, MeOD) δ_H: 0.89 (t, 3H, J=5.81, H-1), 1.20-1.35 (m, 10H, H-2, H-3, H-4, H5, H-6) 1.50 (m, 2H, H-7), 2.38 (m, 2H, H-17), 3.12 dd, J=8.5, 3.0 Hz, 2H, H-10), 3.53 (t, 2H, J=6.5 Hz, H-8), 3.91 (t, 1H, J=7.0 Hz, H-9), 4.29 (t, 1H, J=7.0 Hz, H-16), 7.08 (t, 1H, J=7.5 Hz, H-13), 7.09 (s, 1H, H-11), 7.12 (d, 2H, J= 2.0 Hz, H-18), 7.25 (t, 1H, J=7.5 Hz, H-14), 7.41 (d, 1H, J=8.0, H-12), 7.65 (d, 1H, J=8.0 Hz, H-15). 8.95 (d, 1H, J= 4.0, H19). **^{13}C-NMR** (125 MHz, MeOD): 10.14 (CH_3), 20.25 (CH_2), 23.45 (CH_2), 23.90 (CH_2), 26.82 (CH_2), 28.19 (CH_2), 29.67 ($CHCH_2$), 30.61 (CH_2), 33.41 ($CHCH_2$), 51.33 (COCH), 53.82 (NHCOCH), 65.88 (OCH_2), 108.83 (CH_2C), 111.06 (NHCCH), 117.34 (NHCHC), 118.11 (CHCHC), 118.49 (CHCHC), 122.44 (CCHNH), 123.16 (NHCCHCH), 127.13 (CHC), 127.89 (NCHNH), 131.45 (CH_2CN), 135.55 (NHC), 168.38 (OCHO), 171.88 (NHCO). **LRMS** *m/z* (ESI): 454.1 $[M+H]^+$. **HRMS** *m/z* (ESI): calculated for $C_{25}H_{36}N_5O_3^+$ $[M+H]^+$: Exact Mass: 454.2813 found 454.2814.

*N2,N6-bis(tert-Butoxycarbonyl)-L-lysine (**14**)*[159]

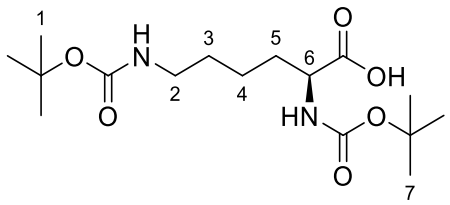

L-Lysine (2 g, 0.01 mol, eq) was dissolved in DCM (10 mL) and 1N NaOH (10 mL) was added and the reaction was stirred rapidly. To this Boc_2O (4.4 g, mmol, 2 eq) was added and the reaction was stirred for 18 hours. DCM (20 mL) and water (20 mL) were added and the pH was adjusted to 4 using dilute HCl. The water layer was removed and the the organic layer was washed a further two times with water. The organic layer was dried over $MgSO_4$. The solvent was removed *in vacuo*. Adapted from literature reference[159]; (2.7 g, 7.9 mmol, %). **^{1}H-NMR:** (400 MHz, MeOD) δ_H: 1.20-1.35 (m, 12H, H-4), 1.45 (s, 9H, H-1), 1.48 (s, 9H, H-7), 1.51-1.58 (m, 2H, H-3 1.65-1.78 (m, 2H, H-5), 1.83-1.99 (m, 2H, H-2), 4.44 (m, 1H, H-6). **^{13}C-NMR** (125 MHz, MeOD): 22.31($NHCH_2CH_2\mathit{C}H_2$), 26.53 ($CH_2\mathit{C}H_2CH$)**,** 27.51, 27.69 ($3\mathit{C}H_3$), 29.00 ($NHCH_2\mathit{C}H_2$), 30.50 ($NH\mathit{C}H_2$), 54.89 (NH*C*H), 79.51, 79.59 ($CH_3\mathit{C}$), 157.02, 157.24 (CO*C*ONH), 174.20 (CH*C*OOH). **LRMS** *m/z* (ESI): 347.3 $[M-H]^-$.

Octyl N2,N6-bis(tert-butoxycarbonyl)-L-lysyl-L-tryptophanate ***(15)***

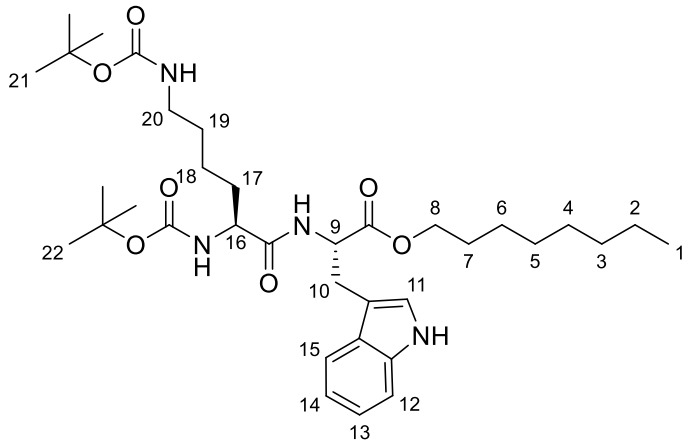

14 (1.0 g, 2.9 mmol, 1 eq), HBTU (1.2 g, 3.2 mmol, 1.1 eq), **1** (1 g, 3.2 mmol, 1.1 eq) and DIPEA (0.94 mL, 0.74 g, 5.8 mmol, 2 eq) were stirred in anhydrous DCM (10 mL) under N_2 gas for 18 hours. DCM (40 mL) was added and then washed three times with water (50 mL). The organic layer was dried over $MgSO_4$ and the solvent removed *in vacuo*. The resulting residue was applied to a silica column and the product was eluted with EtOAc; $\mathbf{R_f}$ = 0.68 (EtOAc). (0.79 g, 1.22 mmol, 42 %). **^{1}H-NMR:** (400 MHz, MeOD) δ_H: 0.90 (t, 3H, J=7.0 Hz, H-1), 1.17-1.36 (m, 12H, H-2, H-3, H-4, H5, H-6, H-18), 1.41 (s, 9H, H-22), 1.44 (s, 9H, H-21), 1.45-1.56 (m, 2H, J=7.04Hz, H-7), 1.67-1.76 (m, 2H, H-19), 1.86-195 (m, 2H, H-17), 2.94 (t, 2H, J= 7.5 Hz, H-20), 3.18 (dd, J=8.5, 2.5 Hz, 2H, H-10), 3.91 (t, 1H, J=6.5 Hz, H-16), 4.03 (t, 2H, J=6.5 Hz, H-8), 4.77 (t, 1H, J=7.0 Hz, H-9), 7.06 (dt, 2H, J= 7.5, 40 .5 Hz, H-13, H-14) 7.15 (s, 1H, J=4.2 Hz, H-11), 7.34 (d, 1H, J=8.0 Hz, H-12), 7.53 (d, 1H, J=8.0 Hz, H-15). **^{13}C-NMR** (125 MHz, MeOD): 13.30 (*C*H_3), 21.20 (*C*H_2), 22.30 (CH*C*H_2), 26.54 (*C*H_2), 27.10, 27.16 (3*C*H_3). 27.32 (*C*H_2), 28.29 (*C*H_2), 28.89 (CH_2*C*H_2), 29.13 (CH*C*H_2), 29.50 (*C*H_2), 30.72 (*C*H_2), 31.56 (CH*C*H_2), 38.91 (*C*H_2NHCO), 52.50 (CO*C*H), 53.82 (NHCO*C*HNH), 65.40 (*C*H_2), 79.72, 79.79 (CH_3*C*), 109.63 (CH_2*C*), 112.00 (NHC*C*H), 117.61 (CH*C*HC), 118.50 (CHCH*C*H), 121.66 (NHCCH*C*H), 122.98 (C*C*HNH), 127.14 (C*C*), 136.74 (NH*C*), 157.22, 157.54 (NH*C*OOC), 169.24 (O*C*HO), 172.20 (NH*C*O). **LRMS** *m/z* (ESI): 415.2 $[M+Na]^+$. **HRMS** *m/z* (ESI): calculated for $C_{35}H_{56}N_4NaO_7^+$ $[M+Na]^+$: 667.4041 found 667.4038.

*L-Lysyl-L-tryptophan octyl ester; H_2N-KW-Oct (**16**)*

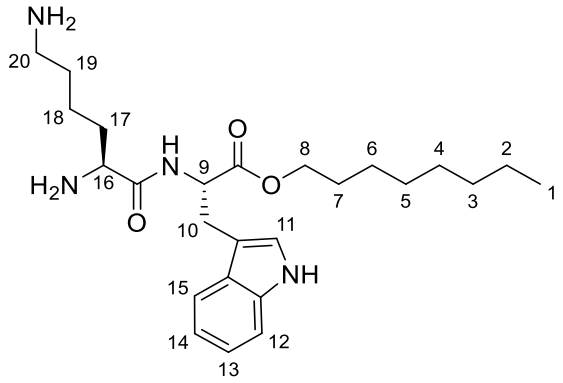

Compound **15** (0.1 g, 0.23 mmol) was stirred in 4N HCl in dioxane (1 mL) for 4 hours. The solvent was removed *in vacuo*; (0.094 g, 0.21 mmol, 94%). **^{1}H-NMR:** (400 MHz, MeOD) δ_H: 0.90 (t, 3H, J=7.0 Hz, H-1), 1.17-1.36 (m, 12H, H-2, H-3, H-4, H5, H-6, H-18), 1.40-1.56 (m, 2H, J=7.04Hz, H-7), 1.67-1.76 (m, 2H, H-19), 1.86-195 (m, 2H, H-17), 2.94 (t, 2H, J= 7.5 Hz, H-20), 3.22 (dd, J=8.5, 2.5 Hz, 2H, H-10), 3.91 (t, 1H, J=6.5 Hz, H-16), 4.03 (t, 2H, J=6.5 Hz, H-8), 4.77 (t, 1H, J=7.0 Hz, H-9), 7.06 (dt, 2H, J= 7.5, 13.5 Hz, H-13, H-14) 7.15 (s, 1H, J=4.2 Hz, H-11), 7.34 (d, 1H, J=8.0 Hz, H-12), 7.53 (d, 1H, J=8.0 Hz, H-15). **^{13}C-NMR** (125 MHz, MeOD): 13.03 (*C*H_3), 21.10 (*C*H_2), 22.30 (CH*C*H_2), 26.75 (*C*H_2), 27.12 (*C*H_2), 28.09 (*C*H_2), 28.89 (CH_2*C*H_2), 29.13 (CH*C*H_2), 29.44 (*C*H_2), 30.72 (*C*H_2), 31.56 (CH*C*H_2), 38.91 (*C*H_2NH_2), 52.50 (CO*C*H), 53.82 (NHCO*C*H), 65.25 (*C*H_2), 109.03 (CH_2*C*), 111.06 (NHC*C*H), 117.61 (CH*C*HC), 118.50 (CHCH*C*H), 121.18 (NHCCH*C*H), 123.17 (C*C*HNH), 127.14 (C*C*), 136.74 (NH*C*), 172.20 (NH*C*O), 168.72 (O*C*HO). **LRMS** *m/z* (ESI): 415.2 [M+Na]$^+$. **HRMS** *m/z* (ESI): calculated for $C_{25}H_{40}N_4NaO_3^+$ [M+Na]$^+$: 467.2993 found 467.2991.

*2-((tert-Butoxycarbonyl)amino)-5-(pyrimidin-2-ylamino)pentanoic acid (**17**)*[160]

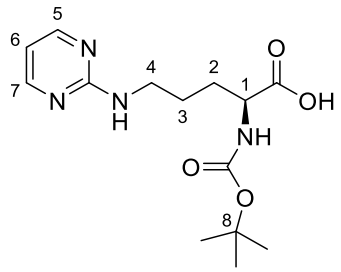

2-Chloropyrimidine (1.3 g, 1.1 mmol, 1.1 eq), Boc-Orn-OH (0.23 g, 1 mol, 1 eq) and K_2CO_3 (0.15 g, 1.1 mol, 1.1 eq) were added to MeOH (10mL) and stirred at 40°C under reflux for 3 days. The solvent was removed *in vacuo* and the resulting brown oil was purified using silica column chromatography. The silica was deactivated and the column and then the product eluted with 20:55:25/MeOH:EtOAc:Acetone. The fractions were pooled and concentrated and dried under high vacuum. The procedure was modified from literature reference[102]; (0.27 g, 0.87 mmol, 87%). **^{1}H-NMR:** (400 MHz, MeOD) δ_H: 1.42 (s, 9H, H-8), 1.66 (m, 2H, H-2), 1.86 (m, 2H, H-3), 3.63 (t, 1H, J=6.0 Hz, H-4), 3.98 (m, 1H, J=6.0 Hz, H-1), 6.55 (t, 1H, J=5.0 Hz, H-6), 8.23 (d, 2H, J=5.0 Hz, H-5, H-7). **^{13}C-NMR** (125 MHz, MeOD): 10.20 (CH_3), 23.45 (CH*C*H_2), 27.41 (CO*C*H), 30.32 (CHCH_2*C*H_2), 46.30 (*C*H_2NH), 58.64 (OCCH_3), 109.59 (NCH*C*H), 156.27 (*C*OOH), 157.82 (N*C*HCH), 162.17 (NH*C*), 162.17 (NH*C*O). **LRMS** *m/z* (ESI): 310.9 $[M+H]^+$. **HRMS** *m/z* (ESI): calculated for $C_{14}H_{22}N_4NaO_4^+$ $[M+Na]^+$: Exact Mass: 333.1533 found 333.1527.

*5-(Pyrimidin-2-ylamino)pentanoic acid-L-tryptophan octyl ester; H_2N-R^1W-Oct (**18**)*

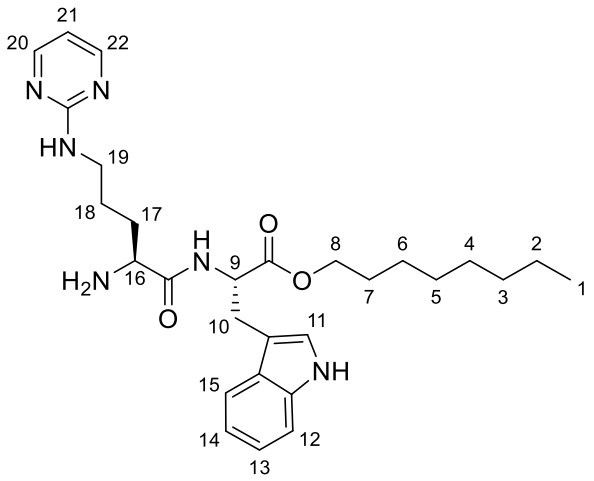

Compound **17** (0.27 g, 0.87 mmol, 1eq), HATU (0.33g, 0.87 mmol, 1eq), **1** (0.28g, 0.87 mmol, 1eq) and DIPEA (0.11g, 0.14 mL, 0.87 mmol, 1eq) were stirred in anhydrous DCM (10 mL) under N_2 gas for 18 hours. The solvent was removed and the resulting oil was stirred in 4N HCl in dioxane (4 mL) for 4 hours. The sample was then purified by RP-HPLC using Synergi™ 4 µm Polar-RP 80 Å and an elution gradient of H_2O + 0.1% TFA /MeCN + 0.1% TFA (100:0 to 0:100) over 30 minutes with a flow rate of 2 mL/min. The fractions were pooled and lyophilized; **^{1}H-NMR:** (400 MHz, MeOD) δ_H: 0.89 (t, 3H, J=5.7 Hz, H-1), 1.17-1.36 (m, 10H, H-2, H-3, H-4, H5, H-6), 1.47 (t, 2H, J=7.0 Hz, H-7), 1.74 (m, 2H, H-18), 1.93 (m, 2H, H-17), 3.18 (dd, J= 8.5, 2.5 Hz, 2H, H-10), 3.28 (t, 2H, J=6.5 Hz, H-19), 3.88 (t, 1H, J=5.9 Hz, H-9), 4.01 (t, 2H, J=6.6 Hz, H-8), 4.77 (t, 1H, J=7.1 Hz, H-16), 6.70 (t, 1H, J=4.8 Hz, H-21), 7.01 (t, 1H, J=7.9 Hz, H-13), 7.09 (t, 1H, J=7.4 Hz, H-14), 7.12 (s, 1H, J=4.2 Hz, H-11), 7.34 (d, 1H, J=8.6 Hz, H-12), 7.53 (d, 1H, J=8.1 Hz, H-15), 8.34 (d, 2H, J=4.8 Hz, H-22, H-20). **^{13}C-NMR** (125 MHz, MeOD): 12.96 (*C*H_3), 22.26 (*C*H_2), 24.18 (*C*H_2), 25.51 (*C*H_2), 27.24 (*C*H_2), 28.90 (CH_2*C*H_2), 28.21 (*C*H_2), 28.80 (*C*H_2), 31.52 (CH*C*H_2), 31.36 (CH*C*H_2), 31.66 (NHCO*C*H), 40.02 (*C*H_2NH), 53.74 (CO*C*H), 65.15 (O*C*H_2), 108.72 (CH_2*C*), 110.07 (NHC*C*H), 111.06 (NCH*C*H_2), 117.75 (C*C*H), 118.07 (CCH*C*H), 121.38 (NHCCH*C*H), 123.11 (C*C*HNH), 127.11 (C*C*), 136.85 (NHC), 162.06 (NH*C*N), 158.05 (N*C*HCH$_2$), 168.86 (NH*C*O), 171.71 (O*C*O). **LRMS** *m/z*

(ESI): 509.1 $[M+H]^+$. **HRMS** *m/z* (ESI): calculated for $C_{28}H_{41}N_6O_3^+$ $[M+H]^+$: Exact Mass: 509.3235 found 509.3237.

*(tert-Butoxycarbonyl)-L-tryptophan (**19**)*[161]

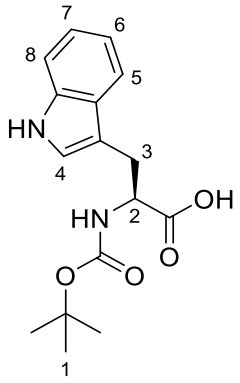

L-tryptophan (2 g, 9 mmol, 1 eq), Boc_2O (3.9 g, 18 mmol, 2 eq) and NaOH (0.7 g, 18 mmol, 2 eq) were added to 1:1 water:THF (40 mL) and stirred for 36 hours. The THF was then removed *in vacuo* and citric acid was added till pH 4 was reached. **19** was extracted in EtOAc (3x 50 mL). The organic layers were pooled and dried with $MgSO_4$. (2.22 g, 7.3 mmol, 81%). $\mathbf{R_f}$**=** 0.64 (EtOAc). **^{1}H-NMR:** (400 MHz, CD_3COCD_3) δ_H: 1.39 (s, 9H, H-1), 3.17-3.29 (m, 1H, H-3a), 3.31-3.40(m, 1H, H-3b), 3.99-4.10 (m, 1H, H-2), 7.07 (dt, J=7.0, 13.5 Hz, 2H, H-6, H-7), 7.24 (s, 1H, H-4), 7.39 (d, J=8.0 Hz, 1H, H-8), 7.64 (d, J=8.0 Hz, 1H, H-5). **^{13}C-NMR** (125 MHz, CD_3COCD_3): 27.40 ($CHCH_2$), 27.68 ($3CH_3$), 59.66 (NH*C*H), 77.70 (CH_3CH), 110.44 (CH_2C), 111.25 (C*C*H), 118.35 (*C*HC), 118.65 (CHCH*C*H), 121.28 (CCH*C*H), 123.49 (C*C*HNH), 127.97 (CH*C*), 136.66 (NH*C*), 155.35 (O*C*O), 173.72 (CH*C*OOH). **LRMS** *m/z* (ESI): 303.1 $[M+H]^+$.

*tert-Butyl (S)-(3-(1H-indol-3-yl)-1-(octylamino)-1-oxopropan-2-yl)carbamate (**20**)*

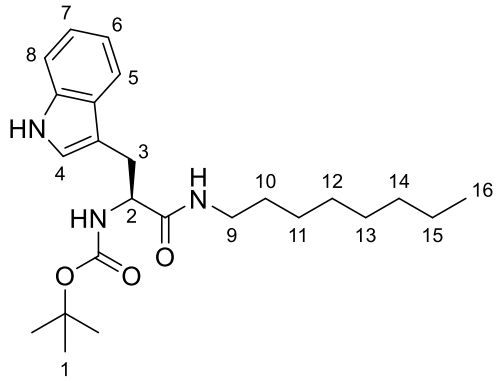

Compound **19** (2.22 g, 7.3 mmol, 1 eq), DCC (2.19 g, 9.9 mmol, 1.1 eq), HOBt (1.37 g, 9.9 mmol, 1.1 eq) and DMAP (0.11 g, 0.9 mmol, 0.1 eq) were stirred in anhydrous DCM under N_2 gas for 30 minutes. 1-Octylamine (1.5 mL, 1.16 g, 9 mmol, 1 eq) was then added and stirred for 18 hours. The solvent was removed *in vacuo* and EtOAc was added to precipitate the by product. The solvent was removed in vacuo and the product was purified by silica chromatography eluting with EtOAc. (2.05 g, 4.9 mmol, 67%). $\mathbf{R_f}$**=** 0.91 (1:1 Petroleum ether:EtOAc). **^{1}H-NMR:** (400 MHz, MeOD) δ_H: 0.89 (t, J= 6.6 Hz, 3H, H-16) 1.10-1.41 (m, 21H, H-1, H-10, H-11, H-12, H-13, H-14, H-15), 2.91-3.25 (m, 3H, H-3, H-9), 4.32-4.37 (m, 1H, H-2), 6.97-7.11 (m, 3H, H-4, H-6, H-7), 7.32 (d, J=7.8 Hz, 1H, H-8), 7.58 (d, J=7.7 Hz, 1H, H-5). **^{13}C-NMR** (125 MHz, MeOD): 13.07 (*C*H_3), 22.33 (*C*H_2), 25.16 (*C*H_2), 26.46 (NHCH*C*H_2CO), 27.28 (3*C*H_3), 28.95 (*C*H_2), 28.99 (*C*H_2), 31.61 (*C*H_2), 33.38 (*C*H_2), 39.05 (NH*C*H_2), 55.74 (NH*C*H), 79.20 (CH_3*C*H), 109.63 (CH_2*C*), 110.87 (C*C*H), 118.26 (*C*HC), 118.37 (CHCH*C*H), 121.04 (CCH*C*H), 123.14 (C*C*HNH), 127.40 (CH*C*), 136.66 (NH*C*), 156.94 (O*C*O), 173.17 (CH*C*ONH). **LRMS** *m/z* (ESI): 414.3 $[M+H]^-$.

*(S)-2-Amino-3-(1H-indol-3-yl)-N-octylpropanamide (**21**)*

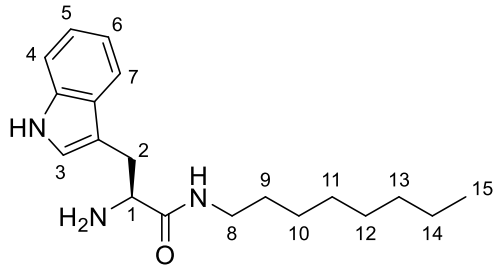

Compound **20** was stirred in HCl (4 M)/dioxane (4 mL) and stirred for 3 hours under N_2. The solvent was removed *in vacuo* and water was added (50 mL). The pH was adjusted to 10 with Na_2CO_3 and then extracted with ethyl acetate (3 x 50 mL). The organic layers were combined and dried with $MgSO_4$. The solvent was removed under reduced pressure. (1.48 g, 4.7 mmol, 96%). **R_f=** 0.49 (1:9 EtOAc:MeOH). **^{1}H-NMR:** (400 MHz, MeOD) δ_H: 0.89 (t, J= 6.5 Hz, 3H, H-15) 1.12-1.49 (m, 12H, H-9, H-10, H-11, H-12, H-13, H-14,), 2.89-2.96 (m, 2H, H-8), 3.16 (dd, J=8.5, 2.5 Hz, 2H, H-2), 4.13-4.18 (m, 1H, H-1), 6.99-7.10 (m, 3H, H-3, H-5, H-6), 7.40 (d, J=8.0 Hz, 1H, H-7), 7.59 (d, J=8.0 Hz, 1H, H-4). **^{13}C-NMR** (125 MHz, MeOD): 13.55 (*C*H_3), 24.87 (*C*H_2), 25.63 (*C*H_2), 26.88 (NHCH*C*H_2CO), 29.21 (*C*H_2), 29.41 (*C*H_2), 29.77 (*C*H_2), 30.54 (*C*H_2), 38.49 (NH*C*H_2), 65.50 (NH_2*C*H), 111.19 (C*C*H), 111.52 (CH_2*C*), 118.43 (*C*HC), 118.80 (CHCH*C*H), 121.03 (CCH*C*H), 123.59 (C*C*HNH), 127.98 (CH*C*), 136.61 (NH*C*), 172.60 (CH*C*ONH). **LRMS** *m/z* (ESI): 316.3 $[M+H]^+$.

*(S)-N-((S)-3-(1H-Indol-3-yl)-1-(octylamino)-1-oxopropan-2-yl)-2-amino-5-guanidinopentanamide (**22**)*

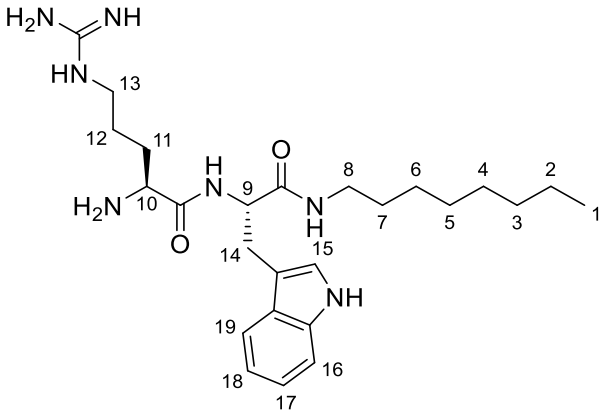

Compound **21** (0.25 g, 0.8 mmol, 1 eq), Fmoc-Arg-OH (0.35 g, 0.9 mmol, 1.1 eq), HATU (0.45 g 1.1 mmol, 1.4 eq) and DIPEA (0.7 mL, 3.2 mmol, 4 eq) were stirred in THF (6 mL) under N_2 for 18 hours. The solvent was removed *in vacuo*. The resulting oil was stirred in 20% piperidine in DCM (10 mL) for 3 hours. The solvent was removed *in vacuo*. The sample was then purified by RP-HPLC using Synergi™ 4 µm Polar-RP 80 Å and an elution gradient of H_2O + 0.1% TFA /MeCN + 0.1% TFA (70:30 to 0:100) over 30 minutes with a flow rate of 2 mL/min. The fractions were pooled and lyophilized. **^{1}H-NMR:** (400MHz, MeOD) δ_H: 0.90 (t, 3H, J=6.6 Hz, H-1), 1.06-1.40 (m, 12H, H-2, H-3, H-4, H-5, H-6, H-7), 1.53-1.65 (m, 2H, H-12), 1.84-1.93 (m, 2H, H-11), 2.81-3.23 (m, 6H, H-8, H-13, H-14) 3.85 (dt, 1H, J= 15.5, 21.7 Hz, H-9), 4.69 (dt, 1H, J= 14.0, 20.1 Hz, H-10), 7.01 (t, 1H, J=7.6 Hz, H-17), 7.09 (t, 1H, J=7.6 Hz, H-18), 7.13 (s, 1H, H-15), 8.15 (d, 1H, J=8.2 Hz, H-16), 8.49 (d, 1H, J=8.0 Hz, H-19). **^{13}C-NMR** (125 MHz, MeOD): 13.03(*C*H_3), 22.31 (*C*H_2), 23.36 (CH*C*H_2), 26.50 (CH_2*C*H_2), 27.93 (*C*H_2), 28.25 (*C*H_2), 28.91 (*C*H_2), 28.96 (CH*C*H_2), 28.97 (*C*H_2), 31.06 (*C*H_2), 39.18 (*C*H_2), 40.44 (*C*H_2NH),54.72 (CO*C*H), 82.46 (NHCO*C*H), 109.4 (CH_2*C*), 110.98 (NHC*C*H), 117.89 (C*C*H), 118.54 (CCH*C*H), 121.20 (NHCCH*C*H), 123.44 (C*C*HNH), 127.24 (C*C*), 136.69 (NHC), 157.35 (NH*C*NH), 168.22 (NH*C*O), 172.12 (NH*C*O). **LRMS** m/z (ESI) 472.4 $[M+H]^+$. **LRMS** *m/z* (ESI): 472.34 $[M+H]^+$. **HRMS** *m/z* (ESI): calculated for $C_{25}H_{42}N_7O_2^+$ $[M+H]^+$: Exact Mass: 472.3395 found 472.3401.

*(9H-Fluoren-9-yl)methyl tert-butyl ((S)-6-(((S)-3-(1H-indol-3-yl)-1-(octylamino)-1-oxopropan-2-yl)amino)-6-oxohexane-1,5-diyl)dicarbamate (**23**)*

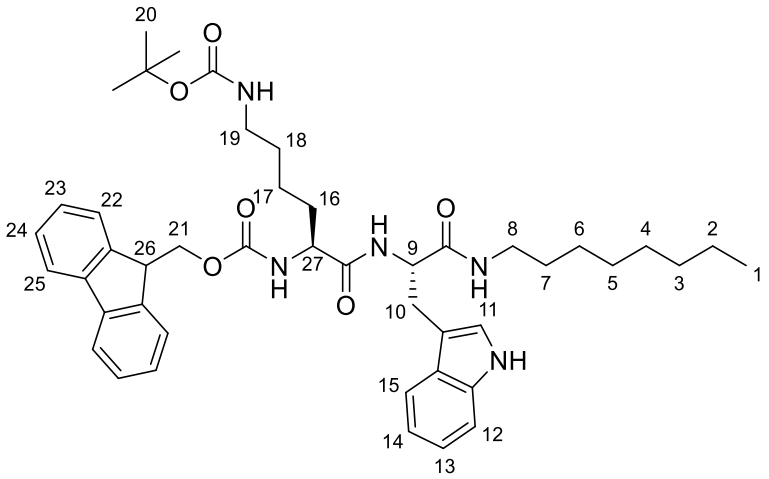

Compound **21** (0.09 g, 0.28 mmol, 1 eq), Fmoc-Lys(Boc)-OH (0.13 g, 0.28 mmol, 1 eq) and HATU (0.14g, 0.39 mmol, 1.4 eq) and DIPEA (0.19 mL, 0.15 g, 1.12 mmol, 4 eq) were dissolved in anhydrous DCM (20 mL). The resulting solution was stirred for 18 hours. The reaction mixture was washed with Na_2CO_3 (3x20 mL) and citric acid (3x20 mL) and then dried with $MgSO_4$. The solvent was removed *in vacuo* and the product was purified by silica chromatography eluting with EtOAc. (0.12 g, 0.15 mmol, 53%). **R_f=** 0.45 (2:3 petroleum ether:EtOAc). **^{1}H-NMR:** (400 MHz, MeOD) δ_H: : 0.87 (t, 3H, J=7.0 Hz, H-1), 1.05-1.31 (m, 14H, H-2, H-3, H-4, H-5, H-6, H-7, H-17), 1.36-1.41 (m, 2H, H-18) 1.43 (s, 9H, H-20), 1.50-1.65 (m, 2H, H-16), 3.04 (dd, J=8.5, 2.5 Hz, 2H,, H-10), 3.06 (t, J= 7.0 Hz, 1H, H-8), 3.13-3.19 (m, 1H, H-19), 4.19 (t, J= 7.0 Hz, 1H, H-27), 4.26 (t, J=7.0 Hz, 1H, H-26), 4.34 (d, J=7.0 Hz, 2H, H-21), 4.59 (t, J=7.0 Hz, 1H, H-9), 7.00 (t J=7.5 Hz, 1H, H-14), 7.05 (t, J=7.5 Hz, 1H, H-13), 7.08 (s, 1H, H-11), 7.28 (d, J=8.0 Hz, 1H, H-12), 7.32 (t, J=7.5 Hz, 2H, H-23), 7.40 (t, J=7.5 Hz, 2H, H-24), 7.56 (d, J=8.0 Hz, 1H, H-15), 7.65 (d, J= 7.5 Hz, 2H, H-22), 7.87 (d, J=7.5 Hz, 2H, H-25). **^{13}C-NMR:** (125 MHz, MeOD): 13.05(CH_3), 22.30 (CH_2), 22.55 (CH_2CH_2), 26.45 ($CHCH_2$), 27.23 ($CHCH_2$), 27.41 ($OCCH_3$), 28.61 ($CHCHCH_2$), 28.90 (CH_2), 28.95 (CH_2), 29.35 (CH_2), 30.94 (CH_2), 31.59 (CH_2), 39.18 (CH_2), 39.60 (CH_2NH), 46.99 (CH_2CC), 54.17 ($NHCOCH$), 55.71 ($COCH$), 66.70 ($NHCOOCH_2$), 78.48 ($OCCH_3$), 109.42 (CH_2C), 110.88 ($NHCCH$), 118.02 (CCH),

118.48 (CCH*C*H), 119.57 (*C*HCHCHCH), 121.07 (NHCCH*C*H), 123.15 (C*C*HNH), 124.86 (CH*C*HCHCH), 127.44 (C*C*), 136.61 (NHC), 143.92 (CH_2CC), 155.15 (NH*C*OO), 157.42 (NH*C*OOCH$_2$), 172.08 (NH*C*O), 173.22 (NH*C*O). 126.80 (CHCH*C*HCH), 127.44 (CHCHCH*C*H). **LRMS** *m/z* (ESI) 788.5 [M+H]+. **HRMS** *m/z* calculated for $C_{45}H_{60}N_5NaO_6^+$ [M+Na]+: 788.4358 found 788.4358.

*(S)-N-((S)-3-(1H-Indol-3-yl)-1-(octylamino)-1-oxopropan-2-yl)-2,6-diaminohexanamide (**24**)*

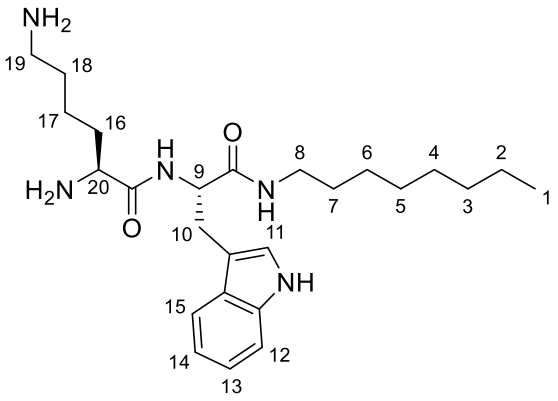

23 (0.12 g, 0.15 mmol) was dissolved in 20% piperidine in DCM (10 mL) and stirred for 1h. DCM (40 mL) was then added to the reaction mixture which was then washed with $NaHCO_3$ (3 x 50 mL). The solution was dried with $MgSO_4$ and the solvent removed *in vacuo*. The resulting yellow oil was stirred in HCl (4 M)/dioxane (4 mL) and stirred for 3 hours under N_2. The solvent was removed *in vacuo*. The sample was then purified by RP-HPLC using Synergi™ 4 µm Polar-RP 80 Å and an elution gradient of H_2O + 0.1% TFA /MeCN + 0.1% TFA (70:30 to 0:100) over 30 minutes with a flow rate of 2 mL/min. The fractions were pooled and lyophilized. **^{1}H-NMR:** (400 MHz, MeOD) δ_H: : 0.90 (t, 3H, J=6.5 Hz, H-1), 1.03-1.13 (m, 2H, H-17), 1.15-1.33 (m, 10H, H-2, H-3, H-4, H-5, H-6), 1.40-1.54 (m, 2H, H-7) 1.64-1.74 (s, 2H, H-19), 1.83-1.90 (m, 2H, H-16), 2.95 (t, J=6.5 Hz, 2H, H-10), 3.16 (dd, J=8.5, 2.5 Hz, 2H, H-10), 4.19 (t, J= 7.0 Hz, 1H, H-20) 4.62 (t, J=7.0 Hz, 1H, H-9), 7.01 (t J=7.5 Hz, 1H, H-14), 7.05-7.13 (m, 2H, H-11, H-13), 7.34 (d, J=8.0 Hz, 1H, H-12), 7.75 (d, J=8.0 Hz, 1H, H-15). **^{13}C-NMR :** (125 MHz, MeOD): 13.54 (*C*H_3), 21.03 (CH_2*C*H_2), 22.31 (*C*H_2), 26.46 (*C*H_2), 26.62 (CH*C*H_2), 27.87 (CHCH*C*H_2), 28.60 (*C*H_2), 28.91 (*C*H_2), 28.96 (*C*H_2), 30.62 (*C*H_2), 31.60 (CH*C*H_2), 38.81 (*C*H_2), 39.29 (*C*H_2NH_2), 52.15 (NHCO*C*H),54.79 (CO*C*H), 109.13 (CH_2*C*), 110.97 (NHC*C*H), 117.90 (C*C*H), 118.48 (CCH*C*H), 121.12 (NHCCH*C*H), 123.27 (C*C*HNH), 127.26 (C*C*), 136.68 (NHC), 168.35 (NH*C*O), 172.04 (NH*C*O). **LRMS** *m/z* (ESI) 444.5 $[M+H]^+$. **HRMS** *m/z* calculated for $C_{25}H_{42}N_5O_2^+$ $[M+H]^+$: 444.3333 found 444.3335.

*tert-Butyl (2-(octylamino)-2-oxoethyl)carbamate (**25**)*

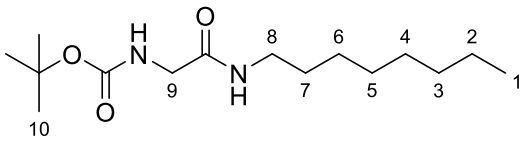

Boc- Gly-OH (2.0 g, 11.0 mmol, 1 eq), EDC.HCl (2.2 g, 12.1 mmol, 1.1 eq) and HOBt (1.6 g, 12.1 mmol, 1.1 eq) were stirred in anhydrous DCM (10 mL) under N_2 gas for 30 minutes. 1-Octylamine (1.8 mL, 1.4 g, 11.0 mmol, 1 eq) was then added and stirred for 18 hours. DCM (40 mL) was added and then was washed three times with water (50 mL). The organic layer was dried over $MgSO_4$ and the solvent was removed *in vacuo.* The product was purified by silica chromatography eluting with EtOAc. (2.1 g, 7.4 mmol, 67%). **R_f=** 0.91 (1:1 Petroleum ether:EtOAc). **^{1}H-NMR:** (400 MHz, MeOD) δ_H: 0.89 (t, J= 6.6 Hz, 3H, H-1) 1.10-1.41 (m, 12H, H-2, H-3, H-4, H-5, H-6, H-7), 1.42 (s, 9H, H-10), 2.91-3.02 (t, 2H, J= 7.0 Hz, H-8), 3.82 (s, 2H, H-9). **^{13}C-NMR** (125 MHz, MeOD): 28.40 (3*C*H_3), 80.01 (CH_3*C*H), 156.92 (O*C*O), 45.54 (NH*C*H_2), 162.82 (CH_2*C*ONH), 39.05 (NH*C*H_2), 31.61 (*C*H_2), 25.16 (*C*H_2), 28.95 (*C*H_2), 28.99 (*C*H_2), 33.38 (*C*H_2), 22.33 (*C*H_2), 13.07 (*C*H_3). **LRMS** *m/z* (ESI): 287.3.

*2-Amino-N-octyl acetamide (**26**)*[162]

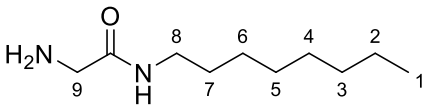

25 (0.80 g, 2.7 mmol) was stirred in 4N HCl in dioxane (3 mL) for 4 hours. The solvent was removed *in vacuo*. (0.50 g, 2.7 mmol, 98%). $\mathbf{R_f}$ = 0.33 (1:9 MeOH:EtOAc). **^{1}H-NMR:** (400 MHz, MeOD) δ_H: 0.90 (t, J= 6.6 Hz, 3H, H-1) 1.13-1.39 (m, 12H, H-2, H-3, H-4, H-5, H-6, H-7), 2.90-3.00 (t, 2H, J= 7.0 Hz, H-8), 3.84 (s, 2H, H-9). **^{13}C-NMR** (125 MHz, MeOD): 12.71 (*C*H_3), 22.33 (*C*H_2), 25.16 (*C*H_2), 28.95 (*C*H_2), 28.99 (*C*H_2), 31.61 (*C*H_2), 33.38 (*C*H_2), 38.52 (NH*C*H_2), 42.14 (NH_2*C*H_2), 169.21 (CH_2*C*ONH). **LRMS** *m/z* (ESI): 187.3

*Octyl N2,N6-bis(tert-butoxycarbonyl)-L-lysylglycinate (**27**)*

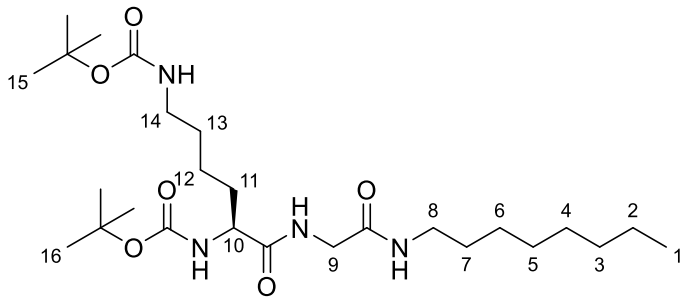

14 (1.0 g, 2.9 mmol, 1 eq), HBTU (1.2 g, 3.2 mmol, 1.1 eq), **26** (0.59 g, 3.2 mmol, 1.1 eq) and DIPEA (0.94 mL, 0.74 g, 5.8 mmol, 2 eq) were stirred in anhydrous DCM (10 mL) under N_2 gas for 18 hours. DCM (40 mL) was added and then washed three times with water (50 mL). The organic layer was dried over $MgSO_4$ and the solvent removed *in vacuo*. The resulting residue was applied to a silica column and the product was eluted with EtOAc. $\mathbf{R_f}$ = 0.76 (EtOAc). (0.67 g, 1.31 mmol, 39 %). **^{1}H-NMR:** (400 MHz, MeOD) δ_H: 0.89 (t, J= 6.6 Hz, 3H, H-1) 1.13-1.39 (m, 12H, H-2, H-3, H-4, H-5, H-6, H-12), 1.45 (s, 9H, H-16), 1.48 (s, 9H, H-15), 1.50-1.59 (m, 2H, H-7), 1.65-1.78 (m, 2H, H-13), 1.83-1.99 (m, 2H, H-11), 2.89-3.02 (t, 2H, J= 7.0 Hz, H-8), 3.20 (m, 2H, H-14), 3.82 (s, 2H, H-9) 4.44 (m, 1H, H-10). **^{13}C-NMR** (125 MHz, MeOD): 12.71 (CH$_3$), 22.31 (NHCH$_2$CH$_2$$CH_2$), 22.71 ($CH_2$), 25.26 ($CH_2$), 26.53 (CH$_2$$CH_2$CH)**,** 27.36, 27.41 (3$CH_3$), 28.95 ($CH_2$), 29.00 (NHCH$_2$$CH_2$) 29.24 ($CH_2$), 30.50 (NH$CH_2$), 31.59 ($CH_2$), 33.36 ($CH_2$), 37.47 (NH$CH_2$), 42.13 (CONH$CH_2$), 55.49 (NH$C$H), 79.40, 79.42 (CH$_3$$C$), 157.01, 157.25 (CO$C$ONH), 170.04 (CH$_2$$C$ONH), 174.59 (CH$C$O). **LRMS** *m/z* (ESI): 537.4 $[M+Na]^+$. **HRMS** *m/z* (ESI): calculated for $C_{26}H_{50}N_4NaO_6^+$ $[M+Na]^+$: 537.3623 found 537.3615.

*Octyl L-lysylglycinate (**28**)*

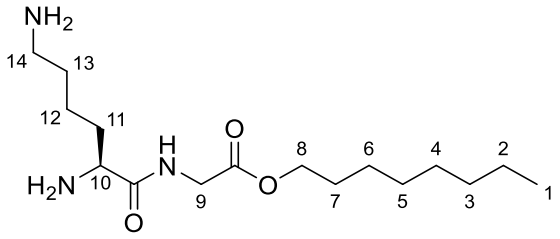

27 (0.67 g, 1.31 mmol) was stirred in 4N HCl in dioxane (3 mL) for 4 hours. The solvent was removed *in vacuo*. (0.39 g, 1.25 mmol, 95%). $\mathbf{R_f}$ = 0.22 (1:9 MeOH:EtOAc). **^{1}H-NMR:** (400 MHz, MeOD) δ_H: 0.89 (t, J= 6.6 Hz, 3H, H-1) 1.13-1.39 (m, 12H, H-2, H-3, H-4, H-5, H-6, H-12), 1.42-1.55 (m, 2H, H-7), 1.63-1.74 (m, 2H, H-13), 1.80-1.89 (m, 2H, H-11), 2.72 (m, 2H, H-14), 2.89-3.03 (t, 2H, J= 7.0 Hz, H-8), 3.79 (s, 2H, H-9) 4.45 (m, 1H, H-10). **^{13}C-NMR** (125 MHz, MeOD): 13.21 (*C*H_3), 22.71 (*C*H_2), 22.86 (NHCH$_2$CH$_2$*C*H$_2$), 25.26 (*C*H_2), 26.24 (CH$_2$*C*H$_2$CH)**,** 28.95 (*C*H_2), 29.24 (*C*H_2), 29.40 (NHCH$_2$*C*H$_2$) 31.92 (*C*H_2), 33.36 (*C*H_2), 35.62 (NH*C*H$_2$), 42.52 (NH$_2$*C*H$_2$), 43.35 (CONH*C*H$_2$), 53.09 (NH$_2$*C*H), 170.02 (CH$_2$*C*ONH), 172.33 (CH*C*O). **LRMS** *m/z* (ESI): 315.4 $[M+Na]^+$. **HRMS** *m/z* (ESI): calculated for $C_{16}H_{35}N_4O_2^+$ $[M+Na]^+$: 315.2755 found 315.2755.

7.2 Peptidomimetic 1

*Methyl 3-hydroxy 4-nitrobenzoic acid (**29**)*[163]

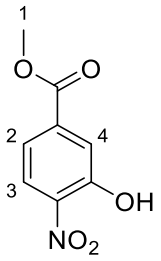

2-Hydroxy-4-nitrobenzoic acid (1.7 g, 9.28 mmol) was dissolved in MeOH (15 mL) and cooled to 0 °C. $SOCl_2$ (1 mL, 1.65 g, 1.5 eq) was added dropwise to the reaction mixture. The reaction mixture was refluxed for 18 hours. MeOH was removed under high vacuum and the resulting solid was dissolved in EtOAc (75 mL) and washed 3 times with water (75 mL). The organic layer was dried with $MgSO_4$ and removed under high vacuum. (1.43 g, 7.26 mmol, 78%). $\mathbf{R_f}$ = 0.60 (3:7/EtOAc:petroleum ether). **^{1}H-NMR:** (400 MHz, MeOD) δ_H: 3.94 (s, 1H, H-1), 7.59 (d, 1H, J=8.7 Hz, H-3), 7.73 (s, 1H, H-4), 8.10 (d, 1H, J=8.7 Hz, H-3). **^{13}C-NMR** (125 MHz, MeOD): 51.84 (*C*H_3O), 119.73 (COH*C*H), 120.43 (C*C*HCH), 125.13 (CCH*C*H), 136.55 (*C*NO_2), 137.84 (CO*C*), 153.11 (*C*OH), 165.06 (O*C*O).

*Methyl 2-(indol-3-ethoxy)-4-nitrobenzoic acid (**30**)*[164]

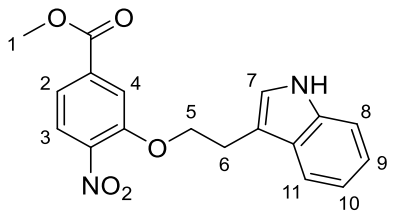

Compound **29** (1.43 g, 7.26 mmol, 1 eq), 3-(2-bromoethyl)indole (1.78 g, 8 mmol, 1.1 eq), Cs_2CO_3 (4.73 g, 14.5 mmol, 2 eq) were stirred in DMF (6 mL) at 70 °C for 20 hours. The reaction mixture was taken up in EtOAc (75 mL) and washed 3 times with Na_2CO_3 *sat.* (75 mL). The organic layer was dried with $MgSO_4$ and dried under high vacuum. Silica column chromatography was carried out and the product was eluted with 2:8/EtOAc:petroleum ether. (0.51 g, 1.5 mmol, 20%). $\mathbf{R_f}$ = 0.41 (3:7/EtOAc:petroleum ether). **^{1}H-NMR:** (400 MHz, MeOD) δ_H: 3.19 (t, 2H, J=6.5 Hz, H-6), 3.86 (s, 3H, H-1), 4.33 (t, 2H, J=6.5 Hz, H-5), 6.99 (t, 1H J=7.5 Hz, H-10), 7.06 (t, 1H, J=7.5 Hz, H-9), 7.12 (s, 1H, H-7), 7.30 (d, 1H, J=8.0 Hz, H-11), 7.55 (d, 2H, J=8.0 Hz, H-8, H-2), 7.66 (s, 1H, H-4), 7.71 (d, J=8.0 Hz, 1H, H-3). **^{13}C-NMR** (125 MHz, MeOD): 24.57 ($CH_2\mathit{C}H_2$), 51.80 ($\mathit{C}H_3O$), 70.01 ($CO\mathit{C}H_2$), 110.19 ($CH_2\mathit{C}$), 110.84 (NHC*C*H), 115.10 (*C*OHCH_2), 118.38 (CHCH*C*H), 117.74 (CH*C*HC), 120.94 (CCH*C*H), 122.91 (C*C*HCH), 124.20 (C*C*H), 124.51 (CCH*C*H), 127.24 (CH*C*), 134.34 (NH*C*), 136.55 (CO*C*CH), 142.77 (CH*C*NO_2), 151.34 (CNO_2COH), 165.69 (O*C*O).

*Methyl 3-(indol-3-ethoxy)-4-aminobenzoic acid (**31**)*[164]

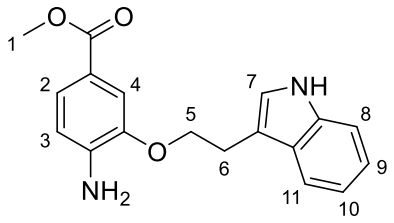

Compound **30** (0.51 g, 1.5 mmol, 1 eq), and Pd/C (0.13 g, 0.8 eq), were stirred in MeOH (10 mL) overnight under H_2 and then filtered. Solvent was removed under high vacuum. (0.43 g, 1.38 mmol, 92%). **R_f =** 0.23 (1:1/EtOAc:petroleum ether). **^{1}H-NMR:** (400 MHz, MeOD) δ_H: 3.27 (t, 2H, J=6.8 Hz, H-6), 3.81 (s, 3H, H-1), 4.28 (t, 2H, J=6.8 Hz, H-5), 6.66 (d, 1H, J=8.1 Hz, H-3), 7.02 (t, 1H, J=7.4 Hz, H-10), 7.10 (t, 1H, J=7.5 Hz, H-9), 7.16 (s, 1H, H-7), 7.34 (d, 1H, J=8.0 Hz, H-11), 7.42-7.46 (m, 2H, H-2, H-4) 7.61 (d, 1H, J=7.8 Hz, H-11). **^{13}C-NMR** (125 MHz, MeOD): 24.90 (CH_2CH_2), 50.69 (CH_3O), 68.93 ($COCH_2$), 110.89 (NHC*C*H), 111.03 (CH_2C), 111.95 (CO*C*H), 112.55 (CCH*C*H), 117.57 (CO*C*CH), 117.80 (CH*C*HC), 118.30 (CHCH*C*H),120.93 (CCH*C*H), 122.34 (C*C*HCH), 123.95 (C*C*H), 127.84 (CH*C*), 129.91 (NH*C*), 143.10 (CH*C*NH_2), 145.01 (CNH_2CO), 167.88 (O*C*O).

*Methyl (S)-2-(2-(indol-3-ethoxy)-4-(2-((((9H-fluoren-9-yl)methoxy)carbonyl)amino)-5-guanidinopentanamido)benzoate (**32**)*

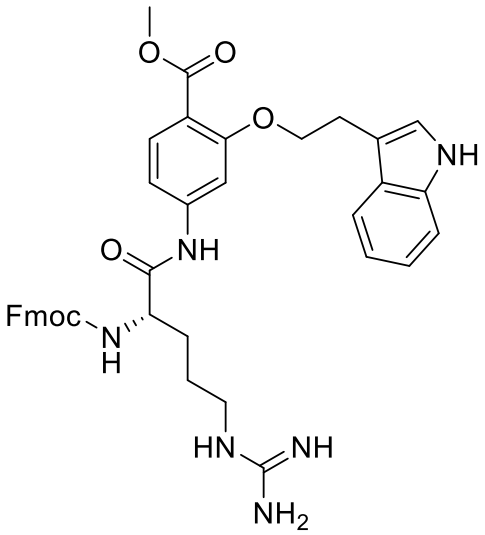

Fmoc-Arg-OH (0.54 g, 1.38 mmol, 1eq) was dissolved in THF (5 mL) and cooled to 0°C. $SOCl_2$ (0.3 mL, 0.49 g, 4.14 mmol, 3 eq) was added dropwise and the reaction was then refluxed for 2 hours. The reaction mixture was concentrated and the $SOCl_2$ was removed under high vacuum. The resulting brown oil was dissolved in THF (5 mL) and to this **31** (0.43 g, 1.38 mmol, 1 eq) and TEA (0.5 mL) was added and the reaction mixture was stirred for 18 hours. The reaction mixture was concentrated under high vacuum. The sample was then purified by RP-HPLC using Synergi™ 4 µm Polar-RP 80 Å and an elution gradient of H_2O + 0.1% TFA /MeCN + 0.1% TFA (100:0 to 0:100) over 30 minutes with a flow rate of 2 mL/min. The fractions containing the desired compound were pooled and lyophilized. **LRMS** *m/z* (ESI): 689.4 $[M+H]^+$. **HRMS** *m/z* (ESI): calculated for $C_{39}H_{40}N_6O_6$ $[M+Na]^+$: 689.3009 found 689.3080.

Only identified by HRMS. Not a sufficient amount to isolate and analyse the product further.

(S)-2-(((Benzyloxy)carbonyl)amino)-5-((tert-butoxycarbonyl)amino) pentanoic acid ***(33)*** [165]

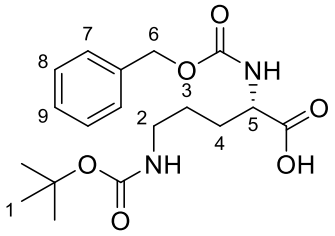

Reaction mixture 1: Orn•HCl (2 g, 15 mmol, 2eq) was stirred in 2M NaOH (20 mL), to this a solution of $Cu(CH_3COO)_2•H_2O$ (1g, 7.5 mmol, 1eq) in water (10 mL) was added. This was followed by the addition of Boc_2 (3.1 g, 9.75 mmol, 1.3 eq) dissolved in acetone (40 mL) After stirring for 24 hours an further volume of acetone (20 mL) was added and stirred for 20 hours. The resulting blue precipitate was collected by filtration, washed with acetone: water (2:1) and water, and then resuspended in acetone (20 mL). To this 10% (w/v) Na_2CO_3 (30mL) and 8-Hydroxyquinoline (1g, 6.75 mmol, 0.9 eq) was added and stirred for 1.5 hours.

Reaction mixture 2: In a separate flask a solution of N-hydroxysuccinimide (0.8 g, 6.75 mmol, 0.9 eq) in water (10 mL) was stirred at -10˚C. To this Na_2CO_3 (0.35 g, 6.75 mmol 0.9 eq) was added followed by the addition of benzyl chloroformate (1.15 g, 6.75 mmol, 0.9 eq) in acetone (10 mL) and stirred at -10˚C for 0.5 hours.

Reaction mixture 1 was added to *reaction mixture 2* and stirred at room temperature for 1.5 hours. The copper quinolinate precipitate (green) was filtered off and washed with water. The filtrate and washings were combined and the acetone was removed *in vacuo.* The resulting aqueous solution was washed with diethyl ether (3x 80 mL) and then acidified to pH 3 using HCl. This was then washed with ethyl acetate (3 x 80 mL). The combined organic layers were dried using $MgSO_4$ and concentrated in vacuo. The resulting green oil was purified using silica chromatography, eluting the product with ethyl acetate.(adapted from literature reference[165]). (0.51 g, 10 mmol, 60%). $\mathbf{R_f}$ = 0.20 (1:4 MeOH:EtOAc). **^{1}H-NMR:** (400 MHz, MeOD) δ_H: 1.42 (s, 9H, H-1), 1.50-1.70 (m, 2H, H-4), 1.79-1.91 (m, 2H, H-3) 3.05 (t, 2H, J=6.5 Hz, H-2), 4.09-4.19 (m, 1H,

H-5), 5.09 (s, 2H, H-6), 7.25-7.38 (m, 5H, H-7, H-8, H-9). **^{13}C-NMR** (125 MHz, MeOD): 26.07 ($NHCH_2\mathit{C}H_2$), 27.38 ($3\mathit{C}H_3$), 28.66 ($CH_2CH_2\mathit{C}H_2$), 39.44 ($NH\mathit{C}H_2$), 53.42 ($\mathit{C}HNH$), 66.21 (OCH_2), 78.62 (C), 127.39 ($CHCH\mathit{C}H$), 127.58 ($C\mathit{C}H$), 128.06 ($CCH\mathit{C}H$), 136.76 (CH_2C), 156.82 ($\mathit{C}O$), 157.26 ($CH\mathit{C}O$), 174.06 ($NH\mathit{C}O$). **LRMS** *m/z* (ESI): 365.2 $[M+H]^-$.

*3-Hydroxy-4-nitro-N-octylbenzamide (**34**)*

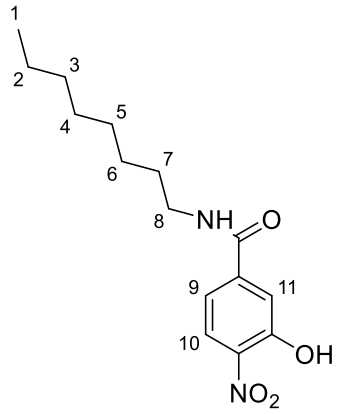

3-hydroxy-4-nitrobenzoic acid (1.00 g, 5.5 mmol, 1 eq), DCC (1.23 g, 6.1 mmol, 1.1 eq) and DMAP (0.07 g, 0.6 mmol, 0.1 eq) were dissolved in anhydrous THF and stirred under N_2 for 30 minutes. 1-Octylamine (0.71 g, 0.92 mL, 5.5 mmol, 1 eq) was then added and stirred for 18h. The solvent was removed *in vacuo* and the resulting oil was dissolved in EtOAc (50 mL) and washed with $NaHCO_3$ (3 x 50 mL). The organic layer was dried with $MgSO_4$. The white precipitate (DCC by-product) was removed by filtration. The solvent was removed *in vacuo*. Silica column chromatography was carried out and the product was eluted with 1:1/EtOAc:petroleum ether. (0.81 g, 4.1 mmol, 75%). $\mathbf{R_f}$ = 0.54 (3:7/EtOAc:petroleum ether). **^{1}H-NMR:** (400 MHz, CD_3COCD_3) δ_H: 0.87 (t, 3H, J=5.5 Hz, H-1), 1.21-1.38 (m, 10H, H-2, H-3, H-4, H-5, H-6), 1.61 (q, 2H, J=6.0 Hz, H-7), 3.40 (q, 2H J=6.5, 6.5Hz, H-8), 7.51 (d, 1H, J=9.0 Hz, H-9), 7.62 (s, 1H, H-10), 8.17 (d, 1H, J=9 Hz, H-11). **^{13}C-NMR** (125 MHz, CD_3COCD_3): 13.44 (*C*H_3), 26.81 (*C*H_2), 28.36 (*C*H_2), 29.10 (*C*H_2), 29.29 (*C*H_2), 29.52 (*C*H_2), 31.67 (*C*H_2), 39.80 (*C*H_2NH), 118.57 (CH*C*HNO$_2$), 118.62 (*C*HCHNO$_2$), 125.29 (COH*C*H), 140.05 (CO*C*), 141.57 (CH*C*NO$_2$), 151.63 (*C*OH), 164.78 (NH*C*O).

*3-(2-(1H-Indol-3-yl)ethoxy)-4-nitro-N-octylbenzamide (**35**)*

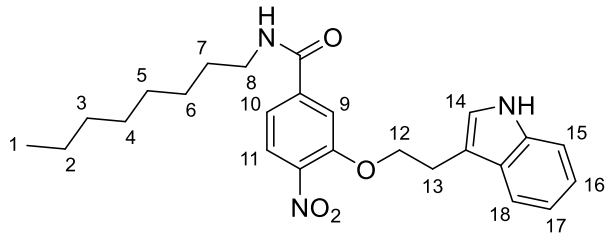

Compound **34** (1.00 g, 5.5 mmol, 1 eq), 3-(2-Bromoethyl)indole (1.30 g, 6.0 mmol, 1.2 eq) and K_2CO_3 (1.25 g, 9.0 mmol, 1.5 eq) were stirred in anhydrous DMF (10 mL) and stirred under N_2 for 18 h. EtOAc (50 mL) and washed with $NaHCO_3$ (3 x 50 mL). The organic layer was dried with $MgSO_4$. The solvent was removed *in vacuo*. Silica column chromatography was carried out and the product was eluted with 1:19/EtOAc:petroleum ether. (0.8 g 2.0 mmol, 36%). R_f = 0.48 (2:3/EtOAc:petroleum ether). **^{1}H-NMR:** (400 MHz, CD_3COCD_3) δ_H: 0.88 (t, 3H, J=6.0 Hz, H-1), 1.22-1.38 (m, 10H, H-2, H-3, H-4, H-5, H-6), 1.55-1.61 (m, 2H, H-7), 3.29 (t, 2H J=6.5 Hz, H-13), 3.39 (dd, 2H, J= 6.0, 12.5 Hz, H-8), 4.44 (t, 2H, J= 7.0 Hz, H-12), 7.09 (dt, 2H, J= 7.0, 14.5 Hz, H-16, H-17), 7.30 (s, 1H, H-14), 7.42 (d, 1H, J= 8.0 Hz, H-10), 7.63 (dd, 2H, J= 8.0, 25.5 Hz, H-15, H-18), 7.79 (s, 1H, H-11), 7.51 (d, 1H, J=9.0 Hz, H-9). **^{13}C-NMR** (125 MHz, CD_3COCD_3): 13.54 (*C*H_3), 24.83 (*C*H_2), 26.86 (*C*H_2), 29.12 (*C*H_2), 29.22 (*C*H_2), 29.41 (*C*H_2), 31.70 (*C*H_2), 32.50 (COCH_2*C*H_2), 39.92 (*C*H_2NH), 70.04 (CO*C*H_2), 110.55 (CH_2*C*), 111.35 (NHC*C*HCH), 113.51 (CO*C*H), 118.32 (CHCH*C*H), 118.78 (CHCH*C*HCH), 119.04 (C*C*HCH), 121.30 (NHCCH*C*H), 123.40 (C*C*HNH), 124.86 (CCH*C*H), 127.59 (*C*CH), 136.68 (NH*C*CH), 140.05 (CO*C*), 141.47 (*C*NO_2), 151.63 (*C*OCH_2), 164.78 (*C*O).

*3-(2-(1H-Indol-3-yl)ethoxy)-4-amino-N-octylbenzamide (**36**)*

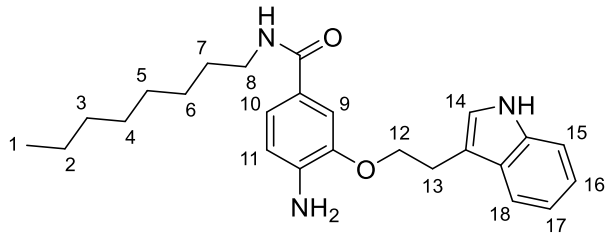

Compound **35** (1.1 g, 2.5 mmol, 1 eq), and Pd/C (0.26 g, 2.0 mmol, 0.8 eq), were stirred in MeOH (10 mL) overnight under H_2 and then filtered. Solvent was removed under high vacuum. (0.94 g, 2.3 mmol, 92%). $\mathbf{R_f}$ = 0.20 (9:1/EtOAc:MeOH). **^{1}H-NMR:** (400 MHz, CD_3COCD_3) δ_H: 0.89 (t, 3H, J=6.0 Hz, H-1), 1.15-1.31 (m, 10H, H-2, H-3, H-4, H-5, H-6), 1.52-1.59 (m, 2H, H-7), 3.30 (t, 2H J=6.5 Hz, H-13), 3.41 (dd, 2H, J= 6.0, 12.5 Hz, H-8), 4.44 (t, 2H, J= 7.0 Hz, H-12), 6.97 (s, 1H, H-11), 7.10 (dt, 2H, J= 7.0, 14.5 Hz, H-16, H-17), 7.30 (s, 1H, H-14), 7.42 (d, 1H, J= 8.0 Hz, H-10), 7.63 (dd, 2H, J= 8.0, 25.5 Hz, H-15, H-18), 7.51 (d, 1H, J=9.0 Hz, H-9). **^{13}C-NMR** (125 MHz, CD_3COCD_3): 13.05 (*C*H_3), 24.51 (*C*H_2), 26.85 (*C*H_2), 29.08 (*C*H_2), 29.21 (*C*H_2), 29.40 (*C*H_2), 31.71 (*C*H_2), 32.55 (COCH$_2$*C*H_2), 40.01 (*C*H_2NH), 69.14 (CO*C*H_2), 110.05 (CH_2*C*), 111.58 (NHC*C*HCH), 113.51 (CO*C*H), 117.61 (CCH*C*H), 118.32 (CHCH*C*H), 118.58 (CHCH*C*HCH), 119.42 (C*C*HCH), 121.88 (NHCCH*C*H), 123.45 (C*C*HNH), 127.90 (*C*CH), 136.00 (NH*C*CH), 139.32 (CNH$_2$), 140.05 (CO*C*), 144.44 (*C*OCH$_2$), 165.02 (*C*O). **LRMS** *m/z* (ESI): 430.4 $[M+Na]^+$. **HRMS** *m/z* (ESI): calculated for $C_{25}H_{34}N_3NaO_2^+$ $[M+Na]^+$: 430.2465 found 430.2466.

*3-(2-(1H-Indol-3-yl)ethoxy)-4-(2-amino-5-guanidinopentanamido)-N-octylbenzamide; Peptidomimetic 1 (**37**)*

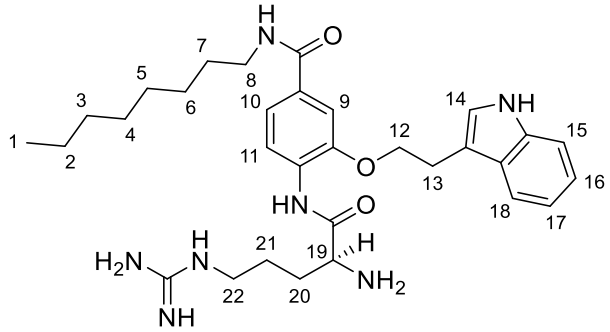

Fmoc-Arg-OH (0.15 g, 0.3 mmol, 1 eq) was dissolved in THF under N_2 and cooled to 0˚C. $SOCl_2$ (80 µL, 0.13 g, 1.11 mmol, 3 eq) was added dropwise then the reaction was heated to reflux for 2 hours. The solvent was then removed *in vacuo*. The resulting residue was dissolved in THF and **36** (0.2 g, 0.37 mmol, 1 eq) and TEA (0.25 mL, 0.18 g, 1.85 mmol, 5 eq) were added. The reaction mixture was stirred under N_2 overnight. The solvent was removed *in vacuo*. Piperidine (20%) in DCM (The resulting oil was purified by RP-HPLC using Synergi™ 4 µm Polar-RP 80 Å and an elution gradient of H_2O/MeCN (50:50 to 0:100) over 30 minutes with a flow rate of 2 mL/min. **^{1}H-NMR:** (400 MHz, CD_3COCD_3) δ_H: 0.89 (t, 3H, J=6.0 Hz, H-1), 1.15-1.42 (m, 12H, H-2, H-3, H-4, H-5, H-6, H-7), 1.55-1.67 (m, 2H, H-21), 1.77-1.89 (m, 2H, H-20), 3.14 (t, 2H J=6.5 Hz, H-13), 3.34 (t, 2H, J= 6.0, 12.5 Hz, H-22), 3.37 (t, 2H, J= 6.0 Hz, H-8), 3.73 (t, 3H, J=6.5 Hz, H-19), 4.45 (t, 2H, J= 7.0 Hz, H-12), 7.11 (dt, 2H, J= 7.5, 3.5 Hz, H-16, H-17), 7.20 (s, 1H, H-11), 7.41 (dd, 2H, J= 8.0, 4.0 Hz, H-15, H-18), 7.57 (s, 1H, H-14), 7.64 (d, 1H, J= 8.0 Hz, H-10), 8.15 (d, 1H, J=9.0 Hz, H-9). **^{13}C-NMR:** (125 MHz, CD_3COCD_3): 13.01 (*C*H_3), 22.35 (CH_2*C*H_2CH_2NH), 22.37 (*C*H_2), 26.01 (*C*H_2), 26.71 (*C*$H_2CH_2CH_2NH$),29.02 (*C*H_2), 29.08 (*C*H_2), 29.35 (*C*H_2), 31.58 (*C*H_2), 31.99 ($COCH_2$*C*H_2), 47.50 (*C*H_2NH), 48.24 (CH_2CH_2*C*H_2NH), 54.52 (CO*C*H), 69.05 (CO*C*H_2), 110.68 (CH_2*C*), 111.18 (NHC*C*HCH), 113.47 (CO*C*H), 117.70 (CCH*C*H), 117.83 (CHCH*C*H), 118.57 (CHCH*C*HCH), 119.49 (C*C*HCH), 121.19 (NHCCH*C*H), 122.54 (C*C*HNH), 127.72 (*C*CH), 129.32 (CNH), 131.36 (CO*C*), 131.58 (NH*C*CH),

148.77 (*C*OCH$_2$), 163.99 (*C*O), 167.71 (NH*C*O). **LRMS** *m/z* (ESI): 564.3 [M+Na]$^+$. **HRMS** *m/z* (ESI): calculated for $C_{31}H_{46}N_7O_3^+$ [M+Na]$^+$: 564.3657 found 564.3656.

7.3 Peptidomimetic 2

*Methyl 2-hydroxy 4-nitrobenzoic acid (**38**)*[166]

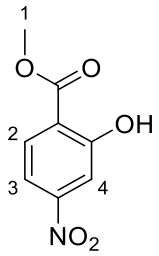

2-Hydroxy-4-nitrobenzoic acid (1.25 g, 6.8 mmol) was dissolved in MeOH (15 mL) and H_2SO_4 *conc.* (0.5 mL) was added. The reaction mixture was refluxed for 18 hours. MeOH was removed under high vacuum and the resulting solid was dissolved in EtOAc (75 mL) and washed 3 times with Na_2CO_3 *sat.* (75 mL) and the organic layer was dried with $MgSO_4$. (0.65 g, 3.3 mmol, 49%). $\mathbf{R_f}$ = 0.63 (3:7/EtOAc:petroleum ether). **^{1}H-NMR:** (400 MHz, MeOD) δ_H: 3.35 (s, 1H, H-1), 7.73 (d, 1H, J=8.7 Hz, H-3), 7.77 (s, 1H, H-4), 8.09 (d, 1H, J=8.7 Hz, H-2). **^{13}C-NMR** (125 MHz, MeOD): 51.71 (*C*H_3O), 111.94 (COH*C*H), 112.92 (CNO_2*C*H), 117.52 (CO*C*) 131.08 (CH*C*H), 151.47 (*C*NO_2), 151.98 (*C*OH), 168.52 (O*C*O).

*Methyl 2-(indol-3-ethoxy)-4-nitrobenzoic acid (**39**)*[167]

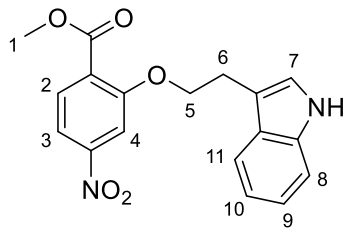

Compound **39** (0.65 g, 3.3 mmol, 1 eq), 3-(2-bromoethyl)indole (0.81 g, 3.6 mmol, 1.1 eq), Cs_2CO_3 (2.15 g, 6.6 mmol, 2 eq) were stirred in DMF (6 mL) at 60°C for 18 hours. The reaction mixture was taken up in EtOAc (75 mL) and washed 3 times with Na_2CO_3 *sat.* (75 mL). The organic layer was dried with $MgSO_4$ and dried under high vacuum. Silica column chromatography was carried out and the product was eluted with 2:8/EtOAc:petroleum ether. (Adapted from literature reference[167]). (0.51 g, 1.5 mmol, 45%). **R_f =** 0.43 (3:7/EtOAc:petroleum ether). **^{1}H-NMR:** (400 MHz, MeOD) δ_H: 3.19 (t, 2H, J=6.5 Hz, H-6), 3.82 (s, 3H, H-1), 4.27 (t, 2H, J=6.5 Hz, H-5), 6.98 (t, 1H J=7.4 Hz, H-10), 7.06 (t, 1H, J=7.4 Hz, H-9), 7.15 (s, 1H, H-7), 7.30 (d, 1H, J=8.0 Hz, H-11), 7.54 (d, 1H, J=7.8 Hz, H-8), 7.65-7.70 (m, 2H, H-3, H-2), 7.72 (s, 1H, H-4). **^{13}C-NMR** (125 MHz, MeOD): 24.50 (CH_2CH_2), 51.57 (CH_3O), 69.79 ($COCH_2$), 107.59 (NHCCH), 110.57 (CH_2C), 110.83 (CNO_2CH), 112.86 (CCH), 114.30 (CCHCH), 117.84 (CHCHC), 118.32 (CHCHCH), 120.92 (CCHCH), 126.25 (COCCH), 127.38 (CHC), 131.19 (CCHCH), 136.52 (NHC), 150.50 ($CHCNO_2$), 158.20 ($COCH_2$), 165.85 (OCO).

*Methyl 2-(indol-3-ethoxy)-4-aminobenzoic acid (**40**)*[168]

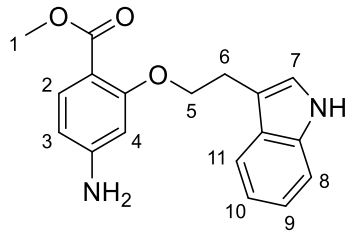

Compound **40** (0.51 g, 1.5 mmol, 1 eq), and Pd/C (0.13 g, 0.8 eq), were stirred in MeOH (10 mL) overnight under H_2 and then filtered through Celite. Solvent was removed under high vacuum. (Adapted from literature reference[168]). (0.23 g, 0.74 mmol, 50%). $\mathbf{R_f}$ = 0.24 (1:1/EtOAc:petroleum ether). **^{1}H-NMR:** (400 MHz, $(CD_3)_2CO$) δ_H: 3.24 (t, 2H, J=7.0 Hz, H-6), 3.74 (s, 3H, H-1), 4.38 (t, 2H, J=7.0 Hz, H-5), 6.24-6.28 (m, 1H, H-3), 6.37 (s, 1H, H-4), 7.02 (t, 1H, J=7.4 Hz, H-10), 7.09 (t, 1H, J=7.4 Hz, H-9), 7.32-7.42 (m, 2H, H-7, H-2), 7.59-7.67 (m, 2H, H-8, H-11). **^{13}C-NMR** (125 MHz, $(CD_3)_2CO$): 25.01 ($CH_2\mathit{C}H_2$), 50.22 ($\mathit{C}H_3O$), 68.87 ($CO\mathit{C}H_2$), 98.10 ($CNH_2\mathit{C}H$), 105.75 ($CCH\mathit{C}H$), 107.62 ($CH_2\mathit{C}$), 111.27 ($NHC\mathit{C}H$), 111.34 ($CO\mathit{C}CH$), 118.35 ($CH\mathit{C}HC$), 118.55 ($CHCH\mathit{C}H$), 121.09 ($CCH\mathit{C}H$), 123.48 ($C\mathit{C}H$), 127.72 ($CH\mathit{C}$) 133.70 ($C\mathit{C}HCH$), 136.40 ($NH\mathit{C}$), 154.16 ($CH\mathit{C}NH_2$), 161.19 ($\mathit{C}OCH_2$), 165.88 ($O\mathit{C}O$).

*Methyl 2-(indol-3-ethoxy)-4-(octylamino) benzoic acid (**41**)*

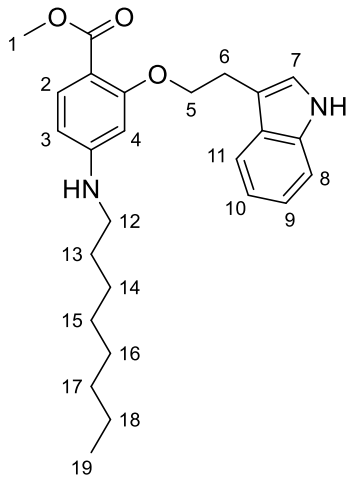

Compound **40** (0.23 g, 0.74 mmol, 1 eq), was dissolved in MeOH (3 mL) and AcOH (40 μL, 1eq). Octanal (0.12 mL, 0.10g, 0.74 mmol, 1 eq) and $NaCNBH_3$ (0.09g, 1.48 mmol, 2 eq) were added and stirred for 24 hrs under N_2. EtOAc (50 mL) was added and washed 3x with Na_2CO_3 (50 mL). The organic layer was dried with $MgSO_4$ and concentrated under high vacuum. Silica column chromatography was carried out and the product was eluted with EtOAc. (Adapted from literature reference[152]). (0.08 g, 0.19 mmol, 26%). $\mathbf{R_f}$ = 0.85 (1:1/EtOAc:petroleum ether). **^{1}H-NMR:** (400 MHz, $(CD_3)_2CO$) δ_H: 0.86, (t, 3H, J= 6.3 Hz, H-19), 1.19-1.43 (m, 10H, H-,14, H-15, H-16, H-17, H-18), 1.55-1.65 (m, 2H, H-13), 3.13 (t, 2H, J=7.0 Hz, H-6), 3.25 (t, 2H, J= 7.0 Hz, H-12), 3.74 (s, 3H, H-1), 4.22 (t, 2H, J=7.0 Hz, H-5), 6.22 (d, 1H, J= 8.0 Hz, H-2), 6.27 (s, 1H, H-7), 7.06 (dt, 2H, J=, 7.3 10.0 Hz, H-9, H-10), 7.36-7.41 (m, 2H, H-3, H-4), 7.65 (dd, 2H, J= 8.0, 3.0 Hz, H-8, H-11). **^{13}C-NMR** (125 MHz, $(CD_3)_2CO$): 16.15 (CH_3), 25.09 (CH_2CH_2), 27.74 ($CH_2CH_2CH_2CH_3$), 29.59 ($NHCH_2CH_2CH_2$), 30.22 (CH_2CH_3),31.80 ($CH_2CH_2CH_3$), 31.90 ($CH_2CH_2CH_2CH_2$), 34.31 ($NHCH_2CH_2$), 45.48 ($NHCH_2$), 52.85 (CH_3O), 71.63 ($COCH_2$), 98.94(CNH_2CH), 106.64 (CCHCH), 109.75 (COCCH), 113.86 (NHCCH), 114.08 (CH_2C), 121.02 (CHCHC), 121.23 (CHCHCH), 123.77 (CCHCH), 126.01 (CCH), 130.41 (CHC), 136.18 (CCHCH), 139.15 (NHC), 156.65 ($CHCNHCH_2$), 163.95 ($COCH_2$), 168.54 (OCO), **LRMS** *m/z* (ESI): 445.4 $[M+Na]^+$. **HRMS** *m/z* (ESI): calculated for $C_{26}H_{34}N_2NaO_3^+$ $[M+Na]^+$: 445.2462 found 445.2468.

*2-(Indol-3-ethoxy)-4-(octylamino) benzoic acid (**42**)*

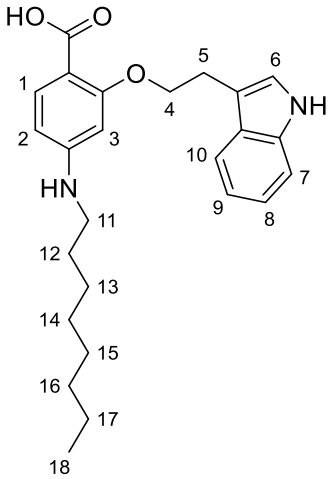

Compound **41** (0.08 g, 0.19 mmol) was dissolved in MeOH (3 mL) and 6M NaOH (1 mL) was added and refluxed overnight. The solution was acidified using HCl and the precipitate was collected by filtration. (0.04 g, 0.09 mmol, 50%). $\mathbf{R_f}$ = 0.85 (EtOAc). **^{1}H-NMR:** (400 MHz, $(CD_3)_2CO$) δ_H: 0.86, (t, 3H, J= 6.2 Hz, H-19), 1.15-1.40 (m, 10H, H-13, H-14, H-15, H-16, H-17), 1.62-1.76 (m, 2H, H-112), 3.22 (t, 2H, J=7.3 Hz, H-11), 3.35 (t, 2H, J= 6.8 Hz, H-5), 4.50 (t, 2H, J=6.8 Hz, H-4), , 7.06 (dt, 2H, J= 32.3, 7.3 Hz, H-8, H-9), 7.29-7.35 (m, 2H, H-2, H-3), 7.40 (d, 1H, J= 8.0 Hz, H-10) 7.66 (d, 1H, J=8.9 Hz, H-7) 7.79 (s, 1H, H-6). **^{13}C-NMR** (125 MHz, $(CD_3)_2CO$): 13.45 (CH_3), 22.93 (CH_2CH_3), 22.93 ($NHCH_2CH_2CH_2$), 26.76 (CH_2CH_2), 28.14 ($CH_2CH_2CH_2CH_2$), 28.37 ($CH_2CH_2CH_2CH_3$), 29.06 ($CH_2CH_2CH_3$), 29.52 ($NHCH_2CH_2$), 44.74 ($NHCH_2$), 69.42 ($COCH_2$), 110.29 (COCCH), 111.37 (CNH_2CH), 111.90 (NHCCH), 114.14 (CCH), 118.29 (CCHCH), 118.73 (CHCHC), 121.37 (CHCHCH), 123.24 (CCHCH), 127.54 (CHC), 132.21 (CCH), 133.89 (CCHCH), 139.33 (CNH), 140.98 (NHCCH), 164.01 ($COCH_2$), 164.51 (OCO). **LRMS** *m/z* (ESI): 431.4 $[M+Na]^+$. **HRMS** *m/z* (ESI): calculated for $C_{25}H_{32}N_2NaO_3^+$ $[M+Na]^+$: 431.2305 found 431.2296.

7.4 Peptidomimetic 3

*Methyl 4-bromo-2-hydroxybenzoate (**43**)*[169]

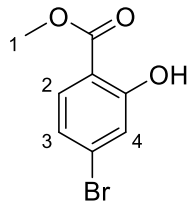

4-Bromo-2-hydroxybenzoic acid (0.5 g, 2.3 mmol) was dissolved in anhydrous MeOH (10 mL), stirred and cooled to 0˚C. $SOCl_2$ (0.5 mL) was added dropwise and then the reaction mixture was heated to reflux for 16h. The solvent was removed *in vacuo*. (0.52 g, 2.3 mmol, 99%). $\mathbf{R_f}$ = 0.58 (3:7/EtOAc:petroleum ether). **^{1}H-NMR:** (400 MHz, MeOD) δ_H: 3.94 (s, 3H, H-1), 7.04 (d, 1H, J=8.5 Hz, H-3), 7.15 (s, 1H, H-4), 7.72 (d, 1H, J=9.0 Hz, H-2). **^{13}C-NMR** (125 MHz, MeOD): 51.56 (*C*H_3O), 120.42 (COH*C*H), 121.95 (C*C*H*C*H), 131.05 (C*C*HCH).

*Methyl 2-hydroxy-4-(oct-1-yn-1-yl)benzoate (**44**)*

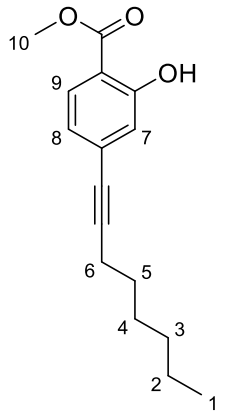

Compound **43** (1.0 g, 4.35 mmol, 1.1 eq), 1-octyne (0.60 mL, 0.44 g, 3.95 mmol, 1 eq), $Pd(PPh_3)_4$ (0.45 g, 0.39 mmol, 0.1 eq), CuI (0.07 g, 0.39 mmol, 0.1 eq) and DIPEA (2.75 mL, 2.04 g, 15.8 mmol, 5 eq) were added to anhydrous THF under N_2 and refluxed for 18 hours. The solvent was removed *in vacuo* and the product was dissolved in petroleum ether. This was filtered and applied to a silica column and the product was eluted with petroleum ether. (0.91 g, 3.5 mmol, 89%). $\mathbf{R_f}$ = 0.68 (Petroleum ether). **^{1}H-NMR:** (400 MHz, MeOD) δ_H: 0.91 (t, 3H, J=6.0 Hz, H-1), 1.22-1.39 (m, 4H, H-2, H-3), 1.40-1.48 (m, 2H, H-4), 1.50-1.64 (m, 2H, H-5), 2.40 (t, 2H, J= 7.0 Hz, H-6), 3.92 (s, 3H, H-10), 6.85 (d, 1H, J= 8.0 Hz, H-8), 6.89 (s, 1H, H-7), 7.72 (d, 1H, J= 8.0 Hz, H-9). **^{13}C-NMR** (125 MHz, MeOD): 13.04 (CH$_3$), 18.69 (CH$_2$), 22.25 (CH$_2$), 28.27 (CH$_2$), 28.32 (CH$_2$), 31.11 (CH$_2$), 51.51 (CCOOCH$_3$), 79.46 (CH$_2$CCC), 93.53 (CH$_2$$C$CC), 111.38 (COH$C$CH), 119.50 (C$C$HCOH), 122.05 (CH$C$H), 129.52 (COHC$C$H), 131.47 (CH$_2CCC$), 160.69 (CCH$C$OH), 169.95 (C$C$OOCH$_3$).

*Methyl 2-(2-(1H-indol-3-yl)ethoxy)-4-(oct-1-yn-1-yl)benzoate (**45**)*

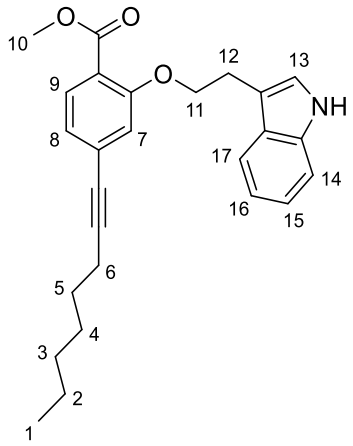

Compound **44** (0.23 g, 0.92 mmol, 1 eq), 3-(2-bromoethyl)indole (0.25 g, 1.11 mmol, 1.2 eq) and $CsCO_3$ (0.58 g, 1.84 mmol, 2 eq) were refluxed in anhydrous acetone for 18 hours. The solvent was removed *in vacuo* and the resulting oil was dissolved in EtOAc. This was washed three times with Na_2CO_3. The organic layer was dried over $MgSO_4$ and the solvent was removed in vacuo. Silica column chromatography was carried out and the product was eluted with 1:4/EtOAc:petroleum ether. (0.20 g, 0.47 mmol, 52%). $\mathbf{R_f}$ = 0.32 (1:4/EtOAc:petroleum ether). **^{1}H-NMR:** (400 MHz, MeOD) δ_H: 0.89 (t, 3H, J=5.5 Hz, H-1), 0.92-1.39 (m, 8H, H-2, H-3, H-4, H-5) 2.43 (t, 2H, J=7.0 Hz, H-6), 3.28 (t, 2H, J=6.5 Hz, H-12), 3.84 (s, 3H, H-10), 4.33 (t, 2H, J= 5.5 Hz, H-11), 6.99-7.08 (m, 2H, H-8, H-16) 7.09-7.15 (m, 2H, H-13, H-15), 7.35-7.43 (m, 2H, H-7, H-17), 7.65-7.70 (m, 2H, H-9, H-14). **^{13}C-NMR** (125 MHz, MeOD): 13.45 (*C*H_3), 22.37 (*C*H_2), 25.05 (*C*H_2), 28.41 (COCH$_2$*C*H$_2$), 28.43 (*C*H_2), 31.52 (*C*H_2), 31.81 (*C*H_2), 51.21 (CCOO*C*H_3), 69.32 (CO*C*H_2CH$_2$), 79.93 (C*C*), 102.1 (*C*), 111.25 (NH*C*CH), 113.75 (CH$_2$*C*), 116.12 (C*C*HCO), 118.35 (CHCHCH*C*H), 118.62 (CHCH*C*HCH), 120.28 (*C*CHCH), 121.17 (NHCCH*C*H), 123.18 (C*C*HNH), 127.72 (CH*C*), 128.16 (CH*C*H), 129.02 (CC*C*), 131.14 (C*C*HCH), 142.96 (NH*C*), 158.13 (CCH*C*O), 165.99 (C*C*OOCH$_3$). **LRMS** *m/z* (ESI): 426.3 [M+Na]$^+$. **HRMS** *m/z* (ESI): calculated for $C_{25}H_{34}N_3NaO_3^+$ [M+Na]$^+$: Exact Mass: 426.2040 found 426.2046.

*2-(2-Indolyl-3-yl ethoxy)-4-(oct-1-yn-1-yl)benzoic acid (**46**)*

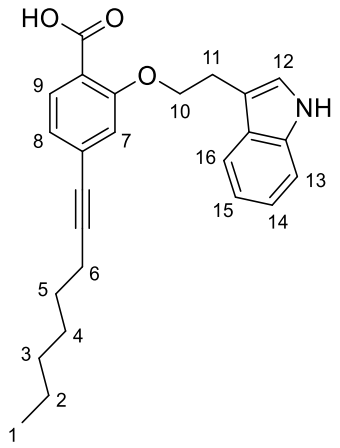

Compound **45** (0.20 g, 0.47 mmol, 1 eq), was stirred in THF (1 mL), MeOH (1 mL), water (1 mL) and 6M NaOH (0.25 mL) at 60˚C for 2 hours. The solvent was removed *in vacuo* and water (40 mL) was added. This was then acidified to pH 3 and washed with EtOAc (3 x 40 mL). The organic fractions were combined and dried over $MgSO_4$. (0.17 g, 0.44 mmol, 95%). **R_f =** 0.49 (EtOAc). **^{1}H-NMR:** (400 MHz, $(CD_3)_2CO$) δ_H: 0.90 (t, 3H, J=5.5 Hz, H-1), 1.09-1.66 (m, 8H, H-2, H-3, H-4, H-5) 2.44 (t, 2H, J=7.0 Hz, H-6), 3.37 (t, 2H, J=6.5 Hz, H-10), 4.53 (t, 2H, J= 5.5 Hz, H-11), 7.08 (dt, J=7.0, 15.5 Hz, 2H, H-14, H-15), 7.22 (s, 1H, H-12), 7.35 (s, 1H, H-7), 7.42 (d, J=8.0 Hz, 1H, H-8), 7.62 (d, J= 8.0 Hz, 1H, H-16), 7.87 (d, J=8.0 Hz, 1H, H-13), 7.94 (d, J=8.0 Hz, 1H, H-9). **^{13}C-NMR** (125 MHz, $(CD_3)_2CO$): 14.35 (CH_3), 19.80 (CH_2), 23.22 (CH_2), 25.92 ($COCH_2CH_2$), 29.28 (CH_2), 29.32 (CH_2), 32.07 (CH_2), 32.41 (CH_2), 70.06 ($COCH_2CH_2$), 80.66 (C*C*), 94.56 (*C*), 111.39 (CH_2C), 111.99 (NH*C*CH), 116.88 (C*C*HCO), 119.08 (*C*CHCH), 119.21 (CHCHCH*C*H), 119.64 (CHCH*C*HCH),122.24 (CH*C*H), 122.27 (NHCCH*C*H), 122.42 (C*C*HNH), 128.52 (CH*C*), 130.93 (C*C*C), 133.24 (C*C*HCH), 137.73 (NH*C*), 158.72 (CCH*C*O), 165.81 ($CCOOCH_3$). **LRMS** *m/z* (ESI): 388.4 $[M-H]^-$. **HRMS** *m/z* (ESI): calculated for $C_{25}H_{26}N_3O_3^-$ $[M-H]^-$: Exact Mass: 388.1918 found 388.1922.

*2-(2-Indolyl-3-yl ethoxy)-4-(oct-1-yn-1-yl)benzoyl)arginine (**47**)*

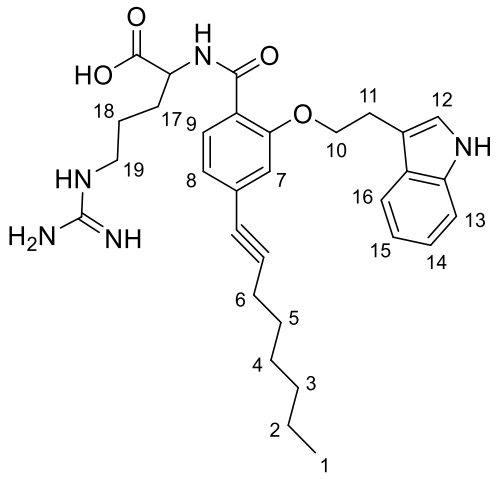

Compound **46** (0.25 g, 0.64 mmol, 1 eq), Arg-O^{t}Bu (0.16 g, 0.70 mmol, 1.1 eq), HATU (0.31 g, 0.83 mmol, 1.3 eq) and DIPEA (0.22 mL, 0.16 g, 1.28 mmol, 2 eq) were dissolved in DCM and stirred under N_2 for 18 hours. The solvent was removed *in vacuo*. To the resulting oil HCl (4M in dioxane) (5 mL) was added under N_2 and stirred for 4 hours. The solvent was removed *in vacuo* to give an orange oil. *Product not isolated but identified by MS.* **LRMS** *m/z* (ESI): 546.4 $[M+H]^+$. **HRMS** *m/z* (ESI): calculated for $C_{31}H_{41}N_5O_4^+$ $[M+H]^+$: Exact Mass: 546.3075 found 546.3068.

*2-(2-Indolyl-3-yl ethoxy)-4-octylbenzoyl)-L-arginine; peptidomimetic 3 (**48**)*

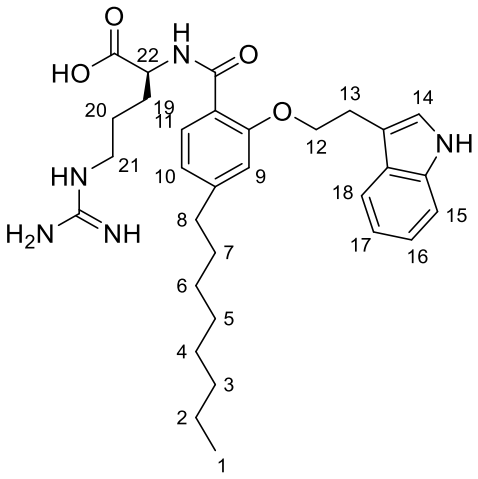

The crude reaction mixture of **47** (0.1 g) was added to Pd/C (0.03 g, 0.28 mmol) and dissolved in MeOH (2 mL) under H_2 and stirred for 18 hours. The sample was then purified by RP-HPLC using Synergi™ 4 µm Polar-RP 80 Å and an elution gradient of H_2O/MeCN (80:20 to 0:100) over 45 minutes with a flow rate of 2 mL/min. The fractions containing the product were pooled and lyophilized. **^{1}H-NMR:** (400MHz, $(CD_3)_2CO$) δ_H: 0.87 (t, 3H, J=5.5 Hz, H-1), 1.35-1.47 (m, 10H, H-2, H-3, H-4, H-5, H-6) 1.48 (t, 2H, J=7.0 Hz, H-7), 1.66-1.74 (m, 2H, H-19), 1.75-1.81 (m, 2H, H-20), 3.45-3.53 (m, 2H, H-21), 2.63 (t, J= 6.0 Hz, 2H, H-12), 2.82 (t, 2H, J=7.0 Hz, H-8), 3.37 (t, 2H, J=6.5 Hz, H-13), 4.53 (t, 2H, J= 5.5 Hz, H-11), 4.54-4.59 (m, 1H, H-22), 6.90 (d, J=8.0 Hz, 1H, H-10), 6.98-7.04 (m, 2H, H-9, H-15), 7.15 (t, J=7.5 Hz, 1H, H-17), 7.15 (s, 1H, H-14), 7.35 (d, J= 8.0 Hz, 1H, H-15), 7.58 (d, J= 8.0 Hz, 1H, H-18), 7.92 (d, J= 8.0 Hz, 1H, H-11). **^{13}C-NMR** (125 MHz, $(CD_3)_2CO$): 13.02 (CH_3), 21.65 ($NHCHCH_2CH_2$), 22.36 ($NHCHCH_2CH_2$), 24.22 (CH_2), 24.52 (CH_2), 28.91 ($COCH_2CH_2$), 29.11 (CH_2), 30.65 (CH_2), 31.06 (CH_2), 35.55 (CH_2), 40.43 (CH_2), 44.30 (CH_2NH), 52.27 (NHCH), 68.77 ($COCH_2CH_2$), 110.47 (CH_2C), 110.96 (CH_2C), 112.67 (NHCCH), 117.84 (CCH), 118.40 (CHCHCHCH), 120.84 (CHCHCHCH), 121.14 (CHCH), 121.84 (NHCCHCH), 122.29 (CCHNH), 123.91 (CHCOC), 127.37 (CHC), 131.13 (COCCH), 136.94 (NHC), 149.56 (CCHCO), 157.46 (NHC), 166.05 (CCO), 173.93 (NHCHCOOH). **LRMS** *m/z* (ESI): 550.5 $[M+H]^+$. **HRMS** *m/z* (ESI): calculated for $C_{31}H_{44}N_5O_4^+$ $[M+H]^+$: Exact Mass: 550.3388 found 550.3394.

7.5 Peptidomimetic 4

*tert-Butyl 3-(2-bromoethyl)-1H-indole-1-carboxylate (**49**)*[170]

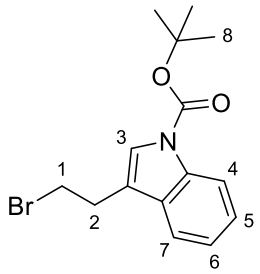

3-(2-Bromoethyl)indole (2 g, 8.9 mmol,1 eq), Boc_2O (3.88 g, 17.8 mmol, 2 eq), TEA (2.40 mL, 1.80 g, 1.78 mmol, 2 eq), and DMAP (0.11 g, 0.9 mmol, 0.1 eq) were added to DCM (40 mL) and stirred overnight. The reaction mixture was washed 3 times with water (40 mL). The organic layer was dried over $MgSO_4$ and reduced *in vacuo*. The resulting residue was applied to a silica column and the product was eluted with 20:80 EtOAc/Petroleum ether. (2.54 g, 7.9 mmol, 88%). **R_f =** 0.85 (20:80 EtOAc/Petroleum ether). **^{1}H-NMR:** (400 MHz, $(CD_3)_2CO$) δ_H: 1.69 (s, 9H, H-8), 3.32 (t, 2H, J= 7.5 Hz, H-2), 3.79 (t, 2H, J= 7.5 Hz, H-1), 7.31 (dt, 2H, J= 7.5, 24.0 Hz, H-5, H-6), 7.63-7.67 (m, 2H, H-3, H-7), 8.16 (d, 1H, J= 8.0 Hz, H-4). **^{13}C-NMR** (125 MHz, $(CD_3)_2CO$): 28.25 ($3CH_3$), 29.36 (BrCH*C*H_2), 32.81 (Br*C*H_2), 84.32 (OCO*C*), 110.99 (CH_2*C*), 115.99 (NHC*C*H), 118.91 (CHCH*C*), 119.80 (CHCHCH*C*H), 123.38 (CHCH*C*H), 124.62 (NHCCH*C*H), 125.54 (CH_2C*C*H), 130.98 (CCHNH*C*), 150.29 (*C*O). **LRMS** *m/z* (ESI): 346.2 $[M+Na]^+$. **HRMS** *m/z* (ESI): calculated for $C_{15}H_{18}BrNNaO_2$ $[M+Na]^+$: Exact Mass: 346.0413 found 346.0406.

Data in agreement with literature reference.

*tert-Butyl 3-(2-(2-nitro-5-(octylcarbamoyl)phenoxy)ethyl)-1H-indole-1-carboxylate (**50**)*

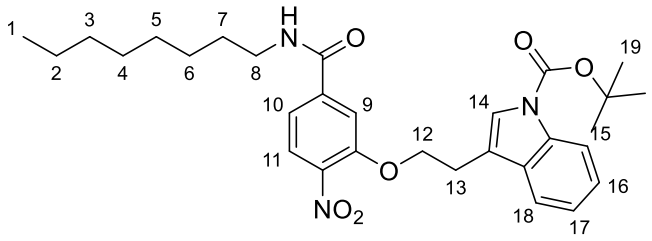

Compound **34** (1.00 g, 5.5 mmol, 1 eq), **49** (2.07 g, 6.0 mmol, 1.2 eq) and K_2CO_3 (1.25 g, 9.0 mmol, 1.5 eq) were stirred in anhydrous DMF (10 mL) and stirred under N_2 for 18 h. EtOAc (50 mL) and washed with $NaHCO_3$ (3 x 50 mL). The organic layer was dried with $MgSO_4$. The solvent was removed *in vacuo*. Silica column chromatography was carried out and the product was eluted with 1:19/EtOAc:petroleum ether. (1.07 g 2.0 mmol, 36%). R_f = 0.80 (2:3/EtOAc:petroleum ether). **^{1}H-NMR:** (400 MHz, CD_3COCD_3) δ_H: 0.90 (t, 3H, J=6.0 Hz, H-1), 1.20-1.38 (m, 10H, H-2, H-3, H-4, H-5, H-6), 1.52-1.59 (m, 2H, H-7), 1.65 (s, 9H, H-19), 3.30 (t, 2H J=6.5 Hz, H-13), 3.38 (dd, 2H, J= 6.0, 12.5 Hz, H-8), 4.44 (t, 2H, J= 7.0 Hz, H-12), 7.09 (dt, 2H, J= 7.0, 14.5 Hz, H-16, H-17), 7.30 (s, 1H, H-14), 7.42 (d, 1H, J= 8.0 Hz, H-10), 7.63 (dd, 2H, J= 8.0, 2.5 Hz, H-15, H-18), 7.79 (s, 1H, H-11), 7.51 (d, 1H, J=9.0 Hz, H-9). **^{13}C-NMR** (125 MHz, CD_3COCD_3): 15.54 (CH_3), 25.00 (CH_2), 26.33 (CH_2), 28.27 ($3CH_3$), 29.42 (CH_2), 29.44 (CH_2), 29.90 (CH_2), 31.35 (CH_2), 32.50 ($COCH_2CH_2$), 40.23 (CH_2NH), 70.04 ($COCH_2$), 75.03 ($COCO$), 110.55 (CH_2C), 111.35 ($NHCCHCH$), 113.51 ($COCH$), 118.32 ($CHCHCH$), 118.78 ($CHCHCHCH$), 119.04 ($CCHCH$), 121.30 ($NHCCHCH$), 123.40 ($CCHNH$), 124.86 ($CCHCH$), 127.59 (CCH), 136.68 ($NHCCH$), 140.05 (COC), 141.47 (CNO_2), 151.63 ($COCH_2$), 162.65 (CO), 168.78 ($COCONC$).

*tert-Butyl 3-(2-(5-(benzyl(octyl)carbamoyl)-2-nitrophenoxy)ethyl)-1H-indole-1-carboxylate (**51**)*

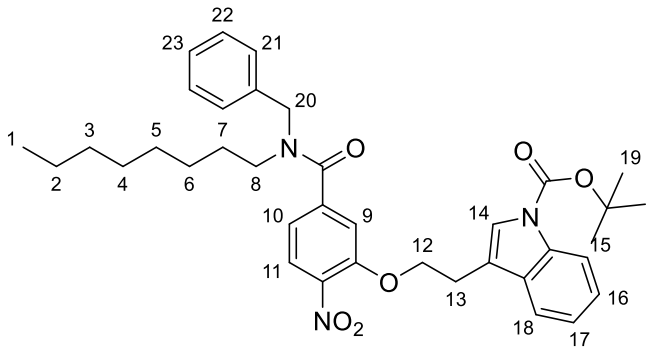

Compound **50** (1.07 g, 2.0 mmol, 1 eq) and NaH (60 % dispersion in mineral oil) (0.4 g, 10 mmol, 5 eq) were stirred in THF (5 mL) at 0 °C for 10 minutes and then allowed to come to room temperature. Benzyl bromide (mL, g, 4.0 mmol, 2 eq) was then added dropwise and the reaction mixture stirred for 18 hours. The THF was removed *in vacuo*. The reaction mixture was taken up in EtOAc (75 mL) and washed 3 times with Na_2CO_3 *sat.* (75 mL). The organic layer was dried with $MgSO_4$ and dried under high vacuum. Silica column chromatography was carried out and the product was eluted with 1:9/EtOAc:petroleum ether. (1.23 g, 1.96 mmol, 98%). $\mathbf{R_f}$ = 0.80 (1:9/EtOAc:petroleum ether). **^{1}H-NMR:** (400 MHz, MeOD) δ_H: 0.89 (t, 3H, J=6.0 Hz, H-1), 1.22-1.37 (m, 10H, H-2, H-3, H-4, H-5, H-6), 1.51-1.60 (m, 2H, H-7), 1.65 (s, 9H, H-26), 3.32 (t, 2H J=6.5 Hz, H-13), 3.39 (dd, 2H, J= 6.0, 12.5 Hz, H-8), 4.40 (t, 2H, J= 7.0 Hz, H-12), 5.11 (s, 2H, H-20), 7.10 (dt, 2H, J= 7.0, 14.5 Hz, H-16, H-17), 7.30 (m, 6H, H-14, H-21, H-22, H-23), 7.42 (d, 1H, J= 8.0 Hz, H-10), 7.65 (dd, 2H, J= 8.0, 25.5 Hz, H-15, H-18), 7.50 (d, 1H, J=9.0 Hz, H-9), 7.81 (s, 1H, H-11). **^{13}C-NMR** (125 MHz, MeOD): 14.90 (*C*H_3), 24.88 (*C*H_2), 25.90 (*C*H_2), 27.93 (3*C*H_3), 29.45 (*C*H_2), 29.89 (*C*H_2), 29.78 (*C*H_2), 30.50 (COCH$_2$*C*H$_2$), 32.00 (*C*H_2), 40.29 (*C*H_2NH), 52.32 (N*C*H_2C), 70.41 (CO*C*H_2), 75.01 (*C*OCO), 110.55 (CH$_2$*C*), 111.32 (NHC*C*HCH), 113.50 (CO*C*H), 118.32 (CHCH*C*H), 118.78 (CHCH*C*HCH), 119.40 (C*C*HCH), 121.30 (NHCCH*C*H), 123.40 (C*C*HNH), 124.82 (CCH*C*H), 126.90, 127.81, 127.92(C*Ar*).128.22 (*C*CH), 136.49 (NCH$_2$*C*), 136.68 (NH*C*CH), 140.52 (CO*C*), 141.42 (CNO$_2$), 150.60 (*C*OCH$_2$), 163.65 (*C*O), 169.10 (CO*C*ONC).

*tert-Butyl 3-(2-(2-amino-5-(benzyl(octyl)carbamoyl)phenoxy)ethyl)-1H-indole-1-carboxylate (**52**)*

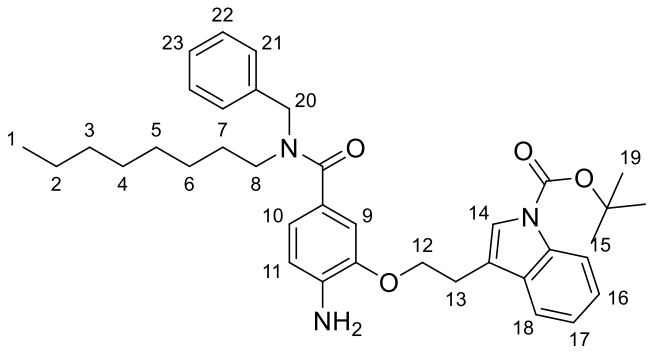

Compound **51** (1.23 g, 1.96 mmol, 1 eq), and Pd/C (0.16 g, 0.8 eq), were stirred in MeOH (10 mL) overnight under H_2 and then filtered through Celite. Solvent was removed under high vacuum. (Adapted from literature reference[168]). (0.61 g, 1.02 mmol, 52%). $\mathbf{R_f}$ = 0.33 (2:1/EtOAc:petroleum ether).**^{1}H-NMR:** (400 MHz, MeOD) δ_H: 0.90 (t, 3H, J=6.0 Hz, H-1), 1.21-1.38 (m, 10H, H-2, H-3, H-4, H-5, H-6), 1.54-1.60 (m, 2H, H-7), 1.68 (s, 9H, H-19), 3.31 (t, 2H J=6.5 Hz, H-13), 3.41 (dd, 2H, J= 6.0, 2.5 Hz, H-8), 4.46 (t, 2H, J= 7.0 Hz, H-12), 5.14 (s, 2H, H-20), 7.11 (dt, 2H, J= 7.0, 10.5 Hz, H-16, H-17), 7.28 (m, 6H, H-14, H-21, H-22, H-23), 7.42 (d, 1H, J= 8.0 Hz, H-10), 7.63 (dd, 2H, J= 8.0, 25.5 Hz, H-15, H-18), 7.51 (d, 1H, J=9.0 Hz, H-9), 7.62 (s, 1H, H-11). **^{13}C-NMR** (125 MHz, MeOD): 15.54 (*C*H_3), 25.00 (*C*H_2), 26.33 (*C*H_2), 29.42 (*C*H_2), 29.44 (*C*H_2), 29.71 (3*C*H_3), 29.90 (*C*H_2), 31.35 (*C*H_2), 32.50 (CO*C*H_2*C*H_2), 40.23 (*C*H_2NH), 54.22 (N*C*H_2C), 70.04 (CO*C*H_2), 75.12 (*C*OCO), 110.55 (CH$_2$*C*), 111.20 (NHC*C*HCH), 113.51 (CO*C*H), 118.34 (CHCH*C*H), 119.02 (CHCH*C*HCH), 119.04 (C*C*HCH), 121.42 (NHCCH*C*H), 123.82 (C*C*HNH), 124.86 (CCH*C*H), 127.61 (*C*CH), 127.41, 128.34, 128.67 (C*Ar*), 136.53 (NCH$_2$*C*), 137.03 (NH*C*CH), 140.05 (CO*C*), 141.47 (CNH$_2$), 151.63 (*C*OCH$_2$), 162.65 (*C*O), 169.00 (CO*C*ONC). **LRMS** *m/z* (ESI): 620.8 $[M+Na]^+$. **HRMS** *m/z* (ESI): calculated for $C_{37}H_{47}N_3NaO_4^+$ $[M+Na]^+$: Exact Mass: 620.3459 found 620.3462.

7.6 Peptidomimetics 5-9

*Methyl 2-(benzyloxy)-4-nitrobenzoate (**53**)*[171]

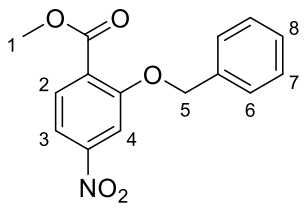

Compound **38** (2.0 g, 0.01 mol, 1 eq), benzyl bromide (1.32 mL, 1.88 g, 0.011 mol, 1.1 eq), Cs_2CO_3 (6.5 g, 0.02 mol, 2 eq) were stirred in DMF (6 mL) at 80 °C for 18 hours. The reaction mixture was taken up in EtOAc (75 mL) and washed 3 times with Na_2CO_3 *sat.* (75 mL). The organic layer was dried with $MgSO_4$ and dried under high vacuum. Silica column chromatography was carried out and the product was eluted with 2:8/EtOAc:petroleum ether. (Adapted from literature reference[167]). (2.0 g, 6.9 mmol, 69%). $\mathbf{R_f}$ = 0.60 (3:7/EtOAc:petroleum ether). **^{1}H-NMR:** (400 MHz, $(CD_3)_2CO$) δ_H: 3.90 (s, 3H, H-1), 5.42 (s, 1H, H-5), 7.33-7.59 (m, 5H, H-6, H-7, H-8), 7.29 (d, 1H, J= 8.5 Hz, H-3), 7.91 (d, 1H, J= 8.0 Hz, H-2), 7.93 (s, 1H, H-4). **^{13}C-NMR** (125 MHz, $(CD_3)_2CO$): 51.12 (OCH_3), 70.59 (OCH_2), 99.48 (CNO_2CH), 104.07 (CO*C*), 107.01 (CCH*C*H), 128.04 (C*C*HCHCH), 129.38 (CCHCH*C*H), 129.90 (CCH*C*HCH), 136.60 (C*C*H), 137.07 (CH_2C), 151.10 ($CHCNO_2$), 162.91 (CH*C*O), 163.24 (O*C*O).

*Methyl 4-amino-2-(benzyloxy)benzoate (**54**)*[82]

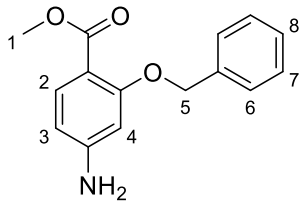

53 (2.0 g, 6.9 mmol, 1 eq), Fe (2 g) and NH_4Cl (2 g) were stirred in 1:1 EtOH and water (10 mL) for 4 hours at 100 °C and then filtered through Celite. Solvent was removed under high vacuum. (1.72 g, 6.6 mmol, 95%). $\mathbf{R_f}$ = 0.52 (1:1/EtOAc:Petroleum ether). **^{1}H-NMR:** (400MHz, $(CD_3)_2CO$) δ_H: 3.80 (s, 3H, H-1), 5.12 (s, 1H, H-5), 6.44 (s, 1H, H-4), 6.82 (d, 1H, J= 8.5 Hz, H-3), 7.23-7.61 (m, 5H, H-6, H-7, H-8), 7.65 (d, 1H, J= 8.0 Hz, H-2). **^{13}C-NMR** (125 MHz, $(CD_3)_2CO$): 51.32 (OCH_3), 70.44 (OCH_2), 98.91 (CNH*C*H), 107.02 (CCH*C*H), 110.28 (CO*C*), 127.63 (C*C*HCHCH), 128.19 (CCHCH*C*H), 129.09 (CCH*C*HCH), 134.68 (C*C*H), 137.91 (CH_2*C*), 153.91 (CH*C*NH), 163.64 (O*C*O), 164.44 (CH*C*O). **LRMS** *m/z* (ESI): 258.2 $[M+H]^+$.

*Methyl 2-(benzyloxy)-4-heptanamidobenzoate (**55**)*

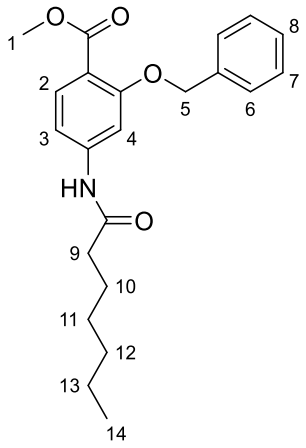

Compound **54** (1.72 g, 6.6 mmol, 1 eq) and DIPEA (2.18 mL, 1.7 g, 13.2 mmol, 2 eq) were stirred in DCM (10 mL) at 0 °C. Heptnoyl chloride (1.1 mL, 1.1 g, 7.26 mmol, 1.1 eq) was then added dropwise over 15 minutes. The reaction was stirred for a further 30 minutes at 0 °C before the solvent was removed *in vacuo*. The resulting oil was purified using silica column chromatography and the product was eluted with 1:4/EtOAc:petroleum ether. (1.63 g, 4.4 mmol, 60%). $\mathbf{R_f}$ = 0.62 (1:4/EtOAc:petroleum ether). **^{1}H-NMR:** (400 MHz, $(CD_3)_2CO$) δ_H: 0.85 (t, 3H, J= 6.5 Hz, H-14), 1.24-1.40 (m, 6H, H-11, H-12, H-13), 1.61-1.74 (m, 2H, H-10), 2.39 (t, 2H, J= 7.5 Hz, H-9), 3.80 (s, 3H, H-1), 5.15 (s, 1H, H-5), 7.12 (d, 1H, J= 7.5 Hz, H-3), 7.26-7.55 (m, 5H, H-6, H-7, H-8), 7.57 (d, 1H, J= 7.5 Hz, H-2), 7.77 (s, 1H, H-4). **^{13}C-NMR** (125 MHz, $(CD_3)_2CO$): 14.35 ($CH_2\mathit{C}H_2CH_2\mathit{C}H_3$), 23.21 ($\mathit{C}H_2CH_2CH_3$), 29.62 ($\mathit{C}H_2CH_2CH_2CH_3$), 26.04 ($COCH_2\mathit{C}H_2$), 32.37 ($COCH_2CH_2\mathit{C}H_2$), 37.88 ($CO\mathit{C}H_2$), 51.79 ($O\mathit{C}H_3$), 70.92 ($O\mathit{C}H_2$), 104.97 (CNH*C*H), 111.40 (CCH*C*H), 115.65 (CO*C*), 127.86 (C*C*HCHCH), 128.41 (CCHCH*C*H), 129.16 (CCH*C*HCH), 133.51 (C*C*H), 138.10 ($CH_2\mathit{C}$), 145.45 (CH*C*NH), 163.25 (CH*C*O), 166.42 (O*C*O), 172.67 (NHCO). **LRMS** *m/z* (ESI): 392.3 $[M+Na]^+$. **HRMS** *m/z* (ESI): calculated for $C_{22}H_{27}NNaO_4^+$ $[M+Na]^+$: Exact Mass: 392.1832 found 392.1833.

*Methyl 4-(N-benzylheptanamido)-2-(benzyloxy)benzoate (**56**)*

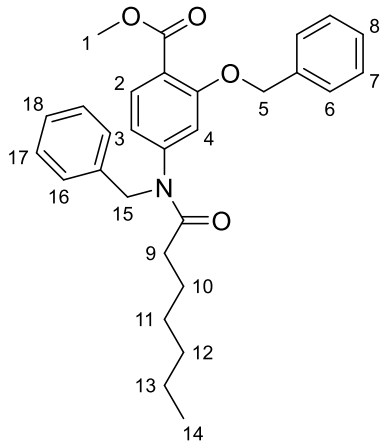

Compound **55** (0.82 g, 2.2 mmol, 1 eq) and NaH (0.10 g, 4.4 mmol, 2 eq) were stirred in dry THF (10 mL) at 0 °C for 0.5 hours. Benzyl bromide (0.30 mL, 0.41 g, 2.3 mmol, 1.1 eq) was then added dropwise and the reaction stirred at room temperature for two hours. The solvent was removed *in vacuo*. The reaction mixture was taken up in EtOAc (75 mL) and washed 3 times with Na_2CO_3 *sat.* (75 mL). The organic layer was dried with $MgSO_4$ and dried under high vacuum. Silica column chromatography was carried out and the product was eluted with 1:9/EtOAc:petroleum ether. (0.96 g, 2.1 mmol, 97%). $\mathbf{R_f}$ = 0.80 (1:9/EtOAc:petroleum ether). **^{1}H-NMR:** (400 MHz, $(CD_3)_2CO$) δ_H: 0.90 (t, 3H, J= 6.5 Hz, H-14), 1.22-1.35 (m, 6H, H-11, H-12, H-13), 1.60-1.71 (m, 2H, H-10), 2.37 (t, 2H, J= 7.5 Hz, H-9), 3.79 (s, 3H, H-1), 5.15 (s, 1H, H-5), 5.17 (s, 2H, H-15), 7.05-7.78 (m, 13H, H-3, H-2, H-4, H-6, H-7, H-8, H-16, H-17, H-18). **^{13}C-NMR** (125 MHz, $(CD_3)_2CO$): 13.15 ($CH_2\mathit{C}H_2CH_2\mathit{C}H_3$), 22.09 ($\mathit{C}H_2CH_2CH_3$), 25.13 ($COCH_2\mathit{C}H_2$), 29.36 ($\mathit{C}H_2CH_2CH_2CH_3$), 31.15 ($COCH_2CH_2\mathit{C}H_2$), 38.82 ($CO\mathit{C}H_2$), 52.00 ($O\mathit{C}H_3$), 52.51 ($N\mathit{C}H_2$), 70.92 ($O\mathit{C}H_2$), 105.27 (CNH*C*H), 110.87 (CCH*C*H), 115.24 (CO*C*), 126.67 (C*C*H), 126.82 (C*C*HCHCH), 127.27(CHCH*C*H), 127.57 (CCHCH*C*H), 128.19 (CH*C*HCH), 128.21 (CCH*C*HCH), 134.08 (C*C*H), 136.90 ($CH_2\mathit{C}$), 138.10 ($CH_2\mathit{C}$), 145.50 (CH*C*NH), 163.25 (CH*C*O), 166.15 (O*C*O), 173.44 (NCO). **LRMS** *m/z* (ESI): 482.3 $[M+Na]^+$. **HRMS** *m/z* (ESI): calculated for $C_{29}H_{33}NNaO_4^+$ $[M+Na]^+$: Exact Mass: 482.2302 found 482.2304.

*4-(N-Benzylheptanamido)-2-(benzyloxy)benzoic acid (**57**)*

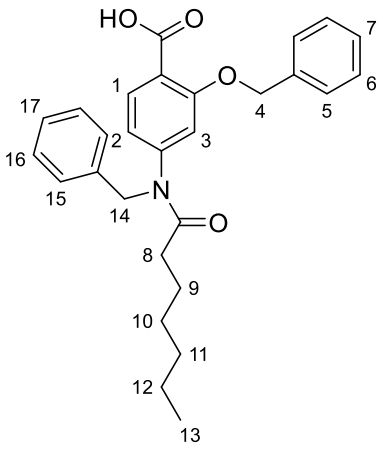

Compound **56** (0.96 g, 2.1 mmol) was dissolved in EtOH (5 mL), water (4 mL) and 6M NaOH (1 mL) was added and refluxed for 5 hours. After removing EtOH *in vacuo* the solution was acidified to pH 4 using HCl and the precipitate was collected by filtration. (0.82 g, 1.8 mmol, 81%). $\mathbf{R_f}$ = 0.70 (4:1/EtOAc:petroleum ether). **^{1}H-NMR:** (400 MHz, MeOD) δ_H: 0.90 (t, 3H, J= 6.5 Hz, H-13), 1.20-1.34 (m, 6H, H-10, H-11, H-12), 1.62-1.68 (m, 2H, H-9), 2.39 (t, 2H, J= 7.5 Hz, H-8), 5.15 (s, 1H, H-4), 5.17 (s, 2H, H-14), 7.02-7.80 (m, 13H, H-1, H-2, H-3, H-5, H-6, H-7, H-15, H-16, H-17,). **^{13}C-NMR** (125 MHz, MeOD): 14.45 ($CH_2CH_2CH_2CH_2CH_3$), 21.99 ($CH_2CH_2CH_2CH_3$), 25.13 ($COCH_2CH_2CH_2$), 28.86 ($CH_2CH_2CH_2CH_2CH_3$), 32.05 ($COCH_2CH_2CH_2CH_2$),38.82 ($COCH_2$), 52.51 (NCH_2), 70.92 (OCH_2), 105.27 (CNHCH), 111.07 (CCHCH), 114.46 (COC), 133.18 (CCH), 126.82 (CCHCHCH), 126.67 (CCH), 127.27(CHCHCH), 127.57 (CCHCHCH), 128.19 (CHCHCH), 128.21 (CCHCHCH), 136.90 (CH_2C), 138.10 (CH_2C), 144.40 (CHCNH), 163.25 (CHCO), 165.35 (COOH), 173.44 (NCO). **LRMS** *m/z* (ESI): 444.4 $[M+Na]^+$. **HRMS** *m/z* (ESI): calculated for $C_{28}H_{31}NNaO_4^+$ $[M+Na]^+$: Exact Mass: 468.2145 found 468.2149.

*Methyl N-2-(4-(N-benzylheptanamido)-2-(benzyloxy)benzoyl)-N6-(tert-butoxycarbonyl)-L-lysinate (**58**)*

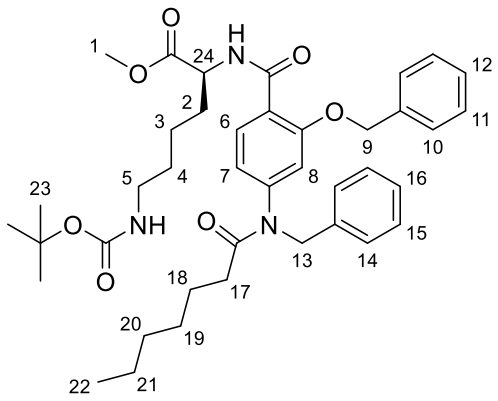

Compound **57** (0.82 g, 1.8 mmol, 1 eq), EDC.HCl (0.42, 2.2 mmol , 1.2 eq), HOBt (0.29 g, 2.2 mmol, 1.2 eq) and DIPEA (0.59 mL, 0.46 g, 3.6 mmol, 2 eq) were stirred in DCM (10 mL) for 15 minutes. H-Lys(Boc)-OMe hydrochloride (0.65 g, 2.2 mmol , 1.2 eq) was added and the reaction was stirred for 18 hours. DCM (40 mL) was added and washed 3 times with Na_2CO_3 *sat.* (75 mL). The organic layer was dried with $MgSO_4$ and dried under high vacuum. Silica column chromatography was carried out and the product was eluted with 2:4/EtOAc:petroleum ether. (0.52 g, 0.75 mmol, 41%). **R_f =** 0.70 (2:4/EtOAc:petroleum ether). **^{1}H-NMR:** (400 MHz, MeOD) δ_H: 0.89 (t, 3H, J= 6.5 Hz, H-22), 1.20-1.40 (m, 8H, H-3, H-19, H-20, H-21), 1.42 (s, 9H, H-23), 1.51-1.60 (m, 2H, H-18), 1.70-1.78 (m, 2H, H-4), 1.69-1.79 (m, 2H, H-2), 2.39 (t, 2H, J= 7.5 Hz, H-17), 2.93 (m, 2H, H-5), 3.32 (s, 3H, H-1), 5.13 (s, 1H, H-9), 5.14 (s, 2H, H-13), 6.81 (d, 1H, J= 8.0 Hz, H-7), 6.94 (s, 1H, H-8), 7.17-7.50 (m, 10H, H-10, H-11, H-12, H-14, H-15, H-16), 7.92 (d, 1H J=8.0 Hz, H-6). **^{13}C-NMR** (125 MHz, MeOD): 13.00 ($CH_2CH_2CH_2CH_3$), 22.13 ($NHCH_2CH_2$), 22.44 ($CH_2CH_2CH_3$), 25.13 ($COCH_2CH_2$), 27.41 ($3CH_3$), 28.53 ($NHCH_2CH_2CH_2$), 28.86 ($CH_2CH_2CH_2CH_3$), 30.53 (CH_2CH), 32.05 ($COCH_2CH_2CH_2$), 35.30 ($COCH_2$), 39.56 ($NHCH_2$), 51.40 ($COOCH_3$), 52.51 (NCH_2), 52.73 (CH_2CH), 71.23 (OCH_2), 78.41 (*C*OCO), 106.17 (CNHCH), 113.56 (CO*C*), 113.96 (CCH*C*H), 128.09 (C*C*HCHCH), 128.37(CHCH*C*H), 128.47 (CCHCH*C*H), 128.60 (CCH*C*HCH), 129.10 (C*C*H), 129.60 (CH*C*HCH), 133.16 (C*C*H), 136.90 (CH_2C), 137.19 (CH_2C), 146.13

(CH*C*NH), 158.46 (CO*C*ONH), 163.25 (CH*C*O), 165.35 (*C*ONHCH), 172.51 (N*C*O), 173.60 (*C*OOCH$_3$). **LRMS** *m/z* (ESI): 710.5 [M+Na]$^+$. **HRMS** *m/z* (ESI): calculated for $C_{40}H_{53}N_3NaO_7^+$ [M+Na]$^+$: Exact Mass: 710.3776 found 710.3780.

*Methyl (4-(N-benzylheptanamido)-2-(benzyloxy)benzoyl)-L-lysinate; peptidomimetic 7 (**59**)*

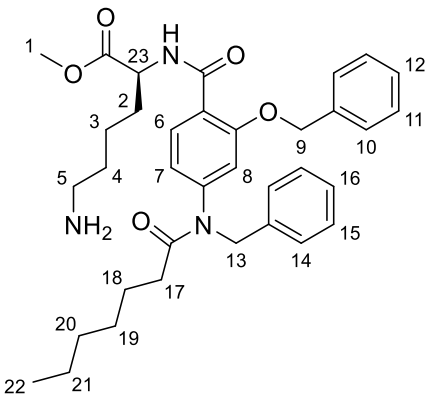

Compound **58** (0.52 g, 0.75 mmol) was stirred in 4N HCl in dioxane (3 mL) for 4 hours. The solvent was removed *in vacuo*. (0.50 g, 0.74 mmol, 98%). $\mathbf{R_f}$ = 0.23 (9:1/EtOAc:MeOH). **^{1}H-NMR:** (400 MHz, MeOD) δ_H: 0.85 (t, 3H, J= 6.5 Hz, H-22), 1.14-1.34 (m, 8H, H-3, H-19, H-20, H-21), 1.48-1.59 (m, 2H, H-18), 1.70-1.78 (m, 2H, H-4), 1.64-1.82 (m, 2H, H-2), 2.15 (t, 2H, J= 7.5 Hz, H-17), 2.94 (m, 2H, H-5), 3.64 (s, 3H, H-1), 4.48 (m, 1H, H-23), 5.21 (s, 1H, H-9), 5.22 (s, 2H, H-13), 6.83 (d, 1H, J= 8.0 Hz, H-7), 7.11 (s, 1H, H-8), 7.18-7.56 (m, 10H, H-10, H-11, H-12, H-14, H-15, H-16), 8.00 (d, 1H J=8.0 Hz, H-6). **^{13}C-NMR** (125 MHz, MeOD): 14.33 ($CH_2CH_2CH_2CH_3$), 22.13 ($NH_2CH_2CH_2$), 22.44 ($CH_2CH_2CH_3$), 25.13 ($COCH_2CH_2$), 28.53 ($NH_2CH_2CH_2CH_2$), 28.86 ($CH_2CH_2CH_2CH_3$), 30.53 (CH_2CH), 32.05 ($COCH_2CH_2CH_2$), 35.30 ($COCH_2$), 39.56 ($NHCH_2$), 52.45 ($COOCH_3$), 52.51 (NCH_2), 53.28 (CH_2CH), 72.26 (OCH_2), 106.17 ($CNHCH$), 113.56 (COC), 114.62 ($CCHCH$), 128.05 ($CCHCHCH$), 129.21 (CCH), 129.25 ($CHCHCH$), 129.28 ($CCHCHCH$), 129.80 ($CCHCHCH$), 129.86 ($CHCHCH$), 133.16 (CCH), 136.63 (CH_2C), 137.37 (CH_2C), 147.13 ($CHCNH$), 163.23 ($CONHCH$), 163.24 ($CHCO$), 172.51 (NCO), 173.05 ($COOCH_3$). **LRMS** *m/z* (ESI): 588.5 $[M+H]^+$. **HRMS** *m/z* (ESI): calculated for $C_{35}H_{46}N_3O_5^+$ $[M+H]^+$: Exact Mass: 588.3432 found 588.3436.

*2-(Benzyloxy)-4-heptanamidobenzoic acid (**60**)*

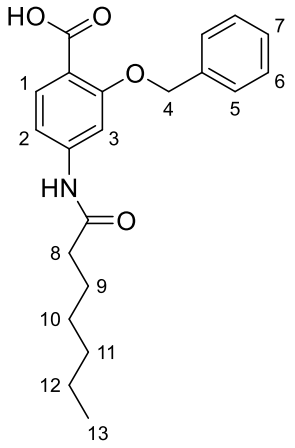

Compounds **55** (0.80 g, 2.2 mmol) was dissolved in EtOH (5 mL), water (4 mL) and 6M NaOH (1 mL) was added and refluxed for 5 hours. After removing EtOH *in vacuo* the solution was acidified to pH 4 using HCl and the precipitate was collected by filtration. (0.78 g, 2.2 mmol, 96%). $\mathbf{R_f}$ = 0.54 (EtOAc). **^{1}H-NMR:** (400 MHz, MeOD) δ_H: 0.90 (t, 3H, J= 6.5 Hz, H-13), 1.26-1.44 (m, 6H, H-10, H-11, H-12), 1.62-1.74 (m, 2H, H-9), 2.38 (t, 2H, J= 7.5, H-8), 5.22 (s, 1H, H-4), 7.10 (d, 1H, J= 8.5 Hz, H-2), 7.26-7.54 (m, 5H, H-5, H-6, H-7), 7.71 (d, 1H, J= 7.5 Hz, H-1), 7.80 (s, 1H, H-3). **^{13}C-NMR** (125 MHz, $(CD_3)_2CO$): 14.49 ($CH_2\mathit{C}H_2CH_2\mathit{C}H_3$), 23.53 ($\mathit{C}H_2CH_2CH_3$), 26.07 ($COCH_2\mathit{C}H_2$), 30.01 ($\mathit{C}H_2CH_2CH_2CH_3$), 32.73 ($COCH_2CH_2\mathit{C}H_2$), 38.16 ($CO\mathit{C}H_2$), 71.82 ($O\mathit{C}H_2$), 112.21 ($CCH\mathit{C}H$), 115.51 ($CO\mathit{C}$), 128.51 ($C\mathit{C}HCHCH$), 129.02 ($CCHCH\mathit{C}H$), 129.56 ($CCH\mathit{C}HCH$), 133.99 ($C\mathit{C}H$), 138.10 ($CH_2\mathit{C}$), 145.66 ($CH\mathit{C}NH$), 145.84 ($CNH\mathit{C}H$), 163.25 ($CH\mathit{C}O$), 163.75 ($\mathit{C}OOH$), 172.60 (NHCO). **LRMS** *m/z* (ESI): 354.1 $[M-H]^-$. **HRMS** *m/z* (ESI): calculated for $C_{21}H_{24}NO_4^-[M-H]^-$: Exact Mass: 354.1711 found 354.1709.

*Methyl-N-2-(2-(benzyloxy)-4-heptanamidobenzoyl)-N6-(tert-butoxycarbonyl)-L-lysinate (**61**)*

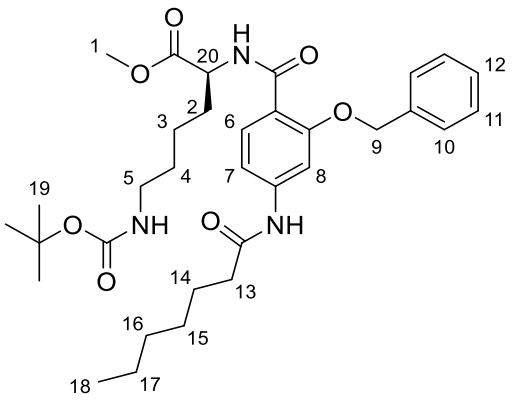

Compound **60** (0.40 g, 0.67 mmol, 1 eq), EDC.HCl (0.15 g, 0.80 mmol , 1.2 eq), HOBt (0.1 g, 0.80 mmol, 1.2 eq) and DIPEA (0.22 mL, 0.17 g, 1.3 mmol, 2 eq) were stirred in DCM (10 mL) for 15 minutes. H-Lys(Boc)-OMe hydrochloride (0.23 g, 0.80 mmol , 1.2 eq) was added and the reaction was stirred for 18 hours. DCM (40 mL) was added and washed 3 times with Na_2CO_3 *sat.* (75 mL). The organic layer was dried with $MgSO_4$ and dried under high vacuum. Silica column chromatography was carried out and the product was eluted with 2:4/EtOAc:petroleum ether. (0.18 g, 0.30 mmol, 45%). **R_f =** 0.49 (2:4/EtOAc:petroleum ether). **^{1}H-NMR:** (400 MHz, MeOD) δ_H: 0.88 (t, 3H, J= 6.5 Hz, H-18), 1.20-1.37 (m, 8H, H-4, H-15, H-16, H-17), 1.38 (s, 9H, H-19), 1.48-1.54 (m, 2H, H-18), 1.62-1.82 (m, 4H, H-4, H-2), 2.41 (t, 2H, J= 7.5 Hz, H-17), 2.97 (m, 2H, H-5), 3.63 (s, 3H, H-1), 4.44 (m, 1H, H-20) 5.25 (s, 1H, H-9), 7.15-7.57 (m, 5H, H-10, H-11, H-12,), 7.63 (d, 1H, J= 8.0 Hz, H-7), 7.93 (s, 1H, H-8), 8.01 (d, 1H J=8.0 Hz, H-6). **^{13}C-NMR** (125 MHz, MeOD): 13.00 ($CH_2CH_2CH_2CH_3$), 23.21 ($CH_2CH_2CH_3$), 23.54 ($NHCH_2CH_2$), 24.46 ($COCH_2CH_2$), 26.06 ($CH_2CH_2CH_2CH_3$), 28.68 ($3CH_3$), 32.05 ($COCH_2CH_2CH_2$), 32.37 ($NHCH_2CH_2CH_2$), 32.51 (CH_2CH), 37.86 ($NHCOCH_2$), 40.80 ($NHCH_2$), 52.20 ($COOCH_3$), 53.37 (CH_2CH), 71.23 (OCH_2), 71.93 (COCO), 104.12 (CNHCH), 112.08 (COC), 113.56 (CCHCH), 129.54 (CCHCHCH), 129.64 (CCHCHCH), 129.67 (CCHCHCH), 136.86 (CCH), 137.19 (CH_2C), 144.87 (CHCNH), 158.46 (COCONH), 158.62 (CONHCH), 163.25 (CHCO),

173.39 (*C*OOCH$_3$), 172.66 (NH*C*O). **LRMS** *m/z* (ESI): 620.5 $[M+Na]^+$. **HRMS** *m/z* (ESI): calculated for $C_{33}H_{47}N_3NaO_7^+$ $[M+Na]^-$: Exact Mass: 620.3306 found 620.3308.

*Methyl (2-(benzyloxy)-4-heptanamidobenzoyl)-L-lysinate; peptidomimetic 5 (**62**)*

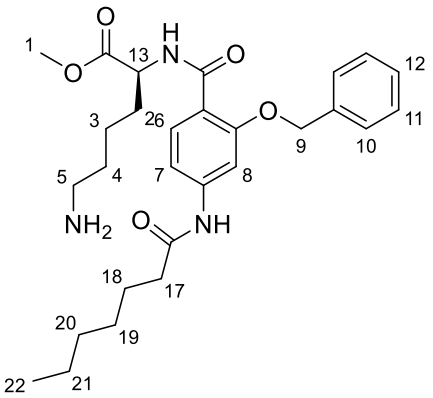

Compound **61** (0.18 g, 0.30 mmol) was stirred in 4N HCl in dioxane (3 mL) for 4 hours. The solvent was removed *in vacuo*. (0.14 g, 0.28 mmol, 93%). $\mathbf{R_f}$ = 0.23 (9:1/EtOAc:MeOH). **^{1}H-NMR:** (400 MHz, MeOD) δ_H: 0.92 (t, 3H, J= 6.5 Hz, H-22), 1.23-1.41 (m, 8H, H-4, H-19, H-20, H-21), 1.45-1.57 (m, 2H, H-18), 1.60-1.80 (m, 2H, H-2), 2.41 (t, 2H, J= 7.5 Hz, H-17), 2.78 (m, 2H, H-5), 3.69 (s, 3H, H-1), 4.47 (m, 1H, H-13), 5.26 (s, 1H, H-9), 7.15-7.48 (m, 5H, H-10, H-11, H-12,), 7.58 (d, 1H, J= 8.0 Hz, H-7), 7.87 (s, 1H, H-8), 7.94 (d, 1H J=8.0 Hz, H-6). **^{13}C-NMR** (125 MHz, MeOD): 14.39 ($CH_2CH_2CH_2CH_3$), 23.51 ($CH_2CH_2CH_3$), 23.60 ($NH_2CH_2CH_2$), 26.72 ($COCH_2CH_2$), 26.72 ($CH_2CH_2CH_2CH_3$), 30.02 ($COCH_2CH_2CH_2$), 32.42 (CH_2CH), 32.74 ($NH_2CH_2CH_2CH_2$), 38.17 ($NHCOCH_2$), 40.43 (NH_2CH_2), 52.87 ($COOCH_3$), 53.64 (CH_2CH), 72.57 (OCH_2), 105.10 ($CNHCH$), 112.08 (COC), 113.56 ($CCHCH$), 129.54 ($CCHCHCH$), 129.64 ($CCHCHCH$), 129.67 ($CCHCHCH$), 137.19 (CH_2C), 137.22 (CCH), 144.87 ($CHCNH$), 158.62 ($CONHCH$), 163.75 ($CHCO$), 172.66 ($NHCO$), 175.16 ($COOCH_3$). **LRMS** *m/z* (ESI): 498.2 $[M+H]^+$. **HRMS** *m/z* (ESI): calculated for $C_{28}H_{40}N_3O_5^+$ $[M+H]^+$: Exact Mass: 498.2962 found 498.2964.

*Methyl 2-(2-(1H-indol-3-yl)ethoxy)-4-heptanamidobenzoate (**63**)*

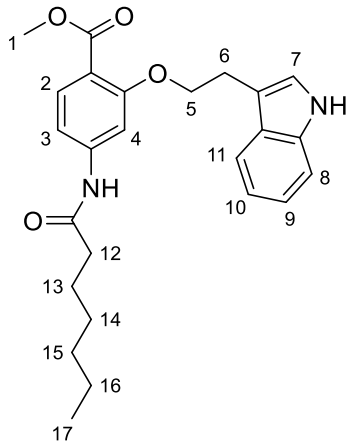

Compound **40** (1.0 g, 2.8 mmol, 1 eq) and DIPEA (0.92 mL, 0.72 g, 5.6 mmol, 2 eq) were stirred in DCM (10 mL) at 0 °C. Heptanoyl chloride (0.46 mL, 0.45 g, 3.1 mmol, 1.1 eq) was then added dropwise over 15 minutes. The reaction was stirred for a further 30 minutes at 0 °C before the solvent was removed *in vacuo*. The resulting oil was purified using silica column chromatography and the product was eluted with 1:4/EtOAc:petroleum ether. (0.80 g, 1.9 mmol, 67%). $\mathbf{R_f}$ = 0.39 (1:4/EtOAc:petroleum ether). **^{1}H-NMR:** (400 MHz, $(CD_3)_2CO$) δ_H: 0.85 (t, 3H, J= 6.5 Hz, H-17), 1.22-1.40 (m, 6H, H-14, H-15, H-16), 1.59-1.72 (m, 2H, H-13), 2.37 (t, 2H, J= 7.5 Hz, H-12), 3.27 (t, 2H, J=7.0 Hz, H-6), 3.80 (s, 3H, H-1), 4.25 (t, 2H, J=7.0 Hz, H-5), 7.06 (dt, 2H, J= 7.0, 10.5 Hz, H-9, H-10), 7.36-7.41 (m, 2H, H-7, H-8), 7.65-7.74 (m, 3H, H-2, H-4, H-11). **^{13}C-NMR** (125 MHz, $(CD_3)_2CO$): 14.32 ($CH_2CH_2CH_2CH_3$), 25.63 ($CH_2CH_2CH_3$), 25.81 ($COCH_2CH_2$), 26.03 (CH_2CH_2), 29.34 ($CH_2CH_2CH_2CH_3$), 32.34 ($COCH_2CH_2CH_2$), 37.86 ($COCH_2$), 51.71 (CH_3O), 70.01 ($COCH_2$), 104.44 (CNHCH), 107.62 (CH_2C), 110.92 (NHCCH), 112.13 (CCHCH), 115.58 (COCCH), 119.28 (CHCHC), 119.51 (CHCHCH), 122.05 (CCHCH), 123.48 (CCH), 128.62 (CHC), 133.17 (CCHCH), 137.54 (NHC), 145.35 (CHCNH), 166.66 (OCO), 160.42 ($COCH_2$), 172.61 (NHCO). **LRMS** *m/z* (ESI): 445.3 $[M+Na]^+$. **HRMS** *m/z* (ESI): calculated for $C_{25}H_{30}N_2NaO_4^+$ $[M+Na]^+$: Exact Mass: 445.2098 found 445.2098.

2-(2-(1H-indol-3-yl)ethoxy)-4-heptanamidobenzoic acid (**64**)

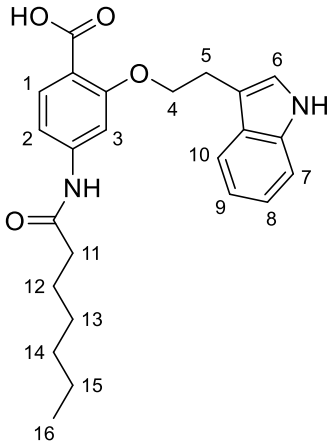

63 (0.80 g, 1.9 mmol) was dissolved in EtOH (5 mL), water (4 mL) and 6M NaOH (1 mL) was added and refluxed for 5 hours. After removing EtOH *in vacuo* the solution was acidified to pH 4 using HCl and the precipitate was collected by filtration. (0.76 g, 1.9 mmol, 97%). $\mathbf{R_f}$ = 0.49 (EtOAc). **^{1}H-NMR:** (500 MHz, $(CD_3)_2CO$) δ_H: 0.85 (t, 3H, J= 6.5 Hz, H-16), 1.22-1.40 (m, 6H, H-13, H-14, H-15), 1.59-1.72 (m, 2H, H-12), 2.39 (t, 2H, J= 7.5 Hz, H-11), 3.39 (t, 2H, J=7.0 Hz, H-5), 4.52 (t, 2H, J=7.0 Hz, H-4), 7.07 (dt, 2H, J= 7.0, 15.5 Hz, H-8, H-9), 7.36-7.41 (m, 2H, H-6, H-7), 7.65-7.74 (m, 3H, H-1, H-3, H-10). **^{13}C-NMR** (125 MHz, $(CD_3)_2CO$): 164.53 (*C*OOH), 115.58 (CO*C*CH), 133.34 (C*C*HCH), 102.98 (CCH*C*H), 145.19 (CH*C*NH), 96.98 (CNH*C*H), 158.75 (*C*OCH_2), 69.57 (CO*C*H$_2$), 25.06 (CH_2*C*H$_2$), 110.31 (CH_2*C*), 123.48 (C*C*H), 137.54 (NH*C*), 110.92 (NHC*C*H), 121.39(CCH*C*H), 118.76 (CHCH*C*H), 118.28 (CH*C*HC), 128.62 (CH*C*), 171.80 (NHCO), 36.89 (CO*C*H$_2$), 25.81 (COCH$_2$*C*H$_2$), 31.44 (COCH$_2$CH$_2$*C*H$_2$), 29.34 (*C*H$_2$CH$_2$CH$_2$CH$_3$), 22.29 (*C*H$_2$CH$_2$CH$_3$), 13.41 (CH$_2$*C*H$_2$CH$_2$*C*H$_3$). **LRMS** m/z (ESI): 407.2 $[M-H]^-$. **HRMS** m/z (ESI): calculated for $C_{24}H_{27}N_2O_4^-$ $[M+H]^-$: Exact Mass: 407.1976 found 407.1981.

*Methyl-N-2-(2-(2-(1H-indol-3-yl)ethoxy)-4-heptanamidobenzoyl)-N6-(tert-butoxycarbonyl)-L-lysinate (**65**)*

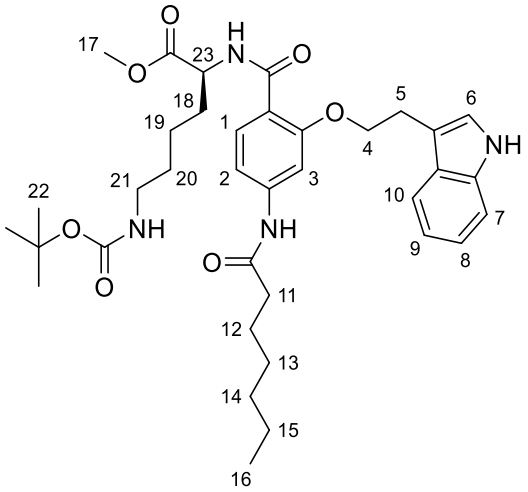

Compound **64** (0.50 g, 1.2 mmol, 1 eq), EDC.HCl (0.26 g, 1.4 mmol , 1.2 eq), HOBt (0.19 g, 1.4 mmol, 1.2 eq) and DIPEA (0.40 mL, 0.30 g, 2.4 mmol, 2 eq) were stirred in DCM (10 mL) for 15 minutes. H-Lys(Boc)-OMe hydrochloride (0.41 g, 1.4 mmol , 1.2 eq) was added and the reaction was stirred for 18 hours. DCM (40 mL) was added and washed 3 times with Na_2CO_3 *sat.* (75 mL). The organic layer was dried with $MgSO_4$ and dried under high vacuum. Silica column chromatography was carried out and the product was eluted with 1:4/EtOAc:petroleum ether. (0.47 g, 0.7 mmol, 58%). **R_f =** 0.51 (1:4/EtOAc:petroleum ether). **^{1}H-NMR:** (500 MHz, $(CD_3)_2CO$) δ_H: 0.88 (t, 3H, J= 6.5 Hz, H-16), 1.18-1.42 (m, 8H, H-19, H-13, H-14, H-15), 1.38 (s, 9H, H-22), 1.43-1.54 (m, 2H, H-12), 1.62-1.74 (m, 4H, H-18, H-20), 2.41 (t, 2H, J= 7.5 Hz, H-11), 2.55 (t, 2H, J= 7.5 Hz, H-21), 3.44 (t, 2H, J=7.0 Hz, H-5), 3.69 (s, 3H, H-1), 4.49 (t, 2H, J=7.0 Hz, H-4), 4.59 (m, 1H, H-23), 7.08 (dt, 2H, J= 7.0, 15.5 Hz, H-8, H-9), 7.21 (d, 1H, J=8.5 Hz, H-7), 7.33 (s, 1H, H-6), 7.41 (d, 1H J=8.0 Hz, H-2), 7.63 (d, 1H, J= 8.0 Hz, H-10), 7.84 (s, 1H, H-3), 8.01 (d, 1H, J= 8.0 Hz, H-1). **^{13}C-NMR** (125 MHz, $(CD_3)_2CO$): 14.32 ($CH_2CH_2CH_2CH_3$), 21.35 ($CH_2CH_2CH_3$), 22.09 ($NHCH_2CH_2$), 25.06 (CH_2CH_2), 25.29 ($COCH_2CH_2$), 26.51 ($CH_2CH_2CH_2CH_3$), 28.61 ($COCH_2CH_2CH_2$), 28.68 ($3CH_3$), 30.65 (CH_2CH), 31.32 ($NHCH_2CH_2CH_2$), 37.84 ($COCH_2$), 40.87 ($NHCH_2$), 52.32 (CH_2CH), 53.31 ($COOCH_3$), 68.76 ($COCH_2$), 71.93 (COCO), 103.80 (CNHCH), 110.42 (CH_2C), 111.81 (CCHCH), 112.01 (NHCCH),

112.08 (CO*C*), 115.19 (CO*C*CH), 118.24 (CH*C*HC), 118.63 (CHCH*C*H), 122.13 (C*C*H), 122.19 (CCH*C*H), 127.38 (CH*C*), 133.27 (C*C*HCH), 136.76 (NH*C*), 145.19 (CH*C*NH), 157.96 (*C*OCH$_2$), 163.23 (CO*C*ONH), 164.85 (*C*ONHCH), 172.63 (*C*OOCH$_3$), 173.63 (NH*C*O). **LRMS** *m/z* (ESI): 673.5 $[M+Na]^+$. **HRMS** *m/z* (ESI): calculated for $C_{36}H_{50}N_4NaO_7^+$ $[M+Na]^+$: Exact Mass: 673.3572 found 673.3576.

*Methyl (2-(2-(1H-indol-3-yl)ethoxy)-4-heptanamidobenzoyl)-L-lysinate; peptidomimetic 6 (**66**)*

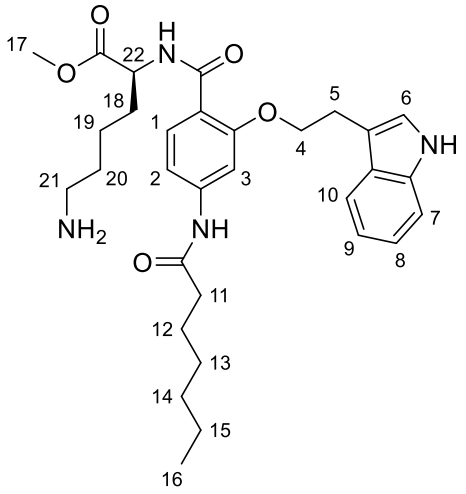

Compound **65** (0.47 g, 0.7 mmol,) was stirred in 4N HCl in dioxane (3 mL) for 4 hours. The solvent was removed *in vacuo*. (0.38 g, 0.7 mmol, 99%). $\mathbf{R_f}$ = 0.23 (9:1/EtOAc:MeOH). **^{1}H-NMR:** (500 MHz, MeOD) δ_H: 0.90 (t, 3H, J= 6.5 Hz, H-16), 1.20-1.40 (m, 8H, H-19, H-13, H-14, H-15), 1.43-1.54 (m, 2H, H-18), 1.64-1.73 (m, 4H, H-20), 2.39 (t, 2H, J= 7.5 Hz, H-11), 2.55 (t, 2H, J= 7.5 Hz, H-21), 3.38 (t, 2H, J=7.0 Hz, H-5), 3.69 (s, 3H, H-17), 4.48 (t, 2H, J=7.0 Hz, H-4), 4.56 (m, 1H, H-22) 7.08 (m, 3H, H-6, H-8, H-9), 7.34 (d, 1H J=7.0 Hz, H-2), 7.57 (d, 1H, J= 8.0 Hz, H-10), 7.78 (s, 1H, H-7), 7.94 (d, 1H, J= 8.0 Hz, H-1). **^{13}C-NMR** (125 MHz, MeOD): 12.97 ($CH_2CH_2CH_2CH_3$), 22.09 ($NHCH_2CH_2$), 22.18 ($CH_2CH_2CH_3$), 25.06 (CH_2CH_2), 25.29 ($COCH_2CH_2$), 26.51 ($CH_2CH_2CH_2CH_3$), 28.61 ($COCH_2CH_2CH_2$), 30.65 (CH_2CH), 31.32 ($NHCH_2CH_2CH_2$), 36.75 ($COCH_2$), 46.51 ($NHCH_2$), 51.50 ($COOCH_3$), 52.22 (CH_2CH), 68.57 ($COCH_2$), 103.33 ($CNHCH$), 110.42 (CH_2C111.01 ($NHCCH$), 111.33 ($CCHCH$),), 112.08 (COC), 115.19 ($COCCH$), 117.86 ($CHCHC$), 118.45 ($CHCHCH$), 121.21 ($CCHCH$), 122.13 (CCH), 127.38 (CHC), 131.81 ($CCHCH$), 136.76 (NHC), 145.19 ($CHCNH$), 157.96 ($COCH_2$), 165.69 ($CONHCH$), 172.40 ($COOCH_3$), 173.80 ($NHCO$). **LRMS** *m/z* (ESI): 551.4 $[M+H]^+$. **HRMS** *m/z* (ESI): calculated for $C_{36}H_{50}N_4NaO_7^+$ $[M+H]^+$: Exact Mass: 551.3228 found 551.3222.

*tert-Butyl 3-(2-(2-(methoxycarbonyl)-5-nitrophenoxy)ethyl)-1H-indole-1-carboxylate (**67**)*

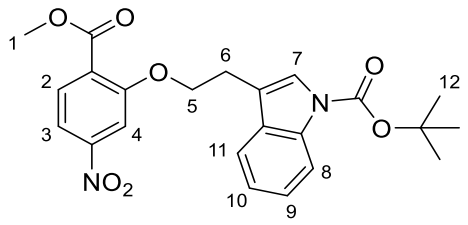

Compound **39** (1.5 g, 7.6 mmol, 1 eq), **49** (2.8 g, 8.3 mmol, 1.1 eq), K_2CO_3 (2.8 g, 15.2 mmol, 2 eq) were stirred in DMF (8 mL) at 50°C for 20 hours. The reaction mixture was taken up in EtOAc (75 mL) and washed 3 times with Na_2CO_3 *sat.* (75 mL). The organic layer was dried with $MgSO_4$ and dried under high vacuum. The resulting residue was applied to a silica column and the product was eluted with 20:80 EtOAc/Petroleum ether. (2.5 g, 5.8 mmol, 81%). $\mathbf{R_f}$ = 0.69 (3:7/EtOAc:petroleum ether). **^{1}H-NMR:** (400 MHz, $(CD_3)_2CO$) δ_H: 1.67 (s, 9H, H-12), 3.28 (t, 2H, J=6.5 Hz, H-6), 3.89 (s, 3H, H-1), 4.55 (t, 2H, J=6.5 Hz, H-5), 7.29 (dt, 2H, J= 7.0, 15.5 Hz, H-8, H-9), 7.62-7.77 (m, 2H, H-8, H-11), 7.86-7.89 (m, 2H, H-3, H-7), 7.95 (s, 1H, H-4), 8.14 (d, 1H, J= 8.0 Hz, H-2). **^{13}C-NMR** (125 MHz, $(CD_3)_2CO$): 24.50 ($CH_2\mathit{C}H_2$), 28.27 ($3\mathit{C}H_3$), 51.57 ($\mathit{C}H_3O$), 69.79 ($CO\mathit{C}H_2$), 75.03 ($\mathit{C}OCO$), 107.59 ($NC\mathit{C}H$), 110.57 ($CH_2\mathit{C}$), 110.83 ($CNO_2\mathit{C}H$), 112.86 ($C\mathit{C}H$), 114.30 ($CCH\mathit{C}H$), 117.84 ($CH\mathit{C}HC$), 118.32 ($CHCH\mathit{C}H$), 120.92 ($CCH\mathit{C}H$), 126.25 ($CO\mathit{C}CH$), 127.38 ($CH\mathit{C}$), 131.19 ($C\mathit{C}HCH$), 136.52 ($N\mathit{C}$), 150.50 ($CH\mathit{C}NO_2$), 158.20 ($\mathit{C}OCH_2$), 165.85 ($O\mathit{C}O$), 168.78 ($CO\mathit{C}ONC$).

*tert-Butyl 3-(2-(5-amino-2-(methoxycarbonyl)phenoxy)ethyl)-1H-indole-1-carboxylate (**68**)*

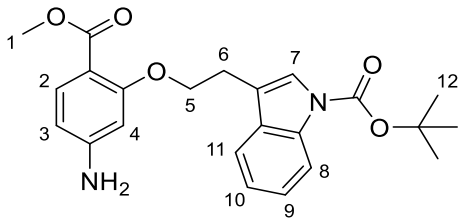

Compound **67** (2.5 g, 5.8 mmol, mmol, 1 eq), Fe (3 g) and NH_4Cl (3 g) were stirred in 1:1 EtOH and water (10 mL) for 4 hours at 100 °C and then filtered through Celite. Solvent was removed under high vacuum. (2.3 g, 5.4 mmol, 93%). $\mathbf{R_f}$ = 0.33 (1:1/EtOAc:petroleum ether). **^{1}H-NMR:** (400 MHz, $(CD_3)_2CO$) δ_H: 1.68 (s, 9H, H-12), 3.24 (t, 2H, J=7.0 Hz, H-6), 3.74 (s, 3H, H-1), 4.38 (t, 2H, J=7.0 Hz, H-5), 6.24-6.28 (m, 1H, H-3), 6.37 (s, 1H, H-4), 7.02 (t, 1H, J=7.4 Hz, H-10), 7.09 (t, 1H, J=7.5 Hz, H-9), 7.32-7.42 (m, 2H, H-7, H-2), 7.59-7.67 (m, 2H, H-8, H-11). **^{13}C-NMR** (125 MHz, $(CD_3)_2CO$): 25.01 ($CH_2\mathit{C}H_2$), 28.70 ($3\mathit{C}H_3$), 50.22 ($\mathit{C}H_3O$), 68.87 ($CO\mathit{C}H_2$), 72.32 ($\mathit{C}OCO$), 98.10 ($CNH_2\mathit{C}H$), 105.75 ($CCH\mathit{C}H$), 107.62 ($CH_2\mathit{C}$), 111.27 ($NHC\mathit{C}H$), 111.34 ($CO\mathit{C}CH$), 118.35 ($CH\mathit{C}HC$), 118.55 ($CHCH\mathit{C}H$), 121.09 ($CCH\mathit{C}H$), 123.48 ($C\mathit{C}H$), 127.72 ($CH\mathit{C}$), 133.70 ($C\mathit{C}HCH$), 136.40 ($NH\mathit{C}$), 154.16 ($CH\mathit{C}NH_2$), 161.19 ($\mathit{C}OCH_2$), 165.88 ($O\mathit{C}O$), 168.81 ($CO\mathit{C}ONC$). **LRMS** *m/z* (ESI): 433.2 $[M+Na]^+$. **HRMS** *m/z* (ESI): calculated for $C_{23}H_{26}N_2NaO_5^+$ $[M+Na]^+$: Exact Mass: 433.1734 found 433.1734.

*tert-Butyl 3-(2-(5-heptanamido-2-(methoxycarbonyl)phenoxy)ethyl)-1H-indole-1-carboxylate (**69**)*

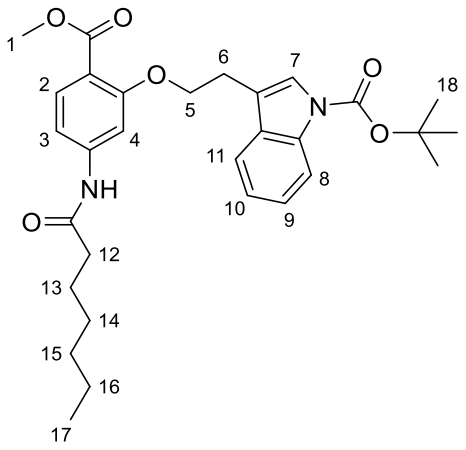

Compound **68** (2.3 g, 5.4 mmol, 1 eq) and DIPEA (1.78 mL, 1.4 g, 10.8 mmol, 2 eq) were stirred in DCM (10 mL) at 0 °C. Heptanoyl chloride (0.89 mL, 0.87 g, 5.9 mmol, 1.1 eq) was then added dropwise over 15 minutes. The reaction was stirred for a further 30 minutes at 0 °C before the solvent was removed *in vacuo*. The resulting oil was purified using silica column chromatography and the product was eluted with 1:4/EtOAc:petroleum ether. (1.82 g, 3.3 mmol, 62%). $\mathbf{R_f}$ = 0.39 (1:4/EtOAc:petroleum ether). **^{1}H-NMR:** (400 MHz, $(CD_3)_2CO$) δ_H: 0.85 (t, 3H, J= 6.5 Hz, H-17), 1.21-1.39 (m, 6H, H-14, H-15, H-16), 1.59-1.64 (m, 2H, H-13), 1.66 (s, 9H, H-18) 2.36 (t, 2H, J= 7.5 Hz, H-12), 3.21 (t, 2H, J=7.0 Hz, H-6), 3.79 (s, 3H, H-1), 4.29 (t, 2H, J=7.0 Hz, H-5), 7.21-7.36 (m, 3H, H-3, H-9, H-10), 7.65-7.77 (m, 4H, H-4, H-7, H-8, H-11). 8.14 (d, 1H, J= 8.0 Hz, H-2). **^{13}C-NMR** (125 MHz, $(CD_3)_2CO$): 14.34 ($CH_2CH_2CH_2CH_2CH_3$), 25.37 ($CH_2CH_2CH_2CH_3$), 26.03 (CH_2CH_2), 28.31 ($3CH_3$), 29.36 ($CH_2CH_2CH_2CH_2CH_3$), 29.62 ($COCH_2CH_2$), 32.35 ($COCH_2CH_2CH_2$), 37.87 ($COCH_2$), 51.79 (CH_3O), 69.00 ($COCH_2$), 84.07 ($COCO$), 104.52 ($CNHCH$), 111.14 ($NCCH$), 115.14 ($CCHCH$), 115.52 (CH_2C), 118.04 ($CHCHC$), 118.14 ($COCCH$), 119.96 ($CHCHCH$), 123.37 ($CCHCH$), 125.14 (CCH), 131.53 (CHC), 133.17 ($CCHCH$), 136.30 (NC), 145.38 ($CHCNH$), 150.38 ($COCH_2$), 160.62 (OCO), 166.59 ($COCONC$), 172.62 (NHCO). **LRMS** m/z (ESI): 545.2 $[M+Na]^+$. **HRMS** m/z (ESI): calculated for $C_{23}H_{26}N_2NaO_5^+$ $[M+H]^+$: Exact Mass: 545.2617found 545.2619.

*tert-Butyl 3-(2-(5-(N-benzylheptanamido)-2-(methoxycarbonyl)phenoxy)ethyl)-1H-indole-1-carboxylate (**70**)*

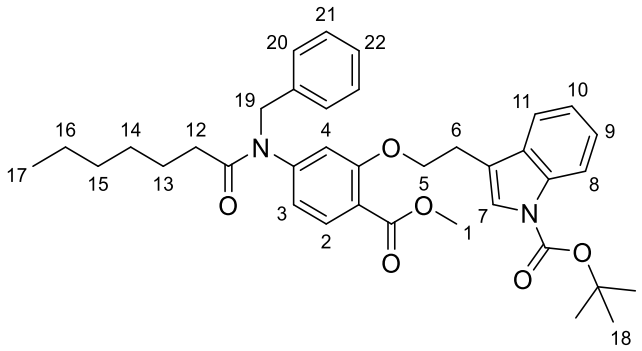

Compound **69** (0.70 g, 1.3 mmol, 1 eq) and potassium tert-butoxide (0.29 g, 2.6 mmol, 2 eq) were stirred in dry THF (10 mL) for 0.5 hours. Benzyl bromide (0.17 mL, 0.24 g, 1.4 mmol, 1.1 eq) was then added dropwise and the reaction stirred for 18 hours. The solvent was removed *in vacuo*. The reaction mixture was taken up in EtOAc (75 mL) and washed 3 times with water (75 mL). The organic layer was dried with $MgSO_4$ and dried under high vacuum. Silica column chromatography was carried out and the product was eluted with 1:9/EtOAc:petroleum ether. (0.5 g, 0.8 mmol, 67%) $\mathbf{R_f}$ = 0.34 (1:9/EtOAc:petroleum ether). **^{1}H-NMR:** (400 MHz, $(CD_3)_2CO$) δ_H: 0.81 (t, 3H, J= 6.5 Hz, H-17), 1.11-1.25 (m, 6H, H-14, H-15, H-16), 1.50-1.61 (m, 2H, H-13), 1.67 (s, 9H, H-18) 2.16 (t, 2H, J= 7.5 Hz, H-12), 3.14 (t, 2H, J=7.0 Hz, H-6), 3.49 (s, 3H, H-1), 4.24 (t, 2H, J=7.0 Hz, H-5), 5.31 (s, 2H, H-19), 6.73-7.75 (m, 12H, H-2, H-3, H-7, H-8, H-9, H-10, H-11, H-20, H-21, H-22), 8.14 (d, 1H, J= 8.0 Hz, H-2), 8.13 (d, 1H, J= 8.0 Hz, H-3). **^{13}C-NMR** (125 MHz, $(CD_3)_2CO$): 13.47 ($CH_2CH_2CH_2CH_3$), 20.46 ($CH_2CH_2CH_3$), 26.03 (CH_2CH_2), 28.31 ($3CH_3$), 28.50 ($CH_2CH_2CH_2CH_3$), 31.44 ($COCH_2CH_2$), 33.96 ($COCH_2CH_2CH_2$), 40.93 ($COCH_2$), 51.29 (CH_3O), 51.94 ($NCOCH_2$), 69.24 ($COCH_2$), 83.28 (COCO), 110.46 (Ar-*C*), 110.79 (Ar-*C*H), 113.86 (Ar-*C*H), 115.04 (Ar-*C*H), 117.02 (Ar-*C*), 118.83 (Ar-*C*H), 119.96 (Ar-*C*H), 122.39 (Ar-*C*H), 124.26 (Ar-*C*H), 128.26 (Ar-*C*H), 128.32 (Ar-*C*H), 128.45 (Ar-*C*H), 132.03 (Ar-*C*H), 136.61 (Ar-*C*), 138.21 (Ar-*C*), 138.21 (Ar-*C*), 145.38 (CH*C*N), 150.38 ($COCH_2$), 160.62 (O*C*O), 166.59 (CO*C*ONC), 172.62 (N*C*O). **LRMS** *m/z* (ESI):

636.5 $[M+Na]^+$. **HRMS** (ESI): calculated for $C_{37}H_{45}N_2NaO_6^+$ $[M+Na]^+$: Exact Mass: 636.3092 found 636.3079.

*2-(2-(1H-Indol-3-yl)ethoxy)-4-(N-benzylheptanamido)benzoic acid (**71**)*

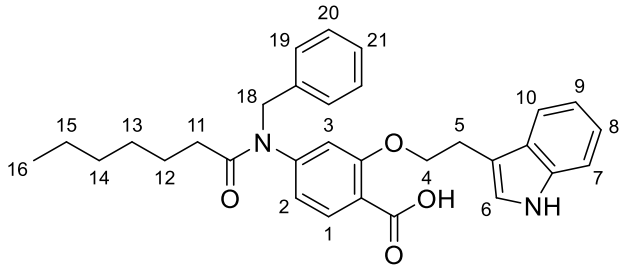

Compound **70** (0.5 g, 0.8 mmol) was dissolved in EtOH (5 mL), water (4 mL) and 6M NaOH (0.5 mL) was added and refluxed for 5 hours. After removing EtOH *in vacuo* the solution was acidified to pH 4 using HCl and the precipitate was collected by filtration. (0.42 g, 1.9 mmol, 95%). $\mathbf{R_f}$ = 0.58 (EtOAc). **^{1}H-NMR:** (400 MHz, $(CD_3)_2CO$) δ_H: 0.82 (t, 3H, J= 6.5 Hz, H-16), 1.08-1.28 (m, 6H, H-13, H-14, H-15), 1.55-1.62 (m, 2H, H-12), 2.19 (t, 2H, J= 7.5 Hz, H-11), 3.26 (t, 2H, J=7.0 Hz, H-4), 4.36 (t, 2H, J=7.0 Hz, H-5), 5.37 (s, 2H, H-19), 6.82-7.63 (m, 12H, H-2, H-3, H-7, H-8, H-9, H-10, H-11, H-20, H-21, H-22), 8.14 (d, 1H, J= 8.0 Hz, H-2), 7.87 (d, 1H, J= 8.0 Hz, H-2). **^{13}C-NMR** (125 MHz, $(CD_3)_2CO$): 13.47 ($CH_2CH_2CH_2CH_3$), 22.36 ($CH_2CH_2CH_3$), 25.32 (CH_2CH_2), 26.21($CH_2CH_2CH_2CH_3$), 27.38 ($COCH_2CH_2CH_2$), 31.71 ($COCH_2CH_2$), 34.06 ($COCH_2$), 52.11 ($NCOCH_2$), 72.06 ($COCH_2$), 109.98 (Ar-CH), 110.40 (Ar-C), 111.35 (Ar-CH), 115.04 (Ar-CH), 118.31 (Ar-CH), 118.72 (Ar-C), 118.86 (Ar-CH), 121.42 (Ar-CH), 123.21 (Ar-CH), 128.07 (Ar-CH), 128.40 (Ar-CH), 128.54 (Ar-CH), 132.94 (Ar-CH), 136.65 (Ar-C), 138.08 (Ar-C), 138.40 (Ar-C), 147.92 (CHCN), 158.56 ($COCH_2$), 165.02 (COOH), 171.67 (NCO). **LRMS** *m/z* (ESI): 497.2 $[M-H]^-$. **HRMS** *m/z* (ESI): calculated for $C_{31}H_{33}N_2O_4^-$ $[M-H]^-$: Exact Mass: 497.2446 found 497.2440.

*Methyl-N2-(2-(2-(1H-indol-3-yl)ethoxy)-4-(N-benzylheptanamido)benzoyl)-N6-(tert-butoxycarbonyl)-L-lysinate (**72**)*

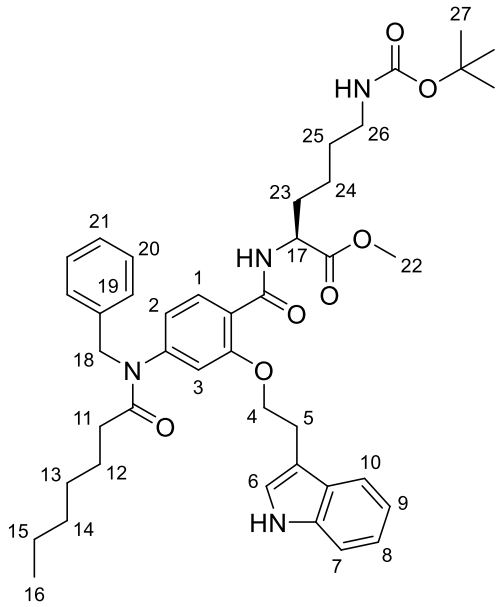

Compound **71** (0.42 g, 1.9 mmol, 1 eq), EDC.HCl (0.43 g, 2.3 mmol , 1.2 eq), HOBt (0.31 g, 2.3 mmol, 1.2 eq) and DIPEA (0.62 mL, 0.49 g, 3.8 mmol, 2 eq) were stirred in DCM (10 mL) for 15 minutes. H-Lys(Boc)-OMe hydrochloride (0.68 g, 2.3 mmol , 1.2 eq) was added and the reaction was stirred for 18 hours. DCM (40 mL) was added and washed 3 times with Na_2CO_3 *sat.* (75 mL). The organic layer was dried with $MgSO_4$ and dried under high vacuum. Silica column chromatography was carried out and the product was eluted with 3:4/EtOAc:petroleum ether. (0.21 g, 0.3 mmol, 15%). **R_f =** 0.56 (3:4/EtOAc:petroleum ether). **^{1}H-NMR:** (400 MHz, $(CD_3)_2CO$) δ_H: 0.83 (t, 3H, J= 6.5 Hz, H-16), 1.20-1.37 (m, 8H, H-24, H-13, H-14, H-15), 1.40 (s, 9H, H-27), 1.48-1.54 (m, 2H, H-12), 1.58-1.75 (m, 4H, H-23, H-25), 2.21 (t, 2H, J= 7.5 Hz, H-11), 2.91 (m, 2H, H-26), 3.25 (t, 2H, J=7.0 Hz, H-4), 3.70 (s, 3H, H-22), 4.33 (t, 2H, J=7.0 Hz, H-5), 4.44 (m, 1H, H-17), 5.37 (s, 2H, H-18), 6.82-7.55 (m, 10H, H-1, H-3, H-7, H-8, H-9, H-10, H-11, H-20, H-21, H-22), 7.88 (d, 1H, J= 8.0 Hz, H-2). **^{13}C-NMR** (125 MHz, $(CD_3)_2CO$): 12.94 ($CH_2CH_2CH_2CH_3$), 22.09 ($NHCH_2CH_2$), 22.42 ($CH_2CH_2CH_3$), 24.42 ($CH_2CH_2CH_2CH_3$), 25.27 (CH_2CH_2), 27.38 ($COCH_2CH_2CH_2$), 27.40 ($3CH_3$), 30.83 (CH_2CH), 31.20 ($NHCH_2CH_2CH_2$), 31.71 ($COCH_2CH_2$), 33.89 ($COCH_2$), 39.58 ($NHCH_2$), 51.40 ($NCOCH_2$), 52.32 (CH_2CH), 52.69 ($COOCH_3$),

71.93 (*C*OCO), 72.06 (CO*C*H_2), 111.02 (Ar-*C*), 111.20 (Ar-*C*H), 113.35 (Ar-*C*H), 117.84 (Ar-*C*H), 118.44 (Ar-*C*H), 120.00 (Ar-*C*H), 121.20 (Ar-763.5*C*H), 122.18 (Ar-*C*H), 127.26 (Ar-*C*H), 127.33 (Ar-*C*H), 128.00 (Ar-*C*H), 128.20 (Ar-*C*), 132.13 (Ar-*C*H), 136.75 (Ar-*C*), 137.20 (Ar-*C*), 138.01 (Ar-*C*), 146.17 (CH*C*N), 157.54 (*C*OCH_2), 164.85 (*C*ONHCH), 165.15 (CO*C*ONH), 171.67 (N*C*O), 172.50 (*C*OOCH_3). **LRMS** *m/z* (ESI): 763.5 $[M+Na]^+$. **HRMS** *m/z* (ESI): calculated for $C_{43}H_{56}N_4NaO_7^+$ $[M+Na]^+$: Exact Mass: 763.4041 found 763.4037.

*Methyl (2-(2-(1H-indol-3-yl)ethoxy)-4-(N benzylheptanamido) benzoyl)-L-lysinate; peptidomimetic 8 (**73**)*

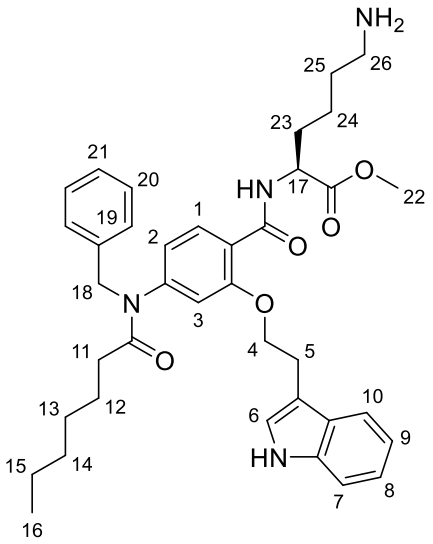

Compound **72** (0.21 g, 0.3 mmol,) was stirred in 4N HCl in dioxane (3 mL) for 4 hours. The solvent was removed *in vacuo*. (0.16 g, 0.23 mmol, 76%). $\mathbf{R_f}$ = 0.30 (9:1/EtOAc:MeOH). **^{1}H-NMR:** (400 MHz, MeOD) δ_H: 0.83 (t, 3H, J= 6.5 Hz, H-16), 1.10-1.30 (m, 8H, H-24, H-13, H-14, H-15), 1.31-1.43 (m, 2H, H-12), 1.41-1.52 (m, 2H, H-25),), 1.53-1.63 (m, 2H, H-23), 2.17 (t, 2H, J= 7.5 Hz, H-11), 2.74 (m, 2H, H-26), 3.27 (t, 2H, J=7.0 Hz, H-6), 3.73 (s, 3H, H-22), 4.37 (t, 2H, J=7.0 Hz, H-5), 4.50 (m, 1H, H-17), 5.31 (s, 2H, H-19), 6.74-7.56 (m, 12H, H-2, H-3, H-7, H-8, H-9, H-10, H-11, H-20, H-21, H-22), 7.92 (d, 1H, J= 8.0 Hz, H-2). **^{13}C-NMR** (125 MHz, MeOD): 12.94 ($CH_2CH_2CH_2CH_3$), 22.09 ($NH_2CH_2CH_2$), 22.91 ($CH_2CH_2CH_3$), 24.63 (CH_2CH_2), 25.25 ($CH_2CH_2CH_2CH_3$), 28.53 ($COCH_2CH_2CH_2$), 30.80 (CH_2CH), 31.88 ($COCH_2CH_2$), 31.20 ($NH_2CH_2CH_2CH_2$), 33.89 ($COCH_2$), 38.99 (NH_2CH_2), 51.40 ($NCOCH_2$), 51.54 ($COOCH_3$), 52.25 (CH_2CH), 69.06 ($COCH_2$), 110.25 (Ar-*C*), 111.04 (Ar-*C*H), 113.32 (Ar-*C*H), 117.83 (Ar-*C*H), 118.45 (Ar-*C*H), 121.23 (Ar-*C*H), 122.24 (Ar-*C*H), 122.90 (Ar-*C*H), 127.26 (Ar-*C*), 127.33 (Ar-*C*H), 128.20 (Ar-*C*H), 128.56 (Ar-*C*H), 136.71 (Ar-*C*), 137.20 (Ar-*C*), 137.40 (Ar-*C*), 146.30 ($CHCN$), 157.53 ($COCH_2$), 164.85 ($CONHCH$), 165.24 (NCO), 172.20 ($COOCH_3$), 132.08 (Ar-*C*H). **LRMS** *m/z* (ESI): 641.5 $[M+H]^+$. **HRMS** *m/z* (ESI): calculated for $C_{38}H_{49}N_4O_5^+$ $[M+Na]^+$: Exact Mass: 641.3697 found 641.3693.

*tert-Butyl 3-(2-(N-(3-(2-(1-(tert-butoxycarbonyl)-1H-indol-3-yl)ethoxy)-4-(methoxycarbonyl)phenyl)heptanamido)ethyl)-1H-indole-1-carboxylate (**74**)*

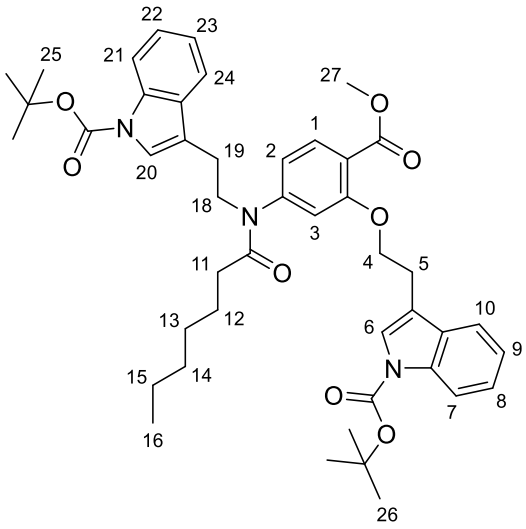

Compound **69** (0.70 g, 1.1 mmol, 1 eq) and potassium tert-butoxide (0.25 g, 2.2 mmol, 2 eq) were stirred in dry THF (10 mL) for 0.5 hours. **49** (0.39 g, 1.2 mmol, 1.1 eq) was then added and the reaction stirred 18 hours. The solvent was removed *in vacuo*. The reaction mixture was taken up in EtOAc (75 mL) and washed 3 times with water (75 mL). The organic layer was dried with $MgSO_4$ and dried under high vacuum. Silica column chromatography was carried out and the product was eluted with 1:9/EtOAc:petroleum ether. (0.18 g, 0.2 mmol, 20%) $\mathbf{R_f}$ = 0.23 (1:9/EtOAc:petroleum ether). **^{1}H-NMR:** (400 MHz, $(CD_3)_2CO$) δ_H: 0.81 (t, 3H, J= 6.5 Hz, H-16), 1.08-1.27 (m, 6H, H-13, H-14, H-15), 1.43-1.62 (m, 2H, H-12), 1.63 (s, 9H, H-26), 1.67 (s 9H, H-25), 2.09 (t, 2H, J= 7.5 Hz, H-11), 3.19 (t, 2H, J=7.0 Hz, H-19), 3.26 (t, 2H, J=7.0 Hz, H-5), 3.86 (s, 3H, H-27), 4.20 (t, 2H, J=7.0 Hz, H-18), 4.30 (t, 2H, J=7.0 Hz, H-4), 6.90-8.01 (m, 13H, H-1, H-2, H-3, H-7, H-8, H-9, H-10, H-20, H-21, H-22, H-23, H-24). **^{13}C-NMR** (125 MHz, $(CD_3)_2CO$): 13.44 ($CH_2CH_2CH_2CH_3$), 20.46 ($CH_2CH_2CH_3$), 26.03, 28.60 (CH_2CH_2), 27.37, 27.40 ($3CH_3$), 28.50 ($CH_2CH_2CH_2CH_3$), 31.44 ($COCH_2CH_2$), 33.96 ($COCH_2CH_2CH_2$), 40.93 ($COCH_2$), 50.88 (CH_3O), 51.33 ($NCOCH_2$), 68.08 ($CNCH_2$), 69.29 ($COCH_2$), 83.18, 83.26 (*C*OCO), 110.06 (Ar-*C*), 111.23 (Ar-*C*H), 113.87 (Ar-*C*H), 114.24 (Ar-*C*H), 117.20 (Ar-*C*), 118.23 (Ar-*C*H), 119.02 (Ar-*C*H), 122.30 (Ar-*C*H), 125.62 (Ar-*C*H), 128.05

(Ar-*C*H), 128.23 (Ar-*C*H), 128.66 (Ar-*C*H), 130.24 (Ar-*C*), 132.66 (Ar-*C*H), 135.43 (Ar-*C*), 135.60 (Ar-*C*), 138.21 (Ar-*C*), 138.33 (Ar-*C*), 144.58 (CH*C*N), 149.49 (*C*OCH$_2$), 160.62 (O*C*O), 165.68, 165.79 (CO*C*ON), 171.61 (N*C*O). **LRMS** *m/z* (ESI): 788.5 $[M+Na]^+$. **HRMS** *m/z* (ESI): calculated for $C_{45}H_{55}N_3NaO_8^+$ $[M+Na]^+$: Exact Mass: 788.3881 found 788.3889.

*2-(2-(1-(tert-Butoxycarbonyl)-1H-indol-3-yl)ethoxy)-4-(N-(2-(1-(tert-butoxycarbonyl)-1H-indol-3-yl)ethyl)heptanamido)benzoic acid (**75**)*

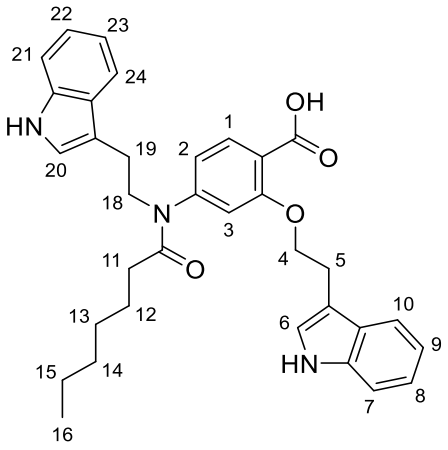

Compound **74** (0.18 g, 0.2 mmol) was dissolved in EtOH (5 mL), water (4 mL) and 6M NaOH (0.5 mL) was added and refluxed for 5 hours. After removing EtOH *in vacuo* the solution was acidified to pH 4 using HCl and the precipitate was collected by filtration. (0.17 g, 0.2 mmol, 95%). $\mathbf{R_f}$ = 0.58 (EtOAc). **^{1}H-NMR:** (400 MHz, $(CD_3)_2CO$) δ_H: 0.85 (t, 3H, J= 6.5 Hz, H-16), 1.21-1.32 (m, 6H, H-13, H-14, H-15), 1.32-1.50 (m, 2H, H-12), 2.12 (t, 2H, J= 7.5 Hz, H-11), 3.20 (t, 2H, J=7.0 Hz, H-19), 3.33 (t, 2H, J=7.0 Hz, H-5), 4.22 (t, 2H, J=7.0 Hz, H-18), 4.34 (t, 2H, J=7.0 Hz, H-4), 6.98-8.12 (m, 13H, H-1, H-2, H-3, H-7, H-8, H-9, H-10, H-20, H-21, H-22, H-23, H-24). **^{13}C-NMR** (125 MHz, $(CD_3)_2CO$): 14.02 ($CH_2CH_2CH_2CH_3$), 20.46 ($CH_2CH_2CH_3$), 25.44, 26.04 (CH_2CH_2), 28.52 ($CH_2CH_2CH_2CH_3$), 32.62 ($COCH_2CH_2$), 33.05 ($COCH_2CH_2CH_2$), 40.92 ($COCH_2$), 51.89 ($NCOCH_2$), 68.98 ($CNCH_2$), 70.34 ($COCH_2$), 110.20 (Ar-*C*H), 111.34 (Ar-*C*), 114.72 (Ar-*C*H), 115.22 (Ar-*C*), 116.40 (Ar-*C*H), 118.32 (Ar-*C*H), 119.32 (Ar-*C*H), 122.32 (Ar-*C*H), 124.42 (Ar-*C*H), 125.02 (Ar-*C*H), 127.98 (Ar-*C*H), 128.64 (Ar-*C*H), 129.11 (Ar-*C*H), 130.45 (Ar-*C*), 132.36 (Ar-*C*H), 135.81 (Ar-*C*), 136.13 (Ar-*C*), 138.20 (Ar-*C*), 138.54 (Ar-*C*), 144.50 (CH*C*N), 150.09 ($COCH_2$), 161.22 (*C*OOH), 172.60 (N*C*O). **LRMS** *m/z* (ESI): 550.2 $[M-H]^-$. **HRMS** *m/z* (ESI): calculated for $C_{34}H_{33}N_3O_4^-$ $[M-H]^-$: Exact Mass: 550.2711 found 550.2712.

*Methyl-N-2-(2-(2-(1H-indol-3-yl)ethoxy)-4-(N-(2-(1H-indol-3-yl)ethyl)heptanamido)benzoyl)-N6-(tert-butoxycarbonyl)-L-lysinate (**76**)*

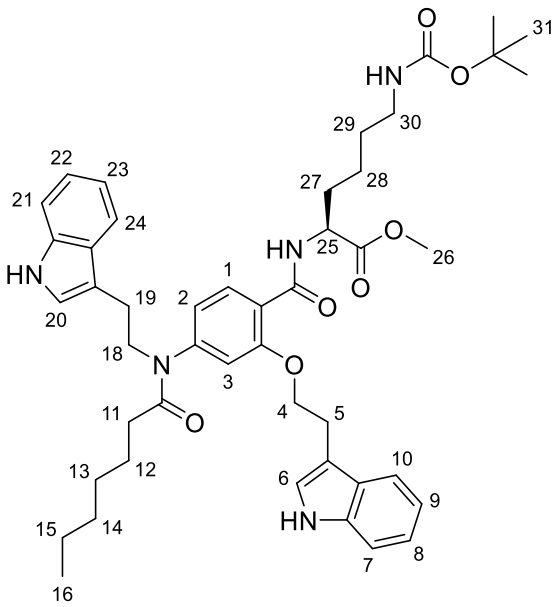

Compound **75** (0.17 g, 0.2 mmol, 1 eq), EDC.HCl (0.05 g, 0.24 mmol, 1.2 eq), HOBt (0.03 g, 0.24 mmol, 1.2 eq) and DIPEA (0.06 mL, 0.05 g, 0.4 mmol, 2 eq) were stirred in DCM (10 mL) for 15 minutes. H-Lys(Boc)-OMe hydrochloride (0.07 g, 0.24 mmol , 1.2 eq) was added and the reaction was stirred for 18 hours. DCM (40 mL) was added and washed 3 times with Na_2CO_3 *sat.* (75 mL). The organic layer was dried with $MgSO_4$ and dried under high vacuum. Silica column chromatography was carried out and the product was eluted with 3:4/EtOAc:petroleum ether. (0.08 g, 0.08 mmol, 42%). **R_f =** 0.23 (3:4/EtOAc:petroleum ether). **^{1}H-NMR:** (400 MHz, $(CD_3)_2CO$) δ_H: 0.85 (t, 3H, J= 6.5 Hz, H-16), 1.18-1.38 (m, 8H, H-28, H-13, H-14, H-15), 1.42 (s, 9H, H-31), 1.48-1.54 (m, 2H, H-12), 1.58-1.75 (m, 4H, H-27, H-29), 2.23 (t, 2H, J= 7.5 Hz, H-11), 2.92 (m, 2H, H-30), 3.21 (t, 2H, J=7.0 Hz, H-19), 3.29 (t, 2H, J=7.0 Hz, H-5), 3.71 (s, 3H, H-26), 4.20 (t, 2H, J=7.0 Hz, H-18), 4.31 (t, 2H, J=7.0 Hz, H-4), 4.54 (m, 1H, H-25), 6.85-8.09 (m, 13H, H-1, H-2, H-3, H-7, H-8, H-9, H-10, H-20, H-21, H-22, H-23, H-24). **^{13}C-NMR** (125 MHz, $(CD_3)_2CO$): 14.15 ($CH_2CH_2CH_2CH_3$), 20.30 ($CH_2CH_2CH_3$), 22.14 ($NHCH_2CH_2$), 26.19 28.02, (CH_2CH_2), 28.22 ($3CH_3$), 28.28 ($CH_2CH_2CH_2CH_3$), 30.34 (CH_2CH), 32.42 ($NHCH_2CH_2CH_2$), 32.62 ($COCH_2CH_2$), 33.00 ($COCH_2CH_2CH_2$), 40.92 ($COCH_2$), 41.81 ($NHCH_2$), 50.95 ($NCOCH_2$), 51.22

(CH_2CH), 52.70 ($COOCH_3$), 69.89 ($COCO$), 69.98 ($CNCH_2$), 72.40 ($COCH_2$), 110.11 (Ar-*C*), 111.34 (Ar-*C*H), 114.25 (Ar-*C*H), 114.92 (Ar-*C*), 116.90 (Ar-*C*H), 117.88 (Ar-*C*H), 118.41 (Ar-*C*H), 120.12 (Ar-*C*H), 124.51 (Ar-*C*H), 128.02 (Ar-*C*H), 128.64 (Ar-*C*H), 129.17 (Ar-*C*H), 132.70 (Ar-*C*H), 132.23 (Ar-*C*), 134.10 (Ar-*C*), 135.24 (Ar-*C*), 137.92 (Ar-*C*), 138.06 (Ar-*C*), 145.02 (CH*C*N), 149.98 ($COCH_2$), 164.44 ($CONHCH$), 164.55 ($COCONH$), 172.40 (NCO), 173.20 ($COOCH_3$). **LRMS** *m/z* (ESI): 816.6 $[M+Na]^+$. **HRMS** *m/z* (ESI): calculated for $C_{46}H_{59}N_4NaO_7^+$ $[M+Na]^+$: Exact Mass: 816.4307 found 816.4306.

*Methyl (2-(2-(1H-indol-3-yl)ethoxy)-4-(N-(2-(1H-indol-3-yl)ethyl)heptanamido)benzoyl)-L-lysinate; peptidomimetic 9 (**77**)*

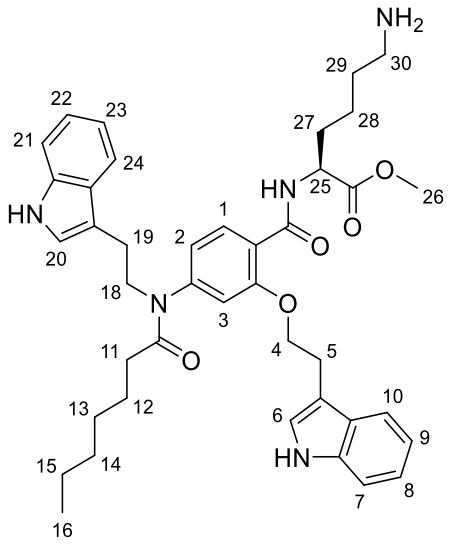

Compound **76** (0.08 g, 0.08 mmol) was stirred in 4N HCl in dioxane (1 mL) for 4 hours. The solvent was removed *in vacuo*. (0.04 g, 0.05 mmol, 62%). $\mathbf{R_f}$ = 0.30 (9:1/EtOAc:MeOH). **^{1}H-NMR:** (400 MHz, MeOD) δ_H: 0.87 (t, 3H, J= 6.5 Hz, H-16), 1.22-1.40 (m, 8H, H-28, H-13, H-14, H-15), 1.42-1.50 (m, 2H, H-12), 1.53-1.73 (m, 4H, H-27, H-29), 2.18 (t, 2H, J= 7.5 Hz, H-11), 2.90 (m, 2H, H-30), 3.19 (t, 2H, J=7.0 Hz, H-19), 3.28 (t, 2H, J=7.0 Hz, H-5), 3.71 (s, 3H, H-26), 4.21 (t, 2H, J=7.0 Hz, H-18), 4.31 (t, 2H, J=7.0 Hz, H-4), 4.59 (m, 1H, H-25), 6.86-8.05 (m, 13H, H-1, H-2, H-3, H-7, H-8, H-9, H-10, H-20, H-21, H-22, H-23, H-24). **^{13}C-NMR** (125 MHz, MeOD): 14.15 ($CH_2CH_2CH_2CH_3$), 20.54 ($CH_2CH_2CH_3$), 22.63 ($NH_2CH_2CH_2$), 26.41, (CH_2CH_2), 29.12 ($CH_2CH_2CH_2CH_3$), 32.38 (CH_2CH), 32.62 ($COCH_2CH_2$), 33.15 ($COCH_2CH_2CH_2$), 34.34 ($NH_2CH_2CH_2CH_2$), 40.92 ($COCH_2$), 41.22 (NH_2CH_2), 50.20 (CH_2CH), 51.73 ($COOCH_3$), 52.16 ($NCOCH_2$) 69.23 ($CNCH_2$), 70.56 ($COCH_2$), 110.00 (Ar-*C*H), 111.45 (Ar-*C*), 114.20 (Ar-*C*), 115.22 (Ar-*C*H), 117.21 (Ar-*C*H), 117.77 (Ar-*C*H), 118.34 (Ar-*C*H), 121.78 (Ar-*C*H), 123.28 (Ar-*C*H), 125.23 (Ar-*C*H), 127.82 (Ar-*C*H), 128.55 (Ar-*C*H), 129.18 (Ar-*C*H), 129.88 (Ar-*C*), 133.46 (Ar-*C*H), 135.60 (Ar-*C*), 136.32 (Ar-*C*), 138.69 (Ar-*C*), 139.02 (Ar-*C*), 146.23 (CH*C*N), 150.99 ($COCH_2$), 165.25 (*C*ONHCH), 171.02 (N*C*O), 172.40 ($COOCH_3$). **LRMS** *m/z* (ESI):

694.5 $[M+H]^+$. **HRMS** *m/z* (ESI): calculated for $C_{41}H_{52}N_5O_5^+$ $[M+Na]^+$: Exact Mass: 694.3963 found 694.3966.

7.7 Peptidomimetics 10-12

*1-Octylurea (**78**)*

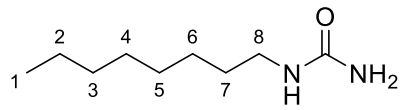

1-Octylamine (2.55 mL, 2.0 g, 0.015 mol, 1 eq) and HCl (0.72 mL, 1 eq) were stirred in hot ethanol (20 mL) for 15 minutes before KOCN (5.02g, 0.062 mol, 4 eq) in water (20 mL) was added. The solution was stirred for 16 hours. The ethanol was removed *in vacuo*. Water (30 mL) was added and this was washed three times with Et_2O (3x 50mL). The organic layers were combined and dried over $MgSO_4$. (Adapted from literature reference[155]). (2.10 g, 0.012 mol, 80%). **^{1}H-NMR:** (400 MHz, $(CD_3)_2CO$) δ_H: 0.91 (t, 3H, J= 6.5 Hz, H-1), 1.24-1.44 (m, 10H, H-2, H-3, H-3, H-4, H-5, H-6), 1.55-1.70 (m, 2H, H-7), 2.77 (t, 2H, J= 7.0 Hz, H-8). **^{13}C-NMR** (125 MHz, $(CD_3)_2CO$): 14.46 (*C*H_3), 23.72 (*C*H_2), 27.99 (*C*H_2), 30.45 (*C*H_2), 31.23 (*C*H_2), 31.45 (*C*H_2), 33.00 (*C*H_2), 41.78 (*C*H_2NH), 163.75 (*C*O).

*1-((Octyl)aminocarbonyl)-3-(ethoxycarbonyl) thiourea (**79**)*

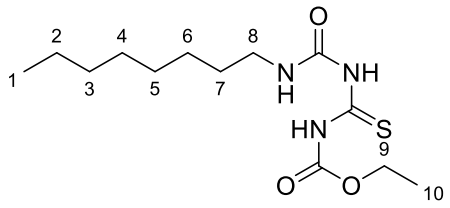

Compound **78** (2.10 g, 0.012 mol, 1 eq) and ethoxycarbonyl isothiocyanate (1.78 mL, 1.96 g, 0.015 mol, 1.2 eq) were stirred in toluene (8 mL) at 60˚C for 4 hours. The solvent was removed *in vacuo*. The resulting residue was applied to a silica column and the product was eluted with 20:80 EtOAc/Petroleum ether. (Adapted from literature reference[155]). (2.25 g, 7.4 mmol, 66 %). **R_f =** 0.25 (20:80 EtOAc/Petroleum ether). **^{1}H-NMR:** (400 MHz, $(CD_3)_2CO$) δ_H: 0.88 (t, 3H, J= 6.5 Hz, H-1), 1.10 (t, 3H, J= 6.5 Hz, H-10), 1.26-1.40 (m, 10H, H-2, H-3, H-3, H-4, H-5, H-6), 1.52-1.60 (m, 2H, H-7), 3.40 (t, 2H, J= 7.0 Hz, H-8), 4.27 (q, 2H, J=7.0, 7.0 Hz, H-9). **^{13}C-NMR** (125 MHz, $(CD_3)_2CO$): 13.47 ($COOCH_2CH_3$), 14.76 (CH_3), 22.46 (CH_2), 26.72 (CH_2), 29.01 (CH_2), 29.07 (CH_2), 29.43 (CH_2), 29.71 (CH_2), 39.74 (CH_2NH), 65.30 ($COOCH_2$), 152.60 (NHCOO), 163.30 (NCON) 179.20 (NHCSNH). **LRMS** *m/z* (ESI): 326.2 $[M+Na]^+$. **HRMS** *m/z* (ESI): calculated for $C_{13}H_{26}N_3O_3SNa^+$ $[M+Na]^+$: 326.1509 found 326.1502.

*6-(Methylthio)-3-octyl-1,3,5-triazine-2,4(1H,3H)-dione (**80**)*

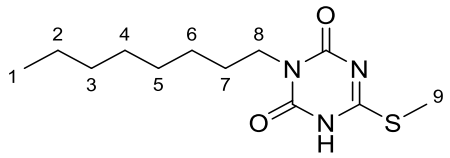

Compound **79** (2.25 g, 7.4 mmol, 1 eq) and NaOMe (0.41 g, 7.4 mmol, 1 eq) were refluxed in anhydrous methanol (30 mL) for 45 minutes. The reaction mixture was cooled to room temperature and MeI (1.41 mL, 3.16 g, 0.022 mol, 3 eq) were added and the reaction mixture was stirred for 4 hours. The solvent was removed *in vacuo*. The resulting residue was dissolved in EtOAc (50 mL) and washed three times with water (3 x 50mL). The organic layer was dried using $MgSO_4$. The resulting residue was applied to a silica column and the product was eluted with 60:40 EtOAc/Petroleum ether. (Adapted from literature reference[155]). (0.78 g, 2.8 mmol, 38 %). $\mathbf{R_f}$ = 0.53 (60:40 EtOAc/Petroleum ether). **^{1}H-NMR:** (400MHz, $(CD_3)_2CO$) δ_H: 0.88 (t, 3H, J= 6.5 Hz, H-1), 1.24-1.36 (m, 10H, H-2, H-3, H-3, H-4, H-5, H-6), 1.56-1.63 (m, 2H, H-7), 2.52 (s, 3H, H-9) 3.78 (t, 2H, J= 7.0 Hz, H-8). **^{13}C-NMR** (125 MHz, $(CD_3)_2CO$): 12.31 ($CSCH_3$), 13.48 (CH_3), 22.40 (CH_2), 26.62 (CH_2), 27.28 (CH_2), 29.10 (CH_2), 29.43 (CH_2), 31.36 (CH_2), 40.81 (CH_2NCO), 168.15 (NCONCS). **LRMS** *m/z* (ESI): 270.1 $[M-H]^-$. **HRMS** *m/z* (ESI): calculated for $C_{12}H_{20}N_3O_2S^-$ $[M-H]^-$: 270.1282 found 270.1278.

*1-Benzyl-6-(methylthio)-3-octyl-1,3,5-triazine-2,4(1H,3H)-dione (**81**)*

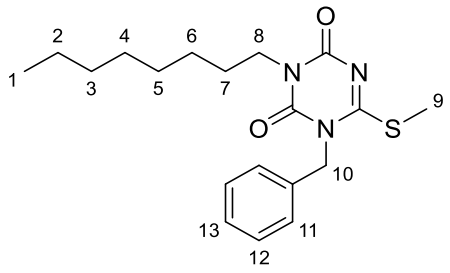

Compound **80** (0.78 g, 2.92 mmol, 1 eq) and benzyl bromide (1.72 mL, 2.48 g, 14.5 mmol, 5 eq) were stirred in DMF (3 mL) at 0 ˚C. To this NaH (1.16 g, 29 mmol, 10 eq) was added in two halves. The reaction was allowed to come to room temperature and was stirred for 16 hours. The reaction was taken up in EtOAc (50 mL) and washed 3 times with water and dried with $MgSO_4$. The solvent was removed *in vacuo*. The resulting residue was applied to a silica column and the product was eluted with 50:50 EtOAc/Petroleum ether. (Adapted from literature reference[155]). (0.33 g, 0.91 mmol mmol, 32 %). $\mathbf{R_f}$ = 0.75 (50:50 EtOAc/Petroleum ether). **^{1}H-NMR:** (400 MHz, $(CD_3)_2CO$) δ_H: 0.89 (t, 3H, J= 6.5 Hz, H-1), 1.21-1.36 (m, 10H, H-2, H-3, H-3, H-4, H-5, H-6), 1.59-1.70 (m, 2H, H-7), 2.49 (s, 3H, H-9), 3.86 (t, 2H, J= 7.0 Hz, H-8), 5.15 (s, 2H, H-10), 7.25-7.41 (m, 5H, H-11, H-12, H-13). **^{13}C-NMR** (125 MHz, $(CD_3)_2CO$): 14.46 (CH_3), 15.21 ($CSCH_3$), 23.36 (CH_2), 27.59 (CH_2), 28.14 (CH_2), 30.01 (CH_2), 30.05 (CH_2), 32.58 (CH_2), 43.07 (CH_2NCO), 48.81 (NCH_2), 128.12 (NCH_2CCH), 128.66 (CCHCHCH), 129.49 (CCHCHCH), 136.24 (NCH_2CCH), 152.42 (CNCO), 163.23 (CH_2NCO), 170.45 (NCONCS). **LRMS** *m/z* (ESI): 362.3 $[M+H]^+$. **HRMS** *m/z* (ESI): calculated for $C_{19}H_{28}N_3O_2S^+[M+H]^+$: 362.1897 found 362.1887.

*6-((2-Aminoethyl)amino)-1-benzyl-3-octyl-1,3,5-triazine-2,4(1H,3H)-dione (**82**)*

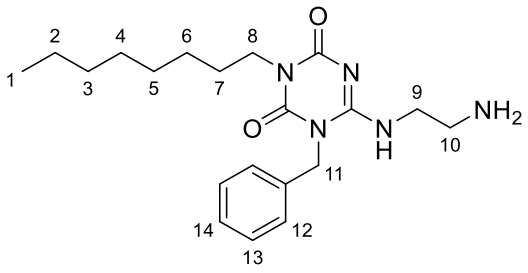

Compound **81** (0.33 g, 0.91 mmol, 1 eq) and ethylenediamine (0.30 mL, 0.27 g, 4.55 mmol, 5 eq) were refluxed in toluene for 6 hours. The solvent was removed in vacuo. The residue was dissolved in EtOAc (50 mL) and washed twice with water (2 x 50 mL), then dried with $MgSO_4$. The resulting residue was applied to a silica column and the product was eluted with 8:2 EtOAc/MeOH. (Adapted from literature reference[155]). (0.29 g, 0.80 mmol, 87%). **^{1}H-NMR:** (400 MHz, $(CD_3)_2CO$) δ_H: 0.87 (t, 3H, J= 6.0 Hz, H-1), 1.20-1.35 (m, 10H, H-2, H-3, H-3, H-4, H-5, H-6), 1.53-1.65 (m, 2H, H-7), 3.29 (t, 2H, J= 6.0 Hz, H-10), 3.51 (t, 2H, J= 6.0 Hz, H-9), 3.86 (t, 2H, J= 7.0 Hz, H-8), 5.19 (s, 2H, H-11), 7.18-7.41 (m, 5H, H-12, H-13, H-14). **^{13}C-NMR** (125 MHz, $(CD_3)_2CO$): 14.40 (CH_3), 23.33 (CH_2), 27.62 (CH_2), 28.61 (CH_2), 30.01 (CH_2), 30.14 (CH_2), 33.56 (CH_2), 42.63 ($CNHCH_2CH_2$), 43.16 (CH_2NCO), 45.67 (NCH_2), 51.16 ($CNHCH_2CH_2$), 127.52 ($CCHCHCH$), 128.32 ($CCHCHCH$), 129.61 (NCH_2CCH), 136.40 (NCH_2CCH), 152.53 ($CNCO$), 154.53 (CH_2NCO), 163.24 ($NCONCNH$). **LRMS** *m/z* (ESI): 374.4 $[M+H]^+$. **HRMS** *m/z* (ESI): calculated for $C_8H_{11}N_2O^+$ $[M+H]^+$: 374.2551 found 374.2552.

*1-(2-((1-Benzyl-5-octyl-4,6-dioxo-1,4,5,6-tetrahydro-1,3,5-triazin-2-yl)amino)ethyl)guanidine (**83**)*

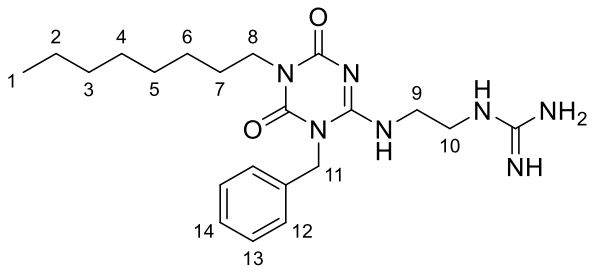

Compound **82** (0.29 g, 0.80 mmol, 1 eq), 1*H*-Pyrazole-1-carboxamidine hydrochloride (0.80 mmol, 1 eq) and DIPEA (0.80 mmol, 1 eq) in MeCN for 18 hours. The precipitate which formed was removed by filtration. (Adapted from literature reference[155]). (0.29 g, 0.80 mmol, 87%). **^{1}H-NMR:** (400 MHz, MeOD) δ_H: 0.89 (t, 3H, J= 7.0 Hz, H-1), 1.21-1.40 (m, 10H, H-2, H-3, H-3, H-4, H-5, H-6), 1.57-1.67 (m, 2H, H-7), 3.35 (t, 2H, J= 7.0 Hz, H-10), 3.51 (t, 2H, J= 7.0 Hz, H-9), 3.87 (t, 2H, J= 7.0 Hz, H-8), 5.16 (s, 2H, H-11), 7.22-7.38 (m, 5H, H-12, H-13, H-14). **^{13}C-NMR** (125 MHz, MeOD): 13.04 (*C*H_3), 22.31 (*C*H_2), 27.62 (*C*H_2), 26.44 (*C*H_2), 27.32 (*C*H_2), 28.96 (*C*H_2), 31.54 (*C*H_2), 40.00 (CNH*C*H_2CH_2), 42.03 (*C*H_2NCO), 43.30 (CNHCH$_2$*C*H_2), 44.93 (N*C*H_2), 125.99 (CCH*C*HCH), 127.53 (CCHCH*C*H), 128.53 (NCH$_2$C*C*H), 134.53 (NCH$_2$*C*CH),151.10 (CN*C*O), 155.07 (CH$_2$N*C*O), 155.69 (NCON*C*NH), 157.58 (NH*C*NH). **LRMS** *m/z* (ESI): 415.2 $[M+H]^+$. **HRMS** *m/z* (ESI): calculated for $C_9H_{12}N_2O^+$ $[M+H]^+$: 415.2696 found 415.2698.

*6-((3-Aminopropyl)amino)-1-benzyl-3-octyl-1,3,5-triazine-2,4(1H,3H)-dione (**84**)*

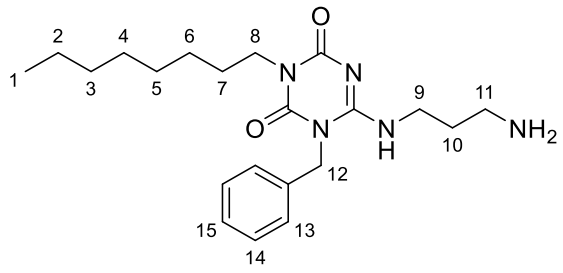

Compound **81** (0.33 g, 0.91 mmol, 1 eq) and *N*-Boc-1,3-propanediamine (0.79 g, 4.55 mmol, 5 eq) were refluxed in toluene for 6 hours. The solvent was removed *in vacuo*. The residue was dissolved in EtOAc (50 mL) and washed twice with water (2 x 50 mL), then dried with $MgSO_4$. The resulting residue was applied to a silica column and the product was eluted with 8:2 EtOAc/MeOH. (Adapted from literature reference[155]). (0.20 g, 0.52 mmol, 57%). **^{1}H-NMR:** (400 MHz, MeOD) δ_H: 0.90 (t, 3H, J= 7.0 Hz, H-1), 1.26-1.37 (m, 10H, H-2, H-3, H-3, H-4, H-5, H-6), 1.56-1.68 (m, 2H, H-7), 1.87 (p, 2H, J= 7.0, 7.0 7.0, 7.0 Hz, H-10) 2.84 (t, 2H, J= 7.0 Hz, H-11), 3.48 (t, 2H, J= 7.0 Hz, H-9), 3.89 (t, 2H, J= 7.0 Hz, H-8), 5.17 (s, 2H, H-12), 7.23-7.40 (m, 5H, H-13, H-14, H-15). **^{13}C-NMR** (125 MHz, MeOD): 13.04 (*C*H_3), 22.31 (*C*H_2), 26.44 (*C*H_2), 27.62 (*C*H_2), 27.32 (*C*H_2), 28.96 (*C*H_2), 31.54 (*C*H_2), 40.00 (CNH*C*H_2CH_2), 42.03 (*C*H_2NCO), 43.30 (CNHCH_2*C*H_2), 44.93 (N*C*H_2), 125.99 (CCH*C*HCH), 127.53 (CCHCH*C*H), 128.53 (NCH_2C*C*H), 134.53 (NCH_2*C*CH), 151.10 (CN*C*O), 155.07 (CH_2N*C*O), 155.69 (NCON*C*NH), 157.58 (CH_2NH_2), **LRMS** *m/z* (ESI): 387.4 $[M+H]^+$. **HRMS** *m/z* (ESI): calculated for $C_9H_{13}N_2O^+$ $[M+H]^+$: 387.2634 found 387.2639.

7.8 Biological methods

Bacteria	Use
E. coli (TOP10)	Transformations, antimicrobial testing, general
P. Fluorescens	antimicrobial testing
B. subtilis (W23)	antimicrobial testing, isolation of UDPMurNAc-pentapeptide
E. coli (C43)	Overexpression of toxic proteins

Table 24: table of bacteria used during the project and the uses of them

7.8.1 Antibiotic stock preparation

The antibiotics used in the inoculations and agar plates are shown in Table 25. The stock concentrations were filter sterilised before use.

Antibiotic	Stock concentration	Working concentration	Dissolved in
Ampicillin	100 mg/mL	100 µg/mL	1:1 EtOH:dH_2O
Kanamycin	50 mg/mL	50 µg/mL	dH_2O
tetracycline	10 mg/mL	10 µg/mL	dH_2O

Table 25: antibiotic preparation conditions.

7.8.2 LB agar plate preparation

The LB agar media is made up as described in Table 26 and then autoclaved. The media is melted in the microwave and allowed to cool to ~55 °C. If antibiotics are required they are added at the corresponding working concentration (Table 25) before the agar is poured into petri dishes (~25 mL per plate). The plates are allowed to set before use.

Reagent	Quantity
bacteriological peptone	10 g/L
yeast extract	5 g/L
NaCl	5 g/L
Agar	12 g/L

Table 26: LB agar composition

Miles and Misra CFU/mL calculation[111]

P. Fluorescens, E. coli (TOP10) and *B. subtilis* (W23) colonies were isolated from an agar plate and inoculated in 5 mL of LB broth (Table 27) overnight at 37 °C. A dilution series of the seeded MH2 (Table 28) was performed to get 10^{-1}, 10^{-2}, 10^{-3}, 10^{-4}, 10^{-5}, 10^{-6}, 10^{-7} and 10^{-8} fold dilutions. The dilution series was performed by taking 0.5 mL of the seeded MH2 and diluting it with 4.5 mL of MH2. Then 0.5 mL of this was taken and was diluted with 4.5 mL of MH2. This was repeated until the dilution series was complete.

From each dilution 20 µL was pipetted onto an agar plate. An L-shaped cell spreader was used to assure the solution was evenly distributed across the plate. The plates were then inverted and incubated overnight at 37 °C or 30 °C. The colonies were counted and multiplied by 50 and the dilution that gave a CFU/mL of 1000 was chosen for MIC calculations.

Reagent	Quantity
bacteriological peptone	10 g/L
yeast extract	5 g/L
NaCl	5 g/L

Table 27: LB broth composition

Reagent	Quantity
casein acid hydrolysate	17.5 g/L
beef extract	3 g/L
starch	1.5 g/L

Table 28: MH2 media composition

7.8.3 Antimicrobial testing - micro titre broth dilution technique[87]

On a sterile 96-welled plate (which had a sterilised lid), 190 µl of the seeded broth (CFU/mL = 1000) was added to each well. 2.5 mg/mL solutions of dipeptide or peptidomimetic were serially diluted to obtain 7 different concentrations (1250, 625, 312.5, 186, 78.2, 39, and 19.5 µg/mL). 10 µL of these diluted inhibitors were added to the 96-well plate to give a final volume of 200 µL and final concentrations of 125, 62.5, 31.25, 15.63, 7.82, 3.90, 1.95 and 0.97 µg/mL. 10 µL of water, MeOH and DMSO were added to separate wells to serve as a growth control. Each test condition was tested in triplicate.

The sterile lid was placed on the plate 96-well plate and incubated overnight at 30 or 37°C. The optical density (OD_{595}) was the measured using a HIDEX Sense Microplate Reader 425-301. The inhibitor concentration which reduced the growth by 50 % was considered the IC_{50} of the compound.

7.8.4 Synthesis of Uridine 5'Diphospho N-acetylmuramyl-L-Ala-γ-D-Glu-m-DAP-D-Ala-D-Ala (UDP-MurNAc-pentapeptide)

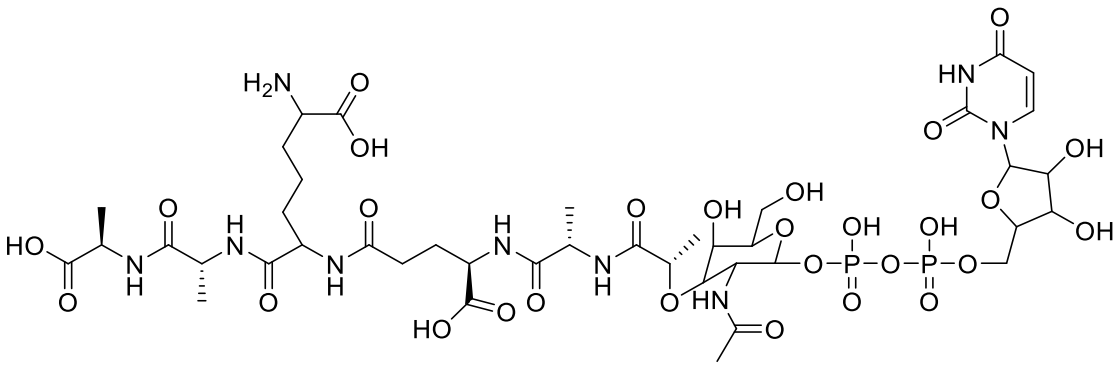

UDP-MurNAc-pentapeptide was isolated from cultures of *Bacillus subtillis* W23.[28,172,173] 50 mL of PYP media was inoculated with *B. subtillis* W23 and incubated at 37°C overnight. 4x 10mL of this was added to 4x 500mL of PYP media in 2 L flasks to give 2% of the *B. subtillis* culture which was then grown to at OD_{600} = 1.2 at 37°C. The cultures were then chilled on ice again and cells pelleted by centrifugation at 4400 rpm at 4°C for 30 minutes. The 4 pellets were suspended in 4x 50 mL CWSM media. This was then added to 4x 75 mL of prewarmed CWSM in 4x 250mL conical flasks and then incubated at 37°C for 45 minutes. The cultures were chilled on ice again and cells pelleted by centrifugation at 4400 rpm at 4°C for 30 minutes and then stored at -20°C overnight. The thawed cells were (~8 g wet weight) were re-suspended in ice cold 5% (w/v) TCA (5 mL/g cells). The pellet was extracted a further two times with half volumes of ice cold TCA. The supernatants (80 mL) were pooled and extracted 3 times with equal volumes of ice cold diethyl ether (3x 80 mL). The aqueous phase was neutralised with 3 M NaOH. The traces of ether were evaporated by rotary evaporation and the sample lyophilised overnight. The sample was dissolved in water and clarified by centrifugation.

PYP medium (pH 7.2) and cell wall synthesis medium (CSWM) (pH 7.4) contained the ingredients described in Table 29 and Table 30 respectively. The PYP and CWSM were autoclaved without $MgCl_2$, $FeSO_4$, glucose, antibiotics and amino acid residues, these ingredients were filter sterilised and then added to the autoclaved media.

Reagent	Quantity
bacteriological peptone	20 g/L
yeast extract	1.5 g/L
K_2HPO_4	4.5 g/L

Table 29: PYP media composition

Reagent	Quantity
Na_2HPO_4	0.26 g/L
NH_4Cl	2.0 g/L
KCl	4.0 g/L
$MgCl_2$	4.0 g/L
Na_2SO_4	0.15 g/L
$FeSO_4$	0.1 g/L
glucose	2.0 g/L
uracil	40 mg/L
L-glutamic acid	120 mg/L
Meso-diaminopimelic acid	120 mg/L
L-alanine	50 mg/L
chloramphenicol	50 mg/L
ampicillin	50 mg/L
vancomycin	12.5 mg/L

Table 30: CWSM media composition

Isolation of the substrate was carried out by RP-HPLC using Synergi™ 4 µm Polar-RP 80 Å and an elution with a gradient of 0:100 to 30:70 Acetonitrile/ 0.05M aqueous NH_4HCO_3 and monitored at 262 nm as previously carried out by Siricilla *et al*.[122] Each peak was collected and subjected to LC-MS by Lijiang Song after being desalted by by RP-HPLC using Synergi™ 4 µm Polar-RP 80 Å and an elution with an isocratic gradient of 10:90 MeCN/water. The peak containing the substrate was identified and collected. The fractions were pooled and lyophilised and then desalted. **HRMS** m/z (ESI): calculated for $C_{41}H_{66}N_9O_{28}P_2^+$ $[M+H]^+$: Exact Mass: 1194.3487 found 1194.3464.

7.8.5 MraY inhibitioin assay - continuous fluorescence plate reader

A HIDEX Sense Microplate Reader 425-301 was used to determine the inhibitory activity of dipeptides and peptidomimetics at an excitation wavelength of 340 nm and emission wavelength of 535 nm to monitor the formation of dansyl-Lipid I. Membranes containing overexpressed MraY were treated with a master mix containing dansyl-tagged UDP-MurNAc-pentapeptide and lipid carrier undecaprenyl phosphate (C_{55}-P). Dansyl-tagged UDP-MurNAc-pentapeptide was provided by Namrita Modgill (summer student).

The lipid carrier C_{55}-P was purchased from Larodan Fine Chemicals in a chloroform/methanol (2:1) + 3 % (v/v) ammonia solution. 20 µL of the 10 mg/mL stock solution (total 0.2 mg) was transferred to a small vial. The solvents were removed from this sample using a gentle stream of $N_{2(g)}$. Once the solution was completely dried it was redissolved in 2 mL of a buffer solution. The lipid carrier buffer solution contained 50 mM Tris Base (pH 7.5), 2 mM β-mercaptoethanol, 1mM $MgCl_2$, 20 % glycerol and 0.5 % TritonX100. The solution 100 µg/mL was sonicated until it became clear.

Preparation of the Master Mix (MM)

The master mix contained a mixture of buffer A, water, dansyl-UDP-MurNAc-pentapeptide and lipid carrier C_{55}-P Buffer A contained a final concentration of 100 mM Tris base (pH 7.5) and 25 mM $MgCl_2$. The master mix contained 21.0 µM Dansyl-UDP-MurNAc-pentapeptide and 47.2 µM C_{55}-P.

Preparation of Membrane-bound MraY

Agnes Mihalyi (PhD) overexpressed *E. coli* MraY in *E. coli* DH5α cells and stored them in a membrane buffer containing 50 mM Tris (pH 7.5) 2 mM β-mercaptoethanol and 1 mM $MgCl_2$. The final protein concentrations of membranes containing overexpressed *E. coli* MraY were 0.72 mg/mL

Plate reader assay protocol

To a black 96-well plate, 10 μL of overexpressed MraY membranes was added to 85 μL of master mix and 5 μL of the inhibitor (final concentration 100 μg/mL in MeOH or DMSO). MeOH and DMSO were used as the negative controls. Tunicamycin at a final concentration of 50 μg/mL in MeOH, was used as a positive controls.

Had inhibition at this concentration of compound been seen a serial dilution would have been carried out.

Fluorescence measurements (excitation wavelength of 340 nm and emission wavelength of 535 nm) were taken before the addition of membranes, t =0, then at 10 second intervals for 10 minutes.

7.8.6 Radiochemical inhibition assay

Assays were carried out as described by A. Lloyd *et al*. (2004).[22] A solution of [^{14}C]-UDPMurNAc-pentapeptide (1-4 nCi) which was prepared by Agnes Mihalyi was added to the master mix (described below). Into an eppendorf 80 μL of master mix was added to 10 μL of inhibitor or DMSO. To start the reaction 10 μL containing 20-50 μg of over expressed MraY membranes in a buffer containing 100 mM Tris (pH 7.5), 17.5 M $MgCl_2$, 4.0 % (v/v) glycerol, 2.3 % (v/v) DMSO, 0.1 % Triton X-100 was added. The total reaction volume was 100 μL. The mixture was then left for 30 minutes to allow the lipid product to form. The reaction was quenched with 50 % 6M pyridinium acetate (100 μL) and vortexed. To this 50 % butanol (200 μL) was added and the mixture was vortexed again. The reaction mixture was centrifuged at 13,000 x g for 2 minutes causing the separation of the two layers. 200 μL of butanol was added to 5 mL ScintiSafe scintillation liquid and quantified by liquid scintillation counting.

The controls were as follows:

- Scintillation fluid only, to show background radiation
- No enzyme, to serve as an extraction control i.e how much unconverted substrate is in the butanol layer
- No inhibitor, which gives 100 % enzyme activity
- Negative control, using 100 μg/mL tunicamycin

The typical composition of master mix:

- 1500 µL of assay buffer (200 mM Tris pH 7, 50 mM $MgCl_2$)
- 1000 µL of undecaprenyl phosphate stock solution (0.1 mg/mL in 50 mM Tris pH 7.5, 2 mM β-mercaptoethanol, 1 mM $MgCl_2$, 20 % glycerol and 0.5 % Triton-X100)
- 100 µL DMSO
- 60 µL [^{14}C]-UDPMurNAc-pentapeptide (24,500 dpm/10 µL)
- 340 µL water

7.8.7 Chemical competency transformation

5 µL of plasmid DNA were added to 50 µL of *E. coli* TOP10 competent cells (prepared by James Williamson, Post Doc) and incubated in ice for 30 minutes. The samples were then transferred to a 42 °C water bath and incubated for 45 seconds and then immediately transferred to ice for 3 minutes. 300 µL of LB was added to the sample and incubated at 37°C with shaking (180 rpm) for 1 hour. 100 µL of the seeded LB was poured to an LB agar plate. An L-shaped cell spreader was used to assure the mixture was evenly distributed across the plate. The agar plate was incubated overnight at 37 °C.

7.8.8 Protection assay- IC50 of inhibitors against E. coli overexpressing MraY

A single colony of the appropriate bacteria was isolated from the transformed plate and inoculated in 5mL of MH2+Amp (100 µg/mL) or MH2+Kan (50 µg/mL) overnight at 37 °C with shaking. This start-up culture was diluted 100-fold with MH2 (with the appropriate antibiotic at the concentration stated) and induced with 0.5 mM IPTG. To a sterile 96-well microtitre plate, 190 µl of the IPTG-induced seeded broth was added to each well. 10 µL of dipeptide was added to the deep 96-well plate to give a final volume of 200 µL and final inhibitor concentrations of 500, 450, 400, 350, 300, 250, 125, 62.5, 31.25, 15.63, 7.82, 3.90, 1.95 and 0.98 µg/mL. Each inhibitor concentration was tested in triplicate. 10 µL of water, MeOH and DMSO were added to separate wells to serve as a growth controls. MH2 was also used as a negative control. The sterile lid was replaced on the plate and incubated at 37 °C with shaking for 8 hours. The optical density (OD_{595}) was the measured using a HIDEX Sense

Microplate Reader 425-301. The inhibitor concentration which reduced the growth by 50 % was considered the IC_{50} of the compound.

7.8.9 General procedure for restriction digests

Plasmids were digested after isolation using a Monarch miniprep kit. Restriction digests of plasmids were conducted at 37 °C for 1 hour using 0.5-1 µl of Thermo Fisher fast digest restriction enzyme, and the buffer conditions suggested by the manufacturer. The digested fragments were purified by gel electrophoresis and gel extraction.

7.8.10 General procedure for Agarose gel electrophoresis

Agarose and TBE buffer (Table 31) 0.8% (w/v) were microwaved until the agarose had dissolved and then cooled slightly before Gel Red (0.003%) was added and the gel was set. Once set the gel was placed into the electrophoresis tank and submerged in TBE buffer. The samples of plasmid DNA (20 µL) were pipetted into separate wells. The DNA ladder which in this case was 1kb generuler (thermoscientific) was added to a separate well. The gel was run at 100V for 45 minutes and visualised under UV light. The relevant bands were cut from the gel and the DNA isolated using a Monarch gel extraction kit.

Reagent	Quantity for 1 L	Final concentration
Tris base	121.1 g	1 M
Boric acid	61.8 g	1 M
EDTA (disodium salt)	7.4 g	0.02 M

Table 31: TBE electrophoresis buffer (10X)

7.8.11 General procedure for ligations

The ligations between the cut plasmids and inserts or PCR products were performed using a 3:1 molar ratio of insert to vector. T4 ligase (1 μL) and 10x ligase buffer (2 μL) were mixed with vector (50 ng) and insert and made up to 20 μL with dH_2O. The reaction was incubated for 40 minutes at room temperature and then at 4 °C overnight, and 5 μL used to transform *E. coli* TOP10 chemically competent cells or *E. coli* C43 electro-competent cells.

7.8.12 General procedure for PCR

Amplification of the kanamycin cassette was carried out using Phusion polymerase using the manufacturer's conditions. The primers used are shown in Table 32. Mixture: 1 μL forward primer (kan cassette, 10 μM), 1 μL reverse primer (kan cassette, 10 μM), 1 μL template DNA (50 ng/μL), 0.4 μL dNTPs (10 mM), 4 μL Phusion GC buffer, 0.2 μL Phusion polymerase, 0.6 μL DMSO and dH2O to make upto 20 μL. Conditions: 98 °C 30 s Denaturation, 98 °C 10 s Denaturation 65 °C 30 s Annealing 72 °C 30 s Extension (25 cycles) 72 °C 600s extension. PCR products were analysed by agarose gel electrophoresis in TBE buffer using a gel of 0.8 % agarose in TBE buffer with GelRed under UV light for detection.

Primer	Forward	Reverse
Kan cassette	GGGATTCGTCTGTTGCAGGAAGA	CGACTTCAGCGAGACCGTTATAG

Table 32: table of primers used in PCR

7.8.13 Transformation of plasmid DNA into Electrocompetent E. coli C43

The plasmid DNA was firstly transformed into chemically competent TOP10. A single colony was then inoculated in 5 mL LB+Amp (100 μg/mL) and incubated overnight at 37 °C. The plasmids were then isolated using a Monarch miniprep kit. This plasmid was then transformed in to electro-competent cells.

Firstly the electro-competent *E. coli* C43 cells were made. A single colony of *E. coli* C43 was inoculated in 20 mL of LB and incubated overnight at 37 °C. The cells were pelleted (4000 g for 15 minutes) and the supernatant discarded. The pellet was resuspended in 10 mL 10% glycerol. The cells were pelleted again and then resuspended in 10 mL 10% glycerol. The cells were pelleted a final time and then resuspended in 0.5 mL 10% glycerol and then transferred aliquots of 100 μL.

The electroporation cuvettes and electrocompetent cells were placed on ice. Once the cells had defrosted transfer 100 μL of the cells were transferred to a chilled electroporation cuvette and then 1 μL of the DNA solution was added and mixed. Electroporate at 1.8 kV. Immediately add 900 μL of LB to the cuvette, gently mix up and down then transfer into a 1.5 mL Eppendorf microcentrifuge tube. Incubate and shake at 37°C for 1 hour. 100 μL of the seeded LB was poured to an LB agar plate. An L-shaped cell spreader was used to assure the mixture was evenly distributed across the plate. The agar plate was incubated overnight at 37 °C.

7.8.14 AlamarBlue™ Assay

A single colony of *E. coli* was isolated from an agar plate and inoculated in 5mL of MH2 overnight at 37 °C with shaking. This start-up culture was diluted 100-fold with MH2 to give a volume of 10 mL. The culture was then incubated at 37 °C until $OD_{(595)}$=0.8 was reached.

On a sterile 96-well plate (which had a sterilised lid), 90 μl of the seeded broth was added to each well. 2.5 mg/mL solutions of dipeptide or peptidomimetic were serially diluted to obtain 7 different concentrations (1250, 625, 312.5, 186, 78.2, 39, and 19.5 μg/mL). 10 μL of these diluted inhibitors were added to the 96-well plate to give a final volume of 200 μL and final concentrations of 250, 125, 62.5, 31.25, 15.63, 7.82, 3.90, 1.95 and 0.97 μg/mL. 10 μL of water, MeOH and DMSO were added to separate wells to serve as a growth control. Each test condition was tested in triplicate.

The sterile lid was placed on the plate 96-well plate and incubated for 1 hour at 37°C. To each well 10 μL of alamarBlue™ was added and the plate was incubated for a further 2-3 hours. The fluorescence was read on the HIDEX Sense Microplate Reader 425-301 using an excitation wavelength of 530 nm and emission wavelength of 580

nm. The inhibitor concentration which reduced the growth by 50 % was considered the IC50 of the compound.

REFERENCES

1 B. C. Chung, J. Zhao, R. A. Gillespie, D. Kwon, Z. Guan, J. Hong, P. Zhou and S.-Y. Lee, *Science*, 2013, **341**, 1012–1016.

2 M. Winn, R. J. M. Goss, K.-I. Kimura and T. D. H. Bugg, *Nat. Prod. Rep.*, 2010, **27**, 279–304.

3 K. Ogura and T. Koyama, *Chem. Rev.*, 1998, **98**, 1263–1276.

4 T.-P. Ko, Y.-K. Chen, H. Robinson, P.-C. Tsai, Y.-G. Gao, A. P.-C. Chen, A. H.-J. Wang and P.-H. Liang, *J. Biol. Chem.*, 2001, **276**, 47474–47482.

5 R. T. Gale and E. D. Brown, *Curr. Opin. Microbiol.*, 2015, **27**, 69–77.

6 A. Bouhss, A. E. Trunkfield, T. D. H. Bugg and D. Mengin-Lecreulx, *FEMS Microbiol. Rev.*, 2008, 208–233.

7 B. G. Spratt, *Eur. J. Biochem.*, 1977, **72**, 341–352.

8 J. Grandchamps, M. Nguyen-Distèche, C. Damblon, J. M. Frère and J. M. Ghuysen, *Biochem. J.*, 1995, **307**, 335–339.

9 S. S. Patel, J. A. Balfour and H. M. Bryson, *Drugs*, 1997, **53**, 637–656.

10 K. J. Stone and J. L. Strominger, *Proc. Natl. Acad. Sci.*, 1971, **68**, 3223–3227.

11 J.-C. Kim and B. Jeon, *J. Antimicrob. Chemother.*, 2016, **71**, 1260–1263.

12 P. Fulco and R. P. Wenzel, *Expert Rev. Anti. Infect. Ther.*, 2006, **4**, 939–945.

13 E. Gordon, N. Mouz, E. Duée and O. Dideberg, *J. Mol. Biol.*, 2000, **299**, 477–485.

14 F. Volke, R. Waschipky, A. Pampel, A. Donnerstag, G. Lantzsch, H. Pfeiffer, W. Richter, G. Klose and P. Welzel, *Chem. Phys. Lipids*, 1997, **85**, 115–123.

15 C. De Witte, B. Taminiau, B. Flahou, V. Hautekiet, G. Daube, R. Ducatelle and F. Haesebrouck, *Vet. Res.*, 2018, **49**, 35.

16 B. Ostash and S. Walker, *Nat. Prod. Rep.*, 2010, **27**, 1594.

17 C. Liu, A. Bayer, S. E. Cosgrove, R. S. Daum, S. K. Fridkin, R. J. Gorwitz, S. L. Kaplan, A. W. Karchmer, D. P. Levine, B. E. Murray, M. J. Rybak, D. A. Talan and H. F. Chambers, *Clin. Infect. Dis.*, 2011, **52**, 285–292.

18 J. R. Knox and R. F. Pratt, *Antimicrob. Agents Chemother.*, 1990, **34**, 1342–1347.

19 T. D. H. Bugg, S. Dutka-Malen, M. Arthur, P. Courvalin and C. T. Walsh, *Biochemistry*, 1991, **30**, 2017–2021.

20 Y. Liu, J. P. G. L. M. Rodrigues, A. M. J. J. Bonvin, E. A. Zaal, C. R. Berkers, M. Heger, K. Gawarecka, E. Swiezewska, E. Breukink and M. R. Egmond, *J. Biol. Chem.*, 2016, **291**, 15057–15068.

21 D. Pless and F. Neuhaus, *J. Biol. Chem.*, 1973, **248**, 1568–1576.

22 A. J. Lloyd, P. E. Brandish, A. M. Gilbey and T. D. H. Bugg, *J. Bacteriol.*, 2004, **186**, 1747–1757.

23 T. D. H. Bugg and R. V. Kerr, *J. Antibiot. (Tokyo).*, 2019, **72**, 865–876.

24 T. Koga, T. Fukuoka, N. Doi, T. Harasaki, H. Inoue, H. Hotoda, M.

Kakuta, Y. Muramatsu, N. Yamamura, M. Hoshi and T. Hirota, *J. Antimicrob. Chemother.*, 2004, **54**, 755–760.

25 B. V. Nikonenko, V. M. Reddy, M. Protopopova, E. Bogatcheva, L. Einck and C. A. Nacy, *Antimicrob. Agents Chemother.*, 2009, **53**, 3138–3139.

26 E. Bogatcheva, T. Dubuisson, M. Protopopova, L. Einck, C. A. Nacy and V. M. Reddy, *J. Antimicrob. Chemother.*, 2011, **66**, 578–587.

27 R. K. Sharma, R. P. Reddy, W. Tegge and R. Jain, *J. Med. Chem.*, 2009, **52**, 7421–7431.

28 P. E. Brandish, M. K. Burnham, J. T. Lonsdale, R. Southgate, M. Inukai and T. D. H. Bugg, *J. Biol. Chem.*, 1996, **271**, 7609–7614.

29 P. E. Brandish, K.-I. Kimura, M. Inukai, R. Southgate, J. T. Lonsdale and T. D. H. Bugg, *Antimicrob. Agents Chemother.*, 1996, **40**, 1640–1644.

30 A. T. Tran, E. E. Watson, V. Pujari, T. Conroy, L. J. Dowman, A. M. Giltrap, A. Pang, W. R. Wong, R. G. Linington, S. Mahapatra, J. Saunders, S. A. Charman, N. P. West, T. D. H. Bugg, J. Tod, C. G. Dowson, D. I. Roper, D. C. Crick, W. J. Britton and R. J. Payne, *Nat. Commun.*, 2017, **8**, 14414.

31 B. C. Chung, E. H. Mashalidis, T. Tanino, M. Kim, A. Matsuda, J. Hong, S. Ichikawa and S. Lee, *Nature*, 2016, **533**, 557–560.

32 J. K. Hakulinen, J. Hering, G. Brändén, H. Chen, A. Snijder, M. Ek and P. Johansson, *Nat. Chem. Biol.*, 2017, **13**, 265–267.

33 E. H. Mashalidis, B. Kaeser, Y. Terasawa, A. Katsuyama, D.-Y. Kwon, K. Lee, J. Hong, S. Ichikawa and S.-Y. Lee, *Nat. Commun.*, 2019, **10**, 2917.

34 S. Hirano, S. Ichikawa and A. Matsuda, *Bioorg. Med. Chem.*, 2008, **16**, 5123–5133.

35 A. Muramatsu, S. Miyakoshi, Y. Ogawa, T. Ohnuki, M. M. Ishii, M. Arai, T. Takatsu and M. Inkai, *J. Antibiot. (Tokyo).*, 2003, **56**, 259–267.

36 R. Young, *Microbiol. Rev.*, 1992, **56**, 430–481.

37 F. Sanger, G. M. Air, B. G. Barrell, N. L. Brown, A. R. Coulson, J. C. Fiddes, C. A. Hutchison, P. M. Slocombe and M. Smith, *Nature*, 1977, **265**, 687–695.

38 K. D. Young and R. Young, *J. Virol.*, 1982, **44**, 993–1002.

39 B. Henrich, W. Lubitz and R. Plapp, *Mol. Gen. Genet. MGG*, 1982, **185**, 493–497.

40 U. Bläsi and W. Lubitz, *J. Gen. Virol.*, 1985, **66**, 1209–1213.

41 K. J. Buckley and M. Hayashi, *Mol. Gen. Genet. MGG*, 1986, **204**, 120–125.

42 S. Mendel, J. M. Holbourn, J. A. Schouten and T. D. H. Bugg, *Microbiology*, 2006, **152**, 2959–2967.

43 A. Witte, G. Wanner, U. Bläsi, G. Halfmann, M. Szostak and W. Lubitz, *J. Bacteriol.*, 1990, **172**, 4109–4114.

44 D. Maratea, K. Young and R. Young, *Gene*, 1985, **40**, 39–46.

45 T. G. Bernhardt, D. K. Struck and R. Young, *J. Biol. Chem.*, 2001, **276**, 6093–6097.

46 T. G. Bernhardt, W. D. Roof and R. Young, *Proc. Natl. Acad. Sci. U. S. A.*, 2000, **97**, 4297–4302.

47 T. G. Bernhardt, W. D. Roof and R. Young, *Mol. Biol.*, 2002, **45**, 99–108.

48 M. T. Rodolis, A. Mihalyi, A. O'Reilly, J. Slikas, D. I. Roper, R. E. W. Hancock and T. D. H. Bugg, *ChemBioChem*, 2014, **15**, 1300–1308.

49 K. Hilpert, R. Volkmer-Engert, T. Walter and R. E. W. Hancock, *Nat. Biotechnol.*, 2005, **23**, 1008–1012.

50 B. Gomes, M. T. Augusto, M. R. Felício, A. Hollmann, O. L. Franco, S. Gonçalves and N. C. Santos, *Biotechnol. Adv.*, 2018, **36**, 415–429.

51 L. Townsend, R. L. Williams, O. Anuforom, M. R. Berwick, F. Halstead, E. Hughes, A. Stamboulis, B. Oppenheim, J. Gough, L. Grover, R. A. H. Scott, M. Webber, A. F. A. Peacock, A. Belli, A. Logan and F. de Cogan, *J. R. Soc. Interface*, 2017, **14**, 20160657.

52 K. V. R. Reddy, R. D. Yedery and C. Aranha, *Int. J. Antimicrob. Agents*, 2004, **24**, 536–547.

53 R. E. W. Hancock and H.-G. Sahl, *Nat. Biotechnol.*, 2006, **24**, 1551–1557.

54 N. H. O'Driscoll, O. Labovitiadi, T. P. T. Cushnie, K. H. Matthews, D. K. Mercer and A. J. Lamb, *Curr. Microbiol.*, 2013, **66**, 271–278.

55 K. Saikia, Y. D. Sravani, V. Ramakrishnan and N. Chaudhary, *Sci. Rep.*, 2017, **7**, 42994.

56 D. I. Chan, E. J. Prenner and H. J. Vogel, *Biochim. Biophys. Acta - Biomembr.*, 2006, **1758**, 1184–1202.

57 Z. Liu, A. Brady, A. Young, B. Rasimick, K. Chen, C. Zhou and N.

R. Kallenbach, *Antimicrob. Agents Chemother.*, 2007, **51**, 597–603.

58 S. Hou, Z. Liu, A. W. Young, S. L. Mark, N. R. Kallenbach and D. Ren, *Appl. Environ. Microbiol.*, 2010, **76**, 1967–1974.

59 H. B. Albada, P. Prochnow, S. Bobersky, S. Langklotz, P. Schriek, J. E. Bandow and N. Metzler-Nolte, *ACS Med. Chem. Lett.*, 2012, **3**, 980–984.

60 A. Pokorny and P. F. F. Almeida, *Biochemistry*, 2005, **44**, 9538–9544.

61 M. Selsted, M. Novotny, W. Morris, Y.-Q. Tang, W. Smith and J. Cullor, *J. Biol. Chem.*, 1992, **267**, 4292–4295.

62 S. E. Blondelle and R. A. Houghten, *Trends Biotechnol.*, 1996, **14**, 60–65.

63 J. A. Killian, I. Salemink, M. R. R. de Planque, G. Lindblom, R. E. Koeppe and D. V. Greathouse, *Biochemistry*, 1996, **35**, 1037–1045.

64 L. Yang, T. M. Weiss, R. I. Lehrer and H. W. Huang, 2009, **79**, 2002–2009.

65 M.-C. Gagnon, E. Strandberg, A. Grau-Campistany, P. Wadhwani, J. Reichert, J. Burck, F. Rabanal, M. Auger, J.-F. Paquin and A. Ulrich, *Biochemistry*, 2017, **56**, 1680–1695.

66 V. Castelletto, C. J. C. Edwards-Gayle, I. W. Hamley, G. Barrett, J. Seitsonen, J. Ruokolainen, L. R. de Mello and E. R. da Silva, *Chem. Commun.*, 2020, **56**, 615–618.

67 T. R. Insel, *Neuron*, 2010, **65**, 768–779.

68 A. Mizuno, K. Matsui and S. Shuto, *Chem. - A Eur. J.*, 2017, **23**, 14394–14409.

69 A. S. Ripka and D. H. Rich, *Curr. Opin. Chem. Biol.*, 1998, **2**, 441–452.

70 P. Wipf, J. Xiao and C. R. J. Stephenson, *Chim. Int. J. Chem.*, 2009, **63**, 764–775.

71 L. Pauling and R. B. Corey, *Proc. Natl. Acad. Sci.*, 1951, **37**, 729–740.

72 B. N. Bullock, A. L. Jochim and P. S. Arora, *J. Am. Chem. Soc.*, 2011, **133**, 14220–14223.

73 K. H. Khoo, C. S. Verma and D. P. Lane, *Nat. Rev. Drug Discov.*, 2014, **13**, 217–236.

74 B. P. Orner, J. T. Ernst and A. D. Hamilton, *J. Am. Chem. Soc.*, 2001, **123**, 5382–5383.

75 J. M. Rodriguez and A. D. Hamilton, *Angew. Chemie Int. Ed.*, 2007, **46**, 8614–8617.

76 S. Thompson and A. D. Hamilton, *Org. Biomol. Chem.*, 2012, **10**, 5780.

77 S. Thompson, R. Vallinayagam, M. J. Adler, R. T. W. Scott and A. D. Hamilton, *Tetrahedron*, 2012, **68**, 4501–4505.

78 J.-M. Ahn and S.-Y. Han, *Tetrahedron Lett.*, 2007, **48**, 3543–3547.

79 N. Busschaert, S. Thompson and A. D. Hamilton, *Chem. Commun.*, 2017, **53**, 313–316.

80 J. M. Davis, A. Truong and A. D. Hamilton, *Org. Lett.*, 2005, **7**, 5405–5408.

81 H. Yin, G. Lee, K. A. Sedey, O. Kutzki, H. S. Park, B. P. Orner, J. T. Ernst, H.-G. Wang, S. M. Sebti and A. D. Hamilton, *J. Am. Chem.*

Soc., 2005, **127**, 10191–10196.

82 P. Prabhakaran, V. Azzarito, T. Jacobs, M. J. Hardie, C. A. Kilner, T. A. Edwards, S. L. Warriner and A. J. Wilson, *Tetrahedron*, 2012, **68**, 4485–4491.

83 L. R. Whitby and D. L. Boger, *Acc. Chem. Res.*, 2012, **45**, 1698–1708.

84 G. Meng, J. Pu, Y. Li, A. Han, Y. Tian, W. Xu, T. Zhang, X. Li, L. Lu, C. Wang, S. Jiang and K. Liu, *J. Med. Chem.*, 2019, **62**, 8773–8783.

85 C. G. Cummings and A. D. Hamilton, *Curr. Opin. Chem. Biol.*, 2010, **14**, 341–346.

86 A. Nefzi, C. Dooley, J. M. Ostresh and R. A. Houghten, *Bioorg. Med. Chem. Lett.*, 1998, **8**, 2273–2278.

87 M. T. Rodolis, University of Warwick, 2013.

88 E. Fischer and A. Speier, *Berichte der Dtsch. Chem. Gesellschaft*, 1895, **28**, 3252.

89 J. M. Palomo, *RSC Adv.*, 2014, **4**, 32658–32672.

90 A. El-Faham and F. Albericio, *Chem. Rev.*, 2011, **111**, 6557–6602.

91 L. A. Carpino, *J. Am. Chem. Soc.*, 1993, **115**, 4397–4398.

92 L. A. Carpino, H. Imazumi, A. El-Faham, F. J. Ferrer, C. Zhang, Y. Lee, B. M. Foxman, P. Henklein, C. Hanay, C. Mügge, H. Wenschuh, J. Klose, M. Beyermann and M. Bienert, *Angew. Chemie - Int. Ed.*, 2002, **41**, 441–445.

93 M. Beyermann, P. Henklein, A. Klose, R. Sohr and M. Bienert, *Int. J. Pept. Protein Res.*, 1991, **37**, 252–256.

94 J. Coste, D. Le-Nguyen and B. Castro, *Tetrahedron Lett.*, 1990, **31**, 205–208.

95 L. A. Carpino and G. Y. Han, *J. Org. Chem.*, 1972, **37**, 3404–3409.

96 A. Isidro-llobet, M. Álvarez and F. Albericio, *Chem. Rev.*, 2009, **109**, 2455–2504.

97 A. Stierandova, N. F. Sepetov, G. V Nikiforovich and M. Lebl, *Int. J. Pept. Protein Res.*, 1994, **43**, 31–38.

98 H. Gaussier, H. Morency, M. C. Lavoie and M. Subirade, *Appl. Environ. Microbiol.*, 2002, **68**, 4803–4808.

99 A. O. Okaru, T. S. Brunner, S. M. Ackermann, T. Kuballa, S. G. Walch, M. Kohl-Himmelseher and D. W. Lachenmeier, *J. Anal. Methods Chem.*, 2017, **2017**, 1–7.

100 J. Sloop, *Reports Org. Chem.*, 2013, **3**, 1–12.

101 M. B. Strøm, B. E. Haug, M. L. Skar, W. Stensen, T. Stiberg and J. S. Svendsen, *J. Med. Chem.*, 2003, **46**, 1567–1570.

102 S. Ulhaq, E. C. Chinje, M. A. Naylor, I. J. Stratford and M. D. Threadgill, *Bioorganic Med. Chem.*, 1999, **7**, 1787–1796.

103 K. Beaumont, R. Webster, I. Gardner and K. Dack, *Curr. Drug Metab.*, 2003, **4**, 461–485.

104 D. Jornada, G. dos Santos Fernandes, D. Chiba, T. de Melo, J. dos Santos and M. Chung, *Molecules*, 2015, **21**, 42.

105 C. Wong and G. Whitesides, in *Tetrahedron Organic Chemistry Series*, 1994, pp. 41–130.

106 D. Rich and J. Singh, in *Major Methods of Peptide Bond Formation*, 1979, pp. 241–261.

107 J. S. Albert, A. D. Hamilton, A. C. Hart, X. Feng, L. Lin and Z. Wang, in *Encyclopedia of Reagents for Organic Synthesis*, John Wiley & Sons, Ltd, Chichester, UK, 2017, pp. 1–9.

108 E. Valeur and M. Bradley, *Chem. Soc. Rev.*, 2009, **38**, 606–631.

109 Y. Chen, C. T. Mant and R. S. Hodges, *J. Chromatogr. A*, 2007, **1140**, 112–120.

110 I. Wiegand, K. Hilpert and R. E. W. Hancock, *Nat. Protoc.*, 2008, **3**, 163–175.

111 A. A. Miles, S. S. Misra and J. O. Irwin, *Epidemiol. Infect.*, 1938, **38**, 732–749.

112 G. Sezonov, D. Joseleau-Petit and R. D'Ari, *J. Bacteriol.*, 2007, **189**, 8746–8749.

113 H. Nikaido, The Limitations of LB Medium, https://schaechter.asmblog.org/schaechter/2009/11/the-limitations-of-lb-medium.html, (accessed 11 May 2017).

114 J. H. Mueller and J. Hinton, *Exp. Biol. Med.*, 1941, **48**, 330–333.

115 J. N. Pendleton, S. P. Gorman and B. F. Gilmore, *Expert Rev. Anti. Infect. Ther.*, 2013, **11**, 297–308.

116 L. D. Renner, J. Zan, L. I. Hu, M. Martinez, P. J. Resto, A. C. Siegel, C. Torres, S. B. Hall, T. R. Slezak, T. H. Nguyen and D. B. Weibel, *Appl. Environ. Microbiol.*, 2017, **83**, 1–13.

117 S. Santajit and N. Indrawattana, *Biomed Res. Int.*, 2016, **2016**, 1–8.

118 G. L. French, *J. Antimicrob. Chemother.*, 2006, **58**, 1107–1117.

119 A. Mihalyi, S. Jamshidi, J. Slikas and T. D. H. Bugg, *Bioorg. Med. Chem.*, 2014, **22**, 4566–4571.

120 C. Watanakunakorn, *J. Antimicrob. Chemother.*, 1984, **14**, 7–18.

121 J. L. Allison, R. E. Hartman, R. S. Hartman, A. D. Wolfe, J. Ciak, F. E. Hahn, J. L. Walter, R. Army, R. E. Hartman, R. S. Hartman, A. D. Wolfe, J. Ciak and E. Fred, *J. Bacteriol.*, 1961, **83**, 609–615.

122 S. Siricilla, K. Mitachi, K. Skorupinska-tudek, E. Swiezewska and M. Kurosu, *Anal. Biochem.*, 2014, **461**, 36–45.

123 S. Tabor, in *Current Protocols in Molecular Biology*, John Wiley & Sons, Inc., Hoboken, NJ, USA, 2001.

124 B. Miroux and J. E. Walker, *J. Mol. Biol.*, 1996, **260**, 289–298.

125 G. Suleyman and M. J. Zervos, *Expert Opin. Drug Saf.*, 2016, **15**, 153–167.

126 E. P. Abraham and E. Chain, *Nature*, 1940, **146**, 837–837.

127 I. R. Hooper, in *The Naturally Occurring Aminoglycoside Antibiotics*, 1982, pp. 1–35.

128 R. L. Yenofsky, M. Fine and J. W. Pellow, *Proc. Natl. Acad. Sci.*, 1990, **87**, 3435–3439.

129 H. Träuble and P. Overath, *Biochim. Biophys. Acta - Biomembr.*, 1973, **307**, 491–512.

130 R. C. Borra, M. A. Lotufo, S. M. Gagioti, F. de M. Barros and P. M. Andrade, *Braz. Oral Res.*, 2009, **23**, 255–262.

131 N. Silanikove and F. Shapiro, 2012, pp. 395–404.

132 S. Anoopkumar-Dukie, J. B. Carey, T. Conere, E. O'Sullivan, F. N. van Pelt and A. Allshire, *Br. J. Radiol.*, 2005, **78**, 945–947.

133 J. O'Brien, I. Wilson, T. Orton and F. Pognan, *Eur. J. Biochem.*,

2000, **267**, 5421–5426.

134 P. Chibueze, S. Di, O. Charles and U. Remigius, *Open Access J. Toxicol.*, 2016, **1**, 555–557.

135 D. C. Morrison and D. M. Jacobs, *Immunochemistry*, 1976, **13**, 813–818.

136 World Health Organization model list of essential medicines: 21st list 2019, https://apps.who.int/iris/handle/10665/325771, (accessed 1 November 2019).

137 K. Fosgerau and T. Hoffmann, *Drug Discov. Today*, 2015, **20**, 122–128.

138 M. Zeng, F. Zhang, F.-X. Wu, Y. Li, J. Wang and M. Li, *Bioinformatics*, 2019, **4**, 1114–1120.

139 D. E. Scott, A. R. Bayly, C. Abell and J. Skidmore, *Nat. Rev. Drug Discov.*, 2016, **15**, 533–550.

140 H. Yin, G. Lee, K. A. Sedey, J. M. Rodriguez, H. Wang, S. M. Sebti and A. D. Hamilton, *J. Am. Chem. Soc.*, 2005, **127**, 5463–5468.

141 R. N. Boyd and R. T. Morrison, *Organic Chemistry*, Prentice Hall, 6th edn., 1992.

142 H. Ledon, *Org. Synth.*, 1979, **59**, 66.

143 J. Pandey, M. Mishra, S. S. Bisht, A. Sharma and R. P. Tripathi, *tetrahedron Lett.*, 2008, **49**, 695–698.

144 V. M. Rinne, T. Suuronen, O. Kyrylenko, S. Kyrylenko, E. Kuusisto, A. J. Tervo, T. Ja, A. Salminen and E. A. A. Wallen, *Bioorg. Med. Chem.*, 2007, **17**, 2448–2451.

145 M. . Cezari and L. Juliano, *Int. J. Pept. Protein Res.*, 1996, **9**, 88–

91.

146 L. Carpino, B. Cohen, K. Stephens, J. Sadat-Aalaee, J. Tien and D. Langridge, *J. Org. Chem.*, 1986, **51**, 3732–3734.

147 M. Bhatt and S. El-Morey, *Synthesis (Stuttg).*, 1982, **12**, 1048–1050.

148 J. Remion, A. Colens and L. Ghosez, *J. Chem. Soc., Chem. Commun.*, 1979, **0**, 1180–1181.

149 J. R. Kimmel, in *Methods in Enzymology*, 1967, pp. 584–589.

150 B. Lal and A. K. Gangopadhyay, *Tetrahedron Lett.*, 1996, **37**, 2483–2486.

151 E. Masiukiewicz, S. Wiejak and B. Rzeszotarskat, *Org. Prep. Proced. Int.*, 2002, **34**, 531–537.

152 J. C. Mckew, M. A. Foley, P. Thakker, M. L. Behnke, F. E. Lovering, F. Sum, S. Tam, K. Wu, M. W. H. Shen, W. Zhang, M. Gonzalez, S. Liu, A. Mahadevan, H. Sard, S. P. Khor and J. D. Clark, *J. Med. Chem.*, 2006, **49**, 135–158.

153 S. Amines, R. Hosseinzadeh, H. Alinezhad, S. Ghahari, A. Heydari and S. Khaksar, *Synthesis (Stuttg).*, 2011, **3**, 490–496.

154 K. Sonogashira, *J. Organomet. Chem.*, 2002, **653**, 46–49.

155 C. Congiu, V. Onnis, A. Deplano, S. Salvadori, V. Marconi, D. Maftei, L. Negri, R. Lattanzi and G. Balboni, *Eur. J. Med. Chem.*, 2014, **81**, 334–340.

156 J. L. Ralbovsky, J. G. Lisko, J. M. Palmer, J. Mabus, K. M. Chevalier, M. J. Schulz, A. B. Dyatkin, T. A. Miskowski, S. J. Coats, P. Hornby and W. He, *Bioorg. Med. Chem. Lett.*, 2009, **19**, 2661–2663.

157 M. Hassani, W. Cai, D. C. Holley, J. P. Lineswala, B. R. Maharjan, G. R. Ebrahimian, H. Seradj, M. G. Stocksdale, F. Mohammadi, C. C. Marvin, J. M. Gerdes, H. D. Beall and M. Behforouz, *J. Med. Chem.*, 2005, **48**, 7733–7749.

158 Y.-S. Liu, C. Zhao, D. E. Bergbreiter and D. Romo, *J. Org. Chem.*, 1998, **63**, 3471–3473.

159 C. Ghosh, G. B. Manjunath, P. Akkapeddi, V. Yarlagadda, J. Hoque, D. S. S. M. Uppu, M. M. Konai and J. Haldar, *J. Med. Chem.*, 2014, **57**, 1428–1436.

160 K. Walsh, H. F. Sneddon and C. J. Moody, *ChemSusChem*, 2013, **6**, 1455–1460.

161 D. R. Appleton, R. C. Babcock and B. R. Copp, *Tetrahedron*, 2001, **57**, 10181–10189.

162 M. de Loos, J. H. van Esch, R. M. Kellogg and B. L. Feringa, *Tetrahedron*, 2007, **63**, 7285–7301.

163 J. L. Yap, X. Cao, K. Vanommeslaeghe, K.-Y. Jung, C. Peddaboina, P. T. Wilder, A. Nan, A. D. MacKerell, W. R. Smythe and S. Fletcher, *Org. Biomol. Chem.*, 2012, **10**, 2928.

164 N. S. Murphy, P. Prabhakaran, V. Azzarito, J. P. Plante, M. J. Hardie, C. A. Kilner, S. L. Warriner and A. J. Wilson, *Chem. - A Eur. J.*, 2013, **19**, 5546–5550.

165 E. Masiukiewicz, S. Wiejak and B. Rzeszotarskat, *Org. Prep. Proced. Int.*, 2002, **34**, 531–537.

166 L. Gong, J. H. Hogg, J. Collier, R. S. Wilhelm and C. Soderberg, *Bioorg. Med. Chem. Lett.*, 2003, **13**, 3597–3600.

167 T. Ogiyama, M. Yamaguchi, N. Kurikawa, S. Honzumi and Y. Yamamoto, *Bioorg. Med. Chem.*, 2016, **24**, 3801–3807.

168 N. Li and J. M. J. Frechet, 1985, 1100–1101.

169 P. Innocenti, K.-M. J. Cheung, S. Solanki, C. Mas-Droux, F. Rowan, S. Yeoh, K. Boxall, M. Westlake, L. Pickard, T. Hardy, J. E. Baxter, G. W. Aherne, R. Bayliss, A. M. Fry and S. Hoelder, *J. Med. Chem.*, 2012, **55**, 3228–3241.

170 M. Juárez-Calderón, D. M. Aparicio, D. Gnecco, J. R. Juárez, L. Orea, A. Mendoza, F. Sartillo-Piscil, E. del Olmo and J. L. Terán, *Tetrahedron Lett.*, 2013, **54**, 2729–2732.

171 M. Durcik, D. Lovison, Ž. Skok, C. Durante Cruz, P. Tammela, T. Tomašič, D. Benedetto Tiz, G. Draskovits, Á. Nyerges, C. Pál, J. Ilaš, L. Peterlin Mašič, D. Kikelj and N. Zidar, *Eur. J. Med. Chem.*, 2018, **154**, 117–132.

172 E. J. J. Lugtenberg, *J. Bacteriol.*, 1972, **110**, 26–34.

173 B. Flouret, D. Mengin-Lecreulx and J. van Heijenoort, *Anal. Biochem.*, 1981, **114**, 59–63.